

# Precision Calculations in Supersymmetric Theories

L. Mihaila

*Institute for Theoretical Particle Physics,  
Karlsruhe Institute of Technology (KIT)*

## Abstract

In this review article we report on the newest developments in precision calculations in supersymmetric theories. An important issue related to this topic is the construction of a regularization scheme preserving simultaneously gauge invariance and supersymmetry. In this context, we discuss in detail dimensional reduction in component field formalism as it is currently the preferred framework employed in the literature. Furthermore, we set special emphasis on the application of multi-loop calculations to the analysis of gauge coupling unification, the prediction of the lightest Higgs boson mass and the computation of the hadronic Higgs production and decay rates in supersymmetric models. Such precise theoretical calculations up to the fourth order in perturbation theory are required in order to cope with the expected experimental accuracy on the one hand, and to enable us to distinguish between the predictions of the Standard Model and those of supersymmetric theories on the other hand.

PACS numbers: 11.25.Db 11.30.Pb 12.38.Bx

# Contents

|          |   |           |
|----------|---|-----------|
| <b>1</b> | <b>Introduction</b>   | <b>2</b>  |
| <b>2</b> | <b>Holomorphy and exact beta functions in supersymmetric theories</b>                   | <b>6</b>  |
| <b>3</b> | <b>Dimensional reduction in the component field formalism</b>                           | <b>10</b> |
| 3.1      | Framework . . . . .   | 11        |
| 3.2      | Minimal Subtraction Schemes $\overline{\text{MS}}$ and $\overline{\text{DR}}$ . . . . . | 14        |
| 3.3      | DRED applied to non-supersymmetric theories . . . . .                                   | 15        |
| 3.3.1    | The $\varepsilon$ -scalar self couplings . . . . .                                      | 18        |
| 3.3.2    | Three-loop renormalization constants for a non-supersymmetric theory . .                | 21        |
| 3.3.3    | The general four-loop order results in the $\overline{\text{DR}}$ scheme . . . . .      | 24        |
| 3.3.4    | The four-loop supersymmetric case . . . . .   | 26        |
| 3.3.5    | $\varepsilon$ -scalar mass . . . . .  | 28        |
| <b>4</b> | <b>Dimensional Reduction applied to SUSY-QCD at three loops</b>                         | <b>30</b> |
| 4.1      | Renormalization of the gauge coupling and fermion masses at three loops . . . .         | 30        |
| 4.2      | Renormalization of the squark sector at three loops . . . . .                           | 33        |
| <b>5</b> | <b>The SM gauge beta functions to three loops</b>                                       | <b>41</b> |
| <b>6</b> | <b>Gauge coupling unification in supersymmetric models</b>                              | <b>46</b> |
| 6.1      | Effective field theory approach. Decoupling coefficients. . . . .                       | 47        |
| 6.1.1    | Framework . . . . .   | 47        |
| 6.1.2    | Renormalization scheme . . . . .  | 49        |
| 6.1.3    | Analytical results . . . . .  | 50        |
| 6.1.4    | Numerical analysis . . . . .  | 51        |
| 6.2      | Gauge coupling unification in the minimal SUSY SU(5) model . . . . .                    | 53        |
| 6.2.1    | Input parameters . . . . .  | 56        |
| 6.2.2    | Numerical analysis . . . . .  | 57        |
| <b>7</b> | <b>The mass of the lightest Higgs boson in the MSSM</b>                                 | <b>60</b> |
| 7.1      | Higgs boson mass in the SM . . . . .  | 60        |
| 7.2      | Higgs boson mass in the MSSM . . . . .  | 63        |

|          |   |           |
|----------|---|-----------|
| 7.2.1    | Calculation of $\mathcal{O}(\alpha_t\alpha_s^2)$ corrections in the MSSM . . . . .                      | 64        |
| 7.2.2    | Phenomenological analysis . . . . .   | 69        |
| <b>8</b> | <b>Hadronic Higgs production and decay in susy models</b>   | <b>70</b> |
| 8.1      | Effective field theory formalism . . . . .  | 71        |
| 8.2      | Computation of the coefficient functions $C_1$ and $C_{2q}$ . . . . .                                   | 73        |
| 8.2.1    | Low Energy Theorem . . . . .  | 76        |
| 8.3      | Hadronic Higgs decays . . . . .   | 77        |
| 8.3.1    | Numerical analysis . . . . .  | 80        |
| 8.3.2    | Mass corrections to hadronic Higgs decays . . . . .   | 81        |
| 8.4      | Hadronic Higgs production . . . . .   | 84        |
| 8.4.1    | Numerical analysis . . . . .  | 86        |
| <b>9</b> | <b>Conclusions</b>  | <b>87</b> |
| <b>A</b> | <b>Group Theory</b>   | <b>89</b> |
| <b>B</b> | <b>Modification of the <math>\overline{\text{DR}}</math> scheme: <math>\overline{\text{MDR}}</math></b> | <b>90</b> |

# 1 Introduction

Today we know that the Standard Model(SM) of particle physics [1–5], which is a renormalizable gauge theory for the group  $SU(3)_C \times SU(2)_W \times U(1)$ , is extremely successful at short distances of the order of  $10^{-16}$  cm. Up to now, all experiments verify it without any conclusive hint towards new physics. On the other hand, Einstein’s gravitational theory based on the same concept of gauging the symmetries gives a very good classical theory for long distances. However, the classical theory of gravity could not be quantized due to its abundant number of singularities. There seems to be a deep conflict between the classical theory of gravity and quantum field theory. Thus, it arises naturally the question whether gauging is the only organizing principle or there is a deeper connection between space-time and internal space symmetries. In a long series of “no-go theorems” among which the Coleman-Mandula theorem [6] is the most important one, it was shown that the only possible symmetry group of a consistent four-dimensional quantum field theory is the direct product of the internal symmetry group and the Poincaré group. Precisely, it states that internal symmetries cannot interact non-trivially with space-time symmetry. Surprisingly, there is a unique way of combining non-trivially space-time and inner space symmetries, namely Supersymmetry (SUSY). It was shown by Haag, Lopuszanski, and Sohnius [7] that weakening the assumptions of the Coleman-Mandula theorem by allowing both commuting and anti-commuting symmetry generators, there is a nontrivial extension of the Poincaré algebra, namely, the supersymmetry algebra. The supersymmetry generators transform bosonic particles into fermionic ones and vice versa, but the commutator of two such transformations

yields a translation in space-time. In case of four-dimensional space-time, the algebra generated by the SUSY generators will contain the algebra of Einstein's general relativity.

The first attempts to construct physical models respecting SUSY can be traced back in the early seventies to the works by Golfand and Likhtman [8] and Volkov and Akulov [9]. However, the first known example of a renormalizable supersymmetric four-dimensional quantum field theory is the Wess-Zumino model [10]. Within SUSY it is very natural to extend the concept of space-time to the concept of superspace [11]. Along with the four-dimensional Minkowsky space there are also two new "anti-commuting" coordinates  $\theta_\alpha$  and  $\bar{\theta}_{\dot{\alpha}}$ , that are labeled in Grassmann numbers rather than real numbers

$$\begin{aligned} \{\theta_\alpha, \theta_\beta\} &= 0, & \{\bar{\theta}_{\dot{\alpha}}, \bar{\theta}_{\dot{\beta}}\} &= 0, \\ \theta_\alpha^2 &= 0, & \bar{\theta}_{\dot{\alpha}}^2 &= 0, & \text{with } \alpha, \beta, \dot{\alpha}, \dot{\beta} &= 1, 2. \end{aligned} \quad (1.1)$$

The ordinary space dimensions correspond to bosonic degrees of freedom, the anti-commuting dimensions to fermionic degrees of freedom. The fields are now functions of the superspace variables  $(x_\mu, \theta_\alpha, \bar{\theta}_{\dot{\alpha}})$  and they are organized into supersymmetric multiplets in a natural way [11]. Expanding the multiplets in Taylor series over the Grassmannian variables, one obtains the components of the superfield as the coefficients of the expansion. They are ordinary functions of the space-time coordinates and can be identified with the usual fields. Furthermore, in the superfield notation the manifestly supersymmetric Lagrangians are polynomials of the superfields. In the same way, as the ordinary action is the integral over the space-time of the Lagrangian density, in the supersymmetric case the action may be expressed as an integral over the whole superspace.

As quantum field theories the supersymmetric theories are less divergent as they would be in the absence of SUSY. These properties can be traced back to the cancellation of diagrams containing bosonic or fermionic particles, as for example the cancellation of quadratic divergences present in the radiative corrections to the Higgs boson mass. Even more, it was shown [12–14] that there are parameters of the theory that do not get any radiative corrections, that is a very special feature in quantum field theories. The most important consequence for the particle phenomenology is the fact that in a supersymmetric theory there should be an equal number of bosons and fermions with equal masses. In other words, for every SM particle there should exist a supersymmetric partner with an equal mass. But in Nature we do not observe such a situation. An elegant solution to break SUSY in such a way that its renormalization properties remain valid (in particular the non-renormalization theorems and the cancellation of quadratic divergences) is to introduce the so-called soft terms [15]. In this way, the mass difference between supersymmetric partners can become of the order of SUSY breaking scale. Moreover, there will also be parameters that receive only finite radiative corrections of the order of magnitude of SUSY breaking parameters. This is the case of the Higgs masses and Higgs couplings. Accordingly, the SUSY partners of the SM particles should not be very heavy in order to account for the smallness of the Higgs mass and couplings. For example, requiring for consistency of the perturbation theory that the radiative corrections to the Higgs boson mass do not exceed the mass itself gives [16]

$$\delta M_h^2 \approx g^2 M_{\text{SUSY}}^2 \approx M_h^2, \quad (1.2)$$

where  $M_{\text{SUSY}}$  denotes the mass scale of SM superpartners. Thus, for  $M_h \approx 100$  GeV and

$g \approx 10^{-1}$  one obtains  $M_{\text{SUSY}} \approx 1000$  GeV. This feature is one of the great achievements of supersymmetric theories, namely, the solution to the hierarchy problem in particle physics.

The very old concept of the existence of an organizing principle that allows the unification of all interactions present in Nature is nowadays embedded in the so-called Grand Unified Theories (GUT). The predictions of such theories can be even precisely tested with the help of the experiments conducted at modern particle colliders. The most prominent example concerns, for sure, the prediction of gauge coupling unification. Once the gauge couplings for the electroweak and strong interactions had been precisely measured at the Large Electron-Proton Collider (LEP) [17], we could verify this hypothesis with high precision. The amazing result of evolving the low-energy values of the gauge couplings according to the SM predictions [18–20] is that unification is excluded by more than eight standard deviations. This means that, unification can be achieved only if new physics occurs between the electroweak and the Planck scales. If one considers that a supersymmetric theory describes the new physics, one obtains that unification at an energy scale of about  $10^{16}$  GeV can be realized if the typical supersymmetric mass scale is of the order of  $10^3$  GeV. This observation was interpreted as first “evidence” for SUSY, especially because the supersymmetric mass scale was in the same range as that derived from the solution to the hierarchy problem.

Another virtue of SUSY is that it provides a candidate for the cold dark matter. Nowadays, it is well established that the visible matter amounts to only about 4% of the matter in the Universe. A considerable fraction of the energy is made up from the so-called dark matter. The direct evidence for the existence of dark matter are the flat rotation curves of spiral galaxies (see, for example, Ref. [21] and references cited therein), the gravitational lensing caused by invisible gravitating matter in the sky [22,23], and the formation of large structures like clusters of galaxies. The dark matter is classified in terms of the mass of the constituent particle(s) and its (their) typical velocity: The hot dark matter, consisting of light relativistic particles and the cold one, made of massive weakly interacting particles (WIMPs) [24]. The hot dark matter might consist of neutrinos; however, this hypothesis cannot explain galaxy formation. For the cold dark matter, there is obviously no candidate within the SM. Nevertheless, SUSY provides an excellent candidate for WIMP, namely, the neutralino as the lightest supersymmetric particle.

These three fundamental predictions of SUSY makes it one of the preferred candidates for physics beyond the SM. This explains the enormous efforts devoted to searches for SUSY in particle physics experiments at accelerators, in the deep sky with the help of telescopes, and with the help of underground facilities, that last already for four decades. The exclusion bounds on the supersymmetric mass spectrum is in general model dependent. In the case of the constrained MSSM (CMSSM), the current status is as follows: If one combines the excluded regions from the direct searches at the LHC [25,25], the stringent lower bound on the mass of the pseudo-scalar Higgs from XENON100 [26], the constraints from the relic density from WMAP [27] and those from muon anomalous magnetic moment [28], one can set a lower limit on the WIMP mass of 230 GeV and on strongly interacting supersymmetric particles of about 1300 GeV. If in addition, the mass of the lightest Higgs boson of 125 GeV in agreement with the recent measurement at the LHC [29,30] is imposed, one can exclude strongly interacting superpartners below 2 TeV. Nevertheless, such exclusion bounds concern the gluinos and mainly the first two generation of squarks. On the other hand, for the third generation of squarks, masses of the order of few hundred GeV are still allowed.

In this context, the question whether low-energy SUSY is still a valid candidate for physics beyond the SM arises naturally. Despite the slight tension that appears in particular models, as for example the constrained MSSM,<sup>1</sup> the supersymmetric parameter space is large enough to accommodate all the experimental data known at present. However, the main prediction of low energy SUSY, i.e. the existence of supersymmetric particles at the TeV scale, is falsifiable at the LHC at the full energy run of 14 TeV. If no supersymmetric particle will be found at the TeV scale, we have to give up the main arguments in favour of SUSY, namely, the gauge coupling unification and the solution to the hierarchy problem.

To draw such powerful conclusions, one definitely needs an accurate comparison of the experimental data with the theory predictions based on SUSY models. There are various possibilities to perform such comparisons, one of them being high precision analyses, that requires precision data both at the experimental and theoretical level. On the theory side, the observables for which precise theoretical predictions up to the next-to-next-to leading order in perturbation theory are required, are the electroweak precision observables (EWPO) [31], the muon anomalous magnetic moment [32], the lightest Higgs boson mass [31], the decay rate for the rare decay of a bottom quark into a strange quark and a photon  $\Gamma(\overline{B} \rightarrow X_s \gamma)$  [33] and, of course, the production and decay rates of the Higgs boson at hadron colliders [34]. Details about the various topics can be found in the excellent review articles cited above. In this paper we report on the newest developments in precision calculations within SUSY models and set special emphasis on the recent calculations at the three-loop order involving several different mass scales. The latter constitute in many cases essential ingredients for the state of the art analyses of the experimental data taken currently at the LHC.

This article is organized as follows: In the next section we briefly review the main results concerning the renormalizability of supersymmetric theories that can be derived from their holomorphic properties. In sections 3 and 4 we describe the regularization method based on dimensional reduction applied to non-supersymmetric and supersymmetric theories up to the fourth order in perturbation theory. In the second part of the paper we present the phenomenological applications of such precision calculations. Namely, in sections 5 we concentrate on computation of the three-loop gauge beta functions within the SM that allows us to predict the gauge couplings at high energies with very high accuracy. Furthermore, in section 6 we report on the gauge coupling unification within SUSY models taking into account the most precise theoretical predictions and experimental measurements. Section 7 is devoted to the computation of the lightest Higgs boson mass within SUSY models with three-loop accuracy. In section 8, the hadronic Higgs production and decay in SUSY models are reviewed and the required computations up to the third order in perturbation theory are presented. Finally, we draw our conclusions and present our perspective on precision calculations in SUSY models in section 9. In the Appendix A we give details about the computation of the group invariants required in multi-loop calculations. Appendix B contains the main renormalization constants needed for three-loop calculations in supersymmetric quantum chromodynamics (SUSY-QCD) within the modified minimal subtraction, that has been employed for the computations reviewed in sections 7 and 8.

---

<sup>1</sup>The constrained MSSM model is based on the universality hypothesis and is described by a set of five free parameters defining the mass scale for the Higgs potential and the scalar and fermion masses.

## 2 Holomorphy and exact beta functions in supersymmetric theories

In the last decades, enormous progress has been made in understanding the dynamics of supersymmetric gauge theories. For many models even exact Renormalization Group Equations (RGEs) for the gauge couplings have been derived. However, the connections between the exact results and those obtained in perturbation theory are still not completely elucidated. Shifman and Vainshtein [35] were the first to propose a solution to this puzzle. They based their argumentation on the difference between the quantities involved in the exact beta functions derived within the Wilsonian renormalization approach and those adopted in the common perturbative framework. A different derivation of the exact beta functions was presented in Ref. [36], where only the Wilsonian renormalization approach was used but the authors distinguished between the holomorphic and canonical normalization of the gauge kinetic term in the bare Lagrangian.

Within the Wilsonian framework [37] any field theory is defined by the fundamental Lagrangian, the bare couplings and the cutoff parameter. Varying the cutoff parameter and the bare couplings in a concerted way so that the low-energy physics remains fixed, one finds the dependence of the bare couplings on the cutoff parameter which is encoded in the Wilsonian Renormalization Group Equations (WRGEs). The transition from a fundamental Lagrangian to an effective Lagrangian involves integrating out the high momentum modes of the quantum fields (i.e. degrees of freedom with momenta between some large cutoff scale  $\Lambda$  and some renormalization scale  $\mu$ ). The coefficients of the resulting operators play the role of renormalized couplings and we will call them Wilsonian effective couplings. The virtue of this approach is the lack of any infrared effects, since none of the calculations involves infrared divergences.

Let us consider as an example supersymmetric electrodynamics (SQED). The vector superfield in the Wess-Zumino gauge has the following Grassmannian expansion

$$V(x, \theta, \bar{\theta}) = -\theta\sigma^\mu\bar{\theta}v_\mu(x) + i\theta\theta\bar{\theta}\bar{\lambda}(x) - i\bar{\theta}\bar{\theta}\theta\lambda(x) + \frac{1}{2}\theta\theta\bar{\theta}\bar{\theta}D(x), \quad (2.1)$$

where the physical degrees of freedom correspond to the vector gauge field  $v_\mu$  and the Majorana spinor field  $\lambda$ , known also as gaugino field. The field  $D$  is an auxiliary field without any physical meaning and can be eliminated with the help of equations of motion for the physical fields.

The Lagrangian of the model at an energy scale  $\mu$  can be written as follows

$$L = \frac{1}{4g^2(\mu)} \int d^4x d^2\theta \mathcal{W}^\alpha \mathcal{W}_\alpha + \frac{1}{4}Z(\mu) \int d^4x d^2\theta (\bar{T}e^V T + \bar{U}e^{-V}U), \quad (2.2)$$

where the superfield strength tensor is defined through the following relation

$$\mathcal{W}_\alpha = \frac{1}{8}\bar{D}^2 D_\alpha V = i\lambda_\alpha(x) - \theta_\alpha D(x) - i\theta^\beta F_{\alpha\beta}(x) + \theta^2 \partial_{\alpha\dot{\alpha}} \bar{\lambda}^{\dot{\alpha}}(x), \quad (2.3)$$

with

$$F_{\mu\nu} = \partial_\mu v_\nu - \partial_\nu v_\mu. \quad (2.4)$$

Here  $D$  and  $\bar{D}$  are the supercovariant derivatives. The superfields  $T(x, \theta, \bar{\theta})$  and  $U(x, \theta, \bar{\theta})$  are chiral matter superfields with charges 1 and  $-1$ , respectively.  $g(\mu)$  stands for the gauge coupling

and  $Z(\mu)$  denotes ...

finish

The maximal value of  $\mu$  is equal to  $\Lambda$ , the ultraviolet cutoff parameter. At this point the Lagrangian (2.2) is just the original SQED Lagrangian and the coefficients  $1/g^2(\Lambda)$  and  $Z(\Lambda)$  are bare parameters.

Because the momentum integrals are performed in  $d = 4$  dimension and the regularization is introduced through the cutoff parameter, the Wilsonian renormalization procedure preserves SUSY. Thus, if one calculates the Wilsonian effective Lagrangian, it is manifestly supersymmetric. As a consequence, the resulting effective superpotential (the part of the Lagrangian density that does not contain any derivative) must be a holomorphic function of the couplings [12–14]. This constraint restricts the running of the Wilsonian couplings to just the one-loop order.

For example, let us assume that we integrate out the matter superfields passing to the low-energy limit of the theory. The low-energy effective coupling at the low-energy  $\mu$  is given through the following relation

$$\frac{\pi}{\alpha_W(\mu)} = \frac{\pi}{\alpha_{W,0}(\Lambda)} - 2b_0 \ln \frac{\Lambda}{\mu}, \quad (2.5)$$

where  $\alpha_W(\mu)$  denotes the renormalized or the Wilsonian low-energy effective coupling constant and  $\alpha_{W,0}(\Lambda)$  is the cutoff-dependent bare coupling constant.  $b_0$  is the coefficient of the one-loop beta function of the underlying theory, where the beta function is defined through

$$\beta(\alpha) = \mu^2 \frac{d}{d\mu^2} \alpha = - \left( \frac{\alpha}{\pi} \right)^2 \sum_{n \geq 0} \left( \frac{\alpha}{\pi} \right)^n b_n, \quad \text{with} \quad \alpha = \frac{g^2}{4\pi}. \quad (2.6)$$

Let us emphasize that Eq. (2.5) is exact at all orders. The two- and higher-loop RGEs involve at least  $\ln(\ln(\alpha_{W,0}))$  which is a non holomorphic function of the bare coupling and thus, cannot contribute to Eq. (2.5). In Ref. [35], it was proved through a direct calculation using the supergraphs method that the two-loop contributions to the running of the effective coupling vanishes. The generalization of this assertion to higher loops is based on the extension of the non-renormalization theorem for  $F$ -terms in supersymmetric theories [12–14].

As mentioned above, one has to distinguish between the holomorphic Wilsonian gauge couplings and the physically-measurable momentum-dependent effective gauge couplings present in the one-particle irreducible generating functional. Unlike the Wilsonian couplings, the physical couplings do not depend on the ultraviolet cutoff scale but on momenta of the particles involved. The dependence of the physical couplings on the overall momentum scale is governed by the Gell-Mann-Low equations [38], which have different physical meaning as the WRGEs and have different  $\beta$ -functions [39, 40] beyond one loop. Going from the effective Lagrangian in the Wilsonian approach to the classical effective action  $\Gamma$  means to integrate out all of the degrees of freedom down to zero momentum, that will generate non-holomorphic corrections.  $\Gamma$  is often interpreted as a sort of effective Lagrangian, but in general it does not have the form of a supersymmetric Lagrangian with holomorphic coefficients.

The connection between the Wilsonian gauge coupling  $\alpha_W$  and a physical gauge coupling  $\alpha_{ph}$  was derived in the so called Novikov-Shifman-Vainshtein-Zakharov renormalization scheme (NSVZ) [35]. This scheme requires a manifestly supersymmetric regularization procedure. In addition, the definition of the physical couplings is close to that in the momentum subtraction



scheme (MOM). The conversion relation reads

$$\frac{\pi}{\alpha_W(\mu)} = \frac{\pi}{\alpha_{ph}(\mu)} + T(R) \ln Z(\mu), \quad (2.7)$$

where  $Z(\mu)$  is the renormalization constant of the matter superfield and the coefficient  $T(R)$  is the Dynkin index of the representation  $R$  of the matter superfield. The factor  $Z(\mu)$  is related to the mass renormalization constants of the matter superfield through the non-renormalization theorems, provided SUSY is preserved. However, in general the  $Z$  factors are not restricted by any holomorphic constraints and thus are not known analytically. They have to be computed order-by-order in perturbation theory. Combining Eqs. (2.7) and (2.5) we get

$$\frac{\pi}{\alpha_{ph}(\mu)} = \frac{\pi}{\alpha_{ph}(\Lambda)} - T(R) \ln \left( \frac{Z(\mu)}{Z(\Lambda)} \right) - 2b_0 \ln \frac{\Lambda}{\mu}. \quad (2.8)$$

Using Eq.(2.6) we obtain for the beta function of the physical coupling in the NSVZ scheme the following relation:

$$\beta_{\text{SQED}}^{\text{NSVZ}}(\alpha_{ph}) = \left( \frac{\alpha_{ph}}{\pi} \right)^2 \frac{1}{2} T(R) (1 - \gamma), \quad (2.9)$$

where we have specified the value of the coefficient  $b_0$  for the SQED case and the superfield anomalous dimension is defined through

$$\gamma = -\mu \frac{d \ln Z(\mu)}{d\mu}. \quad (2.10)$$

Because Eq.(2.5) is exact at all orders, also the relation between the beta-function of  $\alpha_{ph}$  and the anomalous dimension of the matter superfields  $\gamma$  is valid at all orders. Let us remark however, that this relation holds only in the NSVZ scheme. Unfortunately, it is highly non trivial to fulfill the requirements of the NSVZ scheme in practice.

In supersymmetric non-abelian models with several matter supermultiplets, Eq. (2.7) becomes

$$\frac{\pi}{\alpha_W(\mu)} = \frac{\pi}{\alpha_{ph}(\mu)} + \frac{1}{2} C(G) \ln \alpha_{ph}(\mu) + \sum_i T(R_i) \ln Z_i(\mu), \quad (2.11)$$

where  $C(G)$  is the quadratic Casimir operator of the adjoint representation and  $T(R_i)$  is the Dynkin index of the representation  $R_i$  of the matter field  $i$ . The second term stands for the gaugino contribution, while the third one for contributions generated by the matter superfields. A simple calculation provides us with the exact relation between the gauge beta function and the anomalous dimension of the matter superfields

$$\beta^{\text{NSVZ}} = - \left( \frac{\alpha_{ph}}{2\pi} \right)^2 \frac{3C(G) - 2 \sum_i T(R_i) (1 - \gamma_i)}{1 - C(G) \alpha_{ph} / (2\pi)}. \quad (2.12)$$

From Eq. (2.12) it is easy to see that for the derivation of the  $L$ -loop beta functions in the NSVZ scheme one needs the matter anomalous dimensions  $\gamma_i$  at the  $(L - 1)$ -loop order. As will be shown below this feature was intensively exploited in the literature.

In the case of SUSY-Yang-Mills theories the matter superfields are absent, so  $T(R_i) = 0$ , and an exact formula for the gauge coupling beta function can be derived

$$\beta^{NSVZ} = - \left( \frac{\alpha_{ph}}{2\pi} \right)^2 \frac{3C(G)}{1 - C(G) \alpha_{ph}/(2\pi)}. \quad (2.13)$$

Similar relations can also be derived for models with softly-broken SUSY. The line of reasoning is as follows: The powerful supergraph method is also applicable for models with softly-broken SUSY by using the “spurion” external field method [15, 41]. Perhaps, one of the most prominent example is the relation that can be established between the gaugino mass  $m_{\tilde{g}}$  and the gauge beta function. In the presence of the SUSY-breaking gaugino mass term, the coefficient of the gauge kinetic term in the Wilsonian action becomes

$$\left( \frac{1}{g^2} \right)_W \rightarrow \left( \frac{1 - 2m_{\tilde{g}}^2 \theta^2}{g^2} \right)_W, \quad \text{where } \theta \text{ is the Grassman variable.} \quad (2.14)$$

Using the same arguments based on holomorphy, it was shown [42, 43] that a renormalization group invariant (RGI) relation for the gaugino mass can be derived within NSVZ scheme

$$\frac{m_{\tilde{g}} \alpha}{\beta(\alpha)} = \text{RGI}. \quad (2.15)$$

Moreover, it was shown with the help of the spurion formalism that the renormalization constants of softly broken SUSY gauge theory can be related to the renormalization constants of the underlying exact supersymmetric model [44–46]. Even more, the connecting formulas are valid at all orders in perturbation theory. The only necessary assumption for their derivation is the existence of a gauge and SUSY invariant regularization scheme. Thus, such relations are valid only in NSVZ-like regularization schemes.

At this point, a few remarks are in order to comment on the results discussed above. The authors of Ref. [47] state that in  $d = 4$  dimensions the only known regularization to conserve SUSY is the Pauli-Villars scheme for matter superfields and the higher derivative scheme for the gauge superfields. Technically this construction is rather complicated and hardly applicable to multi-loop computations. In Ref. [41], an attempt was made to apply the “supersymmetric dimensional regularization” or “regularization by dimensional reduction” (DRED) [48] within the supergraph formalism. However, as pointed out by Siegel himself [49], this scheme is mathematically inconsistent in its original formulation and a consistent formulation will break supersymmetry in higher orders of perturbation theory. A similar situation occurs also for the application of DRED in component field formalism [50, 51]<sup>2</sup>. Thus, the exact formulas of the NSVZ scheme are not valid, in general, for calculations based on DRED since they do not involve a regularization scheme supersymmetric at all orders. For particle phenomenology, it means that the powerful predictions of Eqs. (2.12) cannot be tested through experiments, since the beta functions are scheme dependent beyond two loops.

The breakthrough regarding this situation was obtained in Refs. [52–56], where it is stated that, if the NSVZ scheme exists it can be perturbatively related to schemes based on DRED. Such

---

<sup>2</sup>A detailed analysis of this issue will be done in the next section.

arguments follow from the equivalence of different renormalization schemes in perturbation theory [57]. Precisely, the computation of the three-loop mass anomalous dimension for the chiral matter superfield in a general non-abelian supersymmetric theory and of the three-loop gauge beta function in the abelian case allowed the derivation of the three- and four-loop gauge beta function for a general supersymmetric theory. Remarkably enough, the derivation (up to a numerical coefficient) of the four-loop gauge beta function was based on a three-loop calculation and theoretical considerations about special relations valid in  $N = 2$  supersymmetric theories and one-loop finite supersymmetric theories.

Let us mention at this point also the calculation of the three-loop gauge beta function for supersymmetric Yang-Mills (SYM) theories of Ref. [58]. For this calculation, DRED was employed in component field formalism rather than superfield formalism, and hence a manifestly not supersymmetric gauge was used. The computations of Refs [55,56] and [58] coincide as a consequence of gauge invariance of the gauge beta function.

Moreover, the authors of Refs. [52,53] noticed that the differential operators relating the beta functions for soft SUSY breaking parameters to the beta functions of the gauge and Yukawa couplings are form invariant under change of scheme (*i.e.* from NSVZ to DRED scheme). Thus, similar relations for the soft SUSY breaking parameter valid to all orders of perturbation theory hold also in a DRED like scheme<sup>3</sup>.

In the next section we will discuss in detail the application of DRED in component field formalism and give some example of important calculations that can be done within this approach. Nevertheless, already now we want to mention the coincidence of all results obtained with DRED in component field formalism and those derived via DRED in supergraphs formalism.

### 3 Dimensional reduction in the component field formalism

The precision of many present or forthcoming experiments in particle physics requires inevitably higher order perturbative calculations in the SM or its extensions like the Minimal Supersymmetric Standard Model (MSSM). Regularization of the divergent loop diagrams arising in the higher order calculations is commonly performed employing Dimensional Regularization (DREG) or its variants, due to its nice feature to respect gauge invariance. Higher order calculations within the SM predominantly use DREG in its original form [59,60], while for calculations within supersymmetric theories DRED as defined in Ref. [48] is commonly employed. It is not *a priori* known whether SUSY as a symmetry of a given Lagrangian is still a symmetry of the full quantum theory in any particular case. Nevertheless, a detailed formal renormalization program has been pursued in Ref. [61] including a proof that SUSY is not anomalous. If the regularized theory does not respect SUSY, the finite amplitude will not satisfy the Ward identities required by SUSY, giving rise to an apparent anomaly. If SUSY is not anomalous, it is possible to restore the invariance by introducing finite counter-terms.

In practice, the choice of regularization scheme is of considerable significance for the extraction of physical predictions. This is the case for the NSVZ scheme we alluded in the previous section, that rarely found direct practical applicability. It rather provides important checks for results

---

<sup>3</sup> Actually, the scheme proposed by the authors of Refs. [52,53] is the so called DRED', for which beta functions of SUSY-breaking parameters do not depend on the unphysical  $\epsilon$ -scalar mass parameter. For more details about the DRED' scheme see section 3.

predicted within DRED. In this section we discuss in detail the application of DRED in the component field formalism and its application to practical calculations.

### 3.1 Framework

DRED consists of continuing the number of space dimensions from 4 to  $d$ , where  $d$  is less than 4, but keeping the dimension of all the fields fixed. In component field language, this means that the vector bosons and fermions preserve their four-dimensional character. Furthermore, it is assumed that all fields depend on  $d$  rather than 4 space-time coordinates, so that the derivatives  $\partial_\mu$  and momenta  $p_\mu$  become  $d$ -dimensional. It is the four-dimensional nature of the fields that is supposed to restore the supersymmetric Ward-Takahashi [62] or Slavnov-Taylor [63] identities, while the  $d$ -dimensional space-time coordinates cures, as in DREG, the singularities of the loop integrals.

However, potential inconsistencies of DRED, arising from the use of purely four-dimensional relations between the Levi-Civita tensor and the metric tensor, have been pointed out by Siegel himself [49]. Even more, inconsistencies of DRED arising without the direct use of Levi-Civita tensors have been revealed in Ref. [51]. The authors have correlated them with the impossibility of decomposing the finite four-dimensional space into a direct sum of infinite-dimensional spaces. The solution proposed by the same authors is to introduce a formal space, called quasi-four-dimensional space ( $Q_4$ ), with “non-integer valued” vector and spinor indices (thus, the two types of indices range over an infinite set of values), obeying certain algebraic identities inspired from the properties of the four-dimensional Minkowski space. The existence of such a space was demonstrated by construction [64] starting from similar arguments as those used to prove the existence of the formal  $d$ -dimensional space of DREG [65]. In this way the consistency of the calculation rules is guaranteed. By construction,  $Q_4$  is represented as the direct sum of two infinite-dimensional spaces:  $Q_d$  which is formally  $d$ -dimensional and is identical with the one of DREG and  $Q_{2\epsilon}$  which is formally  $2\epsilon = 4 - d$ -dimensional<sup>4</sup>

$$Q_4 = Q_d \oplus Q_{2\epsilon}. \quad (3.1)$$

According to the properties of the three formal spaces at hand  $Q_4$ ,  $Q_d$ ,  $Q_{2\epsilon}$  one can derive the following relations for the corresponding metric tensors  $g^{\mu\nu}$ ,  $\hat{g}^{\mu\nu}$ ,  $\bar{g}^{\mu\nu}$  [50, 64]:

$$\begin{aligned} g^{\mu\nu} &= \hat{g}^{\mu\nu} + \bar{g}^{\mu\nu}, & g^{\mu\mu} &= 4, & \hat{g}^{\mu\mu} &= d, & \bar{g}^{\mu\mu} &= 2\epsilon, \\ g^{\mu\nu} \hat{g}_\nu{}^\rho &= \hat{g}^{\mu\rho}, & g^{\mu\nu} \bar{g}_\nu{}^\rho &= \bar{g}^{\mu\rho}, & \hat{g}^{\mu\nu} \bar{g}_\nu{}^\rho &= 0. \end{aligned} \quad (3.2)$$

Furthermore, any quasi-four dimensional vector can be decomposed with the help of the projectors  $\hat{g}^{\mu\nu}$ ,  $\bar{g}^{\mu\nu}$

$$t^\mu = \hat{t}^\mu + \bar{t}^\mu, \quad \hat{t}^\mu = \hat{g}^{\mu\nu} t_\nu, \quad \bar{t}^\mu = \bar{g}^{\mu\nu} t_\nu. \quad (3.3)$$

Imposing the Dirac algebra for the  $\gamma$ -matrices defined in  $Q_4$

$$\{\gamma^\mu, \gamma^\nu\} = 2g^{\mu\nu} \mathbf{1}, \quad (3.4)$$

---

<sup>4</sup>One needs to perform twice the construction of  $n$ -dimensional integrals and metric tensors for  $n = d$  and  $n = 2\epsilon$ . The  $d$ -dimensional integral is the momentum integral in DRED, while  $2\epsilon$  integral is involved only in the definition of the  $2\epsilon$ -dimensional metric tensor.

we can derive similar commutation relations for the components in  $Q_d$  and  $Q_{2\epsilon}$

$$\{\hat{\gamma}^\mu, \hat{\gamma}^\nu\} = 2\hat{g}^{\mu\nu}\mathbf{1}, \quad \{\bar{\gamma}^\mu, \bar{\gamma}^\nu\} = 2\bar{g}^{\mu\nu}\mathbf{1}, \quad \{\bar{\gamma}^\mu, \hat{\gamma}^\nu\} = 0. \quad (3.5)$$

These relations together with the trace condition

$$\text{Tr}\mathbf{1} = 4 \quad (3.6)$$

are sufficient for computing Feynman diagrams. Eq. (3.6) is particularly useful in supersymmetric theories, because it ensures that the numbers of degrees of freedom for fermions and bosons is equal.

For practical computations, it is useful to note that the fermion traces that contain both types of  $\gamma$ -matrices can be factored out as follows

$$\text{Tr}(\hat{\gamma}^{\mu_1} \dots \hat{\gamma}^{\mu_n} \bar{\gamma}^{\nu_1} \dots \bar{\gamma}^{\nu_l}) = \frac{1}{4} \text{Tr}(\hat{\gamma}^{\mu_1} \dots \hat{\gamma}^{\mu_n}) \text{Tr}(\bar{\gamma}^{\nu_1} \dots \bar{\gamma}^{\nu_l}). \quad (3.7)$$

This relation can be derived from Eqs. (3.6) and (3.5) and the algebra of Dirac matrices in  $d$  dimensions. Thus, the Dirac algebra can be performed separately in  $d$  and in  $4 - d = 2\epsilon$  dimensions.

Once we introduced “non-integer valued” spinor indices, we need infinite-dimensional  $\gamma$ -matrices to represent the Dirac algebra. Thus, the Fierz identities valid in the genuine four-dimensional space do not hold anymore in  $Q_4$ . Their use was identified with one of the sources of DRED inconsistencies. Moreover, within  $Q_4$  the invariance of the original Lagrangian under SUSY transformations might be broken. This feature can be directly correlated with the lack of Fierz identities that would ensure the cancellation of Lagrangian variation under SUSY transformations in the genuine four-dimensional space. However, it has been shown [51, 64] that such inconsistencies become active only in the higher orders of perturbation theory, when, for example, traces over at least ten  $\gamma$ -matrices and anti-symmetrization over five indices are involved. Thus, DRED also breaks SUSY, but starting from higher orders of perturbation theory. This explains, why one- and even two-loop calculations of QCD corrections within DRED [66–70] based on genuine four-dimensional Dirac algebra and even Fierz rearrangement provided correct results. Even the supersymmetric character of DRED at low orders has been exploited in the context of QCD with massless quarks in Ref [68]. However, beyond the one-loop level the distinction between  $g^{\mu\nu}$  resulting from contractions of the quasi-four-dimensional vector fields and  $\hat{g}^{\mu\nu}$  resulting from momentum integrals is difficult to follow. It turned out [71] that for higher order computations it is useful to decompose the quasi-four-dimensional vector fields according to Eq. (3.3). As we shall see in the next section, in the case of gauge theories the  $d$ -dimensional components behave as vectors under the gauge transformations whereas the  $2\epsilon$  components as scalars, usually called  $\epsilon$ -scalars.

Representing the underlying space of DRED  $Q_4$  as a formal infinite-dimensional space renders the extension of  $\gamma_5$  as subtle as in DREG. The consistent procedure proposed by 't Hooft-Veltman (HV) [60] for defining  $\gamma_5$  as in four dimensions  $\bar{\gamma}_5 = i\gamma^0\gamma^1\gamma^2\gamma^3$  has in the context of SUSY theories two drawbacks. On the one hand, it is the fact that the mathematically consistent treatment of  $\gamma_5$  in DREG requires  $d > 4$ , whereas for DRED  $d < 4$  is needed. However, it has been shown up to two-loops [72, 73] that the Adler-Bardeen theorem [74] could still be satisfied in DRED with HV scheme, if relations like

$$\hat{\gamma}^i \bar{\gamma}_5 \hat{\gamma}_i = (d - 8) \bar{\gamma}_5, \quad (3.8)$$

which follow in  $d > 4$  are assumed to hold also for  $d < 4$ . On the other hand, the use of a not anti-commuting  $\gamma_5$  leads to the breakdown of symmetries, *e.g.* chiral symmetry of the SM or supersymmetry in case of the MSSM already at the one-loop level. These “spurious anomalies” would spoil the renormalizability and they have to be cured by introducing appropriate counter-terms to restore Ward-Takahashi and Slavnov-Taylor identities order by order in perturbation theory (see Ref [75]). This approach was successfully applied for SM predictions within DREG up to three-loops [76, 77]. However, for the MSSM it becomes much more involved due to the complexity introduced by supersymmetric conditions and it rarely has been employed in practice [73].

The implementation of  $\gamma_5$  in DRED commonly used in practice is inspired by the naive scheme (NS) of DREG. Namely, it is treated rather like a formal object which is not well-defined mathematically but anti-commutes with all  $\gamma$ -matrices

$$\{\hat{\gamma}^\mu, \tilde{\gamma}_5\} = \{\hat{\gamma}^\mu, \tilde{\gamma}_5\} = 0, \quad \text{and} \quad (\tilde{\gamma}_5)^2 = \mathbf{1}. \quad (3.9)$$

Nevertheless, one has to correct the false result that arises from Eqs. (3.9), that the trace of  $\gamma_5$  and four or more  $\gamma$ -matrices vanishes. Paying attention that now two types of  $\gamma$ -matrices occur, the additional constraints read

$$\text{Tr}(\Gamma^\alpha \Gamma^\beta \Gamma^\gamma \Gamma^\delta \tilde{\gamma}_5) = 4i \tilde{\varepsilon}^{\alpha\beta\gamma\delta} + \mathcal{O}(\epsilon), \quad \text{with} \quad \Gamma^\mu = \hat{\gamma}^\mu \text{ or } \bar{\gamma}^\mu. \quad (3.10)$$

The tensor  $\tilde{\varepsilon}^{\alpha\beta\gamma\delta}$  has some similarities with the four-dimensional Levi-Civita tensor: i) it is completely antisymmetric in all indices; ii) when contracted with a second one of its kind gives the following result

$$\tilde{\varepsilon}^{\alpha\beta\gamma\delta} \tilde{\varepsilon}_{\alpha'\beta'\gamma'\delta'} = G_{[\alpha'}^{[\alpha} G_{\beta']}^{\beta} G_{\gamma'}^{\gamma} G_{\delta']}^{\delta]}, \quad G^{\mu\nu} = \hat{g}^{\mu\nu} \text{ or } \bar{g}^{\mu\nu}, \quad (3.11)$$

depending on the nature of Dirac matrices  $\Gamma^\mu$  in Eq. (3.10). Here the square brackets denote complete anti-symmetrization. When taking the limit  $d \rightarrow 4$ ,  $\tilde{\varepsilon}^{\alpha\beta\gamma\delta}$  converts into the four-dimensional Levi-Civita tensor and Eqs. (3.10) and (3.11) ensure that the correct four-dimensional results are reproduced. This last constraint is needed in order to correctly compute fermion triangle diagrams containing an axial vector current, *i.e.* to cope with the Adler-Bardeen-Jackiw anomaly [78].

At this point a comment on Eqs. (3.10) is in order. When we combine it with the cyclic property of traces, it necessary follows that other traces are not well defined in  $d \neq 4$  dimensions. It turns out that there is an unavoidable ambiguity of order  $\mathcal{O}(d - 4)$  when fixing the trace condition in Eq. (3.10). Even if one does not use the cyclic property of the trace, an ambiguity in the distribution of the anomaly between the vector and the axial vector currents shows up [72]. The occurrence of the ambiguity is a characteristic of the extension of  $\gamma_5$  away from  $d = 4$  dimensions. 't Hooft and Veltman have pointed out in their original paper [60] that an ambiguity related to the location of  $\gamma_5$  shows up in HV scheme, too.

The use of an anti-commuting  $\gamma_5$  in  $d \neq 4$  dimensions was applied for the first time to the evaluation of fermion traces with an even number of  $\gamma_5$ 's in Ref. [79], and a few years later extended also to odd  $\gamma_5$  fermion traces in Ref. [80]. The method<sup>5</sup> proved to be effective for SM

---

<sup>5</sup>For more details see [81] and references cited therein.

calculations involving chiral fermions up to two-loop order [82, 83]. The consistency of this  $\gamma_5$  prescription has been verified even in three-loop QCD-electroweak calculations [84, 85]. Within DRED, it has been successfully employed in MSSM calculations at the two- and three-loop order [86–88]. However, let us mention at this point that, for these calculations at most the finite parts of two-loop and the divergent parts of three-loop diagrams are required. For the calculation of finite parts of three-loop diagrams containing two fermion triangle sub-diagrams, the HV scheme has to be applied as the naive scheme does not provide correct results.

Through the consistent formulation of DRED we gain a regularization scheme which proves to be supersymmetric only in the lower orders of perturbation theory. Due to the violation of Fierz identities, SUSY invariance will be broken at higher orders. The first consequence of SUSY breaking is that the all order relations between different anomalous dimension valid in the NSVZ scheme do not hold in DRED. However, although DRED consistently formulated is not a supersymmetric scheme at all orders, it provides so far the best option for computations within SUSY theories.

### 3.2 Minimal Subtraction Schemes $\overline{\text{MS}}$ and $\overline{\text{DR}}$

The common renormalization schemes used for multi-loop calculations are the minimal subtraction (MS), momentum subtraction and on-shell schemes. Minimal subtraction scheme has the advantage of involving the simplest computations, but it is non-physical in the sense that it does not take into account mass threshold effects for heavy particles. Nevertheless, it is the main scheme used in renormalization group (RG) analyses relating the predictions of a given theory at different energy scales. The other two options are computationally much more involved but indispensable for the determination of the parameters of a theory from the quantities measured experimentally. We focus in this section on the minimal subtraction methods.

Minimal subtraction scheme with DREG as regulator [89] or the modified  $\overline{\text{MS}}$  scheme [90] and its variant for DRED — the  $\overline{\text{DR}}$  scheme — are in particular well suited for higher order calculations in perturbation theory. The advantage of these schemes is that all ultra-violet (UV) counter-terms are polynomial both in external momenta and masses [91]. This allows to set to zero certain masses or external momenta, provided no spurious infrared divergences are introduced. This simplifies substantially the calculations of the Feynman integrals. It has been shown [92] by means of the infrared rearrangement (IRR) procedure [92–94] that the renormalization constants within the  $\overline{\text{MS}}$  scheme can be reduced to the calculation of only massless propagator diagrams. This method was used for the first three-loop calculation of the QCD  $\beta$ -function [95], applying it to each individual diagram. But the most effective approach is its use in combination with multiplicative renormalization. This amounts in general to solve recursively the equation

$$Z_a = 1 - K_\epsilon[\Gamma_a(p^2)Z_a], \quad (3.12)$$

where  $K_\epsilon[f(\epsilon)]$  stands for the singular part of the Laurent expansion of  $f(\epsilon)$  in  $\epsilon$  around  $\epsilon = 0$ .  $\Gamma_a(p^2)$  denotes the renormalized Green function with only one external momentum  $p^2$  kept non-zero.  $Z_a$  denotes the renormalization constant associated with the Green function  $\Gamma_a$ . In this case, the renormalization of  $\Gamma_a$  through  $(l + 1)$ -loop order requires the renormalization of the Lagrangian parameters like couplings, masses, gauge parameters, mixing angles, etc. up to  $l$ -loop order. The method was successfully applied to the three-loop calculations of anomalous

dimensions within  $\overline{\text{MS}}$  or  $\overline{\text{DR}}$  schemes [76, 87, 88, 96–99] using the package MINCER [100] written in FORM [101], which computes analytically massless propagator diagrams up to three loops.

Apart from that, a second method was proposed in Ref. [102], which has been used for the calculation of the three- and even four-loop anomalous dimensions of QCD [103–106] and the beta-function of the quartic coupling of the Higgs boson in the SM [98, 107, 108]. It deals with the IRR by introducing an artificial mass for all propagators. Expanding in all particles masses and external momenta, one can reduce the evaluation of the Feynman integrals to massive tadpoles. The analytic evaluation of the massive tadpoles up to three-loop order can be obtained with the help of the package MATAD [109].

A third method was introduced for the evaluation of the renormalization constants for the quark mass [103] and the vector [110] and quark scalar current correlators [111] through four-loops. It is based on global IRR properties and amounts essentially to set to zero the external momentum and let an arbitrary subset of the internal lines to be massive. After non trivial manipulations, the four-loop integrals can be reduced to three-loop massless two-point integrals and one-loop massive vacuum integrals.

The three-loop accuracy for the anomalous dimensions of theories involving not only vector but also Yukawa and quartic scalar interactions (for example the SM [98, 99]) was achieved only very recently. Remarkably, for supersymmetric and softly broken supersymmetric theories like the MSSM the three-loop anomalous dimensions were computed long before [54, 55, 112]. Their derivations used intensively the exact relations established between the various anomalous dimensions in the NSVZ scheme<sup>6</sup> as well as the observation that the NSVZ scheme and DRED can be perturbatively connected.

### 3.3 DRED applied to non-supersymmetric theories

Although DRED was originally proposed as a candidate for an invariant regularization in supersymmetric theories, it proved to be useful also in non-supersymmetric theories. Its use in SM calculations up to three-loop orders was motivated either by the possibility to apply four-dimensional algebra and even Fierz rearrangements [67, 70]<sup>7</sup>, or by the possibility to easily convert a non-supersymmetric gauge theory into a SUSY-Yang-Mills theory and use non-trivial Ward identities as checks of complicated calculations [68, 84, 113]. Apart from the computational advantages, DRED applied to non-supersymmetric theories, in particular to QCD, provides us with a powerful tool to verify its consistency up to three-loop order via the connection that can be established with DREG<sup>8</sup>. Finally, it is motivated by the MSSM, as a softly broken supersymmetric theory, or by various models derived from the MSSM which feature lower symmetries (for example, the intermediate energy theory obtained by integrating out the squarks and sleptons). DRED applied to effective field theories, such that QCD extended to include the Higgs-top Yukawa coupling, was useful for the calculation of the production rate for the Higgs boson in gluon fusion channel within MSSM [114, 115].

In the following, we consider a non-abelian gauge theory with  $n_f$  Dirac fermions  $\psi_f$  transforming according to a representation  $R$  of the gauge group  $\mathcal{G}$ . For the moment we do not take into

---

<sup>6</sup>For more details see section 2

<sup>7</sup>The mathematical inconsistencies alluded to above do not occur at the two-loop level in this calculations.

<sup>8</sup>DRED and DREG are also perturbatively connected.



account any genuine scalar field.

The Lagrangian density (in terms of bare fields) reads

$$\mathcal{L}_B = -\frac{1}{4}F_{\mu\nu}^2 - \frac{1}{2(1-\xi)}(\partial^\mu W_\mu^a)^2 + \partial^\mu \bar{c}^a(\partial_\mu c^a - g f^{abc} c^b W_\mu^c) + i \sum_{f=1}^{n_f} \bar{\psi}_f \not{D} \psi_f \quad (3.13)$$

where the field strength tensor is defined through

$$F_{\mu\nu}^a = \partial_\mu W_\nu^a - \partial_\nu W_\mu^a + g f^{abc} W_\mu^b W_\nu^c \quad (3.14)$$

and

$$D_\mu = \partial_\mu - ig(R^a)W_\mu^a \quad (3.15)$$

is the covariant derivative.  $W_\mu$  is the gauge field,  $c^a$  is the Fadeev-Popov-ghost field,  $f^{abc}$  are the structure constants of the gauge group  $\mathcal{G}$ ,  $\xi$  is the gauge parameter and  $g$  is the gauge coupling.

For the case when the theory admits a gauge invariant fermion mass term we will have  $L_B \rightarrow L_B + L_B^m$ , where

$$L_B^m = -m_f \bar{\psi}_f \psi_f. \quad (3.16)$$

DRED amounts to imposing that all field variables depend only on a subset of the total number of space-time dimensions; in this case  $d$  out of 4 where  $d = 4 - 2\epsilon$ . We can then make the decomposition

$$W_\mu^a(x^j) = \hat{W}_\mu^a(x^j) + \bar{W}_\mu^a(x^j) \quad (3.17)$$

where

$$\hat{W}_\mu^a = \hat{g}_{\mu\nu} W^{\nu,a} \quad \bar{W}_\mu^a = \bar{g}_{\mu\nu} W^{\nu,a} \quad \text{and} \quad \hat{g}_{\mu\mu} = d. \quad (3.18)$$

It is then easy to show that [116]

$$L_B = L_B^d + L_B^\epsilon \quad (3.19)$$

where

$$L_B^d = -\frac{1}{4}\hat{F}_{\mu\nu}^2 - \frac{1}{2(1-\xi)}(\partial^\mu \hat{W}_\mu)^2 + \partial^\mu \bar{c}^a(\partial_\mu c^a - g f^{abc} c^b \hat{W}_\mu^c) + \sum_{f=1}^{n_f} i \bar{\psi}_f \hat{\gamma}^\mu \hat{D}_\mu \psi_f \quad (3.20)$$

and

$$L_B^\epsilon = \frac{1}{2}(\hat{D}_\mu \bar{W}_\nu)^2 - \sum_{f=1}^{n_f} g \bar{\psi}_f \bar{\gamma}^\mu R^a \psi_f \bar{W}_\mu^a - \frac{1}{4}g^2 f^{abc} f^{ade} \bar{W}_\mu^b \bar{W}_\nu^c \bar{W}^{d,\mu} \bar{W}^{e,\nu}. \quad (3.21)$$

$\hat{F}_{\mu\nu}$  and  $\hat{D}_\mu$  denote the projection of the field strength and covariant derivative given in Eqs. (3.14) and (3.15) onto  $Q_d$ , obtained with the help of the operator  $\hat{g}^{\mu\nu}$ . Conventional dimensional regularization (DREG) amounts to using Eq. (3.20) and discarding Eq. (3.21).

Note that under the gauge transformations:

$$\delta \hat{W}_\mu^a = \partial_\mu \Lambda^a + g f^{abc} \hat{W}_\mu^b \Lambda^c, \quad (3.22a)$$

$$\delta \bar{W}_\mu^a = g f^{abc} \bar{W}_\mu^b \Lambda^c, \quad (3.22b)$$

$$\delta \psi^\alpha = ig(R^a)^{\alpha\beta} \psi^\beta \Lambda^a \quad (3.22c)$$

each term in Eq. (3.21) is separately invariant. The  $\bar{W}_\mu$  fields behave exactly like scalar fields, and are hence known as  $\varepsilon$  scalars. There is therefore no reason to expect the  $\bar{\psi}\psi\bar{W}$  vertex to renormalize in the same way as the  $\bar{\psi}\psi\hat{W}$  vertex (except in the case of supersymmetric theories). The couplings associated with the  $\bar{\psi}\psi\bar{W}$  vertex or with the quartic  $\varepsilon$ -scalar interaction are called *evanescent couplings*. They were first described in Ref. [117], and later independently discovered by van Damme and 't Hooft [118]. The vertices  $\hat{W}\bar{W}\bar{W}$  and  $\hat{W}\hat{W}\bar{W}\bar{W}$ , on the other hand, are renormalized in the same way as  $\hat{W}\hat{W}\hat{W}$ ,  $\bar{C}C\hat{W}$ , etc. because of the gauge invariance [119]. Thus we can conclude that  $\hat{W}$  is the gauge particle, while  $\bar{W}$  acts as matter field transforming according to the adjoint representation. In order to avoid confusion, we denote in the following the gauge particles with  $G_\mu^a$  and the  $\varepsilon$  scalars with  $\varepsilon_\mu^a$

$$\hat{W}_\mu^a \rightarrow G_\mu^a \quad \bar{W}_\mu^a \rightarrow \varepsilon_\mu^a. \quad (3.23)$$

Since  $\varepsilon$  scalars are present only on internal lines we could, in fact, choose the wave function renormalization of  $\varepsilon_\mu$  and  $G_\mu$  to be the same. However, such a renormalization prescription will break unitarity [118]. The crucial point is the correct renormalization of sub-divergences, which requires that vertices involving  $\varepsilon$  scalars renormalize in a different way as their gauge counterparts. Thus, to renormalize the  $\varepsilon$  scalars one has to treat them as new fields present in the theory.

For the renormalization of the theory we distinguish two new types of couplings: a Yukawa like coupling  $g_e$  associated with the vertex  $\bar{\psi}\psi\varepsilon$  and a set of  $p$  quartic couplings  $\lambda_r$  associated with vertices containing four  $\varepsilon$  scalars. The number  $p$  is given by the number of independent rank four tensors  $H^{abcd}$  which are non-vanishing when symmetrized with respect to  $(ab)$  and  $(cd)$  interchange. We address the issue of the quartic vertex renormalization in more detail in the next section.

The renormalization constants for the couplings, masses as well as fields and vertices are defined as

$$\begin{aligned} g^0 &= \mu^\varepsilon Z_g g, & g_e^0 &= \mu^\varepsilon Z_e g_e, & \sqrt{\lambda_r^0} &= \mu^\varepsilon Z_{\lambda_r} \sqrt{\lambda_r}, \\ 1 - \xi^0 &= (1 - \xi) Z_3, & m_f^0 &= m_f Z_{m_f}, & m_\varepsilon^0 &= m_\varepsilon Z_m^\varepsilon, \\ \psi^0 &= \sqrt{Z_2} \psi, & G_\mu^{0,a} &= \sqrt{Z_3} G_\mu^a, & \varepsilon_\mu^{0,a} &= \sqrt{Z_3^\varepsilon} \varepsilon_\mu^a, \\ c^{0,a} &= \sqrt{\tilde{Z}_3} c^a, & \Gamma_{\bar{\psi}\psi G}^0 &= Z_1 \Gamma_{\bar{\psi}\psi G}, & \Gamma_{\bar{\psi}\psi \varepsilon}^0 &= Z_1^\varepsilon \Gamma_{\bar{\psi}\psi \varepsilon}, \\ \Gamma_{\bar{c}c G}^0 &= \tilde{Z}_1 \Gamma_{\bar{c}c G}, & \Gamma_{\varepsilon\varepsilon G}^0 &= Z_1^{\varepsilon\varepsilon G} \Gamma_{\varepsilon\varepsilon G}, & \Gamma_{\varepsilon\varepsilon GG}^0 &= Z_1^{\varepsilon\varepsilon GG} \Gamma_{\varepsilon\varepsilon GG}, \\ \Gamma_{GGGG}^0 &= Z_1^{4G} \Gamma_{GGGG}, & \Gamma_{\varepsilon\varepsilon\varepsilon\varepsilon}^0 &= Z_1^{4\varepsilon} \Gamma_{\varepsilon\varepsilon\varepsilon\varepsilon}, \end{aligned} \quad (3.24)$$

where  $\mu$  is the renormalization scale and the bare quantities are marked by the superscript “0”.  $\Gamma_{xyz}(w)$  stands for one-particle irreducible Green functions involving the external particles  $x, y, z, (w)$ . Eq. (3.20) takes under renormalization the usual expression in terms of renormalized parameters as in DREG scheme. The renormalized Lagrangians  $L^\varepsilon$  is the new term that distinguishes DRED from DREG and it is given by

$$\begin{aligned} L^\varepsilon &= \frac{1}{2} Z^{\varepsilon\varepsilon} (\partial_\mu \varepsilon_\nu^a)^2 + Z^{\varepsilon\varepsilon G} g f^{abc} \partial_\mu \varepsilon_\nu^a G^{b,\mu} \varepsilon^{c,\nu} + Z^{\varepsilon\varepsilon GG} g^2 f^{abc} f^{ade} G_\mu^b \varepsilon_\nu^c G^{d,\mu} \varepsilon^{e,\nu} \\ &- Z^{\psi\psi\varepsilon} g_e \bar{\psi} R^a \gamma^\mu \psi \varepsilon_\mu^a - \frac{1}{4} \sum_{r=1}^p Z_{\lambda_r} \lambda_r H_r^{abcd} \varepsilon_\mu^a \varepsilon_\nu^c \varepsilon^{b,\mu} \varepsilon^{d,\nu}. \end{aligned} \quad (3.25)$$

Strictly speaking, Eq. (3.25) should also have a mass term for the  $\varepsilon$  scalars; but since this mass term does not affect renormalization of the couplings and fermion masses we omit it here. We discuss this issue in more detail in section 3.3.5.

The charge renormalization constants are obtained from the Slavnov-Taylor identities. For example, if one computes the  $N$ -point Green function with external fields  $\phi_1, \dots, \phi_n$  and denote its coupling constant by  $g$ , one obtains

$$Z_g = \frac{Z_{\phi_1 \dots \phi_N}}{\sqrt{Z_{\phi_1} \dots Z_{\phi_N}}}, \quad (3.26)$$

where the  $Z_{\phi_i}$  are the wave function renormalization constants for the  $\phi_i$ ,  $Z_{\phi_1 \dots \phi_N}$  is the corresponding vertex renormalization constant, and  $Z_g$  the charge renormalization. Within the minimal subtraction scheme, one is free to choose any masses and external momenta, as long as infra-red divergences are avoided. One can set all masses to zero, as well as one of the two independent external momenta in three-point functions. In this case, one arrives at three-loop integrals with one non-vanishing external momentum  $q$  which can be calculated with the help of MINCER. One can also calculate the three-point functions setting a common mass  $m$  to all particles and expanding the Feynman integrals in the limit  $m^2/q^2 \ll 1$  with the help of asymptotic expansions [102]. This approach is much more tedious, but possible infra-red singularities would manifest in  $\ln m^2/q^2$  terms. If such terms are absent in the final expression, the limit  $m \rightarrow 0$  can be taken and the result should coincide with the one obtain with the massless set-up<sup>9</sup>.

Precisely, the charge renormalization of the gauge coupling can be derived from the ghost-gauge boson, fermion-gauge boson,  $\varepsilon$ -scalar-gauge boson vertices or from the gauge boson self interaction

$$Z_g = \frac{\tilde{Z}_1}{\tilde{Z}_3 \sqrt{Z_3}} = \frac{Z_1}{Z_2 \sqrt{Z_3}} = \frac{Z_1^{\varepsilon \varepsilon G}}{Z_3^{\varepsilon} \sqrt{Z_3}} = \text{etc.} \quad (3.27)$$

as a consequence of gauge invariance.

Similarly, for the charge renormalization constants of the evanescent couplings it holds the following relations

$$Z_e = \frac{Z_1^{\varepsilon}}{Z_2 \sqrt{Z_3^{\varepsilon}}} \quad Z_{\lambda_r} = \frac{Z_1^{4\varepsilon}}{(Z_3^{\varepsilon})^2}. \quad (3.28)$$

In general,  $Z_g \neq Z_e$  even at one-loop order. However, in supersymmetric theories  $Z_g = Z_e$  should hold at all orders because of SUSY. This can be understood following the same line of reasoning as for the derivation of the equality of the charge renormalization constants for the interactions involving gluons and those involving gluinos.

### 3.3.1 The $\varepsilon$ -scalar self couplings

Let us discuss the structure of the quartic  $\varepsilon$ -scalar couplings for an arbitrary gauge group. These interactions are invariant under the symmetry  $\mathcal{G} \otimes O(2\varepsilon)$ , where only  $\mathcal{G}$  is gauged. The number of independent quartic  $\varepsilon$ -scalar couplings is given by the number of independent rank  $n = 4$  tensors

---

<sup>9</sup> For a comprehensive overview about the multi-loop techniques within DREG see the review article [120].

$H^{abcd}$  invariant with respect to  $(a, b)$  and  $(c, d)$  exchange, because of the  $O(2\epsilon)$  invariance. It has been shown that for  $\mathcal{G} = SU(N), SO(N), SP(N)$  with  $N \geq 4$  there are four such tensors [121]. For the case  $N = 3$  only three independent tensors can be built [122], while for  $N = 2$  their number reduces to two [119]. The answer to the general question concerning rank  $n$  tensors is not yet known. For the explicit construction of the set of tensors  $H^{abcd}$  we consider first the  $SU(N)$  group and then generalize the results for the other two groups.

A natural choice for a basis for rank  $n = 4$  tensors when  $N \geq 4$  is given by [123]<sup>10</sup>

$$\begin{aligned} K_1 &= \delta^{ab}\delta^{cd} & K_4 &= d^{abe}d^{cde} & K_7 &= d^{abe}f^{cde} \\ K_2 &= \delta^{ac}\delta^{bd} & K_5 &= d^{ace}d^{bde} & K_8 &= d^{ace}f^{bde} \\ K_3 &= \delta^{ad}\delta^{bc} & K_6 &= d^{ade}d^{bde} & K_9 &= d^{ade}f^{bce}. \end{aligned} \quad (3.29)$$

Here  $d^{abc}$  stands for the completely symmetric rank  $n = 3$  tensors. The dimension of the basis reduces to 8 in the case of  $SU(3)$ . This is achieved via the relation [123, 124]

$$K_4 + K_5 + K_6 = \frac{1}{3}(K_1 + K_2 + K_3) \quad (3.30)$$

which is not valid for  $N \geq 4$ .

To describe the  $\varepsilon$ -scalar quartic interactions one needs to construct rank  $n = 4$  tensors invariant w.r.t. exchange of pairs of indices. Thus, one has to take linear combinations of the basis tensors and symmetrized them with respect to the pair of indices  $(ab)$  and  $(cd)$ . A possible choice for  $N \geq 4$  is given by

$$\begin{aligned} H_1 &= \frac{1}{2}K_1, \\ H_2 &= \frac{1}{2}(K_2 + K_3), \\ H_3 &= \frac{1}{2}K_4, \\ H_4 &= \frac{1}{2}(K_5 + K_6). \end{aligned} \quad (3.31)$$

Note that the absence of a  $d - f$  type term from Eqs. (3.31) follows from the identity [123]

$$K_8 + K_9 = -f^{abe}d^{cde}. \quad (3.32)$$

However, for practical purposes a basis constructed with the help of the structure constants  $f^{abc}$  and avoiding the use of the  $d$ -tensors is more suited. For example, it would allow to explore more easily the supersymmetric case and to generalize to other groups. It is natural to consider the alternative choice [97, 117]

$$\begin{aligned} \overline{H}_1 &= \frac{1}{2}(f^{ace}f^{bde} + f^{ade}f^{bce}), \\ \overline{H}_2 &= \delta^{ac}\delta^{bd} + \delta^{ad}\delta^{bc} + \delta^{ab}\delta^{cd}, \\ \overline{H}_3 &= \frac{1}{2}(\delta^{ac}\delta^{bd} + \delta^{ad}\delta^{bc}) - \delta^{ab}\delta^{cd}, \\ \overline{H}_4 &= \frac{1}{2}(f^{aef}f^{bfg}f^{cgh}f^{dhe} + f^{aef}f^{bfg}f^{dgh}f^{che}). \end{aligned} \quad (3.33)$$

---

<sup>10</sup>An alternative way to define a basis which has the virtue of being immediately generalizable to any group [122] is in terms of traces of products of the generators in the defining representation, thus  $\text{Tr}(T^a T^b T^c T^d)$ ,  $\text{Tr}(T^a T^b)$   $\text{Tr}(T^c T^d)$  etc.

Let us introduce the coupling constants

$$\alpha_s = \frac{g^2}{4\pi}, \quad \alpha_e = \frac{g_e^2}{4\pi} \quad \text{and} \quad u_r = \frac{\lambda_r}{4\pi}. \quad (3.34)$$

Then we can write the last term in Eq. (3.25)

$$\sum_{r=1}^4 Z_{\lambda_r} \lambda_r H_r^{abcd} = 4\pi \sum_{r=1}^4 Z_{u_r} u_r H_r^{abcd} = 4\pi \sum_{r=1}^4 Z_{\eta_r} \eta_r \overline{H}_r^{abcd}, \quad (3.35)$$

where  $\eta_r$  denote the quartic  $\varepsilon$ -scalar couplings in the basis  $\overline{H}^{abcd}$ . The renormalization constants  $Z_\eta$ ,  $Z_u$ , etc. have been computed through one loop in the  $\overline{\text{DR}}$  scheme for a general gauge group in Ref. [117, 121] and in Ref. [97] for  $SU(3)$ . The calculation performed in Ref. [97] has employed the method of Ref. [102] to introduce an artificial mass for all propagators in order to avoid spurious infrared divergences. For the calculation of the results in terms of group invariants the package `color` [125] has been used. For completeness, we reproduce here the one-loop results for the couplings  $\eta_r$ .

$$\begin{aligned} Z_{\eta_1} = & 1 + \frac{1}{\epsilon} \left[ -\frac{\alpha_s^{\overline{\text{DR}}}}{\pi} C_A \frac{3}{2} + \frac{\eta_1}{\pi} C_A \frac{1}{2} + \frac{\eta_2}{\pi} C_A 2 - \frac{\eta_3}{\pi} \frac{7}{2} - \frac{\eta_2}{\pi} \frac{\eta_4}{\eta_1} C_A - \frac{\eta_3}{\pi} \frac{\eta_4}{\eta_1} C_A \frac{1}{2} \right. \\ & + \frac{\eta_4}{\pi} \frac{C_A^4 (-61 + 7N_A) + 48D_4(AA)(N_A - 1)/N_A}{36C_A^2(N_A - 3)} + \frac{\alpha_e}{\pi} T_f \\ & - \frac{\alpha_e}{\pi} \frac{\alpha_e}{\eta_1} \frac{4C_A(2 + N_A)D_4(RA)/I_2(R) + 5C_A^3(7C_A - 2C_R)N_A - 16(2 + N_A)D_4(AA)}{2(25C_A^4N_A - 12D_4(AA)(2 + N_A))} T_f \\ & - \frac{\eta_4}{\pi} \frac{\eta_4}{\eta_1} \frac{1}{54C_A N_A (N_A - 3)(25C_A^4N_A - 12D_4(AA)(2 + N_A))} \\ & \left( -144D_4(AA)^2(2 + N_A)(1 + 2N_A) + 216C_A^2D_4(AAA)N_A(2 + N_A)(N_A - 3) \right. \\ & \left. - 12C_A^4D_4(AA)N_A(-191 - 56N_A + N_A^2) - 25C_A^8N_A^2(4N_A + 23) \right) \Big], \\ Z_{\eta_2} = & 1 + \frac{1}{\epsilon} \left[ -\frac{\alpha_s^{\overline{\text{DR}}}}{\pi} C_A \frac{3}{2} - \frac{\eta_1}{\pi} C_A \frac{1}{6} + \frac{\eta_3}{\pi} \frac{N_A - 1}{6} + \frac{\eta_4}{\pi} C_A^2 \frac{13}{12} + \frac{\eta_2}{\pi} \frac{2(8 + N_A)}{3} \right. \\ & + \frac{\eta_3}{\pi} \left( \frac{\eta_1}{\eta_2} C_A \frac{1}{6} + \frac{\eta_4}{\eta_2} C_A^2 \frac{1}{6} - \frac{\eta_3}{\eta_2} \frac{(N_A - 1)}{12} \right) \\ & - \frac{\eta_4}{\pi} \frac{\eta_4}{\eta_2} \frac{2}{9} \frac{72D_4(AA)^2/N_A - 90C_A^2D_4(AAA) + 25C_A^4D_4(AA)}{25C_A^4N_A - 12D_4(AA)(2 + N_A)} \\ & \left. + \frac{\alpha_e}{\pi} \left( T_f - \frac{\alpha_e}{\eta_2} 2 \frac{5C_A^2D_4(RA)/I_2(R) + (C_A - 6C_R)D_4(AA)}{25C_A^4N_A - 12D_4(AA)(2 + N_A)} T_f \right) \right], \\ Z_{\eta_3} = & 1 + \frac{1}{\epsilon} \left[ \left( -\frac{\alpha_s^{\overline{\text{DR}}}}{\pi} C_A \frac{3}{2} + \frac{\eta_4}{\pi} C_A^2 \frac{5}{12} + \frac{\eta_2}{\pi} \frac{2(2 + N_A)}{3} + \frac{\eta_3}{\pi} \frac{-26 + 5N_A}{12} \right. \right. \\ & + \frac{\eta_4}{\pi} \frac{\eta_4}{\eta_3} \frac{7}{108} \frac{12D_4(AA) - 5C_A^4N_A}{(N_A - 3)N_A} - \frac{\eta_2}{\pi} \left( \frac{\eta_4}{\eta_3} C_A^2 \frac{2}{3} + \frac{\eta_2}{\eta_3} \frac{(2 + N_A)}{3} \right) \\ & \left. \left. + \frac{\eta_1}{\pi} \left( -C_A \frac{5}{6} - \frac{\eta_2}{\eta_3} \frac{2C_A}{3} + \frac{\eta_4}{\eta_3} \frac{12D_4(AA) - 5C_A^4N_A}{9C_A N_A (N_A - 3)} \right) + \frac{\alpha_e}{\pi} T_f \right] \right], \end{aligned}$$

$$\begin{aligned}
Z_{\eta_4} = 1 + \frac{1}{\epsilon} & \left[ -\frac{\alpha_s^{\overline{\text{DR}}}}{\pi} C_A \frac{3}{2} - \frac{\eta_1}{\pi} C_A \frac{1}{4} + \frac{\eta_2}{\pi} 8 - \frac{\eta_3}{\pi} \frac{1}{2} + \frac{\alpha_s^{\overline{\text{DR}}}}{\pi} \frac{\alpha_s^{\overline{\text{DR}}}}{\eta_4} \frac{3}{4} - \frac{\eta_1}{\pi} \frac{\eta_1}{\eta_4} \frac{1}{4} \right. \\
& + \frac{\eta_4 - 1152 D_4(AAA)(2 + N_A) + 5 C_A^2 (125 C_A^4 N_A + 4 D_4(AA)(98 + N_A))}{48(25 C_A^4 N_A - 12 D_4(AA)(2 + N_A))} \\
& \left. + \frac{\alpha_e}{\pi} \left( T_f + \frac{\alpha_e}{\eta_4} \frac{5 C_A^2 (C_A - 6 C_R) N_A + 12(2 + N_A) D_4(RA)/I_2(R)}{25 C_A^4 N_A - 12 D_4(AA)(2 + N_A)} T_f \right) \right], \quad (3.36)
\end{aligned}$$

with the group invariants defined in Appendix A and the abbreviation  $T_f = I_2(R)n_f$ , where  $n_f$  denotes the number of active fermions. Let us notice at this point the presence of negative power of couplings in the expressions of the renormalization constants. This results into beta functions that are not proportional to the coupling itself. This feature is specific to scalar couplings and it implies that, even if we set such a coupling to zero at a given scale, it will receive non-vanishing radiative corrections due to the other couplings present in the theory.

The above results have been computed using an  $SU(N)$  gauge group. However, they are parametrized in terms of group invariants. Thus they are also valid for other physically interesting groups like  $SO(N)$  and  $SP(N)$ . The explicit values of the group invariants for the three groups can be found in Appendix A.

In the case of  $SU(3)$  group, the invariant  $\overline{H}_4$  becomes a linear combination of  $\overline{H}_i, i = 1, 2, 3$  because of relation (3.30). The same is also true for the coupling  $\eta_4$  that can be expressed in terms of the other three couplings. Thus in this case one can ignore  $\eta_4$ .

Actually, the one- and two-loop renormalization constants for totally symmetric quartic scalar couplings with scalars in an arbitrary representation have been known for long time [126]. However, these results cannot be directly applied to  $\varepsilon$ -scalar self interactions, due to their particular symmetry with respect to exchange between pairs of indices.

### 3.3.2 Three-loop renormalization constants for a non-supersymmetric theory

In this section we report on the explicit computation of the charge  $Z_g$ ,  $Z_e$  and mass  $Z_m^q$ ,  $Z_m^e$  renormalization constants to three-loop order within  $\overline{\text{DR}}$  scheme. This requires the calculation of divergent parts of logarithmically divergent integrals. One can exploit the fact that such contributions are independent of the masses and external momenta. Precisely, one sets all internal masses to zero and keeps only one external momentum different from zero and then solve recursively Eq. (3.12). In practice, use of the automated programs **QGRAF** [127], **q2e** and **exp** [128, 129] and **MINCER** are essential due to the large number of diagrams that occur.

The analytical form of  $Z_g^{\overline{\text{DR}}}$  up to two-loop order is identical to the corresponding result in the  $\overline{\text{MS}}$  scheme. This has been shown by an explicit calculation for the first time in Ref. [71] and is a consequence of the minimal renormalization. The three- and four-loop results for a general theory have been derived in Refs. [97, 121, 130]. For completeness we present in the following the three-loop results

$$\begin{aligned}
Z_g^{\overline{\text{DR}}} = 1 + \frac{\alpha_s^{\overline{\text{DR}}}}{\pi} \frac{1}{\epsilon} & \left( -\frac{11}{24} C_A + \frac{1}{6} T_f \right) + \left( \frac{\alpha_s^{\overline{\text{DR}}}}{\pi} \right)^2 \left[ \frac{1}{\epsilon^2} \left( \frac{121}{384} C_A^2 - \frac{11}{48} C_A T_f \right. \right. \\
& \left. \left. + \frac{1}{24} T_f^2 \right) + \frac{1}{\epsilon} \left( -\frac{17}{96} C_A^2 + \frac{5}{48} C_A T_f + \frac{1}{16} C_R T_f \right) \right]
\end{aligned}$$

$$\begin{aligned}
& + \left( \frac{\alpha_s^{\overline{\text{DR}}}}{\pi} \right)^3 \left[ \frac{1}{\epsilon^3} \left( \frac{-6655}{27648} C_A^3 + \frac{605}{2304} C_A^2 T_f - \frac{55}{576} C_A T_f^2 + \frac{5}{432} T_f^3 \right) \right. \\
& + \frac{1}{\epsilon^2} \left( \frac{2057}{6912} C_A^3 - \frac{979}{3456} C_A^2 T_f + \frac{11}{288} C_R T_f^2 - \frac{121}{1152} C_A C_R T_f + \frac{55}{864} C_A T_f^2 \right) \\
& + \frac{1}{\epsilon} \left( -\frac{3115}{20736} C_A^3 + \frac{1439}{10368} C_A^2 T_f + \frac{193}{3456} C_A C_R T_f - \frac{79}{5184} C_A T_f^2 \right. \\
& \left. \left. - \frac{1}{192} C_R^2 T_f - \frac{11}{864} C_R T_f^2 \right) \right] + \left( \frac{\alpha_s^{\overline{\text{DR}}}}{\pi} \right)^2 \frac{\alpha_e}{\pi} \frac{1}{\epsilon} \left( \frac{1}{32} C_R^2 T_f \right) \\
& + \frac{\alpha_s^{\overline{\text{DR}}}}{\pi} \left( \frac{\alpha_e}{\pi} \right)^2 \frac{1}{\epsilon} \left( \frac{1}{96} C_A C_R T_f - \frac{1}{48} C_R^2 T_f - \frac{1}{96} C_R T_f^2 \right). \tag{3.37}
\end{aligned}$$

The one-loop result for  $Z_e$  can be found in Ref. [119]. For the particular case of QCD, *i.e.*  $\mathcal{G} = SU(3)$  and  $\eta_4 = 0$ , the two-, three- and four-loop results have been computed in Refs. [97, 130]. The two-, three- and four-loop results for a general theory have been derived in Ref. [121]. Because of the complexity of the results, we reproduce below only the two-loop contributions that are however enough for most of the practical applications

$$\begin{aligned}
Z_e = & 1 + \frac{\alpha_s^{\overline{\text{DR}}}}{\pi} \frac{1}{\epsilon} \left( -\frac{3}{4} C_R \right) + \frac{\alpha_e}{\pi} \frac{1}{\epsilon} \left( -\frac{1}{4} C_A + \frac{1}{2} C_R + \frac{1}{4} T_f \right) \\
& + \left( \frac{\alpha_s^{\overline{\text{DR}}}}{\pi} \right)^2 \left[ \frac{1}{\epsilon^2} \left( \frac{11}{32} C_A C_R + \frac{9}{32} C_R^2 - \frac{1}{8} C_R T_f \right) + \frac{1}{\epsilon} \left( \frac{7}{256} C_A^2 - \frac{55}{192} C_A C_R \right. \right. \\
& \left. \left. - \frac{3}{64} C_R^2 - \frac{1}{32} C_A T_f + \frac{5}{48} C_R T_f \right) \right] + \frac{\alpha_s^{\overline{\text{DR}}}}{\pi} \frac{\alpha_e}{\pi} \left[ \frac{1}{\epsilon^2} \left( \frac{3}{8} C_A C_R - \frac{3}{4} C_R^2 \right. \right. \\
& \left. \left. - \frac{3}{8} C_R T_f \right) + \frac{1}{\epsilon} \left( \frac{3}{32} C_A^2 - \frac{5}{8} C_A C_R + \frac{11}{16} C_R^2 + \frac{5}{32} C_R T_f \right) \right] \\
& + \left( \frac{\alpha_e}{\pi} \right)^2 \left[ \frac{1}{\epsilon^2} \left( \frac{3}{32} C_A^2 - \frac{3}{8} C_A C_R + \frac{3}{8} C_R^2 - \frac{3}{16} C_A T_f + \frac{3}{8} C_R T_f + \frac{3}{32} T_f^2 \right) \right. \\
& \left. + \frac{1}{\epsilon} \left( -\frac{3}{32} C_A^2 + \frac{5}{16} C_A C_R - \frac{1}{4} C_R^2 + \frac{3}{32} C_A T_f - \frac{3}{16} C_R T_f \right) \right] \\
& + \frac{\alpha_e}{\pi} \frac{1}{\epsilon} \left[ \frac{\eta_1}{\pi} \left( \frac{1}{32} C_A^2 \right) + \frac{\eta_2}{\pi} \left( \frac{1}{16} C_A - \frac{3}{8} C_R \right) + \frac{\eta_3}{\pi} \left( -\frac{1}{16} C_A \right) \right. \\
& \left. + \frac{\eta_4}{\pi} \left( \frac{1}{192} C_A^3 - \frac{1}{8} D_4(RA) I_2(R) \right) \right] + \left( \frac{\eta_1}{\pi} \right)^2 \frac{1}{\epsilon} \left( -\frac{3}{256} C_A^2 \right) + \left( \frac{\eta_2}{\pi} \right)^2 \frac{1}{\epsilon} \left( \frac{3}{32} (N_A + 2) \right) \\
& + \frac{\eta_1}{\pi} \frac{\eta_3}{\pi} \frac{1}{\epsilon} \left( \frac{3}{64} C_A \right) + \left( \frac{\eta_3}{\pi} \right)^2 \frac{1}{\epsilon} \left( -\frac{3}{128} (N_A - 1) \right) + \frac{\eta_1}{\pi} \frac{\eta_4}{\pi} \frac{1}{\epsilon} \left( -\frac{1}{256} C_A^3 \right) \\
& + \frac{\eta_2}{\pi} \frac{\eta_4}{\pi} \frac{1}{\epsilon} \left( \frac{5}{32} C_A^2 \right) + \frac{\eta_3}{\pi} \frac{\eta_4}{\pi} \frac{1}{\epsilon} \left( \frac{1}{128} C_A^2 \right) + \left( \frac{\eta_4}{\pi} \right)^2 \frac{1}{\epsilon} \left( -\frac{1}{3072} C_A^4 + \frac{1}{32} D_4(AA) \right). \tag{3.38}
\end{aligned}$$

The group invariants  $C_A, C_R, I_2(R), D_4(XY)$  occurring in the above equations are defined in Appendix A and we used the abbreviation  $T_f = I_2(R) n_f$ .

There is also an indirect way to derive the three-loop gauge beta function in the  $\overline{\text{DR}}$  scheme starting from the knowledge of the three-loop gauge beta function in the  $\overline{\text{MS}}$  scheme and the

fact that the gauge couplings defined in the two schemes can be perturbatively related to each other. This method will be discussed in more detail in the next section. Let us mention however that, using the expression for the three-loop gauge beta function in the  $\overline{\text{MS}}$  scheme  $\beta_s^{\overline{\text{MS}}}$  and the two-loop conversion relation of  $\alpha_s$  given in Eq. (3.41) one obtains exactly the same results for  $\beta_s^{\overline{\text{DR}}}$  as given in Eq. (3.37). This is a powerful consistency check for the calculation reviewed in this section. It is interesting to mention that the equality of the two results can be obtained only if one keeps  $\alpha_s^{\overline{\text{DR}}} \neq \alpha_e$  during the calculation and renormalize them differently. The identification of  $\alpha_s^{\overline{\text{DR}}}$  and  $\alpha_e$  leads to inconsistent results. In case of  $\beta_s^{\overline{\text{DR}}}$  the error is a finite, gauge parameter independent term [113]. For quark mass renormalization, this identification (precisely the identification of the renormalization constants for the two couplings) generates much more severe problems. Namely, the renormalization constant for the quark mass  $Z_m^{\overline{\text{DR}}}$  will contain non-local terms at three-loop order and the mass anomalous dimension will erroneously become divergent at this loop order.

The renormalization constant for the fermion masses  $Z_m^{\overline{\text{DR}}}$  has been computed in Ref. [97] to three- and in Ref. [121,130] even to four-loop order. Whereas in [97,121,130] only the anomalous dimensions were given we want to present the explicit three-loop result for the renormalization constant, that reads

$$\begin{aligned}
Z_m^{\overline{\text{DR}}} = & 1 + \frac{\alpha_s^{\overline{\text{DR}}}}{\pi} \frac{1}{\epsilon} \left( -\frac{3}{4} C_R \right) + \left( \frac{\alpha_s^{\overline{\text{DR}}}}{\pi} \right)^2 \left[ \frac{1}{\epsilon^2} \left( \frac{11}{32} C_A C_R + \frac{9}{32} C_R^2 - \frac{1}{8} C_R T_f \right) \right. \\
& + \frac{1}{\epsilon} \left( -\frac{91}{192} C_A C_R - \frac{3}{64} C_R^2 + \frac{5}{48} C_R T_f \right) \left. \right] + \frac{\alpha_s^{\overline{\text{DR}}}}{\pi} \frac{\alpha_e}{\pi} \left( \frac{3}{16} \frac{1}{\epsilon} C_R^2 \right) \\
& + \left( \frac{\alpha_e}{\pi} \right)^2 \frac{1}{\epsilon} \left( \frac{1}{16} C_A C_R - \frac{1}{8} C_R^2 - \frac{1}{16} C_R T_f \right) + \left( \frac{\alpha_s^{\overline{\text{DR}}}}{\pi} \right)^3 \left[ \frac{1}{\epsilon^3} \left( -\frac{121}{576} C_A^2 C_R \right. \right. \\
& - \frac{33}{128} C_A C_R^2 - \frac{9}{128} C_R^3 + \frac{11}{72} C_A C_R T_f + \frac{3}{32} C_R^2 T_f - \frac{1}{36} C_R T_f^2 \left. \right) \\
& + \frac{1}{\epsilon^2} \left( \frac{1613}{3456} C_A^2 C_R + \frac{295}{768} C_A C_R^2 + \frac{9}{256} C_R^3 - \frac{59}{216} C_A C_R T_f - \frac{29}{192} C_R^2 T_f \right. \\
& + \frac{5}{216} C_R T_f^2 \left. \right) + \frac{1}{\epsilon} \left( -\frac{10255}{20736} C_A^2 C_R + \frac{133}{768} C_A C_R^2 - \frac{43}{128} C_R^3 + \left( \frac{281}{2592} \right. \right. \\
& + \frac{1}{4} \zeta_3 \left. \right) C_A C_R T_f + \left( \frac{23}{96} - \frac{1}{4} \zeta_3 \right) C_R^2 T_f + \frac{35}{1296} C_R T_f^2 \left. \right] \\
& + \left( \frac{\alpha_s^{\overline{\text{DR}}}}{\pi} \right)^2 \frac{\alpha_e}{\pi} \left[ \frac{1}{\epsilon^2} \left( -\frac{11}{192} C_A C_R^2 - \frac{15}{64} C_R^3 + \frac{1}{48} C_R^2 T_f \right) + \frac{1}{\epsilon} \left( \frac{5}{256} C_A^2 C_R \right. \right. \\
& + \frac{7}{32} C_A C_R^2 + \frac{9}{64} C_R^3 - \frac{3}{32} C_R^2 T_f \left. \right) \left. \right] + \frac{\alpha_s^{\overline{\text{DR}}}}{\pi} \left( \frac{\alpha_e}{\pi} \right)^2 \left[ \frac{1}{\epsilon^2} \left( -\frac{9}{64} C_A C_R^2 + \frac{9}{32} C_R^3 \right. \right. \\
& + \frac{9}{64} C_R^2 T_f \left. \right) + \frac{1}{\epsilon} \left( -\frac{1}{64} C_A^2 C_R + \frac{7}{32} C_A C_R^2 - \frac{3}{8} C_R^3 - \frac{1}{64} C_A C_R T_f \right. \\
& \left. \left. - \frac{1}{8} C_R^2 T_f \right) \right] + \left( \frac{\alpha_e}{\pi} \right)^3 \left[ \frac{1}{\epsilon^2} \left( -\frac{1}{48} C_A^2 C_R + \frac{1}{12} C_A C_R^2 - \frac{1}{12} C_R^3 \right. \right.
\end{aligned}$$



$$\begin{aligned}
& + \frac{1}{24}C_A C_R T_f - \frac{1}{12}C_R^2 T_f - \frac{1}{48}C_R T_f^2 \Big) + \frac{1}{\epsilon} \Big( \frac{1}{32}C_A^2 C_R - \frac{1}{8}C_A C_R^2 + \frac{1}{8}C_R^3 \\
& - \frac{1}{24}C_A C_R T_f + \frac{5}{48}C_R^2 T_f + \frac{1}{96}C_R T_f^2 \Big) + \left( \frac{\alpha_e}{\pi} \right)^2 \frac{1}{\epsilon} \Big[ \frac{\eta_1}{\pi} \left( -\frac{1}{96}C_A^2 C_R \right) \\
& + \frac{\eta_2}{\pi} \left( -\frac{1}{48}C_A C_R + \frac{1}{8}C_R^2 \right) + \frac{\eta_3}{\pi} \left( \frac{1}{48}C_A C_R \right) + \frac{\eta_4}{\pi} \left( -\frac{1}{576}C_A^3 C_R + \frac{1}{12}C_R D_4(RA) \right) \Big] \\
& + \frac{\alpha_e}{\pi} \frac{1}{\epsilon} \Big[ \left( \frac{\eta_1}{\pi} \right)^2 \left( \frac{1}{256}C_A^2 C_R \right) + \left( \frac{\eta_2}{\pi} \right)^2 \left( -\frac{1}{32}C_R(N_A + 2) \right) + \left( \frac{\eta_3}{\pi} \right)^2 \left( \frac{1}{128}C_R(N_A - 1) \right) \\
& + \left( \frac{\eta_4}{\pi} \right)^2 \left( \frac{1}{9216}C_A^4 C_R - \frac{1}{96}C_R D_4(AA) \right) + \frac{\eta_1}{\pi} \frac{\eta_3}{\pi} \left( -\frac{1}{64}C_A C_R \right) \\
& + \frac{\eta_1}{\pi} \frac{\eta_4}{\pi} \left( \frac{1}{768}C_A^3 C_R \right) + \frac{\eta_2}{\pi} \frac{\eta_4}{\pi} \left( -\frac{5}{96}C_A^2 C_R \right) + \frac{\eta_3}{\pi} \frac{\eta_4}{\pi} \left( -\frac{1}{384}C_A^2 C_R \right) \Big]. \tag{3.39}
\end{aligned}$$

where  $\zeta(3)$  is Riemann's zeta function with  $\zeta(3) = 1.20206\dots$

Again, the consistency of the above results can be proved using the indirect method alluded above. To derive the three-loop quark mass anomalous dimension in the  $\overline{\text{DR}}$  scheme  $\gamma_m^{\overline{\text{DR}}}$ , one needs the three-loop result for  $\gamma_m^{\overline{\text{MS}}}$  and the two-loop conversion relation from the quark mass as given in Eq. (3.42). Full agreement has been found between the two methods [97], that provides a further consistency check of the calculation.

### 3.3.3 The general four-loop order results in the $\overline{\text{DR}}$ scheme

The direct way to compute the renormalization constants in minimal subtraction schemes as  $\overline{\text{MS}}$  or  $\overline{\text{DR}}$  requires the calculation of divergent parts of logarithmically divergent integrals. Up to three loops there are well established methods and automated programs exist to perform such calculations (see, e.g., Refs. [100,109]). Also at four-loop order a similar approach is applicable. Nevertheless, it is technically much more involved [103,104,106,131,132]. There is however an indirect method discussed in Refs. [97,113] to derive the renormalization constants in the  $\overline{\text{DR}}$  scheme starting from their  $\overline{\text{MS}}$  expressions. It relies on the perturbative relation that can be established between the couplings and masses defined in the two schemes and takes into account that the four-loop results in the  $\overline{\text{MS}}$  scheme are known [103,104,106]. For example, to derive the beta-function for the gauge coupling to four-loop order in  $\overline{\text{DR}}$  scheme one needs the relation between the gauge couplings defined in the  $\overline{\text{MS}}$  and  $\overline{\text{DR}}$  schemes up to three-loop order. The latter can be determined using the following arguments.

To compute the relations between running parameters defined in two different renormalization schemes, one has to relate them to physical observables which cannot depend on the choice of scheme. For example, the relationship between the strong coupling constant defined in the  $\overline{\text{MS}}$  and  $\overline{\text{DR}}$  schemes can be obtained from the S-matrix amplitude of a physical process involving the gauge coupling computed in the two schemes. However, beyond one-loop the computation of the physical amplitudes becomes very much involved and requires the computation of multi-loop and multi-scale on-shell Feynman integrals that is a highly non-trivial task. Nevertheless, one can avoid the use of on-shell kinematics introducing a physical renormalization scheme defined through convenient kinematics, for which the renormalization constants can be computed applying the “large-momentum” or the “hard-mass” procedures. Up to three loops, there are well

established methods ( for a details see previous sections) to compute the divergent as well as finite pieces of the Feynman integrals and automated programs exist to perform such calculations. Once the renormalization constants in the physical renormalization scheme are determined, one uses the constraint that the *effective* gauge coupling constant defined in such a scheme is unique and thus, independent on the regularization procedure. Furthermore, one relates the running gauge couplings defined in the two regularization schemes through the following relations

$$\begin{aligned}\alpha_s^{\text{ph}} &= \left(z_s^{\text{ph,X}}\right)^2 \alpha_s^{\text{X}}, \quad z_s^{\text{ph,X}} = Z_s^{\text{X}}/Z_s^{\text{ph,X}}, \quad \text{X} \in \{\overline{\text{MS}}, \overline{\text{DR}}\} \\ \Rightarrow \alpha_s^{\overline{\text{DR}}} &= \left(\frac{Z_s^{\text{ph},\overline{\text{DR}}}}{Z_s^{\text{ph},\overline{\text{MS}}}} \frac{Z_s^{\overline{\text{MS}}}}{Z_s^{\overline{\text{DR}}}}\right)^2 \alpha_s^{\overline{\text{MS}}},\end{aligned}\tag{3.40}$$

where  $Z_s^{\overline{\text{MS}}/\overline{\text{DR}}}$  are the charge renormalization constants using minimal subtraction in DREG/DRED, as defined above. Note that the various  $Z_s$  in Eq. (3.40) depend on differently renormalized  $\alpha_s$ , so that the equations have to be used iteratively at higher orders of perturbation theory. Working out these considerations for the gauge coupling and for the fermion mass up to the three-loop order, one obtains

$$\alpha_s^{\overline{\text{DR}}} = \alpha_s^{\overline{\text{MS}}} \left[ 1 + \frac{\alpha_s^{\overline{\text{MS}}}}{\pi} \frac{1}{12} C_A + \left( \frac{\alpha_s^{\overline{\text{MS}}}}{\pi} \right)^2 \frac{11}{72} C_A^2 - \frac{\alpha_s^{\overline{\text{MS}}}}{\pi} \frac{\alpha_e}{\pi} \frac{1}{8} C_R T_f + \delta_\alpha^{(3)} \right], \tag{3.41}$$

$$\begin{aligned}m^{\overline{\text{DR}}} &= m^{\overline{\text{MS}}} \left[ 1 - \frac{\alpha_e}{\pi} \frac{1}{4} C_R + \left( \frac{\alpha_s^{\overline{\text{MS}}}}{\pi} \right)^2 \frac{11}{192} C_A C_R - \frac{\alpha_s^{\overline{\text{MS}}}}{\pi} \frac{\alpha_e}{\pi} \frac{1}{32} C_R (3C_A + 8C_R) \right. \\ &\quad \left. + \left( \frac{\alpha_e}{\pi} \right)^2 \frac{1}{32} [3C_R + T_f] + \delta_m^{(3)} \right],\end{aligned}\tag{3.42}$$

where we have suppressed the explicit dependence on the renormalization scale  $\mu$ .  $\delta_\alpha^{(3)}$  and  $\delta_m^{(3)}$  denote the three-loop terms and they are obtained from the finite parts of three-loop diagrams (see Ref. [97] for details). They read [117, 121]

$$\begin{aligned}\pi^3 \delta_\alpha^{(3)} &= \frac{1}{96} \alpha_s^{\overline{\text{MS}}} \alpha_e^2 T_f [2C_A^2 - 3C_A C_R + 2C_R^2 - C_A T_f + 7C_R T_f] \\ &\quad - \frac{1}{192} (\alpha_s^{\overline{\text{MS}}})^2 \alpha_e T_f (5C_A^2 + 60C_A C_R + 6C_R^2) \\ &\quad + \frac{1}{9216} \alpha_s^{\overline{\text{MS}}} (36C_A^3 \eta_1^2 - 576C_A \eta_2^2 - 144C_A^2 \eta_1 \eta_3 - 72C_A \eta_3^2 \\ &\quad + 12C_A^4 \eta_1 \eta_4 - 480C_A^3 \eta_2 \eta_4 - 24C_A^3 \eta_3 \eta_4 + C_A^5 \eta_4^2 - 288C_A N_A \eta_2^2 \\ &\quad + 72C_A N_A \eta_3^2) - \frac{1}{96N_A} \alpha_s^{\overline{\text{MS}}} \eta_4^2 C_A D_4(AA) + \frac{1}{48} (\alpha_s^{\overline{\text{MS}}})^2 \eta_4 D_4(AA) \\ &\quad + \frac{1}{4608} (\alpha_s^{\overline{\text{MS}}})^2 (-6C_A^3 \eta_1 + 240C_A^2 \eta_2 + 12C_A^2 \eta_3 - C_A^4 \eta_4) \\ &\quad + \frac{1}{10368} (\alpha_s^{\overline{\text{MS}}})^3 [3049C_A^3 - 416C_A^2 T_f - 138C_A C_R T_f], \\ \pi^3 \delta_m^{(3)} &= -\frac{1}{384} \alpha_e^3 C_R [-10C_A^2 + 14C_A C_R + 27C_R^2 - 7C_A T_f \\ &\quad + 39C_R T_f - 10I_2(R)^2 T_f^2 + 12C_A^2 \zeta_3 - 36C_A C_R \zeta_3 + 24C_R^2 \zeta_3]\end{aligned}\tag{3.43}$$

$$\begin{aligned}
& -\alpha_e^2 C_R \left( \frac{1}{322} [(6C_R - C_A)\eta_2] + \frac{1}{16I_2(R)N_A} D_4(RA)\eta_4 + \frac{1}{384} \alpha_s^{\overline{\text{MS}}} [47C_A^2 + 10C_R^2 \right. \\
& - 3C_A T_f - 19C_R T_f - 165C_A C_R + 144C_R^2 \zeta_3 \\
& - 48C_A T_f \zeta_3 + 48C_R T_f \zeta_3 + 72C_A^2 \zeta_3 - 216C_A C_R \zeta_3] \Big) \\
& + \alpha_e C_R \left( \frac{1}{12288} [-36C_A^2 C_R \eta_1^2 + 1728C_R \eta_2^2 + 144C_A C_R \eta_1 \eta_3 + 72C_R \eta_3^2 - 12C_A^3 C_R \eta_1 \eta_4 \right. \\
& + 1440C_A^2 C_R \eta_2 \eta_4 + 24C_A^2 C_R \eta_3 \eta_4 - C_A^4 C_R \eta_4^2 + 864C_R N_A \eta_2^2 - 72C_R N_A \eta_3^2] \\
& + \frac{1}{3072} (\alpha_s^{\overline{\text{MS}}})^2 [2880C_R^2 \zeta_3 - 168C_A T_f - 1544C_A C_R - 52C_R^2 \\
& - 128C_R T_f + 1440C_A^2 \zeta_3 - 4320C_A C_R \zeta_3 - 79C_A^2] \Big) \\
& + \frac{1}{20736} (\alpha_s^{\overline{\text{MS}}})^3 C_R C_A [4354C_A + 135C_R + 304T_f] + \frac{3}{128N_A} D_4(AA)\eta_4^2. \tag{3.44}
\end{aligned}$$

Inserting Eqs. (3.41) and (3.42) into the definition of the beta function for the gauge coupling Eq. (2.6) and the mass anomalous dimension Eq. (2.10), one can show that

$$\begin{aligned}
\beta_s^{\overline{\text{DR}}} &= \mu^2 \frac{d}{d\mu^2} \frac{\alpha_s^{\overline{\text{DR}}}}{\pi} \\
&= \beta_s^{\overline{\text{MS}}} \frac{\partial \alpha_s^{\overline{\text{DR}}}}{\partial \alpha_s^{\overline{\text{MS}}}} + \beta_e \frac{\partial \alpha_s^{\overline{\text{DR}}}}{\partial \alpha_e} + \sum_r \beta_{\eta_r} \frac{\partial \alpha_s^{\overline{\text{DR}}}}{\partial \eta_r}, \\
\gamma_m^{\overline{\text{DR}}} &= \frac{\mu^2}{m^{\overline{\text{DR}}}} \frac{d}{d\mu^2} m^{\overline{\text{DR}}} \\
&= \gamma_m^{\overline{\text{MS}}} \frac{\partial \ln m^{\overline{\text{DR}}}}{\partial \ln m^{\overline{\text{MS}}}} + \frac{\pi \beta_s^{\overline{\text{MS}}}}{m^{\overline{\text{DR}}}} \frac{\partial m^{\overline{\text{DR}}}}{\partial \alpha_s^{\overline{\text{MS}}}} + \frac{\pi \beta_e}{m^{\overline{\text{DR}}}} \frac{\partial m^{\overline{\text{DR}}}}{\partial \alpha_e} + \sum_r \frac{\pi \beta_{\eta_r}}{m^{\overline{\text{DR}}}} \frac{\partial m^{\overline{\text{DR}}}}{\partial \eta_r}, \tag{3.45}
\end{aligned}$$

where the first equality is due to the definition of  $\beta_s^{\overline{\text{DR}}}$  and  $\gamma_m^{\overline{\text{DR}}}$ , and the second one is a consequence of the chain rule. Let us briefly discuss the order in perturbation theory up to which the individual building blocks are needed. Of course, the  $\overline{\text{MS}}$  quantities are needed to four-loop order; they can be found in Refs. [103–106]. The dependence of  $\alpha_s^{\overline{\text{DR}}}$  and  $m^{\overline{\text{DR}}}$  on  $\alpha_e$  starts at two- and one-loop order [97], respectively. Thus,  $\beta_e$  is needed up to the three-loop level (cf. Eq. (3.45)). On the other hand, both  $\alpha_s^{\overline{\text{DR}}}$  and  $m^{\overline{\text{DR}}}$  depend on  $\eta_r$  starting from three loops and consequently only the one-loop term of  $\beta_{\eta_r}$  enters in Eq. (3.45). The  $\overline{\text{DR}}$  four-loop results were derived for QCD in Ref. [97] and for a general theory in Ref. [117, 121]. The explicit four-loop results are too lengthy to be presented in this review and we refer to the original papers for the explicit results. We discuss however their supersymmetric limit in the next section.

### 3.3.4 The four-loop supersymmetric case

An important check of the complicated formulas derived in the previous sections can be obtained by converting them to a supersymmetric Yang-Mills theory. For this case, one has to replace the fermions by the supersymmetric partner of the gauge bosons, the so-called gauginos. Technically, this amounts to set the fermions in the adjoint representation of the gauge group. In addition, closed fermion loops have to be multiplied by an extra factor 1/2 in order to take into account

the Majorana character of the gauginos. Explicitly, for the derivation of the three- and four-loop results one needs the replacements

$$\begin{aligned}
C_R &\rightarrow C_A \\
I_2(R) &\rightarrow C_A \\
n_f &\rightarrow \frac{1}{2} \\
D_4(RR) &\rightarrow D_4(AA) \\
D_4(RA) &\rightarrow D_4(AA) \\
D_4(RAA) &\rightarrow D_4(AAA) .
\end{aligned} \tag{3.46}$$

Furthermore, SUSY requires that the gauge coupling  $\alpha_s$  equals the evanescent coupling  $\alpha_e$  to all orders of perturbation theory, and therefore, the  $\beta$  functions are also equal  $\beta_e^{\text{SYM}} = \beta_s^{\text{SYM}}$ . Moreover, SUSY also requires that the  $\varepsilon$ -scalar quartic interaction containing the structure constants is equal to the gauge coupling to all orders of perturbation theory. In this case, the other three quartic couplings have to vanish, so that the decomposition Eq. (3.17) holds to all orders of perturbation theory. Indeed, using Eqs. (3.36) one can easily derive the corresponding one-loop beta functions for supersymmetric theories and obtains

$$\beta_{\eta_1}^{\text{SYM}} = \beta_e^{\text{SYM}} = \beta_s^{\text{SYM}} \quad \text{and} \quad \beta_{\eta_2}^{\text{SYM}} = \beta_{\eta_3}^{\text{SYM}} = \beta_{\eta_4}^{\text{SYM}} = 0 , \tag{3.47}$$

when the SUSY restrictions

$$\eta_1 = \alpha_3 = \alpha_s \quad \text{and} \quad \eta_2 = \eta_3 = \eta_4 = 0 . \tag{3.48}$$

are imposed. It is also interesting to notice that the terms in the renormalization constants Eqs. (3.36) that contain negative power of couplings cancel out in the SUSY limit, so that the limit  $\eta_2 = \eta_3 = \eta_4 \rightarrow 0$  can be computed trivially. Thus, if relations (3.48) are imposed at the tree-level, they will not be spoiled by the renormalization at the one-loop order. Checks of this statement at two- and three-loop orders are available so far only for the evanescent coupling  $\alpha_e$  [97, 130].

Applying the substitutions given in Eq. (3.46) and (3.48) one can obtain the four-loop results for the gauge beta-function  $\beta_s^{\text{SYM}}$  [97, 121] and compare it with the expression derived in Ref. [133]

$$\beta_s^{\text{SYM}} = - \left( \frac{\alpha_s}{\pi} \right)^2 \left[ \frac{3}{4} C_A + \frac{3}{8} C_A^2 \frac{\alpha_s}{\pi} + \frac{21}{64} C_A^3 \left( \frac{\alpha_s}{\pi} \right)^2 + \frac{51}{128} C_A^4 \left( \frac{\alpha_s}{\pi} \right)^3 \right] + \mathcal{O}(\alpha_s^6) . \tag{3.49}$$

The method employed in Ref. [133] to obtain the four-loop result was very indirect, in particular relying on the existence of the NSVZ formula for  $\beta_s^{\text{SYM}}$  [134, 135]<sup>11</sup>. It is therefore a remarkable check on both calculations that indeed precise agreement was obtained.

Turning now to the case of softly-broken supersymmetry, there exists an exact result relating  $\beta_s$  and  $\gamma_m$  [42, 52] within the NSVZ scheme:

$$\gamma_m^{\text{SYM}} = \pi \alpha_s \frac{d}{d\alpha_s} \left[ \frac{\beta_s^{\text{SYM}}}{\alpha_s} \right] , \tag{3.50}$$

---

<sup>11</sup>For more details see section 2.

that nevertheless holds in  $\overline{\text{DR}}$  scheme too. Hence, it follows that

$$\gamma_m^{\text{SYM}} = - \left( \frac{\alpha_s}{\pi} \right) \left[ \frac{3}{4} C_A + \frac{3}{4} C_A^2 \frac{\alpha_s}{\pi} + \frac{63}{64} C_A^3 \left( \frac{\alpha_s}{\pi} \right)^2 + \frac{51}{32} C_A^4 \left( \frac{\alpha_s}{\pi} \right)^3 \right] + \mathcal{O}(\alpha_s^5). \quad (3.51)$$

Inserting Eq. (3.46) in Eq. (3.45), one can easily reproduce Eq. (3.51).

The invariant  $D_4(AAA)$  does not occur in either calculation, and the dependence on  $D_4(AA)$ ,  $N_A$ ,  $\zeta_3$ ,  $\zeta_4$  and  $\zeta_5$  all cancel although they appear in individual terms. It is tempting to speculate that this absence of higher order invariants and transcendental numbers (other than  $\pi$ ) is related to the existence of the NSVZ scheme, in which the gauge  $\beta$ -function for any simple gauge group is given (in the supersymmetric case without matter fields) by the expression in Eq. (2.13), which is manifestly free of transcendental numbers to all orders. It is natural to conjecture that the same property holds in the DRED scheme, too.

### 3.3.5 $\varepsilon$ -scalar mass

Although there is in general no tree-level term in the Lagrangian for the mass of the  $\varepsilon$  scalar there are loop induced contributions to it that require the introduction of the corresponding counter term. Let us introduce first the renormalization constant for the  $\varepsilon$ -scalar mass

$$(m_\varepsilon^0)^2 = Z_{m_\varepsilon} m_\varepsilon^2. \quad (3.52)$$

The relevant Feynman diagrams contributing to the  $\varepsilon$ -scalar propagator show quadratic divergences and therefore, one needs to consider only contributions from massive particles. Thus, in this case, only diagrams involving massive fermions have to be taken into account, since they are the only particles allowed by the gauge invariance to have non zero masses. Sample diagrams are shown in Fig. 3.1.

It is advantageous in practice to renormalize  $m_\varepsilon$  on-shell and require that the renormalized mass is zero to each order in perturbation theory. In this scheme the  $\varepsilon$ -scalar mass completely decouples from the physical observables.

At the one-loop order there is only one relevant diagram (cf. Fig. 3.1(a)) which has to be evaluated for vanishing external momentum. A closer look at the two-loop diagrams shows that they develop infrared divergences in the limit  $m_\varepsilon \rightarrow 0$  (cf., e.g., Fig. 3.1(e)). They can be regulated by introducing a small but non-vanishing mass for the  $\varepsilon$ -scalars. After the subsequent application of an asymptotic expansion [136] in the limit  $q^2 = m_\varepsilon^2 \ll M_f^2$  the infra-red divergences manifest themselves as  $\ln(m_\varepsilon)$  terms. Furthermore, one-loop diagrams like the ones in Fig. 3.1(b) and (c) do not vanish anymore and have to be taken into account as well. Although they are proportional to  $m_\varepsilon^2$ , after renormalization they induce two-loop contributions which are proportional to  $M_f^2$ , partly multiplied by  $\ln(m_\varepsilon)$  terms. It is interesting to note that in the sum of the genuine two-loop diagrams and the counter-term contributions the limit  $m_\varepsilon \rightarrow 0$  can be taken which demonstrates the infra-red finiteness of the on-shell mass of the  $\varepsilon$  scalar. The two-loop renormalization constant within QCD has been computed in Ref [137]. It is given by

$$\frac{m_\varepsilon^2}{M_f^2} (Z_{m_\varepsilon}^{\text{OS}} - 1) = - \frac{\alpha_e}{\pi} n_h I_2(R) \left[ \frac{2}{\epsilon} + 2 + 2L_\mu + \epsilon \left( 2 + \frac{1}{6} \pi^2 + 2L_\mu + L_\mu^2 \right) \right]$$

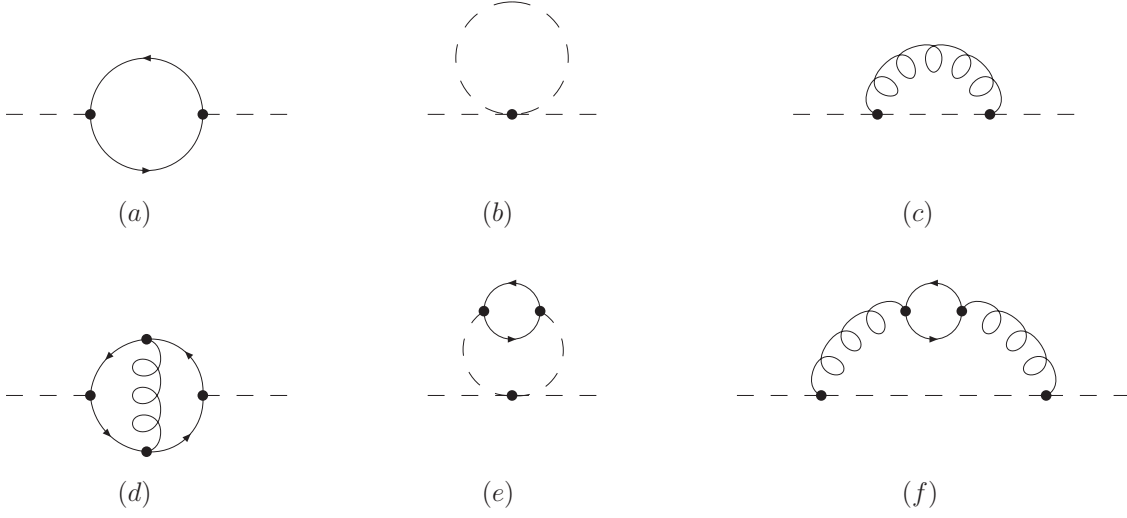


Figure 3.1: One- and two-loop Feynman diagrams contributing to the  $\varepsilon$ -scalar propagator. Dashed lines denote  $\varepsilon$  scalars, curly lines denote the gauge bosons and solid lines denote massive fermions with mass  $M_f$ .

$$\begin{aligned}
& - \left( \frac{\alpha_s^{\overline{\text{DR}}}}{\pi} \right)^2 n_h I_2(R) \left( \frac{3}{4} \frac{1}{\epsilon} + \frac{1}{4} + \frac{3}{2} L_\mu \right) C_A + \frac{\alpha_s^{\overline{\text{DR}}}}{\pi} \frac{\alpha_e}{\pi} n_h I_2(R) \left\{ \frac{1}{\epsilon^2} \left( \frac{3}{8} C_A + \frac{3}{2} C_R \right) \right. \\
& + \frac{1}{\epsilon} \left[ \frac{7}{8} C_A + \frac{3}{2} C_R + \left( \frac{3}{4} C_A + \frac{3}{2} C_R \right) L_\mu \right] + \left( \frac{15}{8} + \frac{1}{16} \pi^2 \right) C_A \\
& + \left( \frac{3}{2} + \frac{1}{8} \pi^2 \right) C_R + \left( \frac{7}{4} C_A + \frac{3}{2} C_R \right) L_\mu + \left( \frac{3}{4} C_A + \frac{3}{4} C_R \right) L_\mu^2 \Big\} \\
& + \left( \frac{\alpha_e}{\pi} \right)^2 n_h I_2(R) \left\{ \frac{1}{\epsilon^2} \left( \frac{1}{4} C_A - \frac{1}{2} C_R - \frac{1}{2} T_f \right) + \frac{1}{\epsilon} \left[ \frac{1}{2} C_R \right. \right. \\
& - \frac{1}{2} (1 + L_\mu) T_f \Big] - \frac{1}{2} C_A + \frac{5}{2} C_R - \left( \frac{1}{2} + \frac{1}{24} \pi^2 \right) T_f \\
& - \left( \frac{1}{2} C_A - 2 C_R + \frac{1}{2} T_f \right) L_\mu - \left( \frac{1}{4} C_A - \frac{1}{2} C_R + \frac{1}{4} T_f \right) L_\mu^2 \Big\} \\
& + \frac{\alpha_e}{\pi} \frac{\eta_1}{\pi} n_h \left[ \frac{3}{16} \frac{1}{\epsilon^2} + \frac{1}{\epsilon} \left( \frac{3}{16} + \frac{3}{8} L_\mu \right) + \frac{3}{16} + \frac{1}{32} \pi^2 + \frac{3}{8} L_\mu + \frac{3}{8} L_\mu^2 \right] \\
& - \frac{\alpha_e}{\pi} \frac{\eta_2}{\pi} n_h \left[ \frac{5}{4} \frac{1}{\epsilon^2} + \left( 5 + \frac{5}{2} L_\mu \right) \frac{1}{\epsilon} + \frac{25}{2} + \frac{5}{24} \pi^2 + 10 L_\mu + \frac{5}{2} L_\mu^2 \right] \\
& - \frac{\alpha_e}{\pi} \frac{\eta_3}{\pi} n_h \left[ \frac{7}{16} \frac{1}{\epsilon^2} + \left( \frac{7}{16} + \frac{7}{8} L_\mu \right) \frac{1}{\epsilon} + \frac{7}{16} + \frac{7}{96} \pi^2 + \frac{7}{8} L_\mu + \frac{7}{8} L_\mu^2 \right], \tag{3.53}
\end{aligned}$$

where  $L_\mu = \ln(\mu^2/M_f^2)$ ,  $T_f = n_f I_2(R)$ , where  $n_f$  and  $n_h$  denotes the number of fermions and heavy fermions, respectively. The overall factor  $n_h$  in front of the one- and two-loop corrections shows that the renormalization of  $m_\varepsilon$  is only influenced by those diagrams which contain a closed heavy fermion loop.

It is also possible to renormalize  $m_\epsilon$  so that  $m_\epsilon^{\text{OS}} \neq 0$  or adopt the  $\overline{\text{DR}}$  scheme for it. In the latter case, the physical observables will depend on  $m_\epsilon$ . In order to get rid of this unphysical dependence, one has to introduce additional finite shifts in the renormalization constants of the physical parameters. This new renormalization scheme is called  $\overline{\text{DR}}'$  and it will be discussed in more detail in the next section. Nevertheless, in context of QCD, the  $\overline{\text{DR}}'$  has rarely been used [138].

## 4 Dimensional Reduction applied to SUSY-QCD at three loops

All the appealing features of supersymmetric theories have to be confirmed by an accurate comparison with the experimental data like those measured in collider experiments [29, 30, 139]. Such an ambitious task requires precision data as well as precision calculations. But, precise predictions for observables implies computations of higher order radiative corrections. Thus, it necessarily rises the question of constructing regularization and renormalization schemes that are gauge and SUSY invariant. As discussed in the previous sections, DRED scheme was proposed as a solution, although it could violate SUSY at higher orders of perturbation theory. Currently, it is believed that DRED preserves SUSY at three-loop order as was explicitly checked in Refs. [87, 88] and that it breaks SUSY at four-loop order, taking into consideration formal arguments [51, 64]. Nevertheless, renormalization by combining DRED with minimal subtraction (the  $\overline{\text{DR}}$  scheme) or the on-shell scheme has become the preferred schemes in higher order supersymmetric calculations [86, 114, 140–142].

### 4.1 Renormalization of the gauge coupling and fermion masses at three loops

As was already reviewed in section 2, for supersymmetric gauge theories one can devise a particular renormalization scheme, the so-called NSVZ scheme [143], where an all-order relation between the gauge  $\beta$  function and the anomalous dimension of the chiral supermultiplet is valid. So, in the absence of the matter supermultiplet, *i.e.* for SUSY-Yang-Mills theory, the  $\beta$  function is known to all orders in the coupling constant. Applying the same method based on the connection between the holomorphic and the NSVZ scheme to softly broken SUSY gauge theory, the authors of Ref. [42] derived the renormalization group equation governing the running of the gaugino and sfermion masses as functions of the gauge and Yukawa coupling  $\beta$  functions, valid to all orders in perturbation theory. Actually, all these calculations received important phenomenological applications only after the authors of Ref. [55] found the three-loop conversion formula between the NSVZ and  $\overline{\text{DR}}$ . This allowed the derivation of three-loop order beta-functions for the parameters of the MSSM in the  $\overline{\text{DR}}$  scheme [144].

The goal of this section is to report on another confirmation of the results for the anomalous dimensions of SUSY-QCD parameters, that is based on a direct calculation of relevant three-loop Feynman diagrams implementing the DRED approach in the component field formalism. The agreement of the two independent and conceptually completely different calculations is a very important check of the two methods on the one side, and on the other side it establishes the DRED as a consistent framework for computations of radiative corrections in supersymmetric theories.

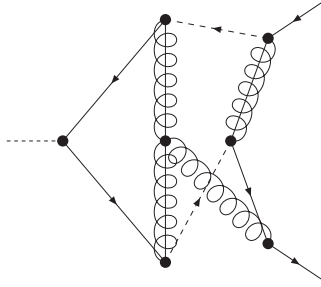


Figure 4.1: Sample diagram for the three-loop  $q\bar{q}\epsilon$  vertex where a non-vanishing trace with a single  $\gamma_5$  matrix occurs. Solid lines are quarks, dashed lines are squarks, slashed springy lines are gluinos, and the external dashed line depicts an  $\epsilon$  scalar. The arrows on the lines denote the charge flow.

The renormalized Lagrangian of a supersymmetric theory will obey SUSY constraints, only if the decomposition of Eq. (3.17) hold at all orders of perturbation theory. Therefore, the renormalized gluon and  $\epsilon$ -scalar coupling constants must be equal, i.e., their  $\beta$  functions must be the same. An all order proof of this statement is currently not available. However, it was explicitly shown [88] that the coupling constant arising from the vertices:  $g\bar{c}\bar{c}$ ,  $ggg$ ,  $gq\bar{q}$ ,  $\tilde{g}q\bar{q}$  and that from the vertices  $q\bar{q}\epsilon$ ,  $\tilde{g}\tilde{g}\epsilon$ , and  $g\epsilon\epsilon$  are equal through three loops.

Even more: in order to renormalize the quartic  $\epsilon$ -scalar vertex, one has to take into account all possible colour structures for it, and attribute to each one a separate coupling constant<sup>12</sup>. For SUSY-QCD, it has been explicitly checked [121] that at the one-loop order only the  $\beta$  function associated with the usual colour structure of the four-gluon interaction, *i.e.*  $f_{abe}f_{cde}$ <sup>13</sup>, does not vanish and it equals the one-loop gauge  $\beta$  function. Thus, through one-loop, one can identify the coupling constant of the corresponding  $\epsilon$ -scalar quartic interaction with the strong coupling constant and set to zero the other three quartic couplings. This order of accuracy is sufficient for the results discussed here, as the  $\epsilon$ -scalar quartic interactions contribute to the anomalous dimensions starting from the two-loop order. A similar observation was made also in the previous section when the SUSY-Yang-Mills theory was discussed at four-loop accuracy. All these tests confirm the consistency of DRED with SUSY at next-to-next-to-next-to-leading order (NNNLO) of perturbation theory.

For the calculation of renormalization constants within supersymmetric theories one can apply the same methods as the ones discussed in section 3.3.2 in the context of non-SUSY theories. Let us however mention at this point, a technical subtlety related to the implementation of  $\gamma_5$  matrix. Traces with a single  $\gamma_5$  and at least four  $\gamma$ -matrices do not contribute to any of the two-point functions<sup>14</sup>. They do contribute for some of the three-point functions though, in particular the  $q\bar{q}\tilde{g}$ , the  $\tilde{g}\tilde{g}\epsilon$ , and the  $q\bar{q}\epsilon$  vertex. An example diagram for the latter vertex is shown in Figure 4.1. Such diagrams contribute (among others) a colour factor  $d_R^{abcd}d_A^{abcd}$  (for the notation, see Appendix A), but they cancel against the same factors from other sources in the

<sup>12</sup>For details see sections 3.3.1 and 3.3.4.

<sup>13</sup> $f_{abe}$  denotes the structure constants of the gauge group.

<sup>14</sup>For a detailed discussion about this aspect see Ref. [145].



final result for the renormalization constants and the  $\beta$  functions. Precisely, the naive scheme for the implementation of the  $\gamma_5$  give rise to incorrect results. One has to supplement it with the relations given in Eqs. (3.10) and (3.11). The first equation takes into account the contributions arising in triangle diagrams containing Dirac fermions, whereas the second one generalizes the contraction properties of the *pseudo* Levi-Civita tensors defined away from  $d = 4$  dimensions.

The results for the three-loop renormalization constants of the gauge coupling constant  $\alpha_s$  are very compact and are given by

$$\begin{aligned}
Z_s = 1 &+ \frac{\alpha_s}{4\pi} \frac{1}{\epsilon} [-3C_A + 2T_f] \\
&+ \left( \frac{\alpha_s}{4\pi} \right)^2 \left\{ \frac{1}{\epsilon^2} [9C_A^2 - 12C_A T_f + 4T_f^2] + \frac{1}{\epsilon} [-3C_A^2 + 2C_A T_f + 4C_R T_f] \right\} \\
&+ \left( \frac{\alpha_s}{4\pi} \right)^3 \left\{ \frac{1}{\epsilon^3} [-27C_A^3 + 54C_A^2 T_f - 36C_A T_f^2 + 8T_f^3] \right. \\
&+ \frac{7}{3\epsilon^2} [9C_A^3 - 12C_A^2 T_f - 12C_A C_R T_f + 4C_A T_f^2 + 8C_R T_f^2] \\
&\left. + \frac{1}{3\epsilon} [-21C_A^3 + 20C_A^2 T_f + 52C_A C_R T_f - 16C_R^2 T_f - 4C_A T_f^2 - 24C_R T_f^2] \right\}, \quad (4.1)
\end{aligned}$$

where we have introduced the notation  $T_f = I_2(R)n_f$ , with  $n_f$  the number of active fermions of the theory and the invariants  $C_R, C_A, I_2(R)$  are explicitly given in the Appendix A.

The case  $T_f = 0$  corresponds to SUSY–Yang–Mills theory that has been treated in detail in sections 2 and 3.3.4. Full agreement has been found between the two methods up to three-loop order.

The three-loop renormalization constants for the gluino mass read

$$\begin{aligned}
Z_{m_{\tilde{g}}} = 1 &+ \frac{\alpha_s}{4\pi} \frac{1}{\epsilon} [-3C_A + 2T_f] \\
&+ \left( \frac{\alpha_s}{4\pi} \right)^2 \left\{ \frac{1}{\epsilon^2} [9C_A^2 - 12C_A T_f + 4T_f^2] + \frac{2}{\epsilon} [-3C_A^2 + 2C_A T_f + 4C_R T_f] \right\} \\
&+ \left( \frac{\alpha_s}{4\pi} \right)^3 \left\{ \frac{1}{\epsilon^3} [-27C_A^3 + 54C_A^2 T_f - 36C_A T_f^2 + 8T_f^3] \right. \\
&+ \frac{4}{\epsilon^2} (9C_A^3 - 12C_A^2 T_f - 12C_A C_R T_f + 4C_A T_f^2 + 8C_R T_f^2) \\
&\left. + \frac{1}{\epsilon} (-21C_A^3 + 20C_A^2 T_f + 52C_A C_R T_f - 16C_R^2 T_f - 4C_A T_f^2 - 24C_R T_f^2) \right\}. \quad (4.2)
\end{aligned}$$

The  $\overline{\text{DR}}$  quark mass renormalization constant is also independent of any mass parameter and is given by the following formula

$$\begin{aligned}
Z_{m_q} = 1 &- \frac{\alpha_s}{4\pi} \frac{1}{\epsilon} 2C_R + \left( \frac{\alpha_s}{4\pi} \right)^2 \left\{ \frac{1}{\epsilon^2} [3C_A C_R + 2C_R^2 - 2C_R T_f] + \frac{1}{\epsilon} [-3C_A C_R + 2C_R^2 + 2C_R T_f] \right\} \\
&+ \left( \frac{\alpha_s}{4\pi} \right)^3 \left\{ \frac{1}{\epsilon^3} \left[ -6C_A^2 C_R - 6C_A C_R^2 - \frac{4}{3}C_R^3 + (8C_A C_R + 4C_R^2)T_f - \frac{8}{3}C_R T_f^2 \right] \right. \\
&\left. + \frac{1}{\epsilon^2} \left[ 10C_A^2 C_R + 2C_A C_R^2 - 4C_R^3 + \left(-\frac{32}{3}C_A C_R - \frac{20}{3}C_R^2\right)T_f + \frac{8}{3}C_R T_f^2 \right] \right\}
\end{aligned}$$

$$\frac{1}{\epsilon} \left[ -4C_A^2 C_R + 4C_A C_R^2 - \frac{16}{3} C_R^3 + \frac{8}{3} C_R T_f^2 + T_f (C_R^2 (\frac{32}{3} - 16\zeta(3)) + C_A C_R (-\frac{4}{3} + 16\zeta(3))) \right] \Big\}, \quad (4.3)$$

where  $\zeta(3)$  is Riemann's zeta function with  $\zeta(3) = 1.20206\dots$ . The results of Eqs. (4.1,4.3,4.2) are in agreement with Refs. [54,55]. Using Eqs. (4.1) and (4.2), it is an easy exercise to confirm the relation derived in Ref. [52] between the anomalous dimension of gluino mass and the gauge  $\beta$ -function that holds also in DRED. This result is similar to the NSVZ relation given in Eq. (2.15) and holds to all orders in perturbation theory. It reads

$$\gamma_n^{\tilde{g}} = (n+1)\beta_n. \quad (4.4)$$

where  $n$  denotes the number of loops.

## 4.2 Renormalization of the squark sector at three loops

In this section, we report on the renormalization of the squark sector of SUSY-QCD up to three loop order within the  $\overline{\text{DR}}$  scheme in the component field approach [146]. These results are on the one side important for the phenomenological analyses aiming to predict the squark masses at the TeV scale with an accuracy of the order of  $\mathcal{O}(50 \text{ GeV})$ , that is required by the precision achieved in the current experimental searches at the LHC. On the other side, they have also genuine theoretical significance, since they provide an independent confirmation of the three-loop results obtained with the help of the NSVZ scheme [45,46,144].

The calculations presented in this section are performed in the framework of SUSY-QCD with  $n_q = 5$  massless quarks and a massive top quark ( $m_t$ ). The scalar super partners of the latter has two mass eigenstates ( $m_{\tilde{t}_1}$  and  $m_{\tilde{t}_2}$ ) which may have different masses and thus a non-vanishing mixing angle occurs. The super partners of the  $n_q$  light quarks are assumed to have degenerate masses ( $m_{\tilde{q}}$ ) and vanishing mixing angles. A generalization to a non-degenerate spectrum is possible in a straightforward way from the formalism for the top squark sector which is discussed in detail in the following.

Unless stated otherwise all parameters in the following derivation are  $\overline{\text{DR}}$  quantities which depend on the renormalization scale  $\mu$ . For the sake of compactness the latter is omitted. Bare quantities are marked by a superscript “(0)”. To define the framework, we start from the bare Lagrangian containing the kinetic energy and the mass terms for the top squarks

$$\mathcal{L}_t^{(0)} = \frac{1}{2} \partial_\mu (\tilde{t}_L^*, \tilde{t}_R^*)^{(0)} \partial^\mu \begin{pmatrix} \tilde{t}_L \\ \tilde{t}_R \end{pmatrix}^{(0)} - \frac{1}{2} (\tilde{t}_L^*, \tilde{t}_R^*)^{(0)} (\mathcal{M}_t^2)^{(0)} \begin{pmatrix} \tilde{t}_L \\ \tilde{t}_R \end{pmatrix}^{(0)}, \quad (4.5)$$

where  $\tilde{t}_L$  and  $\tilde{t}_R$  denote the interaction eigenstates. The top squark mass matrix is given by

$$\begin{aligned} \mathcal{M}_t^2 &= \begin{pmatrix} m_t^2 + M_Z^2 (\frac{1}{2} - \frac{2}{3} \sin^2 \vartheta_W) \cos 2\beta + M_Q^2 & m_t (A_t - \mu_{\text{SUSY}} \cot \beta) \\ m_t (A_t - \mu_{\text{SUSY}} \cot \beta) & m_t^2 + \frac{2}{3} M_Z^2 \sin^2 \vartheta_W \cos 2\beta + M_U^2 \end{pmatrix} \\ &\equiv \begin{pmatrix} m_{\tilde{t}_L}^2 & m_t X_t \\ m_t X_t & m_{\tilde{t}_R}^2 \end{pmatrix} \end{aligned} \quad (4.6)$$

with  $X_t = A_t - \mu_{\text{SUSY}} \cot \beta$ .  $A_t$  is the soft SUSY breaking trilinear coupling, and  $M_{\tilde{U}}$  and  $M_{\tilde{Q}}$  are the soft SUSY breaking masses.

The top squark mass eigenstates are related to the interaction eigenstates through the unitary transformation

$$\begin{pmatrix} \tilde{t}_1 \\ \tilde{t}_2 \end{pmatrix}^{(0)} = \mathcal{R}_{\tilde{t}}^{(0)\dagger} \begin{pmatrix} \tilde{t}_L \\ \tilde{t}_R \end{pmatrix}^{(0)}. \quad (4.7)$$

The unitary matrix  $\mathcal{R}_{\tilde{t}}$  is defined through the diagonalization relation for the mass matrix  $\mathcal{M}_{\tilde{t}}^2$

$$\begin{pmatrix} m_{\tilde{t}_1}^2 & 0 \\ 0 & m_{\tilde{t}_2}^2 \end{pmatrix} = R_{\tilde{t}}^\dagger \mathcal{M}_{\tilde{t}}^2 R_{\tilde{t}}. \quad (4.8)$$

The eigenvalues are the masses of the eigenstates  $\tilde{t}_1$  and  $\tilde{t}_2$ . They read

$$m_{\tilde{t}_{1,2}}^2 = \frac{1}{2} \left[ m_{\tilde{t}_L}^2 + m_{\tilde{t}_R}^2 \mp \sqrt{(m_{\tilde{t}_L}^2 - m_{\tilde{t}_R}^2)^2 + 4m_t^2 X_t^2} \right]. \quad (4.9)$$

The unitary transformation can be parameterized by the mixing angle

$$R_{\tilde{t}} = \begin{pmatrix} \cos \theta_t & -\sin \theta_t \\ \sin \theta_t & \cos \theta_t \end{pmatrix}, \quad (4.10)$$

with

$$\sin(2\theta_t) = \frac{2m_t (A_t - \mu_{\text{SUSY}} \cot \beta)}{m_{\tilde{t}_1}^2 - m_{\tilde{t}_2}^2}. \quad (4.11)$$

The renormalization constants connected to the top squark are extracted from the top squark propagator. At tree-level it is a diagonal  $2 \times 2$  matrix which receives non-diagonal entries at loop-level. In order to be able to write down the renormalized top squark propagator we define the renormalization constants as follows: The wave function renormalization constant is introduced through the relation

$$\begin{pmatrix} \tilde{t}_1 \\ \tilde{t}_2 \end{pmatrix}^{(0)} = \mathcal{Z}_{\tilde{t}}^{1/2} \begin{pmatrix} \tilde{t}_1 \\ \tilde{t}_2 \end{pmatrix}, \quad \text{with} \quad \mathcal{Z}_{\tilde{t}}^{1/2} = \begin{pmatrix} Z_{11}^{1/2} & Z_{12}^{1/2} \\ Z_{21}^{1/2} & Z_{22}^{1/2} \end{pmatrix}, \quad (4.12)$$

where it holds  $\mathcal{Z}_{\tilde{t}}^{1/2} = \mathbf{I} + \mathcal{O}(\alpha_s)$ .

In case of SUSY-QCD, the matrix  $\mathcal{Z}_{\tilde{t}}^{1/2}$  has a particularly symmetric form. This can be derived from the observation that the left- and right-handed components of the top squark fields have the same renormalization constant for their wave functions within SUSY-QCD

$$\begin{pmatrix} \tilde{t}_L \\ \tilde{t}_R \end{pmatrix}^{(0)} = \tilde{Z}_2^{1/2} \begin{pmatrix} \tilde{t}_L \\ \tilde{t}_R \end{pmatrix}. \quad (4.13)$$

Furthermore, if we introduce the renormalization constant for the mixing angle via

$$\theta_t^{(0)} = \theta_t + \delta\theta_t. \quad (4.14)$$

and make use of Eq. (4.7) we obtain

$$\mathcal{Z}_t^{1/2} = \tilde{Z}_2^{1/2} \begin{pmatrix} \cos \delta\theta_t & \sin \delta\theta_t \\ -\sin \delta\theta_t & \cos \delta\theta_t \end{pmatrix}. \quad (4.15)$$

When supersymmetric electroweak (SUSY-EW) corrections are taken into account, Eq. (4.13) becomes

$$\begin{pmatrix} \tilde{t}_L \\ \tilde{t}_R \end{pmatrix}^{(0)} = \begin{pmatrix} \tilde{Z}_L^{1/2} & 0 \\ 0 & \tilde{Z}_R^{1/2} \end{pmatrix} \begin{pmatrix} \tilde{t}_L \\ \tilde{t}_R \end{pmatrix}. \quad (4.16)$$

This assignment takes into account supersymmetric constraints [147] and is sufficient to absorb all divergences. As a consequence also the matrix  $\mathcal{Z}_t^{1/2}$  has a more complicated structure and additional renormalization conditions are required.

Furthermore, the mass matrix Eq. (4.6) has to be renormalized. It can be parameterized as follows

$$\begin{pmatrix} (m_{\tilde{t}_1}^{(0)})^2 & 0 \\ 0 & (m_{\tilde{t}_2}^{(0)})^2 \end{pmatrix} \rightarrow \begin{pmatrix} m_{11}^2 Z_{m_{11}} & m_{12}^2 Z_{m_{12}} \\ m_{21}^2 Z_{m_{21}} & m_{22}^2 Z_{m_{22}} \end{pmatrix} \equiv \mathcal{M}, \quad (4.17)$$

where we require that the off-diagonal elements in the renormalized mass matrix vanish. This ensures that the renormalized fields are the true mass eigenstates. As a consequence, the counter-term  $\delta\theta_t$  takes care of the divergences in the self-energy contribution where a  $\tilde{t}_1$  transforms into a  $\tilde{t}_2$  or vice versa. This can be seen in the explicit formulae given below. The diagonal elements of Eq. (4.17) can be identified with the renormalization constants of the masses

$$(m_{\tilde{t}_i}^{(0)})^2 = m_{ii}^2 Z_{m_{ii}} = m_{\tilde{t}_i}^2 Z_{m_{\tilde{t}_i}}. \quad (4.18)$$

In order to formulate the renormalization conditions it is convenient to consider the renormalized inverse top squark propagator given by

$$i\mathcal{S}^{-1}(p^2) = p^2 \left( \mathcal{Z}_t^{1/2} \right)^\dagger \mathcal{Z}_t^{1/2} - \left( \mathcal{Z}_t^{1/2} \right)^\dagger [\mathcal{M} - \Sigma(p^2)] \mathcal{Z}_t^{1/2} \quad (4.19)$$

where

$$\Sigma(p^2) = \begin{pmatrix} \Sigma_{11}(p^2) & \Sigma_{12}(p^2) \\ \Sigma_{21}(p^2) & \Sigma_{22}(p^2) \end{pmatrix}, \quad (4.20)$$

stands for the matrix of the squark self energies in the mass eigenstate basis.

In the  $\overline{\text{DR}}$  scheme the renormalization conditions read

$$\mathcal{S}_{ij}^{-1}(p^2) \Big|_{\text{pp}} = 0, \quad (4.21)$$

where “pp” stands for the “pole part”.

In order to obtain explicit formulae for the evaluation of the renormalization constants it is convenient to define perturbative expansions of the quantities entering Eq. (4.21). Up to three-loop order we have

$$\begin{aligned} Z_k &= 1 + \left(\frac{\alpha_s}{\pi}\right) \delta Z_k^{(1)} + \left(\frac{\alpha_s}{\pi}\right)^2 \delta Z_k^{(2)} + \left(\frac{\alpha_s}{\pi}\right)^3 \delta Z_k^{(3)} + \mathcal{O}(\alpha_s^4), \\ \delta\theta_t &= \left(\frac{\alpha_s}{\pi}\right) \delta\theta_t^{(1)} + \left(\frac{\alpha_s}{\pi}\right)^2 \delta\theta_t^{(2)} + \left(\frac{\alpha_s}{\pi}\right)^3 \delta\theta_t^{(3)} + \mathcal{O}(\alpha_s^4), \\ \Sigma_{ij} &= \left(\frac{\alpha_s}{\pi}\right) \Sigma_{ij}^{(1)} + \left(\frac{\alpha_s}{\pi}\right)^2 \Sigma_{ij}^{(2)} + \left(\frac{\alpha_s}{\pi}\right)^3 \Sigma_{ij}^{(3)} + \mathcal{O}(\alpha_s^4), \end{aligned} \quad (4.22)$$

where  $i, j \in \{1, 2\}$  and  $k \in \{2, m_{\tilde{t}_1}, m_{\tilde{t}_2}\}$ . Inserting these equations into (4.19) one can solve Eq. (4.21) iteratively order-by-order in  $\alpha_s$ . At one-loop order one gets

$$\begin{aligned} \left\{ \Sigma_{ii}^{(1)} - m_{\tilde{t}_i}^2 \left( \delta\tilde{Z}_2^{(1)} + \delta Z_{m_{\tilde{t}_i}}^{(1)} \right) + p^2 \delta\tilde{Z}_2^{(1)} \right\} \Big|_{\text{pp}} &= 0, \quad i = 1, 2, \\ \left\{ \Sigma_{12}^{(1)} - \delta\theta_t^{(1)} \left( m_{\tilde{t}_1}^2 - m_{\tilde{t}_2}^2 \right) \right\} \Big|_{\text{pp}} &= 0. \end{aligned} \quad (4.23)$$

The terms proportional to  $p^2$  in the first equation of (4.23) are used to compute the wave function renormalization constant which is independent of all occurring masses. Thus they can be set to zero and one obtains

$$\delta\tilde{Z}_2^{(1)} = -\frac{1}{p^2} \Sigma_{11}^{(1)}(p^2) \Big|_{\text{pp}} = -\frac{1}{p^2} \Sigma_{22}^{(1)}(p^2) \Big|_{\text{pp}}. \quad (4.24)$$

Once  $\delta\tilde{Z}_2^{(1)}$  is known Eq. (4.23) is used to obtain  $\delta Z_{m_{\tilde{t}_i}}^{(1)}$  keeping the mass dependence in  $\Sigma_{ii}^{(1)}$  (see below for more details). The second equation of (4.23) is used to obtain the renormalization constant of the mixing angle via

$$\delta\theta_t^{(1)} = \frac{\Sigma_{12}^{(1)}}{m_{\tilde{t}_1}^2 - m_{\tilde{t}_2}^2} \Big|_{\text{pp}}. \quad (4.25)$$

Proceeding to two loops we obtain the equations

$$\begin{aligned} &\left[ \Sigma_{ii}^{(2)} + \delta\tilde{Z}_2^{(1)} \Sigma_{ii}^{(1)} - m_{\tilde{t}_i}^2 \left( \delta\tilde{Z}_2^{(2)} + \delta\tilde{Z}_2^{(1)} \delta Z_{m_{\tilde{t}_i}}^{(1)} + \delta Z_{m_{\tilde{t}_i}}^{(2)} \right) + \delta\tilde{Z}_2^{(2)} p^2 \right. \\ &\quad \left. + (-1)^{(i+1)} \delta\theta_t^{(1)} \left( -2\Sigma_{12}^{(1)} + \delta\theta_t^{(1)} (m_{\tilde{t}_1}^2 - m_{\tilde{t}_2}^2) \right) \right] \Big|_{\text{pp}} = 0, \quad i = 1, 2, \end{aligned} \quad (4.26)$$

$$\begin{aligned} &\left[ -\delta\theta_t^{(2)} (m_{\tilde{t}_1}^2 - m_{\tilde{t}_2}^2) - \delta\theta_t^{(1)} \delta\tilde{Z}_2^{(1)} (m_{\tilde{t}_1}^2 - m_{\tilde{t}_2}^2) - \delta\theta_t^{(1)} \delta Z_{m_{\tilde{t}_1}}^{(1)} m_{\tilde{t}_1}^2 + \delta\theta_t^{(1)} \delta Z_{m_{\tilde{t}_2}}^{(1)} m_{\tilde{t}_2}^2 \right. \\ &\quad \left. + \delta\theta_t^{(1)} \Sigma_{11}^{(1)} - \delta\theta_t^{(1)} \Sigma_{22}^{(1)} + \delta\tilde{Z}_2^{(1)} \Sigma_{12}^{(1)} + \Sigma_{12}^{(2)} \right] \Big|_{\text{pp}} = 0, \end{aligned} \quad (4.27)$$

which are solved for  $\tilde{Z}_2^{(2)}$ ,  $\delta Z_{m_{\tilde{t}_i}}^{(2)}$  and  $\delta\theta_t^{(2)}$  using the same strategy as at one-loop level.

Similarly, at three-loop order we have

$$\begin{aligned} & \left[ (-1)^{i+1} \left\{ \left( \delta\theta_t^{(1)} \right)^2 \left( \delta\tilde{Z}_2^{(1)} (m_{\tilde{t}_1}^2 - m_{\tilde{t}_2}^2) + \delta Z_{m_{\tilde{t}_1}}^{(1)} m_{\tilde{t}_1}^2 - \delta Z_{m_{\tilde{t}_2}}^{(1)} m_{\tilde{t}_2}^2 - \Sigma_{11}^{(1)} + \Sigma_{22}^{(1)} \right) \right. \right. \\ & \quad \left. \left. + \delta\theta_t^{(1)} \left( 2\delta\theta_t^{(2)} (m_{\tilde{t}_1}^2 - m_{\tilde{t}_2}^2) - 2\delta\tilde{Z}_2^{(1)} \Sigma_{12}^{(1)} - 2\Sigma_{12}^{(2)} \right) - 2\delta\theta_t^{(2)} \Sigma_{12}^{(1)} \right\} \right. \\ & \quad \left. + \delta\tilde{Z}_2^{(1)} \left( \Sigma_{ii}^{(2)} - \delta Z_{m_{\tilde{t}_i}}^{(2)} m_{\tilde{t}_i}^2 \right) - \delta\tilde{Z}_2^{(2)} \delta Z_{m_{\tilde{t}_i}}^{(1)} m_{\tilde{t}_i}^2 + \delta\tilde{Z}_2^{(2)} \Sigma_{ii}^{(1)} - \delta\tilde{Z}_2^{(3)} m_{\tilde{t}_i}^2 + \delta\tilde{Z}_2^{(3)} p^2 \right. \\ & \quad \left. - \delta Z_{m_{\tilde{t}_i}}^{(3)} m_{\tilde{t}_i}^2 + \Sigma_{ii}^{(3)} \right] \Big|_{\text{pp}} = 0, \quad i = 1, 2, \end{aligned} \quad (4.28)$$

$$\begin{aligned} & \left[ \delta\theta_t^{(1)} \left( -\delta\tilde{Z}_2^{(1)} \delta Z_{m_{\tilde{t}_1}}^{(1)} m_{\tilde{t}_1}^2 + \delta\tilde{Z}_2^{(1)} \delta Z_{m_{\tilde{t}_2}}^{(1)} m_{\tilde{t}_2}^2 + \delta\tilde{Z}_2^{(1)} \Sigma_{11}^{(1)} - \delta\tilde{Z}_2^{(1)} \Sigma_{22}^{(1)} \right. \right. \\ & \quad \left. \left. - \delta\tilde{Z}_2^{(2)} (m_{\tilde{t}_1}^2 - m_{\tilde{t}_2}^2) - \delta Z_{m_{\tilde{t}_1}}^{(2)} m_{\tilde{t}_1}^2 + \delta Z_{m_{\tilde{t}_2}}^{(2)} m_{\tilde{t}_2}^2 + \Sigma_{11}^{(2)} - \Sigma_{22}^{(2)} \right) \right. \\ & \quad \left. + \delta\theta_t^{(2)} \left( -\delta\tilde{Z}_2^{(1)} (m_{\tilde{t}_1}^2 - m_{\tilde{t}_2}^2) - \delta Z_{m_{\tilde{t}_1}}^{(1)} m_{\tilde{t}_1}^2 + \delta Z_{m_{\tilde{t}_2}}^{(1)} m_{\tilde{t}_2}^2 + \Sigma_{11}^{(1)} - \Sigma_{22}^{(1)} \right) \right. \\ & \quad \left. - \delta\theta_t^{(3)} (m_{\tilde{t}_1}^2 - m_{\tilde{t}_2}^2) + \delta\tilde{Z}_2^{(1)} \Sigma_{12}^{(2)} + \delta\tilde{Z}_2^{(2)} \Sigma_{12}^{(1)} + \Sigma_{12}^{(3)} + \frac{2}{3} \left( \delta\theta_t^{(1)} \right)^3 (m_{\tilde{t}_1}^2 - m_{\tilde{t}_2}^2) \right. \\ & \quad \left. - 2 \left( \delta\theta_t^{(1)} \right)^2 \Sigma_{12}^{(1)} \right] \Big|_{\text{pp}} = 0. \end{aligned} \quad (4.29)$$

Sample diagrams contributing to  $\Sigma_{11}$  up to three loops can be found in Fig. 4.2; the contributions to  $\Sigma_{12}$  and  $\Sigma_{22}$  look very similar. Once the quantities  $\Sigma_{11}$ ,  $\Sigma_{12}$  and  $\Sigma_{22}$  are known to three-loop order it is possible to extract the renormalization constants for the squark wave function and mass and the mixing angle from Eqs. (4.28) and (4.29).

As compared to the corresponding self-energy contributions for fermions or gauge bosons, which after proper projection only lead to logarithmically divergent integrals, the quantities in the above equations have mass dimension two. As a consequence the renormalization constants of the squark masses and the mixing angles depend on the occurring masses, even in a minimal subtraction scheme like  $\overline{\text{DR}}$ . At three-loop order an exact evaluation of the corresponding integrals is not possible. It is nevertheless possible to reconstruct the complete dependence on the occurring masses using repeated asymptotic expansions and in addition some knowledge about the structure of the final result. Thus, one has to keep during the calculation non vanishing squark, gluino and the top quark masses and chose convenient hierarchies between them. For the asymptotic expansion (see, e.g., Ref. [136]) one can use `exp` [128,129]. As a result only one-scale integrals up to three loops appear which can be evaluated with the packages `MINCER` [100] and `MATAD` [109].

After the calculation of the bare self energies one has to renormalize all occurring parameters in the  $\overline{\text{DR}}$  scheme. For the three-loop calculation one needs the counter-terms for  $\alpha_s$ ,  $m_t$ ,  $m_{\tilde{g}}$ ,  $m_{\tilde{t}_i}$ ,

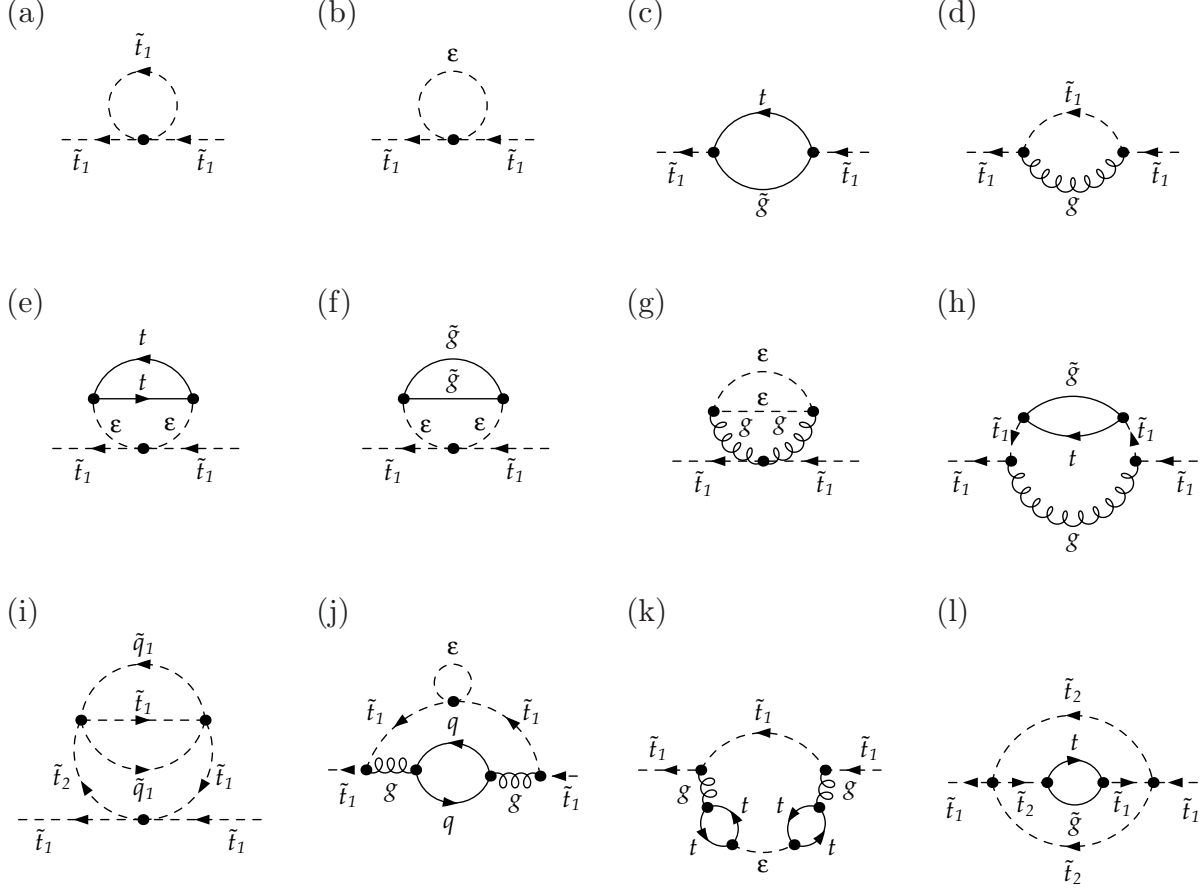


Figure 4.2: Sample diagrams contributing to  $\Sigma_{11}$  at one, two and three loops. The symbols  $t$ ,  $\tilde{t}_i$ ,  $g$ ,  $\tilde{g}$  and  $\epsilon$  denote top quarks, top squarks, gluons, gluinos, and  $\epsilon$  scalars, respectively.

$\theta_t$  and  $m_\epsilon$  to two-loop order and the one for  $m_{\tilde{q}}$  to one-loop approximation. Furthermore, also the QCD gauge parameter has to be renormalized to two loops since it appears in the results for the wave function anomalous dimensions.

At this point some comments on the treatment of the  $\epsilon$  scalar mass,  $m_\epsilon$ , are in order. In practice there are two renormalization schemes for  $m_\epsilon$  which are frequently used, the  $\overline{\text{DR}}$  and on-shell scheme. In the latter one requires that the renormalized mass vanishes in each order in perturbation theory whereas in the  $\overline{\text{DR}}$  prescription only the pole parts are subtracted by the renormalization constant. In the  $\overline{\text{DR}}$  scheme it is important to keep  $m_\epsilon$  different from zero since the renormalization group equations for the squark masses and  $m_\epsilon$  are coupled. A non-vanishing  $\epsilon$ -scalar mass in intermediate steps is also required for the computation of the anomalous dimensions in the  $\overline{\text{DR}}'$  scheme [148] (see below) which was constructed in order to disentangle the running of  $m_\epsilon$  from the one of the squark parameters.

In the following, we present only the results derived in the scheme where the  $\epsilon$  scalar mass is renormalized in  $\overline{\text{DR}}$  scheme. The two-loop results for the renormalization constants of the top

squark mass  $m_{\tilde{t}_1}$  read

$$\begin{aligned}
m_{\tilde{t}_1}^2 \delta Z_{m_{\tilde{t}_1}}^{(1)} &= C_R \left( -m_{\tilde{g}}^2 - m_t^2 + m_{\tilde{g}} m_t s_{2t} + \frac{m_{\tilde{t}_2}^2 - m_{\tilde{t}_1}^2}{4} s_{2t}^2 \right) \frac{1}{\epsilon}, \\
m_{\tilde{t}_1}^2 \delta Z_{m_{\tilde{t}_1}}^{(2)} &= \left\{ C_R^2 \left[ \frac{c_{2t}^2 m_{\tilde{g}}^2 m_t^2}{m_{\tilde{t}_1}^2 - m_{\tilde{t}_2}^2} + \frac{(1 + c_{2t}^2) s_{2t}^2 (m_{\tilde{t}_1}^2 - m_{\tilde{t}_2}^2) + 8m_t^2}{16} - \frac{(1 + c_{2t}^2) m_{\tilde{g}} m_t s_{2t}}{2} \right] \right. \\
&\quad + C_A C_R \left[ \frac{9m_{\tilde{g}}^2}{8} + 3 \frac{s_{2t}^2 (m_{\tilde{t}_1}^2 - m_{\tilde{t}_2}^2) + 4m_t^2}{32} - \frac{3m_{\tilde{g}} m_t s_{2t}}{4} \right] \\
&\quad + C_R T_f \left[ \frac{-3m_{\tilde{g}}^2}{4} - \frac{s_{2t}^2 (m_{\tilde{t}_1}^2 - m_{\tilde{t}_2}^2) + 4m_t^2}{16} + \frac{m_{\tilde{g}} m_t s_{2t}}{2} \right] \left. \right\} \frac{1}{\epsilon^2} \\
&\quad + \left\{ C_R^2 \left[ \frac{3m_{\tilde{g}}^2}{4} + \frac{s_{2t}^2 (m_{\tilde{t}_1}^2 - m_{\tilde{t}_2}^2) + 4m_t^2}{16} - \frac{m_{\tilde{g}} m_t s_{2t}}{2} \right] \right. \\
&\quad + C_A C_R \left[ \frac{-11m_{\tilde{g}}^2}{8} - 3 \frac{s_{2t}^2 (m_{\tilde{t}_1}^2 - m_{\tilde{t}_2}^2) + 4m_t^2}{32} + \frac{3m_{\tilde{g}} m_t s_{2t}}{4} \right] \\
&\quad + C_R T_q \left[ \frac{3m_{\tilde{g}}^2}{4} + \frac{s_{2t}^2 (m_{\tilde{t}_1}^2 - m_{\tilde{t}_2}^2) + 8m_{\tilde{q}}^2 + 4m_t^2}{16} - \frac{m_{\tilde{g}} m_t s_{2t}}{2} \right] \\
&\quad + C_R T_t \left[ \frac{3m_{\tilde{g}}^2}{4} + \frac{s_{2t}^2 (m_{\tilde{t}_1}^2 - m_{\tilde{t}_2}^2) + 4m_{\tilde{t}_1}^2 + 4m_{\tilde{t}_2}^2 - 4m_t^2}{16} - \frac{m_{\tilde{g}} m_t s_{2t}}{2} \right] \left. \right\} \frac{1}{\epsilon} \\
&\quad + m_\epsilon^2 \left( -C_A C_R \frac{3}{8} + C_R T_f \frac{1}{4} \right) \frac{1}{\epsilon}, \tag{4.30}
\end{aligned}$$

where we have introduced the abbreviations  $T_l = n_l I_2(R)$ , with  $l = f, q, t$  and  $c_{nt} = \cos(n\theta_t)$  and  $s_{nt} = \sin(n\theta_t)$ .  $n_q$  denotes the number of light quark flavours and takes in this case the value  $n_q = 5$ .  $n_t = 1$  has been introduced for convenience and it holds  $n_f = n_q + n_t$ . Furthermore  $m_\epsilon$  denotes the  $\overline{\text{DR}}$  renormalized  $\epsilon$ -scalar mass. The corresponding results for  $m_{\tilde{t}_2}$  can be derived from Eq. (4.30) by interchanging  $m_{\tilde{t}_1}$  and  $m_{\tilde{t}_2}$  and changing the sign of  $\theta_t$ .

Finally, for the mixing angle we have

$$\begin{aligned}
(m_{\tilde{t}_1}^2 - m_{\tilde{t}_2}^2) \delta \theta_t^{(1)} &= C_R c_{2t} \left( m_{\tilde{g}} m_t - \frac{s_{2t} (m_{\tilde{t}_1}^2 - m_{\tilde{t}_2}^2)}{4} \right) \frac{1}{\epsilon}, \\
(m_{\tilde{t}_1}^2 - m_{\tilde{t}_2}^2) \delta \theta_t^{(2)} &= \left\{ C_R^2 c_{2t} \left[ (s_{2t}^2 - c_{2t}^2) \left( \frac{m_{\tilde{g}} m_t}{2} - \frac{s_{2t} (m_{\tilde{t}_1}^2 - m_{\tilde{t}_2}^2)}{16} \right) - \frac{2s_{2t} m_{\tilde{g}}^2 m_t^2}{m_{\tilde{t}_1}^2 - m_{\tilde{t}_2}^2} \right] \right. \\
&\quad + C_R C_A c_{2t} \left[ \frac{-3m_{\tilde{g}} m_t}{4} + \frac{3s_{2t} (m_{\tilde{t}_1}^2 - m_{\tilde{t}_2}^2)}{32} \right] + C_R T_f c_{2t} \left[ \frac{m_{\tilde{g}} m_t}{2} - \frac{s_{2t} (m_{\tilde{t}_1}^2 - m_{\tilde{t}_2}^2)}{16} \right] \left. \right\} \frac{1}{\epsilon^2} \\
&\quad + \left\{ C_R^2 c_{2t} \left[ -\frac{m_{\tilde{g}} m_t}{2} + \frac{s_{2t} (m_{\tilde{t}_1}^2 - m_{\tilde{t}_2}^2)}{16} \right] + C_R C_A c_{2t} \left[ \frac{3m_{\tilde{g}} m_t}{4} - \frac{3s_{2t} (m_{\tilde{t}_1}^2 - m_{\tilde{t}_2}^2)}{32} \right] \right. \\
&\quad + C_R T_f c_{2t} \left[ -\frac{m_{\tilde{g}} m_t}{2} + \frac{s_{2t} (m_{\tilde{t}_1}^2 - m_{\tilde{t}_2}^2)}{16} \right] \left. \right\} \frac{1}{\epsilon}. \tag{4.31}
\end{aligned}$$

The three-loop results are also available in electronic form [146], but they are too lengthy to be explicitly given in this review.



In the case of degenerate squark masses, one can take naively the limit  $m_{\tilde{t}_2} \rightarrow m_{\tilde{t}_1}$  in Eqs. (4.30). Furthermore one has to nullify the mixing angle. The quantities  $\delta\theta_t^{(1,2)}$  are not defined in the mass-degenerate case which is reflected by the fact that the limit  $m_{\tilde{t}_2} \rightarrow m_{\tilde{t}_1}$  does not exist in Eqs. (4.31).

For completeness let us also provide the three-loop result for mass-degenerate squarks which is given by

$$\begin{aligned}
m_{\tilde{q}}^2 Z_{m_{\tilde{q}}} = & m_{\tilde{q}}^2 - \frac{\alpha_s}{\pi} \frac{1}{\epsilon} C_R m_{\tilde{g}}^2 + \left(\frac{\alpha_s}{\pi}\right)^2 \frac{1}{16} \left\{ \frac{2}{\epsilon^2} C_R (9C_A - 6T_f) m_{\tilde{g}}^2 \right. \\
& + \frac{1}{\epsilon} \left[ 4C_R [2T_q m_{\tilde{q}}^2 + T_t (m_{\tilde{t}_1}^2 + m_{\tilde{t}_2}^2 - 2M_t^2)] \right. \\
& + [2C_R (-11C_A + 6C_R) + 12C_R T_f] m_{\tilde{g}}^2 + (-6C_A C_R + 4C_R T_f) m_{\tilde{\epsilon}}^2 \left. \right] \left. \right\} \\
& \left(\frac{\alpha_s}{\pi}\right)^3 \frac{1}{64} \left\{ \frac{8}{\epsilon^3} C_R \left[ -9C_A^2 + 12C_A T_f - 4T_f^2 \right] m_{\tilde{g}}^2 + \frac{1}{\epsilon^2} \left[ 8C_R T_q (-3C_A + 2T_f) M_{\tilde{q}}^2 \right. \right. \\
& + 4C_R T_f (-3C_A + 2T_f) (m_{\tilde{t}_1}^2 + m_{\tilde{t}_2}^2 - 2M_t^2) + 2C_R (3C_A - 2T_f)^2 m_{\tilde{\epsilon}}^2 \left. \right] + \\
& + \frac{1}{\epsilon} \left[ C_R (5C_A - 2C_R + 2T_f) [T_q M_{\tilde{q}}^2 + 4T_t (m_{\tilde{t}_1}^2 + m_{\tilde{t}_2}^2 - 2M_t^2)] \right. \\
& + 8C_R m_{\tilde{g}}^2 [-10C_A^2 + 7C_A C_R - 8C_R^2 + 4T_f^2 + 6T_f C_R (3 - 4\zeta(3)) + 24T_f C_A \zeta(3)] \\
& \left. \left. + 2C_R (3C_A - 2T_f) (-5C_A + 2C_R + 2T_f) m_{\tilde{\epsilon}}^2 \right] \right\}, \tag{4.32}
\end{aligned}$$

where we have used the above mentioned abbreviations  $T_l = n_l I_2(R)$ , with  $l = f, q, t$ . The terms that do not involve  $T_t$  can be obtained from  $Z_{m_{\tilde{t}_1}}$  by setting  $m_{\tilde{t}_2} = m_{\tilde{t}_1}$ ,  $m_t = 0$  and  $\theta_t = 0$ .

As mentioned before, the  $\epsilon$  scalar mass needs to be renormalized at two loops within the  $\overline{\text{DR}}$  scheme, in order to obtain the three-loop renormalization constants for squark masses and mixing angles. The corresponding renormalization constant is given by

$$\begin{aligned}
Z_{m_{\tilde{\epsilon}}} = & 1 + \frac{\alpha_s}{\pi} \frac{1}{\epsilon} \left\{ -\frac{3}{4} C_A + \frac{1}{2} T_f + \left[ -\frac{C_A}{2} m_{\tilde{g}}^2 + 2T_q m_{\tilde{q}}^2 + T_t (m_{\tilde{t}_1}^2 + m_{\tilde{t}_2}^2 - 2m_t^2) \right] \frac{1}{2m_{\tilde{\epsilon}}^2} \right\} \\
& + \left(\frac{\alpha_s}{\pi}\right)^2 \left\{ \frac{1}{\epsilon^2} \left[ \frac{9}{16} C_A^2 - \frac{3}{4} C_A T_f + \frac{1}{4} T_f^2 + \left( \frac{3C_A^2 - 2C_A T_f - 2C_R T_f}{4} m_{\tilde{g}}^2 \right. \right. \right. \\
& \left. \left. - \frac{3C_A T_q - 2T_f T_q}{4} m_{\tilde{q}}^2 - \frac{3C_A T_t - 2T_f T_t}{8} (m_{\tilde{t}_1}^2 + m_{\tilde{t}_2}^2 - 2m_t^2) \right) \frac{1}{m_{\tilde{\epsilon}}^2} \right] \\
& \frac{1}{\epsilon} \left[ -\frac{3}{8} C_A^2 + \frac{1}{4} C_A T_f + \left( -\frac{5C_A^2 - 2C_A T_f - 4C_R T_f}{8} m_{\tilde{g}}^2 \right. \right. \\
& \left. \left. + \frac{C_A T_q}{2} m_{\tilde{q}}^2 + \frac{C_A T_t}{4} (m_{\tilde{t}_1}^2 + m_{\tilde{t}_2}^2 - 2m_t^2) \right) \frac{1}{m_{\tilde{\epsilon}}^2} \right] \left. \right\}. \tag{4.33}
\end{aligned}$$

Let us detail at this point on the choice of scheme. When computing the anomalous dimensions for the physical parameters, one has to consider the combined set of differential equations of all  $\overline{\text{DR}}$  parameters appearing in the corresponding renormalization constants. This concerns in particular the unphysical  $\epsilon$ -scalar mass which means that although  $m_{\tilde{\epsilon}}$  is set to zero at one

scale it is different from zero once this scale is changed. A way out from this situation is to renormalize the  $\epsilon$  scalar mass on-shell and set the renormalized mass  $M_\epsilon$  to zero. However, this scheme might become quite involved in practice, because of the on shell two-loop diagrams that have to be computed. Alternatively one could shift the squark masses by a finite term which is chosen such that the  $\epsilon$  scalar decouples from the system of differential equations. The resulting renormalization scheme is called  $\overline{\text{DR}}'$  scheme and has been suggested in Ref. [148]. For this calculation the finite shift is needed up to two loops and is given by [138,148]

$$m_{\tilde{f}}^2 \rightarrow m_{\tilde{f}}^2 - \frac{\alpha_s}{\pi} \frac{1}{2} C_F m_\epsilon^2 + \left(\frac{\alpha_s}{\pi}\right)^2 C_F m_\epsilon^2 \left( \frac{1}{4} T_f (n_q + n_t) + \frac{1}{4} C_F - \frac{3}{8} C_A \right), \quad (4.34)$$

where  $f = t$  or  $f = q$ .

At the end of this section we want to discuss briefly the numerical impact of the higher order corrections on the squark masses. If one chooses the SUSY mass parameters of the order of  $\mathcal{O}(1 \text{ TeV})$ , one observes a moderate shift of a few GeV when going from one to two loops. After switching on the three-loop terms, however, the squark masses are decreased by about 40 GeV which is approximately an order of magnitude larger than the two-loop corrections. Nevertheless it corresponds to a shift in the masses of about 3% which is a reasonable amount for a three-loop SUSY-QCD term. Our observation coincides with the findings of Ref. [144] where also relatively large three-loop corrections for the squarks have been identified.

## 5 The SM gauge beta functions to three loops

In this section we report on the recent calculation of the three-loop gauge beta functions of the SM. In contrast to the supersymmetric theories, the SM beta functions to three loops have been computed only last year. At this point, it becomes probably clear the importance of all order relations for the anomalous dimensions of supersymmetric theories valid in special regularization schemes. In the absence of SUSY and its holomorphic properties, one has to derive the anomalous dimension from a pure diagrammatic computation, which at the three-loop level becomes computationally quite involved.

The SM beta functions are important tools that allow us to relate theory predictions for various parameters at different energy scales. An important example in this respect is the inspection of the gauge coupling unification at high energies, for which precise experimental data of the couplings at the electroweak scale combined with accurate calculations of the RGEs yields precise predictions.

The computation of the beta functions of gauge theories has a long history. The one-loop beta functions in gauge theories along with the discovery of asymptotic freedom have been presented in Refs. [5,149]. The computation of the corresponding two-loop corrections followed a few years later in a series of papers. Namely, for gauge theories without fermions the results were computed in Refs. [150,151], those for gauge theories with fermions neglecting Yukawa couplings in Refs. [152–154] and considering also Yukawa couplings in Ref. [155]. The two-loop gauge coupling beta functions in an arbitrary quantum field theory have been considered in Ref. [156,157]. At the three-loop order, the first computed contributions to the gauge beta functions were those induced through the scalar self-interactions in Refs. [107,108]. An important

contribution to the field was the computation of the three-loop beta function in QCD [95, 96]. Yukawa contributions to it have been obtained in Ref. [158]. The generalization of these results to a general quantum field theory based on a single gauge group has been achieved in Ref. [87]. For QCD, even the four-loop corrections are known from Refs. [104, 106]. In the following we concentrate on the calculation of the beta functions for the three gauge couplings of the SM up to three loops in the  $\overline{\text{MS}}$  scheme. They have been computed for the first time in Ref [99] and confirmed by an independent calculation in Ref. [159].

Let us in a first step fix the notation. We denote the three gauge couplings by  $\alpha_1$ ,  $\alpha_2$  and  $\alpha_3$  and adopt a  $SU(5)$ -like normalization. They are related to the quantities usually used in the SM by the all-order relations

$$\begin{aligned}\alpha_1 &= \frac{5}{3} \frac{\alpha_{\text{QED}}}{\cos^2 \theta_W}, \\ \alpha_2 &= \frac{\alpha_{\text{QED}}}{\sin^2 \theta_W}, \\ \alpha_3 &= \alpha_s,\end{aligned}\tag{5.35}$$

where  $\alpha_{\text{QED}}$  is the fine structure constant,  $\theta_W$  the weak mixing angle and  $\alpha_s$  the strong coupling.

The SM Yukawa interactions are described by (see, e.g., Chapter 11 of Ref. [160])

$$\mathcal{L}_{\text{Yukawa}} = -\bar{Q}_i^L Y_{ij}^U \epsilon H^\star u_j^R - \bar{Q}_i^L Y_{ij}^D H d_j^R - \bar{L}_i^L Y_{ij}^L H l_j^R + \text{h.c.},\tag{5.36}$$

where  $Y^{U,D,L}$  are complex  $3 \times 3$  matrices,  $i, j$  are generation labels,  $H$  denotes the Higgs field and  $\epsilon$  is the  $2 \times 2$  antisymmetric tensor.  $Q^L, L^L$  are the left-handed quark and lepton doublets, and  $u^R, d^R, l^R$  are the right-handed up- and down-type quark and lepton singlets, respectively. The physical mass-eigenstates are obtained by diagonalizing  $Y^{U,D,L}$  by six unitary matrices  $V_{L,R}^{U,D,L}$  as follows

$$\tilde{Y}_{\text{diag}}^f = V_L^f Y^f V_R^{f\dagger}, \quad f = U, D, L.\tag{5.37}$$

As a result the charged-current  $W^\pm$  couples to the physical quark states with couplings parametrized by the Cabibbo-Kobayashi-Maskawa (CKM) matrix  $V_{CKM} \equiv V_L^U V_L^{D\dagger}$ . We furthermore introduce the notation

$$\hat{T} = \frac{1}{4\pi} Y^U Y^{U\dagger}, \quad \hat{B} = \frac{1}{4\pi} Y^D Y^{D\dagger}, \quad \hat{L} = \frac{1}{4\pi} Y^L Y^{L\dagger}.\tag{5.38}$$

Of course, only traces over products of Yukawa matrices can occur because they arise from closed fermion loops. Using Eqs. (5.37) and (5.38) it is straightforward to see that only traces of diagonal matrices have to be taken except for  $\text{tr} \hat{T} \hat{B}$  which is given by

$$\text{tr} \hat{T} \hat{B} = \text{tr} \left[ \begin{pmatrix} \alpha_u & 0 & 0 \\ 0 & \alpha_c & 0 \\ 0 & 0 & \alpha_t \end{pmatrix} V_{CKM} \begin{pmatrix} \alpha_d & 0 & 0 \\ 0 & \alpha_s & 0 \\ 0 & 0 & \alpha_b \end{pmatrix} V_{CKM}^\dagger \right].\tag{5.39}$$

The Yukawa couplings are related to the SM parameters via the tree-level relations

$$\alpha_x = \frac{\alpha_{\text{QED}} m_x^2}{2 \sin^2 \theta_W M_W^2}, \quad \text{with } x = t, b, \tau, c, s, \dots,\tag{5.40}$$

where  $m_x$  and  $M_W$  are the fermion and W boson mass, respectively.

We denote the Higgs boson self-coupling by  $\hat{\lambda}$ , where the Lagrange density contains the following term

$$\mathcal{L} = \dots - (4\pi\hat{\lambda})(H^\dagger H)^2 + \dots \quad (5.41)$$

describing the quartic Higgs boson self-interaction.

The beta functions are obtained by calculating the renormalization constants relating bare and renormalized couplings via the relation

$$\alpha_i^{\text{bare}} = \mu^{2\epsilon} Z_{\alpha_i}(\{\alpha_j\}, \epsilon) \alpha_i. \quad (5.42)$$

Taking into account that  $\alpha_i^{\text{bare}}$  does not depend on  $\mu$  and taking into account that  $Z_{\alpha_i}$  may depend on all couplings leads to the following formula

$$\beta_i = - \left[ \epsilon \frac{\alpha_i}{\pi} + \frac{\alpha_i}{Z_{\alpha_i}} \sum_{j=1, j \neq i}^7 \frac{\partial Z_{\alpha_i}}{\partial \alpha_j} \beta_j \right] \left( 1 + \frac{\alpha_i}{Z_{\alpha_i}} \frac{\partial Z_{\alpha_i}}{\partial \alpha_i} \right)^{-1}, \quad (5.43)$$

where  $i = 1, 2$  or  $3$ . We furthermore set  $\alpha_4 = \alpha_t$ ,  $\alpha_5 = \alpha_b$ ,  $\alpha_6 = \alpha_\tau$  and  $\alpha_7 = \hat{\lambda}$  and neglect the rest of Yukawa couplings.

The first term in the first factor of Eq. (5.43) originates from the term  $\mu^{2\epsilon}$  in Eq. (5.42) and vanishes in four space-time dimensions. The second term in the first factor contains the beta functions of the remaining six couplings of the SM. Note that (for the gauge couplings) the one-loop term of  $Z_{\alpha_i}$  only contains  $\alpha_i$ , whereas at two loops all couplings are present except  $\hat{\lambda}$ . The latter appears for the first time at three-loop level. As a consequence, it is necessary to know  $\beta_j$  for  $j = 4, 5, 6$  to one-loop order and only the  $\epsilon$ -dependent term for  $\beta_7$ , namely  $\beta_7 = -\epsilon\alpha_7/\pi$ . From the second term in the first factor and the second factor of Eq. (5.43) one can read off that three-loop corrections to  $Z_{\alpha_i}$  are required for the computation of  $\beta_i$  to the same loop order.

In the  $\overline{\text{MS}}$  scheme the beta functions are mass independent. This allows us to use the SM in the unbroken phase as a framework for our calculation. In principle each vertex containing the coupling  $g_i = \sqrt{4\pi\alpha_i}$  can be used in order to determine the corresponding renormalization constant via the relation (3.26). In order to compute the individual renormalization constants entering Eq. (3.26) one can proceed as outlined in the previous sections.

A second method that can be used to get an independent result for the renormalization constants of the gauge couplings is a calculation in the background field gauge (BFG) [161, 162]. The basic idea of the BFG is the splitting of all gauge fields in a “quantum” and a “classical” part where in practical calculations the latter only occurs as external particle.

The BFG has the advantage that Ward identities guarantee that renormalization constants for gauge couplings can be obtained from the exclusive knowledge of the corresponding wave function renormalization constant. Thus we have the following formula

$$Z_{\alpha_i} = \frac{1}{Z_{A_i, \text{wf}}}, \quad (5.44)$$

where  $A$  denotes the gauge boson corresponding to the gauge coupling  $\alpha_i$ .

In the BFG calculation it is advisable to adopt Landau gauge in order to avoid the renormalization of the gauge parameters  $\xi_i$ . However, it is not possible to choose Landau gauge from

the very beginning since some Feynman rules for vertices involving a background gauge boson contain terms proportional to  $1/\xi_i$  where  $\xi_i = 0$  corresponds to Landau gauge. To circumvent this problem one has to evaluate the bare integrals for arbitrary gauge parameters. In the final result all inverse powers of  $\xi_i$  cancel and thus the limit  $\xi_i = 0$  can be taken at the bare level.

An important issue in the present calculation is the treatment of  $\gamma_5$  within dimensional regularization. Non-trivial contributions may arise if in the course of the calculation two fermion traces occur where both of them contain an odd number of  $\gamma_5$  matrices and four or more  $\gamma$  matrices. It is straightforward to see that the three-point Green functions that are required for this computation contain at most one-loop triangle sub-diagrams.<sup>15</sup> This could potentially lead to contributions where a careful treatment of  $\gamma_5$  is required. However, all these contributions vanish identically due to anomaly cancellations in the SM (see, e.g., Ref. [163]). This can also be checked by an explicit calculation using the semi-naive regularization prescription for  $\gamma_5$  as discussed in section 3.1. Due to the  $\mathcal{O}(\epsilon)$  ambiguity of the Eq. (3.10), this approach can be directly applied only to diagrams that contain at most simple poles in  $\epsilon$ . Otherwise, finite counter-terms have to be introduced in order to restore Ward-Identities [76]. However, the diagrams contributing to this calculation that contain one-loop triangle sub-diagrams, have at most simple poles in  $\epsilon$ . This explains why one obtains correct results for the three-loop beta functions even without implementing the 't Hooft-Veltman scheme for the regularization of  $\gamma_5$ .

From the technical point of view, all the methods and programs discussed in the previous section can also be applied in this computation. The main difficulty of this calculation is the enormous number of diagrams (of about a million diagrams) that contribute to the individual renormalization factors. In order to handle such an enormous amount of diagrams in a reasonable wall-clock time, one needs to parallelize the calculation.

We are now in the position to present the results for the beta functions of the gauge couplings which are given by

$$\begin{aligned}
\beta_1 = & \frac{\alpha_1^2}{(4\pi)^2} \left\{ \frac{2}{5} + \frac{16n_G}{3} \right\} \\
& + \frac{\alpha_1^2}{(4\pi)^3} \left\{ \frac{18\alpha_1}{25} + \frac{18\alpha_2}{5} - \frac{34\text{tr}\hat{T}}{5} - 2\text{tr}\hat{B} - 6\text{tr}\hat{L} + n_G \left[ \frac{76\alpha_1}{15} + \frac{12\alpha_2}{5} + \frac{176\alpha_3}{15} \right] \right\} \\
& + \frac{\alpha_1^2}{(4\pi)^4} \left\{ \frac{489\alpha_1^2}{2000} + \frac{783\alpha_1\alpha_2}{200} + \frac{3401\alpha_2^2}{80} + \frac{54\alpha_1\hat{\lambda}}{25} + \frac{18\alpha_2\hat{\lambda}}{5} - \frac{36\hat{\lambda}^2}{5} - \frac{2827\alpha_1\text{tr}\hat{T}}{200} \right. \\
& - \frac{471\alpha_2\text{tr}\hat{T}}{8} - \frac{116\alpha_3\text{tr}\hat{T}}{5} - \frac{1267\alpha_1\text{tr}\hat{B}}{200} - \frac{1311\alpha_2\text{tr}\hat{B}}{40} - \frac{68\alpha_3\text{tr}\hat{B}}{5} - \frac{2529\alpha_1\text{tr}\hat{L}}{200} \\
& - \frac{1629\alpha_2\text{tr}\hat{L}}{40} + \frac{183\text{tr}\hat{B}^2}{20} + \frac{51(\text{tr}\hat{B})^2}{10} + \frac{157\text{tr}\hat{B}\text{tr}\hat{L}}{5} + \frac{261\text{tr}\hat{L}^2}{20} + \frac{99(\text{tr}\hat{L})^2}{10} \\
& + \frac{3\text{tr}\hat{T}\hat{B}}{2} + \frac{339\text{tr}\hat{T}^2}{20} + \frac{177\text{tr}\hat{T}\text{tr}\hat{B}}{5} + \frac{199\text{tr}\hat{T}\text{tr}\hat{L}}{5} + \frac{303(\text{tr}\hat{T})^2}{10} \\
& + n_G \left[ -\frac{232\alpha_1^2}{75} - \frac{7\alpha_1\alpha_2}{25} + \frac{166\alpha_2^2}{15} - \frac{548\alpha_1\alpha_3}{225} - \frac{4\alpha_2\alpha_3}{5} + \frac{1100\alpha_3^2}{9} \right] \\
& \left. + n_G^2 \left[ -\frac{836\alpha_1^2}{135} - \frac{44\alpha_2^2}{15} - \frac{1936\alpha_3^2}{135} \right] \right\}, \tag{5.45}
\end{aligned}$$

---

<sup>15</sup> Three-point Green functions involving external fermion lines are not considered here.

$$\begin{aligned}
\beta_2 = & \frac{\alpha_2^2}{(4\pi)^2} \left\{ -\frac{86}{3} + \frac{16n_G}{3} \right\} \\
& + \frac{\alpha_2^2}{(4\pi)^3} \left\{ \frac{6\alpha_1}{5} - \frac{518\alpha_2}{3} - 6\text{tr}\hat{T} - 6\text{tr}\hat{B} - 2\text{tr}\hat{L} + n_G \left[ \frac{4\alpha_1}{5} + \frac{196\alpha_2}{3} + 16\alpha_3 \right] \right\} \\
& + \frac{\alpha_2^2}{(4\pi)^4} \left\{ \frac{163\alpha_1^2}{400} + \frac{561\alpha_1\alpha_2}{40} - \frac{667111\alpha_2^2}{432} + \frac{6\alpha_1\hat{\lambda}}{5} + 6\alpha_2\hat{\lambda} - 12\hat{\lambda}^2 - \frac{593\alpha_1\text{tr}\hat{T}}{40} \right. \\
& - \frac{729\alpha_2\text{tr}\hat{T}}{8} - 28\alpha_3\text{tr}\hat{T} - \frac{533\alpha_1\text{tr}\hat{B}}{40} - \frac{729\alpha_2\text{tr}\hat{B}}{8} - 28\alpha_3\text{tr}\hat{B} - \frac{51\alpha_1\text{tr}\hat{L}}{8} \\
& - \frac{243\alpha_2\text{tr}\hat{L}}{8} + \frac{57\text{tr}\hat{B}^2}{4} + \frac{45(\text{tr}\hat{B})^2}{2} + 15\text{tr}\hat{B}\text{tr}\hat{L} + \frac{19\text{tr}\hat{L}^2}{4} + \frac{5(\text{tr}\hat{L})^2}{2} + \frac{27\text{tr}\hat{T}\hat{B}}{2} \\
& + \frac{57\text{tr}\hat{T}^2}{4} + 45\text{tr}\hat{T}\text{tr}\hat{B} + 15\text{tr}\hat{T}\text{tr}\hat{L} + \frac{45(\text{tr}\hat{T})^2}{2} \\
& + n_G \left[ -\frac{28\alpha_1^2}{15} + \frac{13\alpha_1\alpha_2}{5} + \frac{25648\alpha_2^2}{27} - \frac{4\alpha_1\alpha_3}{15} + 52\alpha_2\alpha_3 + \frac{500\alpha_3^2}{3} \right] \\
& \left. + n_G^2 \left[ -\frac{44\alpha_1^2}{45} - \frac{1660\alpha_2^2}{27} - \frac{176\alpha_3^2}{9} \right] \right\}, \tag{5.46}
\end{aligned}$$

$$\begin{aligned}
\beta_3 = & \frac{\alpha_3^2}{(4\pi)^2} \left\{ -44 + \frac{16n_G}{3} \right\} \\
& + \frac{\alpha_3^2}{(4\pi)^3} \left\{ -408\alpha_3 - 8\text{tr}\hat{T} - 8\text{tr}\hat{B} + n_G \left[ \frac{22\alpha_1}{15} + 6\alpha_2 + \frac{304\alpha_3}{3} \right] \right\} \\
& + \frac{\alpha_3^2}{(4\pi)^4} \left\{ -5714\alpha_3^2 - \frac{101\alpha_1\text{tr}\hat{T}}{10} - \frac{93\alpha_2\text{tr}\hat{T}}{2} - 160\alpha_3\text{tr}\hat{T} - \frac{89\alpha_1\text{tr}\hat{B}}{10} - \frac{93\alpha_2\text{tr}\hat{B}}{2} \right. \\
& - 160\alpha_3\text{tr}\hat{B} + 18\text{tr}\hat{B}^2 + 42(\text{tr}\hat{B})^2 + 14\text{tr}\hat{B}\text{tr}\hat{L} - 12\text{tr}\hat{T}\hat{B} + 18\text{tr}\hat{T}^2 + 84\text{tr}\hat{T}\text{tr}\hat{B} \\
& + 14\text{tr}\hat{T}\text{tr}\hat{L} + 42(\text{tr}\hat{T})^2 \\
& + n_G \left[ -\frac{13\alpha_1^2}{30} - \frac{\alpha_1\alpha_2}{10} + \frac{241\alpha_2^2}{6} + \frac{308\alpha_1\alpha_3}{45} + 28\alpha_2\alpha_3 + \frac{20132\alpha_3^2}{9} \right] \\
& \left. + n_G^2 \left[ -\frac{242\alpha_1^2}{135} - \frac{22\alpha_2^2}{3} - \frac{2600\alpha_3^2}{27} \right] \right\}. \tag{5.47}
\end{aligned}$$

In the above formulas  $n_G$  denotes the number of fermion generations. It is obtained by labeling the closed quark and lepton loops present in the diagrams.

Let us finally briefly discuss the numerical impact of the new three-loop corrections. In Fig. 5.3 from Ref. [99] we reproduce the running of  $\alpha_1$  and  $\alpha_2$  from  $\mu = M_Z$  to the energy scales where these two couplings become equal. The dotted and dashed lines correspond to one- and two-loop running, respectively. One observes a significant change of the curves, which is in particular much bigger than the experimental uncertainty indicated by the dashed band. Thus in case only one- and two-loop perturbative corrections are included the theory uncertainty is much bigger than the experimental one. This changes with the inclusion of the three-loop terms. The results are shown as solid lines which are closed to the corresponding dashed curves. The effect is small, however, still of the order of the experimental uncertainty, in particular for  $\alpha_2$ . The three-loop effects on  $\alpha_3$  predictions are, as expected, much smaller than the experimental uncertainty. For

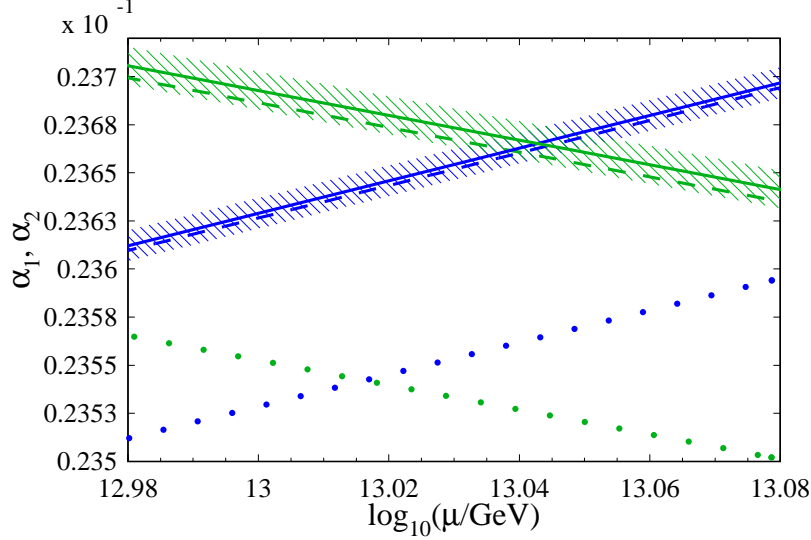


Figure 5.3: The running of the electroweak gauge couplings in the SM from Ref. [99]. The lines with positive slope correspond to  $\alpha_1$ , the lines with negative slope to  $\alpha_2$ . The dotted, dashed and solid lines correspond to one-, two- and three-loop precision, respectively. The bands around the three-loop curves visualize the experimental uncertainty.

this reason, the strong coupling was not displayed in Fig. 5.3. Let us briefly point out that the energy scale at which the electroweak couplings meet each other is of about  $10^{13}$  GeV. Coupling unification at such a low energy scale would imply a too rapid proton decay, in contrast to the experimental results. Thus, even from this partial analysis, we can conclude that the statement that gauge coupling unification cannot be achieved within the SM remains valid even after the inclusion of the three-loop radiative corrections. More details about this topic can be found in the next section.

## 6 Gauge coupling unification in supersymmetric models

An appealing hint in favour of supersymmetry is the apparent unification of gauge couplings at a scale of about  $10^{16}$  GeV [18–20]. Gauge coupling unification is highly sensitive to the heavy particle mass spectrum. This property allows us to probe unification through precision measurements of low-energy parameters like the gauge couplings at the electroweak scale and the supersymmetric mass spectrum. The current precision of the experimental data for the relevant input parameters [160, 164] and the substantial progress on the theory side [88, 112, 144, 165, 166] require renormalization group analyses even at three-loop accuracy. Within this method, one needs  $n$ -loop RGEs and  $(n - 1)$ -loop threshold corrections to achieve  $n$ -loop precision. We have discussed in detail the derivation of RGEs in the previous sections. The first part of this section is devoted to the calculation of threshold corrections. As an example, the determination of the two-loop SUSY-QCD threshold corrections for the strong coupling  $\alpha_s$  and the bottom quark

mass  $m_b$  will be presented. In the second part of this section, we outline the phenomenological analysis of gauge coupling unification within the minimal SUSY SU(5) model.

## 6.1 Effective field theory approach. Decoupling coefficients.

As already stated above, the underlying motivation for the running analysis is to relate physical parameters measured at the electroweak scale with the Lagrange parameters at the GUT scale. The running parameters are most conveniently defined in mass-independent renormalization schemes such as  $\overline{\text{MS}}$  for the SM parameters and  $\overline{\text{DR}}$  for the MSSM parameters. These schemes have the advantage that the gauge beta-functions are mass independent and their computation is much easier than in physical mass dependent schemes. However, quantum corrections to low-energy processes contain logarithmically enhanced contributions from heavy particles with masses much greater than the energy-scale of the process under consideration. In other words in such “unphysical” renormalization schemes the Appelquist-Carazzone decoupling theorem [167] does not hold in its naive form. An elegant approach to get rid of this unwanted behaviour in the  $\overline{\text{MS}}$  or  $\overline{\text{DR}}$  scheme is to formulate an effective theory (ET) (for more details see Refs. [120, 168]) integrating out all heavy particles. The parameters of the ET must be modified (“rescaled”) in order to take into account the effects of the heavy fields. The ET parameters are related to the parameters of the full theory by the so-called matching or decoupling relations.

They have been computed in QCD including corrections up to the four-loop order for the strong coupling [169] and three-loop order for quark masses [168]. In the MSSM the two-loop SUSY-QCD [165, 166, 170] and SUSY-EW [171, 172] expressions are known. Very recently, even the three-loop SUSY-QCD corrections to decoupling coefficient of the strong coupling was computed [173].

In the following, we concentrate on the calculation of the decoupling coefficients for the strong coupling and the bottom-quark mass within SUSY-QCD. They are the most interesting quantities from the phenomenological point of view because they are on the one hand the main ingredients for the study of the gauge and Yukawa coupling unification. On the other hand they are the quantities that receive the largest radiative corrections, for which next-to-next-to-leading-order corrections are essential for high precision predictions.

### 6.1.1 Framework

We consider SUSY-QCD with  $n_f$  active quark and  $n_s = n_f$  active squark flavours and  $n_{\tilde{g}} = 1$  gluinos. Furthermore, we assume that  $n_l = 5$  quarks are light (among which the bottom quark) and that the top quark and all squarks and the gluino are heavy. Integrating out the heavy fields from the full SUSY-QCD Lagrangian, we obtain the Lagrange density corresponding to the effective QCD with  $n_l$  light quarks plus non-renormalizable interactions. The latter are suppressed by negative powers of the heavy masses and will be neglected here. The effective Lagrangian can be written as follows:

$$\mathcal{L}_{\text{eff}}(g_s^0, m_q^0, \xi^0; q^0, G_\mu^{0,a}, c^{0,a}; \zeta_i^0) = \mathcal{L}^{QCD}(g_s^{0'}, m_q^{0'}, \xi^{0'}; q^{0'}, G_\mu^{0',a}, c^{0',a}), \quad (6.48)$$



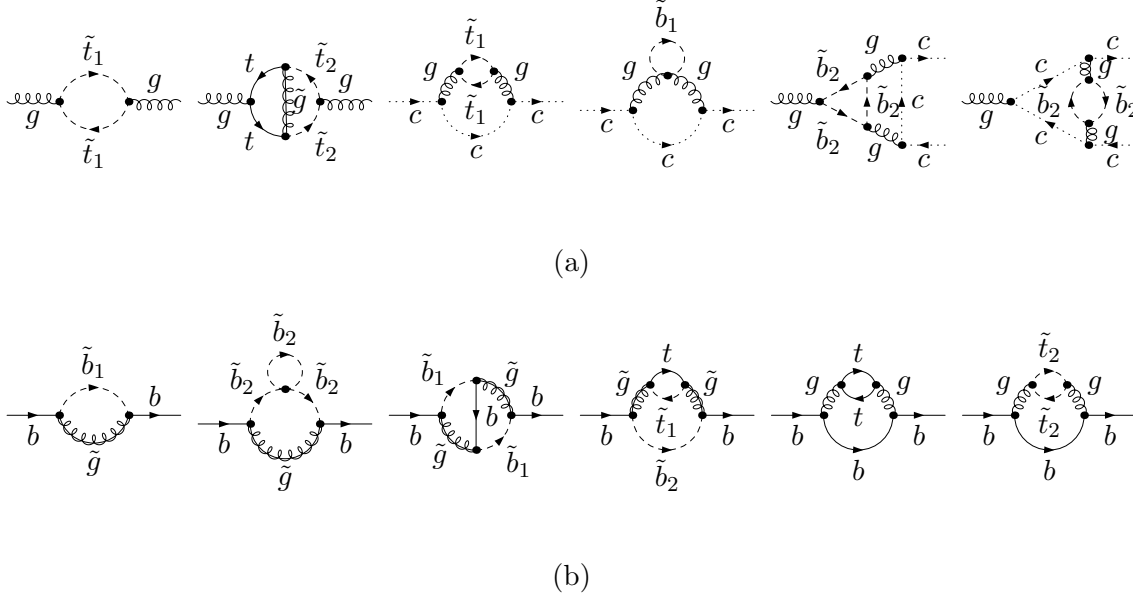


Figure 6.4: Sample diagrams contributing to  $\zeta_3$ ,  $\tilde{\zeta}_3$ ,  $\tilde{\zeta}_1$  and  $\zeta_m$  with gluons ( $g$ ), ghosts ( $c$ ), bottom/top quarks ( $b/t$ ), bottom/top squarks ( $\tilde{b}/\tilde{t}$ ) and gluinos ( $\tilde{g}$ ).

where  $q, G_\mu^a, c^a$  denote the light-quark, the gluon and the ghost fields, respectively,  $m_q$  stands for the light quark masses,  $\xi$  is the gauge parameter and  $g_s = \sqrt{4\pi\alpha_s}$  is the strong coupling. The index 0 marks bare quantities  $\mathcal{L}^{QCD}$  is the usual QCD Lagrangian from which all heavy fields have been discarded. As a result the fields, masses and couplings associated with light particles have to be rescaled. They are labeled by a prime in Eq. (6.48) and are related to the original parameters through decoupling relations:

$$\begin{aligned}
g_s^{0'} &= \zeta_g^0 g_s^0, & m_q^{0'} &= \zeta_m^0 m_q^0, & \xi^{0'} - 1 &= \zeta_3^0 (\xi^0 - 1), \\
q^{0'} &= \sqrt{\zeta_2^0} q^0, & G_\mu^{0',a} &= \sqrt{\zeta_3^0} G_\mu^{0,a}, & c^{0',a} &= \sqrt{\tilde{\zeta}_3^0} c^{0,a}.
\end{aligned} \tag{6.49}$$

Since the decoupling coefficients are universal quantities, they are independent of the momenta carried by the incoming and outgoing particles. The authors of Refs. [168] showed that the bare decoupling coefficients  $\zeta_m^0, \zeta_2^0, \zeta_3^0, \tilde{\zeta}_3^0$  can be derived from the quark, the gluon and the ghost propagators, all evaluated at vanishing external momenta, via the relations

$$\begin{aligned}
\zeta_3^{(0)} &= 1 + \Pi^{0,h}(0), \\
\zeta_2^{(0)} &= 1 + \Sigma_v^{0,h}(0), \\
\zeta_m^{(0)} &= \frac{1 - \Sigma_s^{0,h}(0)}{1 + \Sigma_v^{0,h}(0)}.
\end{aligned} \tag{6.50}$$

The superscript  $h$  indicates that in the framework of DREG or DRED only diagrams containing at least one heavy particle inside the loops contribute and that only the hard regions in the

asymptotic expansion of the diagrams are taken into account.

In Fig. 6.4 are shown sample Feynman diagrams contributing to the decoupling coefficients for the strong coupling (a) and the bottom-quark mass (b).

For the computation of  $\zeta_g$  one has to consider in addition one vertex involving the strong coupling. A convenient choice is the relation:

$$\zeta_g^0 = \frac{\tilde{\zeta}_1^0}{\tilde{\zeta}_3^0 \sqrt{\zeta_3^0}}, \quad (6.51)$$

where  $\tilde{\zeta}_1^0$  denotes the decoupling constant for the ghost-gluon vertex.

The finite decoupling coefficients are obtained upon the renormalization of the bare parameters. They are given by

$$\zeta_g = \frac{Z_g}{Z'_g} \zeta_g^0, \quad \zeta_m = \frac{Z_m}{Z'_m} \zeta_m^0, \quad (6.52)$$

where  $Z'_g$  and  $Z'_m$  correspond to the renormalization constants in the effective theory, and  $Z_g$  and  $Z_m$  denote the same quantities in the full theory. Since we are interested in the two-loop results for  $\zeta_i$ ,  $i = g, m$ , the corresponding renormalization constants for SUSY-QCD and QCD have to be implemented with the same accuracy. Analytical results for the latter up to the three-loop order can be found in the previous sections and the references cited therein, *e.g.* Refs. [120, 174, 175].

### 6.1.2 Renormalization scheme

Apart from the renormalization constants of the external fields, also the renormalization of the input parameters is required. However, for the renormalization of the gluino and squark masses and the squark mixing angle we choose the on-shell scheme. This scheme allows us to use directly the physical parameters in the running analyses making the implementation very simple. The explicit formulae at the one-loop order can be found in Refs. [176, 177]. The two-loop counterterms are known analytically only for specific mass hierarchies [142] and numerically for arbitrary masses [178].

For the computation of the decoupling coefficient for the bottom quark mass at order  $\mathcal{O}(\alpha_s^2)$  one needs to renormalize in addition the bottom quark mass and the trilinear coupling  $A_b$  as well as the  $\epsilon$ -scalar mass. As the bottom-quark mass is neglected w.r.t. heavy particle masses, an explicit dependence of the radiative corrections on  $m_b$  can occur only through bottom Yukawa coupling. In order to avoid the occurrence of large logarithms of the form  $\alpha_s^2 \log(\mu^2/m_b^2)$  with  $\mu \simeq \tilde{M}$ , one has to renormalize the bottom Yukawa coupling in the  $\overline{\text{DR}}$  scheme. In this way, the large logarithms are absorbed into the running mass and the higher order corrections are maintained small.

The renormalization prescription for the trilinear coupling  $A_b$  is fixed by the tree-level relation

$$\sin 2\theta_b = \frac{2m_b(A_b - \mu \tan \beta)}{m_{b_1}^2 - m_{b_2}^2}. \quad (6.53)$$

The parameters  $\mu$  and  $\tan \beta$  do not acquire  $\mathcal{O}(\alpha_s)$  corrections to the one-loop level. Generically, the counter-term for  $A_b$  can be expressed as

$$\delta A_b = \left( 2 \cos 2\theta_b \delta\theta_b + \sin 2\theta_b \frac{\delta m_{\tilde{b}_1}^2 - \delta m_{\tilde{b}_2}^2}{m_{\tilde{b}_1}^2 - m_{\tilde{b}_2}^2} - \sin 2\theta_b \frac{\delta m_b}{m_b} \right) \frac{m_{\tilde{b}_1}^2 - m_{\tilde{b}_2}^2}{2m_b}, \quad (6.54)$$

where  $\delta m_b$  and  $\delta m_{\tilde{b}_{1,2}}^2$  are the counter-terms corresponding to bottom-quark and squark masses, respectively. Due to the use of different renormalization prescriptions for the bottom quark and squark masses and mixing angle, the parameter  $A_b$  is renormalized in a *mixed* scheme.

Finally, the last parameter to be renormalized is the  $\epsilon$ -scalar mass. In softly broken SUSY theories, as it is the case of MSSM or SUSY-QCD, they get a radiatively induced mass. As already discussed in the previous sections, there are different approaches in the literature to perform the renormalization in such a case. To obtain decoupling coefficients independent of the unphysical parameter  $m_\epsilon$ , one has to modify the bottom squark masses by finite quantities [138, 148] according to the relation (4.34). Such finite shifts have to be performed for both renormalization schemes for squark masses  $\overline{\text{DR}}$  and on-shell.

### 6.1.3 Analytical results

The exact one-loop results for the decoupling coefficients of the strong coupling constant  $\zeta_s$  and bottom-quark mass  $\zeta_m$  can be found in Refs. [166, 170, 176]. We list them below up to order  $\mathcal{O}(\epsilon)$

$$\zeta_s = 1 + \frac{\alpha_s^{(\text{SQCD})}}{\pi} \left[ -\frac{1}{6} C_A L_{\tilde{g}} - \frac{1}{6} L_t - \sum_q \sum_{i=1,2} \frac{1}{24} L_{\tilde{q}_i} \right. \\ \left. - \epsilon \left( \frac{C_A}{12} (L_{\tilde{g}}^2 + \zeta(2)) + \frac{1}{12} (L_t^2 + \zeta(2)) - \frac{1}{48} \sum_q \sum_{i=1,2} (L_{\tilde{q}_i}^2 + \zeta(2)) \right) \right], \quad (6.55)$$

$$\zeta_{m_b} = 1 + \frac{\alpha_s^{(\text{SQCD})}}{\pi} C_F \sum_{i=1,2} \left\{ -\frac{(1 + L_{\tilde{b}_i})}{4} \frac{m_{\tilde{b}_i}^2}{(m_{\tilde{b}_i}^2 - m_{\tilde{g}}^2)} + \frac{(3 + 2L_{\tilde{b}_i})m_{\tilde{b}_i}^4 - (3 + 2L_{\tilde{g}})m_{\tilde{g}}^4}{16(m_{\tilde{b}_i}^2 - m_{\tilde{g}}^2)^2} \right. \\ - \frac{(-1)^i X_b m_{\tilde{g}}}{m_{\tilde{b}_1}^2 - m_{\tilde{b}_2}^2} \frac{m_{\tilde{b}_i}^2 L_{\tilde{b}_i} - m_{\tilde{g}}^2 L_{\tilde{g}}}{2(m_{\tilde{b}_i}^2 - m_{\tilde{g}}^2)} + \epsilon \left[ -\frac{m_{\tilde{b}_i}^2 (2 + L_{\tilde{b}_i} (2 + L_{\tilde{b}_i}) + \zeta(2))}{8(m_{\tilde{b}_i}^2 - m_{\tilde{g}}^2)} \right. \\ + \frac{m_{\tilde{b}_i}^4 (7 + 2L_{\tilde{b}_i} (3 + L_{\tilde{b}_i}) + 2\zeta(2)) - m_{\tilde{g}}^4 (7 + 2L_{\tilde{g}} (3 + L_{\tilde{g}}) + 2\zeta(2))}{32(m_{\tilde{b}_i}^2 - m_{\tilde{g}}^2)^2} \\ \left. \left. + \frac{(-1)^i X_b m_{\tilde{g}}}{m_{\tilde{b}_1}^2 - m_{\tilde{b}_2}^2} \frac{m_{\tilde{g}}^2 L_{\tilde{g}} (2 + L_{\tilde{g}}) - m_{\tilde{b}_i}^2 L_{\tilde{b}_i} (2 + L_{\tilde{b}_i})}{4(m_{\tilde{b}_i}^2 - m_{\tilde{g}}^2)} \right] \right\}, \quad (6.56)$$

where  $\zeta(2)$  is Riemann's zeta function with  $\zeta(2) = \pi^2/6$ . In the above equations we have adopted the abbreviations

$$L_i = \ln \frac{\mu^2}{m_i^2}, \quad i \in \{t, \tilde{g}, \tilde{q}_{1,2}, \tilde{b}_{1,2}\}, \quad \text{and} \quad X_b = A_b - \mu_{\text{SUSY}} \tan \beta. \quad (6.57)$$

$\alpha_s^{(\text{SQCD})}$  denotes the strong coupling constant in SUSY-QCD.

The presence of the terms proportional to the parameter  $X_b$  is a manifestation of the supersymmetry breaking. They are generated by the Yukawa interaction between left- and right-handed bottom squarks and the CP-neutral Higgs fields. Their contribution to the decoupling coefficient of the bottom-quark mass can be related through the Low Energy Theorem [179] to the decay rate of the Higgs boson to  $b\bar{b}$  pairs. To one-loop order, the  $X_b$ -term of Eq. (6.56) coincides with the SUSY-QCD corrections to the decay rate  $\phi \rightarrow b\bar{b}$  [180]. To higher orders, the relation between the two parameters becomes more involved<sup>16</sup>. These Yukawa-coupling induced contributions attracted a lot of attention due to the fact that they are the dominant corrections for large values of  $\tan\beta$ . They may in general become comparable with the tree-level bottom-quark mass. Thus, they need to be resummed even at the two-loop level.

The analytical two-loop results for the decoupling coefficients are too lengthy to be displayed here. They are available in Ref [166] together with their expressions for some phenomenologically motivated mass hierarchies. The dominant two-loop contributions to  $\zeta_{m_b}$ , i.e. the terms enhanced by  $\tan\beta$ , have been confirmed by the independent computation of Ref. [172]. Also the dominant SUSY QCD-EW corrections to  $\zeta_{m_b}$  at the two-loop order have been computed in Ref. [172].

#### 6.1.4 Numerical analysis

In this section we discuss briefly the numerical impact of the two-loop decoupling coefficients derived above on the prediction of the strong coupling constant at the GUT scale. As already pointed out, the scale  $\mu_{\text{dec}}$  at which the decoupling of the heavy particles is performed is not fixed by the theory. The dependence of physical observables on this unphysical parameter is a measure of the theoretical uncertainty left over. At fixed order perturbation theory, it is expected that the relations between the running parameters evaluated at high-energy scale and their low-energy values become less sensitive to the choice of  $\mu_{\text{dec}}$ , once higher order radiative corrections are considered.

In Ref. [181] a consistent method for the calculation of the energy evolution of physical parameters was proposed. For example, one derives the SM values  $\alpha_s^{(5)}(\mu_{\text{dec}})$  and at the heavy scale  $\mu_{\text{dec}}$  from the  $n$ -loop SM RGEs. Here  $\mu_{\text{dec}}$  denotes the energy scale at which the heavy particles are supposed to become active, *i.e.* the scale where the matching between the SM and the MSSM is performed. Before the matching procedure, one has to perform also the change of regularization scheme from  $\overline{\text{MS}}$  to  $\overline{\text{DR}}$ . For consistency, the  $n$ -loop running parameters have to be folded with  $(n-1)$ -loop conversion and decoupling relations. The latter are known in SUSY-QCD up to two-loop order [182] and within MSSM to one-loop order [183]. Above the decoupling scale, the energy dependence of the running parameters is governed by the  $n$ -loop MSSM RGEs.

The dependence of  $\alpha_s(\mu_{\text{GUT}})$  on the decoupling scale is displayed in Fig. 6.5 from Ref [166]. The dotted, dashed and solid lines denote the one-, two-, and three-loop running, where the corresponding exact results for the decoupling coefficients have been implemented. One can see the improved stability of the three-loop results w.r.t. the decoupling-scale variation. The uncertainty induced by the current experimental accuracy on  $\alpha_s(M_Z)$ ,  $\delta\alpha_s = 0.001$  [184], is

---

<sup>16</sup>For details see section8

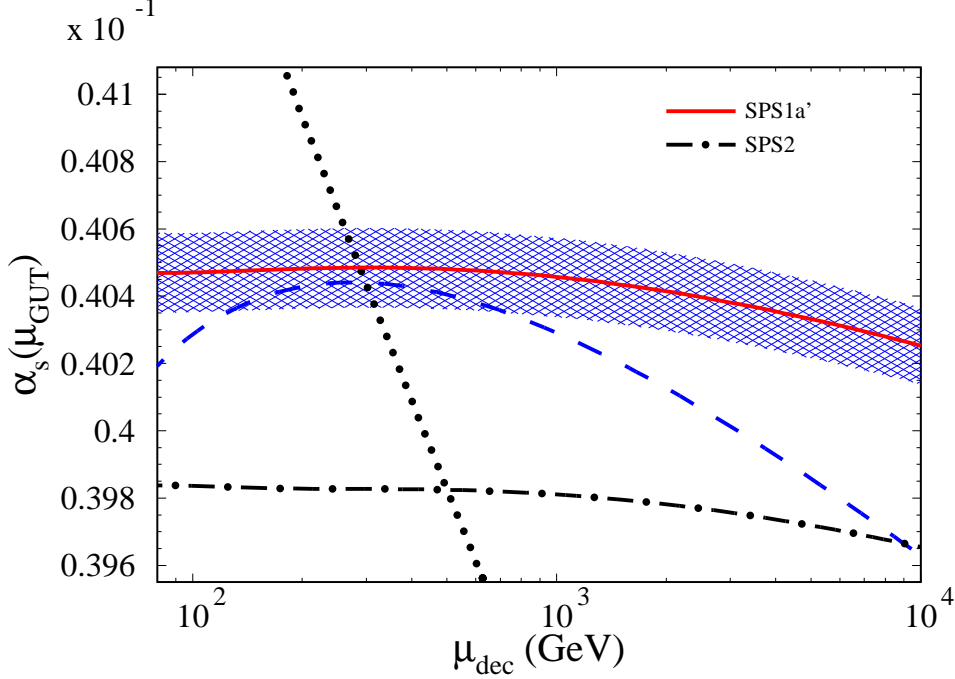


Figure 6.5:  $\alpha_s(\mu_{\text{GUT}})$  as a function of  $\mu_{\text{dec}}$  from Ref [166]. . Dotted, dashed and solid lines denote the one-, two-, and three-loop contributions, respectively, obtained using for the input parameters their values for the SPS1a' benchmark point. The dash-dotted line shows the three-loop running corresponding to the SPS2 point.

indicated by the hatched band.

In order to get an idea of the effects induced by the SUSY mass parameters on  $\alpha_s(\mu_{\text{GUT}})$ , two different mass spectra are shown. As reference was chosen the so called Snowmass Point SPS1a' scenario [185] for which rather low SUSY mass parameters are required:  $m_{\tilde{g}} = 607.1$  GeV,  $m_{\tilde{t}_1} = 366.5$  GeV,  $m_{\tilde{t}_2} = 585.5$  GeV,  $m_{\tilde{b}_1} = 506.3$  GeV,  $m_{\tilde{b}_2} = 545.7$  GeV,  $A_t^{\overline{\text{DR}}}(1 \text{ TeV}) = -565.1$  GeV,  $A_b^{\overline{\text{DR}}}(1 \text{ TeV}) = -943.4$  GeV,  $\mu = 396.0$  GeV, and  $\tan \beta = 10.0$ . In addition the dash-dotted line shows the three-loop results when the SUSY parameters corresponding to the SPS2 [186] scenario are adopted. Their explicit values are  $m_{\tilde{g}} = 784.4$  GeV,  $m_{\tilde{t}_1} = 1003.9$  GeV,  $m_{\tilde{t}_2} = 1307.4$  GeV,  $m_{\tilde{b}_1} = 1296.6$  GeV,  $m_{\tilde{b}_2} = 1520.1$  GeV, and  $\tan \beta = 10.0$ . One clearly notices the great impact of the SUSY-mass pattern on the predicted value of the strong coupling at high energies. Accordingly, for precision studies concerning gauge coupling unification the explicit mass pattern of heavy particles must be taken into account.

At this point, a comment on the chosen mass spectrum is in order. The nature of this plot is rather academic and aims to quantify the mass dependence of the strong coupling constant at high energies. The two mass spectra are already excluded by the direct searches at the LHC. Nevertheless, one can easily estimate that for heavier SUSY particles  $M_{\text{SUSY}} > 1.5$  TeV the value of  $\alpha_s(\mu_{\text{GUT}})$  decreases below the value 0.398. Its implication on the quality of the unification will be discussed in the next section.

## 6.2 Gauge coupling unification in the minimal SUSY SU(5) model

The gauge coupling unification might be predicted, even under the assumption of a minimal particle content of the underlying GUT like in the so-called minimal SUSY SU(5) model [187, 188]. This is the most predictive model among the currently known candidates for SUSY GUTs. However, immediately after its formulation it has been noticed that new dimension-five operators may cause a rapid proton decay. Together with the requirement of gauge coupling unification this aspect was used to even rule out the SUSY SU(5) model [189, 190]. However, subsequent careful analyses have shown that the proton decay rate for the dominant channel  $p \rightarrow K^+ \bar{\nu}$  can be suppressed either by sfermion mixing [191] or by taking into account higher dimensional operators induced at the Planck scale [192–194].

In the following, we review the latest analysis on the gauge coupling unification in the renormalizable version of minimal SUSY SU(5). This model is not the best motivated phenomenologically, but it requires the most severe constraints on the GUT parameters. More precisely, we outline the constraints on the mass of the colour triplet Higgs  $M_{H_c}$  and the grand unification scale<sup>17</sup>  $M_G$  taking into account the latest experimental data for the weak scale parameters and the most precise theoretical predictions currently available. The two parameters are predicted in the “bottom-up” approach, taking into account threshold corrections generated by the superpartners of the SM particles as well as those due to the super-heavy SUSY-GUT particles. In addition, the gauge coupling constants of the SM at the electroweak scale and the MSSM mass spectrum are required as input parameters. The predicted values for the two parameters have to be compared with the constraints derived from the non observation of proton decay.

For completeness, we present below our notation in the framework of minimal SUSY SU(5). The superpotential of the model [187] is given by

$$\begin{aligned} \mathcal{W} = & M_1 \text{Tr}(\Sigma^2) + \lambda_1 \text{Tr}(\Sigma^3) + \lambda_2 \bar{H} \Sigma H + M_2 \bar{H} H \\ & + \sqrt{2} Y_d^{ij} \Psi_i \phi_j \bar{H} + \frac{1}{4} Y_u^{ij} \Psi_i \Psi_j H, \end{aligned} \quad (6.58)$$

where  $\Psi_i$  and  $\phi_i$  ( $i = 1, 2, 3$  is a generation index) are matter multiplets in the **10**- and  $\bar{\mathbf{5}}$ -dimensional representation of SU(5). Their decomposition w.r.t. the SM gauge group SU(3)  $\times$  SU(2)  $\times$  U(1) reads

$$\begin{aligned} \mathbf{5} &= (3, 1, -\frac{1}{3}) \oplus (1, 2, +\frac{1}{2}) \\ \mathbf{10} &= (\bar{3}, 1, -\frac{2}{3}) \oplus (3, 2, \frac{1}{6}) \oplus (1, 1, 1). \end{aligned} \quad (6.59)$$

The field  $H$  ( $\bar{H}$ ) is realized in the **5** ( $\bar{\mathbf{5}}$ ) representation. The gauge group SU(5) is broken to the SM gauge group if the adjoint Higgs boson  $\Sigma \equiv \Phi^a T^a$  ( $a = 1, \dots, 24$ ) living in the **24** representation gets the vacuum expectation value  $\langle \Sigma \rangle = V/(2\sqrt{30}) \times \text{diag}(-2, -2, -2, 3, 3)$ , with  $V = -4\sqrt{30}M_1/(3\lambda_1)$ .<sup>18</sup> Its decomposition w.r.t. the SM gauge group reads

$$\mathbf{24} = (1, 1, 0) \oplus (1, 3, 0) \oplus (8, 1, 0) \oplus (3, 2, -\frac{5}{6}) \oplus (\bar{3}, 2, \frac{5}{6}). \quad (6.60)$$

<sup>17</sup>See below the exact definition of  $M_{H_c}$  and  $M_G$ .

<sup>18</sup>Here, we parametrize as usual the **24** representation like a  $5 \times 5$  matrix.

Choosing  $\langle \bar{H} \rangle = \langle H \rangle \ll V$  and in addition imposing the (tree-level-) fine-tuning condition  $M_2 = -\sqrt{3}\lambda_2 V/\sqrt{40}$ , the iso-doublets in  $H$  and  $\bar{H}$  remain massless. Furthermore, one gets the following super-heavy mass spectrum:

$$M_X^2 = \frac{5}{12}g^2V^2, \quad M_{H_c}^2 = \frac{5}{24}\lambda_2^2V^2, \quad M_\Sigma^2 \equiv M_{(8,1)}^2 = M_{(1,3)}^2 = 25M_{(1,1)}^2 = \frac{15}{32}\lambda_1^2V^2, \quad (6.61)$$

where the indices in round brackets refer to the SU(3) and SU(2) quantum numbers. Here  $M_\Sigma$  denotes the mass of the colour octet part of the adjoint Higgs boson  $\Sigma$  and  $M_{H_c}$  stands for the mass of the colour triplets of  $H$  and  $\bar{H}$ .  $M_X$  is the mass of the gauge bosons and  $g$  is the gauge coupling. The equality  $M_{(8,1)}^2 = M_{(1,3)}^2$  holds only if one neglects operators that are suppressed by  $1/M_{\text{Pl}}$  as we do here.

In the study of the energy evolution of the gauge couplings up to scales of the order  $\mathcal{O}(10^{16})$  GeV, one has to apply the effective field theory (EFT) approach twice: once at an energy scale comparable with the SUSY particle masses and once at the GUT scale. In practice, this translates into the following steps:

1. Running within the SM from  $\mu = M_Z$  to the SUSY scale  $\mu_{\text{SUSY}}$ .

In this step, the three-loop beta function of QCD [95, 96] and up to three-loop RGEs in the electroweak sector [98, 99] are necessary in order to obtain the values of the gauge couplings at  $\mu_{\text{SUSY}} \approx 1$  TeV. At this point we want to stress once again that, the value of  $\mu_{\text{SUSY}}$  is a free parameter. Let us mention that the top-quark threshold effects are taken into account in the determination of the input parameters (for details see next section) and the running analysis is performed in SM with six active quark flavours.

2. SUSY threshold corrections.

In order to still cure the naturalness problem of the SM, the SUSY mass spectrum has to be at most in the TeV range. Thus, for energies of this order of magnitude, it is expected that the SUSY particles become active and the proper matching between the SM and the MSSM has to be performed. The one-loop decoupling relations for  $\alpha_1$  and  $\alpha_2$  [195] and the Yukawa couplings [176] are known since long time. The SUSY-QCD decoupling effects for  $\alpha_3$  and  $m_b$  are known to three- and two-loop order, respectively, as discussed in the previous section. A fully consistent approach would require two-loop threshold corrections not only in the strong but also in the electroweak sector. They are not yet available, nevertheless it is expected that their numerical impact is relatively small.

At this stage also the change of renormalization scheme from  $\overline{\text{MS}}$  to  $\overline{\text{DR}}$  has to be taken into account. To establish the conversion relations between the running parameters in the two schemes, one can use the method discussed in section 3.3.3, where such relations have been derived in the context of non-supersymmetric theories.<sup>19</sup> The conversion relations that are of interest for the numerical analysis discussed in this section are those involving the gauge couplings and the quark masses of the third generation, as only their Yukawa couplings give sizable effects. They are known up to the two-loop order in SUSY-QCD [182]. For

---

<sup>19</sup>For more details see Ref. [182].

the convenience of the reader we cite them below

$$\alpha_s^{\overline{\text{MS}}} = \alpha_s^{\overline{\text{DR}}} \left[ 1 - \frac{\alpha_s^{\overline{\text{DR}}}}{\pi} \frac{C_A}{3} + \left( \frac{\alpha_s^{\overline{\text{DR}}}}{\pi} \right)^2 \left( -\frac{11}{9} C_A^2 + 2 T_f C_R \right) \right], \quad (6.62)$$

$$m_q^{\overline{\text{MS}}} = m_q^{\overline{\text{DR}}} \left[ 1 + \frac{\alpha_s^{\overline{\text{DR}}}}{\pi} C_R + \left( \frac{\alpha_s^{\overline{\text{DR}}}}{\pi} \right)^2 \left( \frac{7}{12} C_A C_R + \frac{7}{4} C_R^2 - \frac{1}{2} T_f C_R \right) \right], \quad (6.63)$$

where the group invariants are defined as in Appendix A and  $T_f = I_2(R) n_f$ , with  $n_f$  the number of active fermions.

3. Running within the MSSM from  $\mu_{\text{SUSY}}$  to the high-energy scale  $\mu_{\text{GUT}}$ .

In this step the three-loop RGEs of the MSSM [88, 112] are required to evolve the gauge and Yukawa couplings from  $\mu_{\text{SUSY}}$  to some very high scale of the order of  $10^{16}$  GeV, that we denote as  $\mu_{\text{GUT}}$ . At this energy scale it is expected that SUSY-GUT particles become active.

4. SUSY-GUT threshold effects.

At the energy scale  $\mu_{\text{GUT}}$ , threshold corrections induced by the non-degenerate SUSY-GUT spectrum have to be taken into account. The one-loop formulas of the decoupling coefficients for a general gauge group have been known for a long time [196–198]. The specification to the minimal SUSY SU(5) reads [199, 200]

$$\begin{aligned} \zeta_{\alpha_1}(\mu) &= 1 + \frac{\alpha^{\text{SU}(5)}(\mu)}{4\pi} \left( -\frac{2}{5} L_{\mu H_c} + 10 L_{\mu X} \right), \\ \zeta_{\alpha_2}(\mu) &= 1 + \frac{\alpha^{\text{SU}(5)}(\mu)}{4\pi} (-2 L_{\mu \Sigma} + 6 L_{\mu X}), \\ \zeta_{\alpha_3}(\mu) &= 1 + \frac{\alpha^{\text{SU}(5)}(\mu)}{4\pi} (-L_{\mu H_c} - 3 L_{\mu \Sigma} + 4 L_{\mu X}), \end{aligned} \quad (6.64)$$

where  $L_{\mu x} = \ln(\mu^2/M_x^2)$  and for simplicity we keep from the list of arguments of the coefficients  $\zeta_{\alpha_i}$  only the decoupling scale.  $\frac{\alpha^{\text{SU}(5)}(\mu)}{4\pi}$  is the gauge coupling constant of the unified theory, *i.e.* of the SUSY SU(5) model.

A suitable linear combination of the three equations above leads to the following two relations

$$\begin{aligned} 4\pi \left( -\frac{1}{\alpha_1(\mu)} + 3 \frac{1}{\alpha_2(\mu)} - 2 \frac{1}{\alpha_3(\mu)} \right) &= -\frac{12}{5} L_{\mu H_c}, \\ 4\pi \left( 5 \frac{1}{\alpha_1(\mu)} - 3 \frac{1}{\alpha_2(\mu)} - 2 \frac{1}{\alpha_3(\mu)} \right) &= -24 \left( L_{\mu X} + \frac{1}{2} L_{\mu \Sigma} \right), \end{aligned} \quad (6.65)$$

where  $\alpha^{\text{SU}(5)}$  has been eliminated. These equations allow the prediction of the coloured triplet Higgs boson mass  $M_{H_c}$  from the knowledge of the MSSM gauge couplings at the energy scale  $\mu = \mu_{\text{GUT}}$ . It is furthermore common to define a new mass parameter  $M_G = \sqrt[3]{M_X^2 M_\Sigma}$ , the so-called grand unified mass scale. It can also be determined from the knowledge of the MSSM gauge couplings at  $\mu_{\text{GUT}}$  through Eq. (6.65). These observations makes it quite easy to test the minimal SUSY SU(5) model once the required experimental data are available in combination with a high-order analysis.



5. Running from  $\mu_{\text{GUT}}$  to the Planck scale  $M_{\text{Pl}}$ .

The last sequence of this approach consists in the running within the SUSY-SU(5) model. The three-loop RGEs for the gauge [55], and the one-loop formulas for the Yukawa and Higgs self couplings [201] are available in the literature. In addition, the perturbativity constraints (*i.e.* all couplings of the theory are smaller than unity) have to be imposed.

### 6.2.1 Input parameters

As can be inferred from the discussion above, to constrain the GUT parameters one needs in addition to the precise running analysis also precise input parameters. Explicitly, one needs the values of weak mixing angle in the  $\overline{\text{MS}}$  scheme [202], the QED coupling constant at zero momentum transfer and its hadronic contribution [203] in order to obtain its counterpart at the  $Z$ -boson scale, and the strong coupling constant [164].<sup>20</sup> Their numerical values and uncertainties are

$$\begin{aligned}\sin^2 \Theta^{\overline{\text{MS}}} &= 0.23119 \pm 0.00014, \\ \alpha &= 1/137.036, \\ \Delta\alpha_{\text{had}}^{(5)} &= 0.02761 \pm 0.00015, \\ \alpha_s(M_Z) &= 0.1184 \pm 0.0020.\end{aligned}\tag{6.66}$$

To determine the value of  $\alpha$  in the  $\overline{\text{MS}}$  scheme, it is necessary to take into account the hadronic  $\Delta\alpha_{\text{had}}^{(5)}$ , leptonic  $\Delta\alpha_{\text{lep}}^{(5)}$  [204] and top-quark  $\Delta\alpha_{\text{top}}^{(5)}$  [205] contributions to the on-shell value. In addition, the conversion formula to the  $\overline{\text{MS}}$  scheme has to be taken into account. Thus, one obtains

$$\begin{aligned}\alpha^{\overline{\text{MS}}}(M_Z) &= \frac{\alpha}{1 - \Delta\alpha_{\text{lep}}^{(5)} - \Delta\alpha_{\text{had}}^{(5)} - \Delta\alpha_{\text{top}}^{(5)} - (\Delta\alpha^{(5),\overline{\text{MS}}} - \Delta\alpha^{(5),\text{OS}})} \\ &= \frac{1}{127.960 \pm 0.021}.\end{aligned}\tag{6.67}$$

For supersymmetric particle masses of order  $\mathcal{O}(1 \text{ TeV})$  it is appropriate to take into account top-quark threshold effects in a separate step. For convenience, we choose the scale at which we decouple the top-quark to be  $\mu_{\text{dec}} = M_Z$ . The corresponding threshold corrections are available from the Refs. [202, 206, 207] and give the following contributions

$$\begin{aligned}\alpha^{(6),\overline{\text{MS}}}(M_Z) &= 1/(128.129 \pm 0.021), \\ \sin^2 \Theta^{(6),\overline{\text{MS}}}(M_Z) &= 0.23138 \pm 0.00014, \\ \alpha_s^{(6)}(M_Z) &= 0.1173 \pm 0.0020.\end{aligned}\tag{6.68}$$

Even more, the supersymmetric particles can induce sizeable effects in the extraction of the weak mixing angle from experimental data. Such effects are by construction suppressed by the square of the supersymmetric mass scale [195, 208]. For a typical supersymmetric mass scale  $\geq 1 \text{ TeV}$  such corrections can lead to shifts in  $M_{H_c}$  of the order of  $\leq 10\%$ .

---

<sup>20</sup>We adopt the central value from Ref. [164], however, use as our default choice for the uncertainty 0.0020 instead of 0.0007.

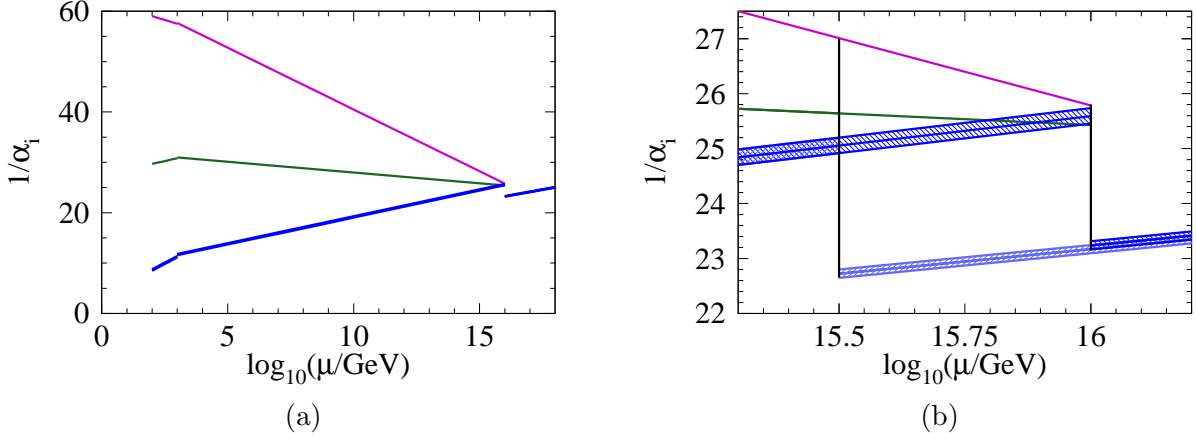


Figure 6.6: Running of the gauge couplings from the electroweak to the Planck scale from Ref [211]. The discontinuity for  $\mu = \mu_{\text{SUSY}}$  and  $\mu = \mu_{\text{GUT}}$  are clearly visible. In panel (b) an enlargement of (a) for the region around  $\mu = \mu_{\text{GUT}}$  is shown where for the decoupling the two values  $\mu_{\text{GUT}} = 10^{15.5} \text{ GeV} \approx 3.2 \cdot 10^{15} \text{ GeV}$  and  $\mu_{\text{GUT}} = 10^{16} \text{ GeV}$  have been chosen.

### 6.2.2 Numerical analysis

For illustration of the numerical effects we adopt the `mSUGRA` [209] scenario for the SUSY breaking mechanism with the following initial parameters

$$\begin{aligned} m_0 &= m_{1/2} = -A_0 = 1000 \text{ GeV}, \\ \tan \beta &= 3, \quad \mu > 0, \end{aligned} \tag{6.69}$$

and generate with the help of the code `SOFTSUSY` [210] the supersymmetric mass spectrum. This results in squark masses of the order of 2 TeV, thus beyond above the exclusion bounds currently established by direct searches at the LHC.

In Fig. 6.6 from Ref. [211] we visualize the running (and decoupling) of the gauge couplings where the parameters of Eq. (6.69) together with  $\mu_{\text{SUSY}} = 1000 \text{ GeV}$  and  $\mu_{\text{GUT}} = 10^{16} \text{ GeV}$  have been adopted. In addition we have chosen  $M_{\Sigma} = 1 \cdot 10^{15} \text{ GeV}$  which leads via Eq. (6.65) to  $M_{H_c} = 1.7 \cdot 10^{15} \text{ GeV}$  and  $M_X = 4.6 \cdot 10^{16} \text{ GeV}$ . One can clearly see the discontinuities at the matching scales and the change of the slopes when passing them. In panel (b) the region around  $\mu = 10^{16} \text{ GeV}$  is enlarged which allows for a closer look at the unification region. The bands indicate  $1\sigma$  uncertainties of  $\alpha_i$  at the electroweak scale (cf. Eq. (6.68)). In panel (b) we furthermore perform the decoupling of the super-heavy masses for two different values of  $\mu_{\text{GUT}}$ . One observes quite different threshold corrections leading to a nice agreement of  $\alpha^{\text{SU}(5)}$  above  $10^{16} \text{ GeV}$ . Fig. 6.6 stresses again that the uncertainty of  $\alpha_s$  is the most important one for the constraints that one can set on GUT models from low-energy data. Furthermore, it illustrates the size of the GUT threshold corrections and emphasizes the importance of precision calculations.

In the following, we discuss the dependence of  $M_{H_c}$  and  $M_G$  on various parameters entering our analysis. We start with varying the supersymmetric mass spectrum and use Eq. (6.65) in order to extract both  $M_{H_c}$  and  $M_G$ . The decoupling scales are fixed to  $\mu_{\text{SUSY}} = 1000 \text{ GeV}$

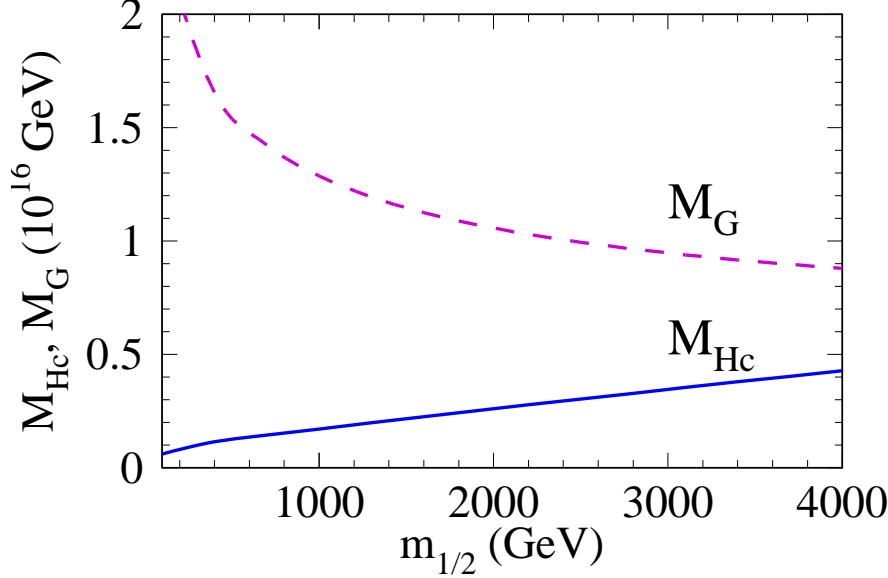


Figure 6.7: Dependence of  $M_{H_c}$  (solid) and  $M_G$  (dashed) on  $m_{1/2}$  from Ref [211].

and  $\mu_{\text{GUT}} = 10^{16}$  GeV, respectively, which ensures that the three-loop effect is rather small. In Fig. 6.7 the parameter  $m_{1/2}$  is varied up to 4 TeV. The solid and dashed lines correspond to  $M_{H_c}$  and  $M_G$ , respectively, which show a substantial variation. On the other hand,  $m_0$ ,  $\tan\beta$  and  $A_0$  have only a minor influence on the GUT masses and thus we refrain from explicitly showing the dependence.

An interesting aspect from the phenomenological point of view is the study of the effects of the experimental uncertainties of  $\alpha_i$  (c.f. Eq. (6.66)) on the prediction of  $M_{H_c}$  and  $M_G$ . For this, we fix the SUSY spectrum as before (see Eq. (6.69)) and set  $\mu_{\text{SUSY}} = M_Z$  which has often been common practice in similar analyses (see, e.g., Ref. [190]). Taking into account correlated errors and performing a  $\chi^2$  analysis leads to ellipses in the  $M_{H_c} - M_G$  plane. In Fig. 6.8 from Ref [211] the results for the two- (dashed lines) and three-loop (continuous lines) analyses are shown. The two concentric ellipses correspond to 68% and 90% confidence level, respectively, where only parametric uncertainties from Eq. (6.68) have been taken into account. Let us, however, stress that an optimistic uncertainty of  $\delta\alpha_s = 0.0010$  has been adopted for this plot. As expected, the uncertainty of  $\alpha_s$  induces the largest contributions to the uncertainties on  $M_{H_c}$  and  $M_G$ . In particular, it essentially determines the semi-major axis of the ellipses. The three-loop corrections induce a significant shift to higher masses of about an order of magnitude for  $M_{H_c}$ . In the same time  $M_G$  increases by about  $2 \cdot 10^{15}$  GeV. This demonstrates the importance of the precision calculations in such type of analyses. As has been discussed in the original paper [211] they are also essential in order to remove the dependence on  $\mu_{\text{SUSY}}$ . In fact, choosing  $\mu_{\text{SUSY}}$  close to the supersymmetric mass scale leads to small three-loop effects, since the two-loop ellipses are essentially shifted on top of the three-loop ones.

At this point a discussion about the additional constraint on the Higgs triplet mass  $M_{H_c}$  that can be derived from the non-observation of the proton decay is in order. The latest upper bound

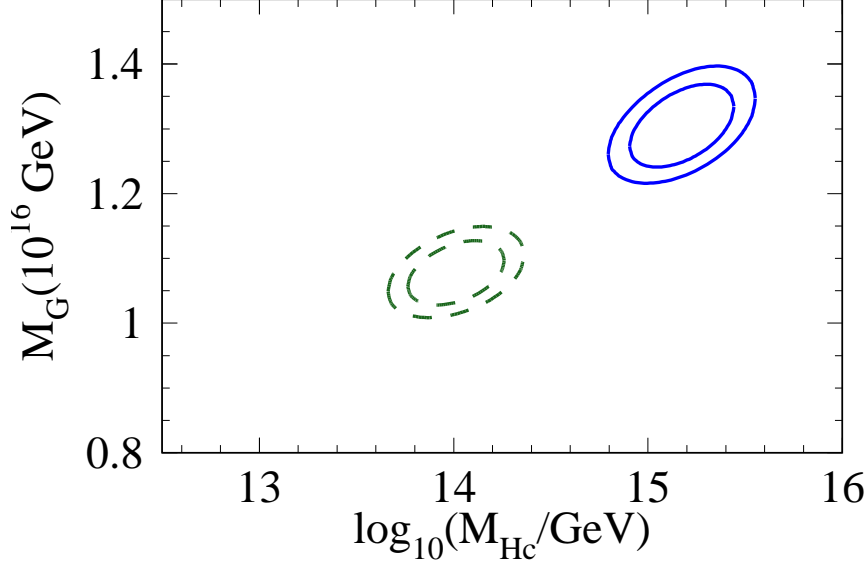


Figure 6.8: Ellipses in the  $M_{H_c} - M_G$  plane obtained from the uncertainties of the gauge couplings at the electroweak scale. The input parameters of Eq. (6.66) have been used whereas  $\delta\alpha_s = 0.0010$  has been chosen. Dashed and solid lines correspond to the two- and three-loop analysis, respectively.

on the proton decay rate for the channel  $p \rightarrow K^+ \bar{\nu}$  [212] is  $\Gamma_{\text{exp}} = 4.35 \times 10^{-34}/\text{y}$ . In order to translate it into a lower bound for the Higgs triplet mass, one needs an additional assumption about the Yukawa couplings that enter the expression of the decay rate  $\Gamma(p \rightarrow K^+ \bar{\nu})$ . As pointed out in Ref. [192] this is because down quark and lepton Yukawa couplings fail to unify within the minimal renormalizable SUSY SU(5) model and so a completely consistent treatment is not possible. Therefore one could either choose<sup>21</sup> (i)  $Y_{ql} = Y_{ud} = Y_d$  or (ii)  $Y_{ql} = Y_{ud} = Y_e$ , which leads to completely different phenomenological consequences. Both choices are equally justified once higher dimensional operators are included. Since these operators further weaken the bounds presented below, we refrain to include these bounds into the analysis presented here. For the case (i) and supersymmetric particle masses around 1 TeV the lower bound for the Higgs triplet mass can be read off from Fig. 2 of Ref. [192] and amounts to  $M_{H_c} \geq 1.05 \times 10^{17}$  GeV whereas for the second choice it becomes  $M_{H_c} \geq 5.25 \times 10^{15}$  GeV. From our phenomenological analysis presented above it turns out that within the minimal SUSY SU(5) model the upper bound for  $M_{H_c}$  is of about  $10^{16}$  GeV. Thus, the substantial increase of about one order of magnitude for the upper bound on  $M_{H_c}$  induced by the three-loop order running analysis attenuates the tension between the theoretical predictions made under the assumption (i) and the experimental data. The choice (ii) for the Yukawa couplings clearly shows that the minimal SUSY SU(5) model cannot be ruled out by the current experimental data on proton decay rates. More experimental information about the SUSY mass spectrum and proton decay rates is required in order to be

<sup>21</sup> $Y_{ql}$  is the Yukawa coupling of the quark and lepton doublet to the Higgs colour triplet.  $Y_{ud}$  is the corresponding coupling for the up and down quark singlet.

able to draw a firm conclusion.

## 7 The mass of the lightest Higgs boson in the MSSM

### 7.1 Higgs boson mass in the SM

Spontaneous symmetry breaking was introduced into the particle physics in the seminal papers [213–215] and the existence of the Higgs boson was postulated by P. Higgs in 1964 in Ref. [216]. The next important step was the incorporation of the spontaneous symmetry breaking into the unified model of the weak and electromagnetic interactions [2,3]. The breakthrough of these ideas came with the proof of the renormalizability of spontaneously-broken gauge theories by G. 't Hooft and M. Veltman [60,217].

The direct Higgs boson searches performed at LEP 1 in  $Z^0 \rightarrow H + \bar{f}f$  and at LEP 2 in  $e^+e^- \rightarrow Z^0 + H$  channels provided us with a lower bound on its mass of  $M_h > 114.4$  GeV at the 95% CL [218]. In parallel to the direct searches, the high precision electroweak data obtained at LEP allowed us to estimate the possible mass range of the Higgs boson within the SM, namely  $M_h = 96^{+31}_{-21}$  GeV [219]. Moreover, the CDF and D0 experiments at the Tevatron [220] excluded a range of Higgs masses between  $156 < M_h < 177$  GeV, as well as lower masses in the range already excluded by LEP. Only very recently, the existence of the Higgs boson could have been experimentally confirmed by the ATLAS and CMS collaborations at the LHC [29,30]. Its mass is around 125 – 126 GeV. Currently, dedicated analysis are performed in order to establish if the observed boson is just the one predicted by the SM or hints towards new physics.

The Higgs boson mass itself is a fundamental parameter of the SM. Together with the top quark mass and the strong coupling constant, it plays a crucial role in determining the stability bounds for the SM electroweak vacuum. The usual way to present this interplay is to display the allowed domains for  $M_h$  as a function of  $\Lambda$ , the scale up to which the SM may remain valid. If  $M_h$  is too large, the RGEs of the SM drive the Higgs self coupling into the non-perturbative regime at some scale  $\Lambda < M_{Planck}$ . This is shown as the upper pair bold lines in Fig. 7.1 that is taken from Ref. [221]. In this case new physics at a scale  $\Lambda$  will be required in order to prevent the Higgs self-coupling to blow-up. On the other hand if  $M_h$  is too small, the RGEs drive the Higgs self-coupling to a negative value. In this case the Higgs potential can develop an instability at high field values  $> \Lambda$ , unless there is new physics at some scale  $< \Lambda$  that prevents the occurrence of an additional minimum in the potential. This is shown as light shaded bands in Fig. 7.1. Between the blow-up and the stability regions, there is a range of intermediate values of  $M_h$  for which the SM can survive up to the Planck scale. Taking into account the current theoretical and experimental errors on  $M_h$ ,  $M_t$  and  $\alpha_s$ , stability up to the Planck scale cannot be yet excluded [222].

Nevertheless, as shown in Fig. 7.2 from Ref. [222] and confirmed by Ref [223], the range of  $M_h$  as revealed by the present searches at the LHC lies right at the edge between electroweak stability and instability regions. The possibility that the SM potential becomes unstable at large field values, below the Planck scale, does not contradict any experimental observation, provided its lifetime is longer than the age of the universe. Indeed, the authors of Ref. [224] found that for  $M_h = 125$  GeV, the instability scale lies around  $10^{11\pm1}$  GeV. In this case, tunneling through

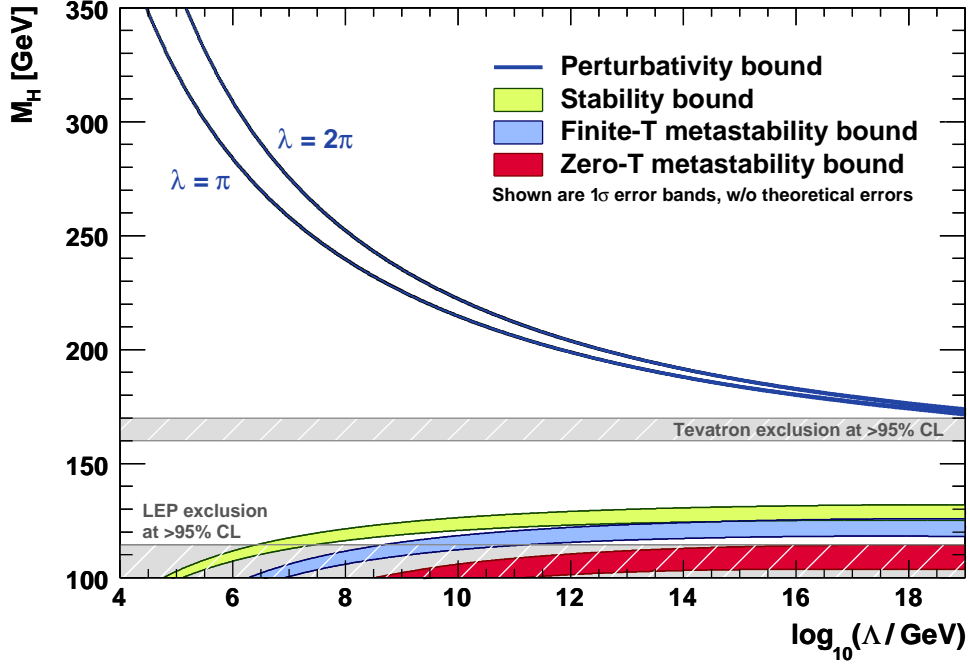


Figure 7.1: The Higgs boson mass as a function of the scale  $\Lambda$  up to which the SM may remain valid obtained from perturbativity (solid dark blue line) and the stability of the electroweak vacuum (shaded regions). The figure is taken from Ref. [221].

quantum fluctuations is slow enough to ensure at least metastability of the electroweak vacuum.

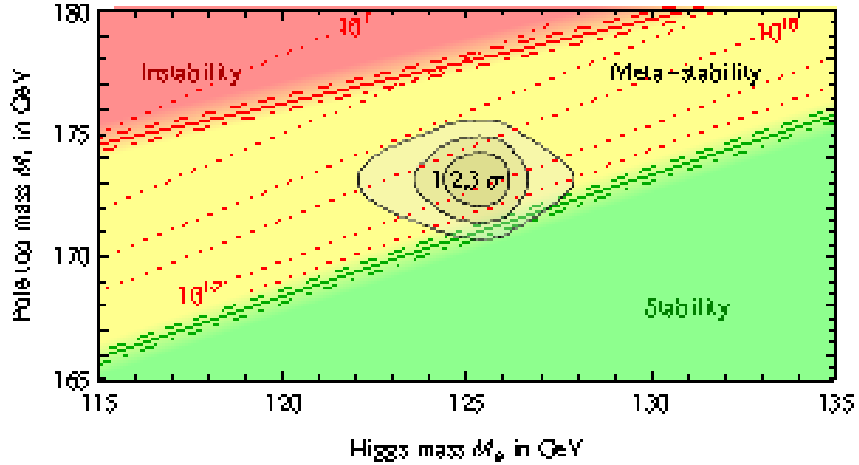


Figure 7.2: Measured value of the top mass and preferred range of  $m_h$  as revealed by the present searches at the LHC, compared to the regions corresponding to absolute stability, meta-stability and instability of the SM vacuum [222]. The three boundaries lines corresponds to  $\alpha_s(M_Z) = 0.1184 \pm 0.0007$ , and the grading of the colours indicates the size of the theoretical errors. The dotted contour-lines show the instability scale  $\Lambda$  in GeV assuming  $\alpha_s(M_Z) = 0.1184$ .

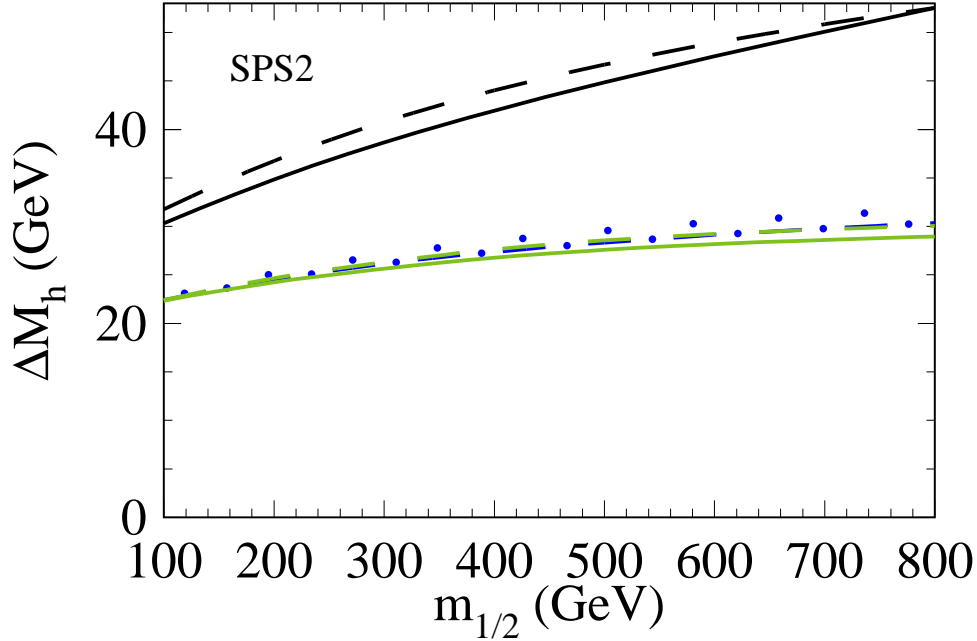


Figure 7.3: Comparison of complete and approximate one- and two-loop corrections to the Higgs boson mass for SPS2 scenario. The solid (full result) and dashed lines ( $m_t^4$  approximation) represent the results in the on-shell scheme where the black and gray curves correspond to the one- and two-loop results, respectively. For comparison, the two-loop  $\overline{\text{DR}}$  results are shown as dash-dotted (full result) and dotted ( $m_t^4$  approximation) curves.

It is also interesting to note that the SM extrapolation of the Higgs parameters (the mass parameter  $m^2$  and quartic coupling  $\lambda$ ) corresponds to near vanishing  $\lambda$  and its beta function at the Planck scale. The coupling  $\lambda = 0$  is the critical value for the electroweak stability. Moreover, the coefficient  $m^2$  of the Higgs bilinear in the scalar potential is also approximately zero (at the Planck scale). This is again a critical value that separates the symmetric phase ( $m^2 > 0$ ) from the broken phase ( $m^2 < 0$ ). At present, we do not know if this is just a numerical coincidence or the consequence of an underlying symmetry.

There are different interpretations in the literature for the near-criticality of the SM parameters. For instance, SUSY implies that  $m^2 = 0$ . If SUSY is softly broken,  $m^2$  would remain near zero, solving the hierarchy problem. Nevertheless, the analysis performed in Ref. [224] shows that the usual low-scale SUSY scenario can accommodate a Higgs mass around 125 GeV only for extreme values of the parameters, *e. g.* large  $\tan\beta$ , heavy stops, or maximal stop mixing. Other explanations of the near-criticality can be given via interpreting the Higgs as a Goldstone boson (composite Higgs modes) or as a consequence of transplanckian dynamics (like in multiverse models). In the following we concentrate on the SUSY explanation.

## 7.2 Higgs boson mass in the MSSM

A natural possibility to counterbalance the effects of the top quark on the evolution of the Higgs self-coupling was found within SUSY models, via the opposite effects induced by the top quark superpartners. The mass of the Higgs boson within SUSY models is linked to the magnitude of its self-coupling, which in turn is fixed by SUSY in terms of the electroweak gauge couplings. Compared to the SM, the MSSM Higgs sector is described by two additional parameters, usually chosen to be the pseudo-scalar mass  $M_A$  and the ratio of the vacuum expectation values of the two Higgs doublets,  $\tan\beta = v_2/v_1$ . The masses of the other Higgs bosons are then fixed by SUSY constraints. In particular, the mass of the light CP-even Higgs boson,  $M_h$ , is bounded from above. At tree-level, this constraint reads  $M_h < M_Z$ . Radiative corrections to the Higgs pole mass raise this bound substantially to values that were inaccessible at LEP [225–227]. The dominant radiative corrections are given by the contribution  $\sim \alpha_t m_t^2 \sim m_t^4$  coming from top- and top squark loops ( $m_t$  is the top quark mass and  $\sqrt{\alpha_t}$  is proportional to the top Yukawa coupling). For illustration, complete and approximate (*i.e.* only contributions  $\sim m_t^4$ ) one- and two-loop corrections to the lightest Higgs boson mass are shown in Fig. 7.3 from Ref. [142].

In this figure, the mass difference  $\Delta M_h = M_h^{i\text{--loop}} - M_h^{\text{tree}}$  is shown as a function of the parameter  $m_{1/2}$  in the scenario SPS2 [228]. The small differences between the solid (full result) and dashed ( $m_t^4$  approximation) lines demonstrate that the leading term  $\sim m_t^4$  approximates the full result to a high accuracy. This motivates the computation of higher order corrections taking into account only the contributions that scale like  $\sim m_t^4$ .

From the one-loop corrections to the Higgs pole masses, that are known without any approximations [176, 229–231], one can show that a second approximation is appropriate: The bulk of the numerical effects can be obtained in the so-called effective-potential approach, for which the external momentum of the Higgs propagator is set to zero. Most of the relevant two-loop corrections have been evaluated in this approach (for reviews, see e.g. Refs. [140, 232]). In addition, two-loop corrections including even CP-violating couplings and improvements from renormalization group considerations have been computed in Refs. [140, 232, 233]. In particular CP violating phases can lead to a shift of a few GeV in  $M_h$ , see, e.g., Refs. [234, 235]. In Ref. [236] a large class of sub-dominant two-loop corrections to the lightest Higgs boson mass have been considered. Furthermore, leading logarithmic corrections at three-loop order have been computed in Ref. [237]. The first complete three-loop calculation of the leading quartic top quark mass terms within supersymmetric QCD has been performed in Refs. [142, 238].

There are by now three computer programs publicly available which include most of the higher order corrections. **FeynHiggs** has been available already since 1998 [233, 239, 240] and has been continuously improved since then [241]. In particular, it contains all numerically important two-loop corrections and accepts both real and complex MSSM input parameters. The second program, **CPSuperH** [242, 243], is based on a renormalization group improved calculation and allows for explicit CP violation. Both programs compute the masses as well as the decay widths of the neutral and charged Higgs bosons. The third program, **H3m** [244], contains all currently available three-loop results. Furthermore, **H3m** constitutes an interface to **FeynHiggs** [245] and various SUSY spectrum generators which allows for precise predictions of  $M_h$  on the basis of realistic SUSY scenarios.



### 7.2.1 Calculation of $\mathcal{O}(\alpha_t \alpha_s^2)$ corrections in the MSSM

In this section we focus on details of the calculation of the lightest Higgs boson mass to three-loop accuracy in SUSY-QCD. It was the first calculation of an observable at this order of accuracy in the framework of SUSY-QCD and it raised technical difficulties specific to higher order calculations.

At tree-level, the mass matrix of the neutral, CP-even Higgs bosons  $h, H$  has the following form:

$$\mathcal{M}_{H,\text{tree}}^2 = \frac{\sin 2\beta}{2} \times \begin{pmatrix} M_Z^2 \cot \beta + M_A^2 \tan \beta & -M_Z^2 - M_A^2 \\ -M_Z^2 - M_A^2 & M_Z^2 \tan \beta + M_A^2 \cot \beta \end{pmatrix}. \quad (7.1)$$

The diagonalization of  $\mathcal{M}_{H,\text{tree}}^2$  gives the tree-level result for  $M_h$  and  $M_H$ , and leads to the well-known bound  $M_h < M_Z$  which is approached in the limit  $\tan \beta \rightarrow \infty$ .

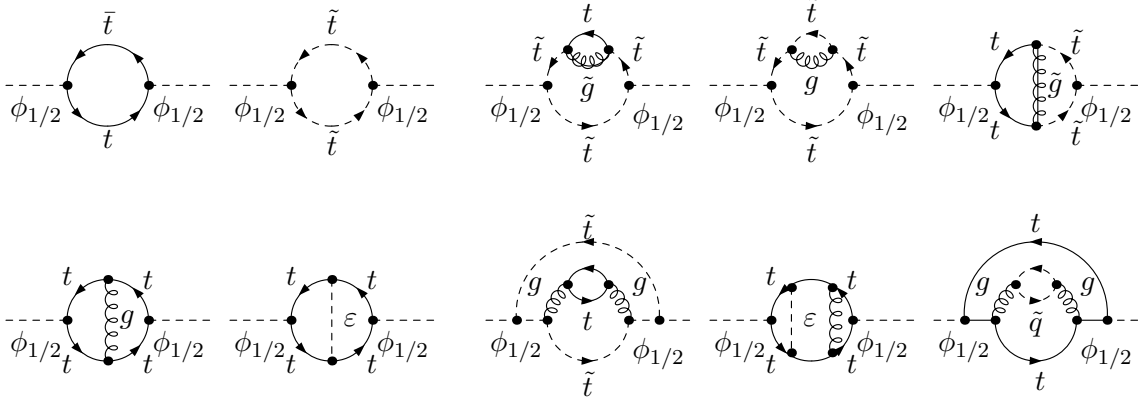


Figure 7.4: Sample diagrams contributing to  $\Sigma_{\phi_1}$ ,  $\Sigma_{\phi_2}$ ,  $\Sigma_{\phi_1\phi_2}$ , etc. to one-, two- and three-loops. Internal solid, dashed, dotted and curly lines correspond to top quarks, top squarks,  $\varepsilon$ -scalar and gluons, respectively. Gluinos are depicted with as curly lines with an additional solid line in the middle. The external dashed line corresponds to the Higgs bosons.

The mass matrix  $\mathcal{M}_H^2$  is obtained from the quadratic terms in the Higgs boson potential constructed from the fields  $\phi_1$  and  $\phi_2$ . They are related to the physical Higgs mass eigenstates via the mixing angle  $\alpha$

$$\begin{pmatrix} H \\ h \end{pmatrix} = \begin{pmatrix} \cos \alpha & \sin \alpha \\ -\sin \alpha & \cos \alpha \end{pmatrix} \begin{pmatrix} \phi_1 \\ \phi_2 \end{pmatrix}. \quad (7.2)$$

As usual,  $h$  stands for the lightest Higgs boson. The mixing angle  $\alpha$  is determined at the leading order through

$$\tan 2\alpha = \tan 2\beta \frac{M_A^2 + M_Z^2}{M_A^2 - M_Z^2}; \quad -\frac{\pi}{2} < \alpha < 0, \quad (7.3)$$

where  $M_Z$  is the mass of the Z boson and  $\tan \beta = v_2/v_1$ . Since  $\phi_1$  does not couple directly to top quarks, it is convenient to perform the calculations of the Feynman diagrams in the  $(\phi_1, \phi_2)$  basis.

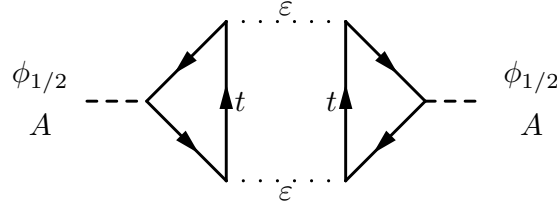


Figure 7.5: Sample diagram contributing a finite term to  $\Sigma_{\phi_1}$ ,  $\Sigma_{\phi_2}$ , etc. when the infra-red divergence are regulated through a small external momentum or a finite  $\varepsilon$ -scalar mass.

Including higher order corrections, one obtains the Higgs boson mass matrix

$$\mathcal{M}_H^2 = \mathcal{M}_{H,\text{tree}}^2 - \begin{pmatrix} \hat{\Sigma}_{\phi_1} & \hat{\Sigma}_{\phi_1\phi_2} \\ \hat{\Sigma}_{\phi_1\phi_2} & \hat{\Sigma}_{\phi_2} \end{pmatrix}, \quad (7.4)$$

which again gives the physical Higgs boson masses upon diagonalization. The renormalized quantities  $\hat{\Sigma}_{\phi_1}$ ,  $\hat{\Sigma}_{\phi_2}$  and  $\hat{\Sigma}_{\phi_1\phi_2}$  are obtained from the self energies of the fields  $\phi_1$ ,  $\phi_2$ ,  $A$ , evaluated at zero external momentum, as well as from tadpole contributions of  $\phi_1$  and  $\phi_2$  (see, e.g., Ref. [140]).

$$\begin{aligned} \hat{\Sigma}_{\phi_1} &= \Sigma_{\phi_1} - \Sigma_A \sin^2 \beta \\ &\quad + \frac{e}{2M_W \sin \vartheta_W} t_{\phi_1} \cos \beta (1 + \sin^2 \beta) \\ &\quad - \frac{e}{2M_W \sin \vartheta_W} t_{\phi_2} \cos^2 \beta \sin \beta, \\ \hat{\Sigma}_{\phi_2} &= \Sigma_{\phi_2} - \Sigma_A \cos^2 \beta \\ &\quad - \frac{e}{2M_W \sin \vartheta_W} t_{\phi_1} \sin^2 \beta \cos \beta \\ &\quad + \frac{e}{2M_W \sin \vartheta_W} t_{\phi_2} \sin \beta (1 + \cos^2 \beta), \\ \hat{\Sigma}_{\phi_1\phi_2} &= \Sigma_{\phi_1\phi_2} + \Sigma_A \sin \beta \cos \beta \\ &\quad + \frac{e}{2M_W \sin \vartheta_W} t_{\phi_1} \sin^3 \beta \\ &\quad + \frac{e}{2M_W \sin \vartheta_W} t_{\phi_2} \cos^3 \beta. \end{aligned} \quad (7.5)$$

In this equation,  $\vartheta_W$  is the weak mixing angle,  $\Sigma_A$  denotes the self energy of the pseudo-scalar Higgs boson and  $t_{\phi_i}$  the tadpole contributions of the field  $\phi_i$ . Typical diagrams to the individual contributions can be found in Fig. 7.4.

Considering the many different mass parameters entering the formula for the Higgs boson mass an exact calculation of the three-loop corrections is currently not feasible. However, it is possible to apply expansion techniques [136] for various limits which allow to cover a large part of the supersymmetric parameter space. After the application of the asymptotic expansion the resulting integrals have to be reduced to an independent set of master integrals. For the case of the Higgs mass corrections there will be only three-loop tadpole integrals that can be handled with the program MATAD [109].

A technical subtlety arises when calculating diagrams like those shown in Fig. 7.5. If both the external momentum and the  $\varepsilon$ -scalar mass are set to zero from the beginning, an infra-red

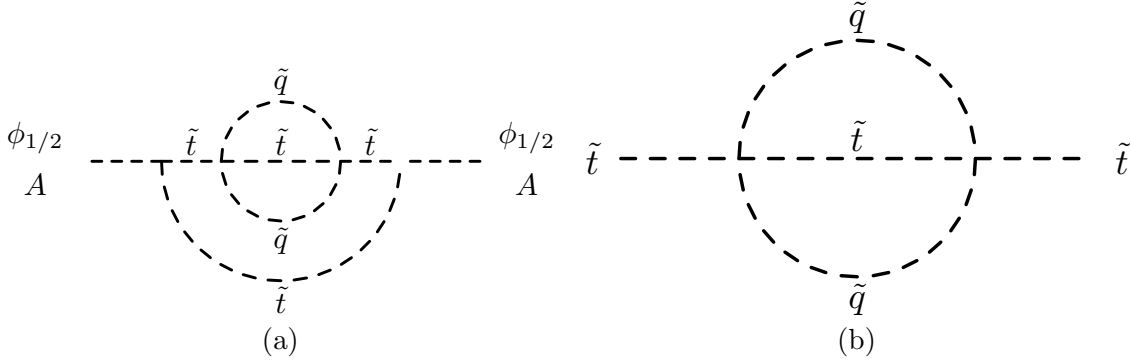


Figure 7.6: (a) Feynman diagram involving a heavy virtual squark contributing to the Higgs boson self energy. (b) Counter-term diagram related to the diagram in (a). The same notation as in Fig. 7.4 has been adopted.

divergence occurs and cancels the ultra-violet divergence of the integral. In effect, the diagram will be of order  $(d - 4)$  due to the  $\varepsilon$ -scalar algebra. In order to avoid this, one can keep the external momentum  $q$  non-zero, though much smaller than all other scales. The ultra-violet pole multiplied by the algebraic factor of  $(d - 4)$  then produces a finite contribution, while the infra-red divergence leads to a contribution  $(d - 4) \ln(q^2)$  that vanishes as  $d \rightarrow 4$ . Instead of the requirement  $q \neq 0$  one could also introduce a nonzero mass for the  $\varepsilon$  scalars in order to regulate the infra-red divergences. In the final result one observes that the regulator is multiplied by an additional factor  $(d - 4)$  leading to a finite result for  $M_\varepsilon \rightarrow 0$ . Alternatively, one can allow a non zero  $\varepsilon$ -scalar mass and shift the squark mass counter-terms so that all  $M_\varepsilon$  dependent contributions in the final result cancel out<sup>22</sup>. All these renormalization prescriptions lead to identical results for the corrections to the Higgs boson mass  $M_h$ , that is a non trivial check of the calculation.

Concerning the renormalization, it is well known that the perturbative series can exhibit a bad convergence behaviour in case it is parametrized in terms of the on-shell quark masses<sup>23</sup> which is due to intrinsically large contributions related to the infra-red behaviour of the theory. Thus, it is tempting to re-parametrize the results for the Higgs boson mass in terms of the top quark mass renormalized in the  $\overline{\text{DR}}$  scheme. Moreover, the two-loop renormalization constants for the masses of the SUSY particles and the top squark mixing angle, that are required for this calculation, are much more complicated in the on-shell scheme as compared to the  $\overline{\text{DR}}$  ones. Thus, it is preferable to adopt the  $\overline{\text{DR}}$  scheme also for these parameters. The renormalization constants for the gluino and  $\varepsilon$ -scalar masses are needed only at the one-loop order. For them, both schemes are accessible. Nevertheless, the  $\varepsilon$ -scalar mass renormalized in the on-shell scheme might be better suited for this type of calculations. In this case, it can be set equal to zero in the three-loop diagrams, that makes the calculation less involved. An extensive discussion about the calculation of the two-loop renormalization constants required in this computation as well as explicit formulae can be found in section 4. In the remainder of this section we will refer to this renormalization scheme as  $\overline{\text{DR}}$  scheme although it contains a mixture of on-shell and  $\overline{\text{DR}}$

<sup>22</sup>This renormalization scheme is equivalent with the  $\overline{\text{DR}}'$  scheme discussed in section 4.2, however it is not identical.

<sup>23</sup>For a typical example we refer to the electroweak  $\rho$  parameter. Using the on-shell top quark mass the four-loop corrections [246–248] are larger by a factor 50 as compared to the  $\overline{\text{MS}}$  scheme.

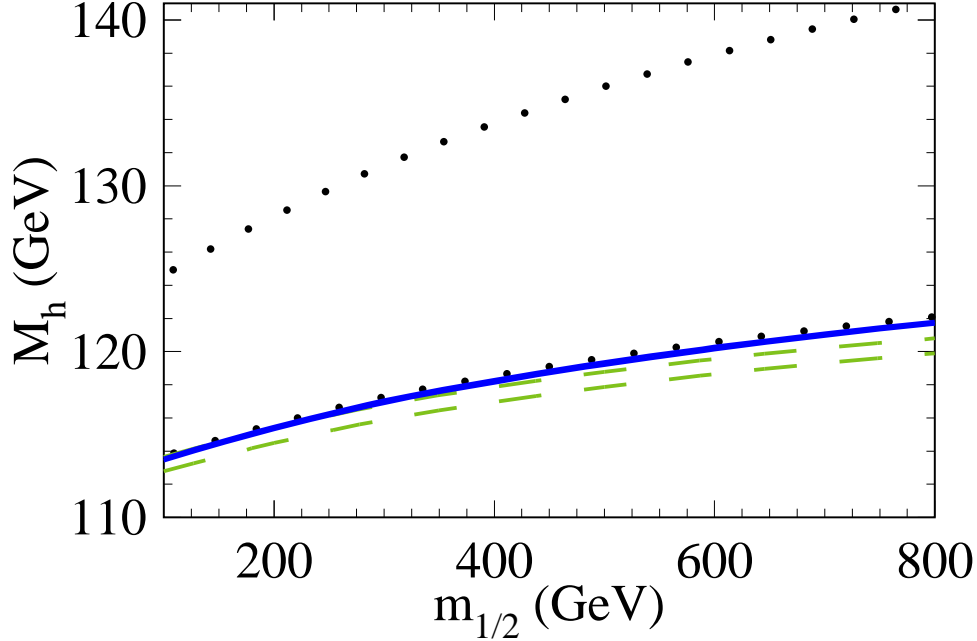


Figure 7.7: Renormalization scheme dependence of  $M_h$  as a function of  $m_{1/2}$  adopting SPS2. Dotted, dashed and solid curves correspond to one-, two- and three-loop results. The  $\overline{\text{DR}}$  (on-shell) results correspond to the lower (upper) curves. The three-loop curves obtained in the two renormalization schemes lay on top of each other.

parameters in order to distinguish between it and the genuine on-shell scheme.

At this point a comment concerning the minimal  $\overline{\text{DR}}$  renormalization constants for the masses of the top squarks is in order. Due to diagrams involving heavy squarks  $\tilde{q}$ , for example Fig. 7.6(a), the squared Higgs boson mass receives contributions which are proportional to  $m_{\tilde{q}}^2$  and thus can lead to unnatural large corrections. For this reason the on-shell scheme for these contributions is better suited, because it avoids the potentially large terms  $\sim m_{\tilde{q}}^2$  from the three-loop diagrams. The renormalization of the mixing angle is free of such enhanced contributions and can be done in the pure  $\overline{\text{DR}}$  scheme. A similar behaviour is observed when the gluino is much heavier than the top squarks [116, 249]. In this case, the two- and three-loop corrections to the Higgs masses contain terms proportional to  $m_{\tilde{g}}$  and  $m_{\tilde{g}}^2$ . These contributions are canceled when the masses are renormalized in the on-shell scheme by the finite parts of the relevant counter-terms. Thus, in order to avoid unnatural large radiative corrections to the Higgs mass for scenarios with heavy gluinos a modified non-minimal renormalization scheme for the top squark masses is required. The additional finite shifts of top squark masses are chosen such that they cancel the power-like behaviour of the gluino contributions. Again, the renormalization of the mixing angle will not be modified as compared to the genuine  $\overline{\text{DR}}$  scheme. The relevant finite shifts for commonly adopted scenarios are explicitly given in Appendix B.

As an illustration of the renormalization scheme issue, we show in Fig. 7.7 from Ref. [142] the

renormalization scheme dependence of  $M_h$  as a function of the parameter  $m_{1/2}$  for the SPS2 scenario. In the left panel of Fig. 7.7 the upper dotted, dashed and solid curve correspond to the one-, two- and three-loop prediction of  $M_h$  in the on-shell scheme whereas the corresponding lower three curves are obtained in the  $\overline{\text{DR}}$  scheme. In the on-shell scheme one observes large positive one-loop corrections which get reduced by 10 to 20 GeV after including the two-loop terms. The three-loop corrections amount to several hundred MeV. They are positive or negative depending on the value of  $m_{1/2}$ . The situation is completely different for  $\overline{\text{DR}}$  mass parameters: the one-loop corrections are significantly smaller and lead to values of  $M_h$  which are already of the order of the two- and three-loop on-shell prediction. The two-loop term leads to a small shift of the order of  $-1$  GeV and the three-loop term to a positive shift of about the same order of magnitude. The final prediction for  $M_h$  is very close to the one obtained after incorporating three-loop on-shell results.<sup>24</sup>

The three-loop results have in general very long expressions. However, for simplifying assumptions about the supersymmetric mass spectrum, like for example the *natural* SUSY, for which the superpartners of the first and second generation of quarks are much heavier than the gluino and third generation of squarks, *i. e.*  $m_{\tilde{q}} \gg m_{\tilde{t}_1} \approx m_{\tilde{t}_2} \approx m_{\tilde{g}}$ , the analytical expressions for the dominant contributions have a quite compact form. Let us mention that in general, for the case of quasi degenerate masses a naive Taylor expansion in the mass differences is sufficient, while for large mass ratios an asymptotic expansion is necessary. For illustration, we give below the three-loop results for the two-point functions contributing to the Higgs boson mass, where for the renormalization of the stop quark masses the modified  $\overline{\text{DR}}$  scheme as given in Eq. (B.53) was adopted.

$$\begin{aligned}
\hat{\Sigma}_{\phi_1} &= \frac{G_F m_t^4 \sqrt{2}}{\pi^2 \cos^2 \beta} \left( \frac{\alpha_s}{4\pi} \right)^2 \frac{A_t^2}{m_{\text{SUSY}}^2} \left[ -\frac{349}{9} + \frac{32}{9} L_{\mu t} + \frac{32}{9} L_{\mu t}^2 + \left( \frac{56}{9} + \frac{64}{9} L_{\mu t} \right) L_{tS} + \frac{32}{9} L_{tS}^2 \right. \\
&\quad \left. + \frac{94}{3} \zeta(3) + \mathcal{O} \left( \frac{m_{\text{SUSY}}^4}{m_{\tilde{q}}^4} \right) \right], \\
\hat{\Sigma}_{\phi_{12}} &= \frac{G_F m_t^4 \sqrt{2}}{\pi^2 \cos \beta \sin \beta} \left[ \frac{\alpha_s}{4\pi} \frac{A_t}{m_{\text{SUSY}}} \left( -2 - 4L_{\mu t} - 2L_{tS} \right) \right. \\
&\quad + \left( \frac{\alpha_s}{4\pi} \right)^2 \left\{ \frac{A_t^2}{m_{\text{SUSY}}^2} \left( \frac{349}{9} - \frac{32}{9} L_{\mu t} - \frac{32}{9} L_{\mu t}^2 + \left( -\frac{56}{9} - \frac{64}{9} L_{\mu t} \right) L_{tS} - \frac{32}{9} L_{tS}^2 - \frac{94}{3} \zeta(3) \right) \right. \\
&\quad + \frac{A_t m_{\text{SUSY}}}{m_{\tilde{q}}^2} \left( 40 - \frac{160}{9} L_{t\tilde{q}} - \frac{40}{3} L_{t\tilde{q}}^2 + L_{tS} \left( \frac{160}{9} + \frac{40}{3} L_{t\tilde{q}} \right) - \frac{80}{3} \zeta(2) \right) \\
&\quad + \frac{A_t}{m_{\text{SUSY}}} \left( -\frac{416}{27} - \frac{364}{27} L_{\mu t} - \frac{100}{3} L_{\mu t}^2 - \frac{304}{9} L_{tS}^2 + \frac{200}{9} L_{t\tilde{q}} - 20 L_{t\tilde{q}}^2 \right. \\
&\quad \left. \left. + L_{tS} \left( -\frac{628}{27} - \frac{400}{9} L_{\mu t} + \frac{80}{3} L_{t\tilde{q}} \right) - 40 \zeta(2) + \frac{106}{3} \zeta(3) \right) \right\} + \mathcal{O} \left( \frac{m_{\text{SUSY}}^4}{m_{\tilde{q}}^4} \right) \Big], \\
\hat{\Sigma}_{\phi_2} &= \frac{G_F m_t^4 \sqrt{2}}{\pi^2 \sin^2 \beta} \left[ \frac{3}{2} L_{tS} + \frac{\alpha_s}{4\pi} \left( 4 + \left( 4 + 16 L_{\mu t} \right) L_{tS} + 4 L_{tS}^2 + \frac{A_t}{m_{\text{SUSY}}} \left( 4 + 8 L_{\mu t} + 4 L_{tS} \right) \right) \right]
\end{aligned}$$

<sup>24</sup>There are regions in the parameter space where the two-loop corrections are accidentally small in the  $\overline{\text{DR}}$  scheme leading to relatively large three-loop terms. Nevertheless the overall size of the two- and three-loop corrections is small.

$$\begin{aligned}
& + \left( \frac{\alpha_s}{4\pi} \right)^2 \left\{ \frac{2764}{9} - \frac{116}{27} L_{\mu t} - \frac{136}{3} L_{\mu t}^2 + \left( -\frac{644}{9} + \frac{164}{3} L_{\mu t} \right) L_{tS}^2 \right. \\
& + 24 L_{tS}^3 + \frac{400}{3} L_{t\bar{q}} - \frac{200}{3} L_{t\bar{q}}^2 - \frac{20}{3} L_{t\bar{q}}^3 - 120 \zeta(2) - 80 L_{t\bar{q}} \zeta(2) + \frac{8}{3} \zeta(3) \\
& - \left( \frac{2216}{27} + \frac{644}{9} L_{\mu t} - \frac{328}{3} L_{\mu t}^2 - 40 L_{t\bar{q}} - 20 L_{t\bar{q}}^2 - 40 \zeta(2) + 16 \zeta(3) \right) L_{tS} \\
& + \frac{m_{\text{SUSY}}^2}{m_{\bar{q}}^2} \left( \frac{42356}{225} + 8 L_{tS}^2 - \frac{2128}{45} L_{t\bar{q}} - \frac{176}{3} L_{t\bar{q}}^2 + \left( \frac{3928}{45} + \frac{152}{3} L_{t\bar{q}} \right) L_{tS} - \frac{400}{3} \zeta(2) \right) \\
& + \frac{A_t m_{\text{SUSY}}}{m_{\bar{q}}^2} \left( -80 + L_{tS} \left( -\frac{320}{9} - \frac{80}{3} L_{t\bar{q}} \right) + \frac{320}{9} L_{t\bar{q}} + \frac{80}{3} L_{t\bar{q}}^2 + \frac{160}{3} \zeta(2) \right) \\
& + \frac{A_t}{m_{\text{SUSY}}} \left( \frac{832}{27} + \frac{728}{27} L_{\mu t} + \frac{200}{3} L_{\mu t}^2 + \frac{608}{9} L_{tS}^2 + L_{tS} \left( \frac{1256}{27} + \frac{800}{9} L_{\mu t} - \frac{160}{3} L_{t\bar{q}} \right) \right. \\
& - \frac{400}{9} L_{t\bar{q}} + 40 L_{t\bar{q}}^2 + 80 \zeta(2) - \frac{212}{3} \zeta(3) \left. \right) \\
& + \frac{A_t^2}{m_{\text{SUSY}}^2} \left( -\frac{349}{9} + \frac{32}{9} L_{\mu t} + \frac{32}{9} L_{\mu t}^2 + \left( \frac{56}{9} + \frac{64}{9} L_{\mu t} \right) L_{tS} + \frac{32}{9} L_{tS}^2 + \frac{94}{3} \zeta(3) \right) \left. \right\} \\
& + \mathcal{O} \left( \frac{m_{\text{SUSY}}^4}{m_{\bar{q}}^4} \right) \Big], \tag{7.6}
\end{aligned}$$

with  $m_t = m_t(\mu_r)$ ,  $m_{\text{SUSY}} = m_{\text{SUSY}}(\mu_r) = m_{\tilde{t}_1}(\mu_r) = m_{\tilde{t}_2}(\mu_r) = m_{\tilde{g}}(\mu_r)$ ,  $L_{\mu t} = \ln(\mu_r^2/m_t^2)$ ,  $L_{tS} = \ln(m_t^2/m_{\text{SUSY}}^2)$  and  $L_{t\bar{q}} = \ln(m_t^2/m_{\bar{q}}^2)$  where  $\mu_r$  is the renormalization scale.

### 7.2.2 Phenomenological analysis

In order to quantify the phenomenological significance of the three-loop contributions, it is interesting to investigate the dependence of  $M_h$  on SUSY parameters. In the following, we adopt the “modified  $m_h^{\text{max}}$ ” scenario as defined in Ref [115]. The relevant MSSM parameters for our analysis are the top squark masses  $m_{\tilde{t}_1} = 370$  GeV and  $m_{\tilde{t}_2} = 1045$  GeV, the gluino mass  $m_{\tilde{g}} = 860$  GeV, the squark mass scale  $m_{\bar{q}} = 1042$  GeV, the top trilinear coupling  $A_t = 1500$  GeV and the mass of the pseudoscalar Higgs  $M_A = 1000$  GeV.

In Fig. 7.8 from Ref. [115] is shown the comparison between the two- (dashed line) and three-loop (full line) predictions for the Higgs boson mass as a function of  $\tan \beta$  parameter. As can be read from the plot, the genuine three-loop corrections amount to around 2 GeV for the given mass spectrum, independently of the value of  $\tan \beta$ . Let us remind the reader that the experimental accuracy on  $M_h$  expected at the LHC is almost an order of magnitude smaller. It is also worth mentioning that the three-loop corrections are positive and increase the predicted value for  $M_h$  beyond 125 GeV. For increasing gluino and third generation squark masses, the light Higgs boson mass becomes larger and values well above 120 GeV can be reached.

We can infer from the above analysis that for a precise comparison with the experimental data expected from the LHC experiments, the three-loop corrections are indispensable. Moreover, the MSSM predictions can easily accommodate a light Higgs boson mass in the range between  $125 < M_h < 127$  GeV as observed in the current experiments at the LHC.

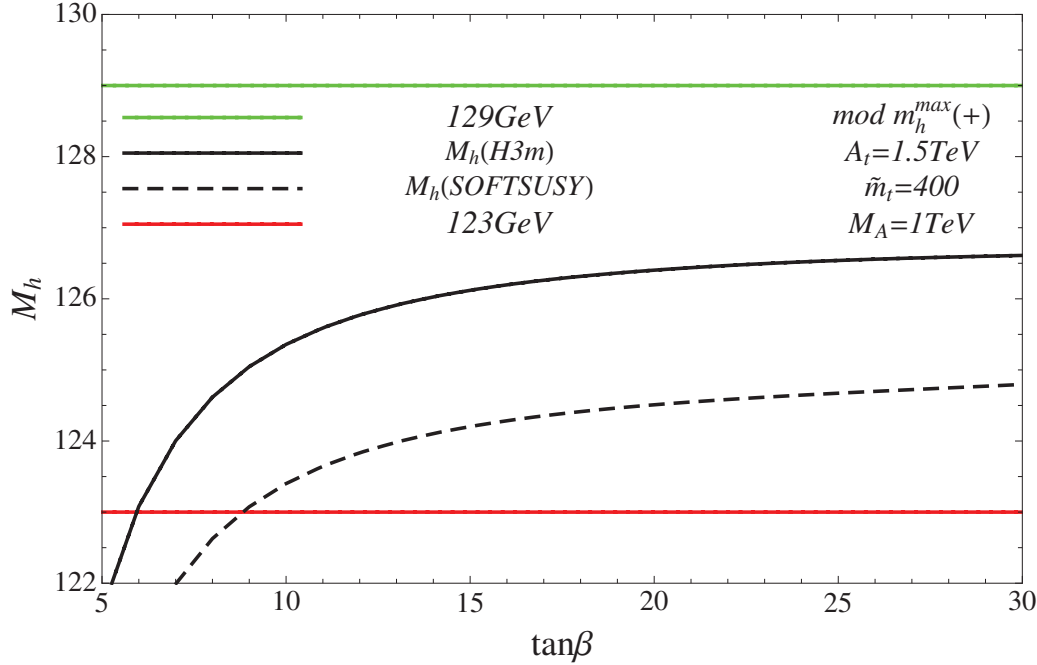


Figure 7.8: The light Higgs boson mass as a function of  $\tan\beta$  to three-loop accuracy from Ref. [115]

## 8 Hadronic Higgs production and decay in susy models

After the discovery of the new scalar particle with the mass around 125 GeV the most important question to be answered is whether it is indeed the Higgs boson predicted by the SM or it has another origin. To obtain the answer one has to study in detail the interaction properties of this new scalar with the SM particles. This task requires the comparison of the theory predictions for the production cross sections and the decay rates of the newly discovered scalar particle with the experimental data. In most of the cases, a precision of the theory predictions at the percent level is required in order to cope with the experimental accuracy. This implies that radiative corrections even at next-to-next to leading order (NNLO) have to be taken into account.

In the current section we concentrate on the radiative corrections up to NNLO to the hadronic Higgs production and decays within the MSSM. It turns out that in most of the cases only the NNLO SUSY-QCD corrections have to be taken into account. If available in the literature, also the NNLO top-Yukawa corrections, expected to be the next dominant contributions, will be discussed. As the exact analytic calculations are not always feasible, several theoretical methods employing phenomenologically well motivated simplifying assumptions will be presented.

## 8.1 Effective field theory formalism

In this section we want to derive the effective field theory formalism (EFT) following the method of operator product expansion (OPE) introduced by Wilson [250]<sup>25</sup>. The main idea is again to disentangle the long and short distance physics from each other. Precisely, the long distance physics is described by local operators constructed from light degrees of freedom  $\mathcal{O}_i$ , whereas the effects of the heavy degrees of freedom are absorbed into coefficient functions of the operators. For QCD the relevant local operators have dimension four. Their renormalization and the issue of operator mixing under renormalization have been studied in detail in the literature [251–253]. For all processes studied in this section, the low energy effective theory is QCD with five active flavours supplemented with a light Higgs boson. For completeness, we briefly review the main results concerning the renormalization of the local dimension four operators below.

In the following we assume for simplicity that the fundamental theory is described by the SUSY-QCD particle content together with the two Higgs doublets of the MSSM,  $\phi_i$ , with  $i = 1, 2$ . The corresponding interactions are described by the following Lagrangian

$$\mathcal{L} = \mathcal{L}_{\text{QCD}} + \mathcal{L}_{\text{SQCD}} + \sum_{i=1,2} \mathcal{L}_{q\phi_i} + \sum_{i=1,2} \mathcal{L}_{\tilde{q}\phi_i} \quad (8.1)$$

where

$$\mathcal{L}_{q\phi_i} = - \sum_{q=1}^6 \frac{m_q}{v} g_q^{\phi_i} \bar{q} q \phi_i \quad \text{and} \quad \mathcal{L}_{\tilde{q}\phi_i} = - \sum_{q=1}^6 \sum_{r,k=1,2} \frac{m_q}{v} g_{\tilde{q};kr}^{\phi_i} \tilde{q}_k^* \tilde{q}_r \phi_i. \quad (8.2)$$

$\mathcal{L}_{\text{QCD}} + \mathcal{L}_{\text{SQCD}}$  denotes the supersymmetric extension of the full QCD Lagrangian with six quark flavours. The couplings  $g_q^{\phi_i}$  and  $g_{\tilde{q};kr}^{\phi_i}$  are defined in Table 8.1, where  $v = \sqrt{v_1^2 + v_2^2}$ , with  $v_i, i = 1, 2$ , is obtained from the vacuum expectation values of the two Higgs doublets of the MSSM. The fields  $\tilde{q}_i$ , with  $i = 1, 2$ , denote as before the squark mass eigenstates, while  $\theta_q$  stands for the mixing angle defined through:

$$\sin 2\theta_q = \frac{2m_q X_q}{m_{\tilde{q}_1}^2 - m_{\tilde{q}_2}^2}, \quad X_q = A_q - \mu_{\text{SUSY}} \begin{cases} \tan \beta, & \text{for down-type quarks} \\ \cot \beta, & \text{for up-type quarks} \end{cases}, \quad (8.3)$$

where  $A_q$  is the trilinear coupling and  $\mu_{\text{SUSY}}$  the Higgs-Higgsino bilinear coupling.

We assume further the mass of the lightest Higgs boson  $h$  to be much smaller than the mass of the top quark and of the SUSY particles, as well as all the other Higgs bosons. In this case, the physical phenomena at low energies can be described by an effective theory containing five quark flavours and the light Higgs

$$\mathcal{L} \longrightarrow \mathcal{L}_Y^{\text{eff}} + \mathcal{L}_{\text{QCD}}^{(5)}, \quad (8.4)$$

where  $\mathcal{L}_{\text{QCD}}^{(5)}$  denotes the Lagrangian of QCD with five active flavours.

At leading order in the heavy masses, the effective Lagrangian  $\mathcal{L}_Y^{\text{eff}}$  can be written as a linear

---

<sup>25</sup>For a pedagogical overview of the method see also Ref [65].



|      |                |                             |   |                             |
|------|----------------|-----------------------------|---|-----------------------------|
| f    | $g_q^{\phi_1}$ | $g_{\tilde{q};11}^{\phi_1}$ | $g_{\tilde{q};12}^{\phi_1} = g_{\tilde{q};21}^{\phi_1}$ | $g_{\tilde{q};22}^{\phi_1}$ |
| up   | 0              | $-\mu S_q/S_\beta$          | $-\mu C_q/S_\beta$                                      | $\mu S_q/S_\beta$           |
| down | $1/C_\beta$    | $(2m_q + A_q S_q)/C_\beta$  | $A_q C_q/C_\beta$                                       | $(2m_q - A_q S_q)/C_\beta$  |
| f    | $g_q^{\phi_2}$ | $g_{\tilde{q};11}^{\phi_2}$ | $g_{\tilde{q};12}^{\phi_2} = g_{\tilde{q};21}^{\phi_2}$ | $g_{\tilde{q};22}^{\phi_2}$ |
| up   | $1/S_\beta$    | $(2m_q + A_q S_q)/S_\beta$  | $A_q C_q/S_\beta$                                       | $(2m_q - A_q S_q)/S_\beta$  |
| down | 0              | $-\mu S_q/C_\beta$          | $-\mu C_q/C_\beta$                                      | $\mu S_q/C_\beta$           |

Table 8.1: Yukawa coupling coefficients for up and down type quark and squark, where  $S_q = \sin 2\theta_q$  and  $C_q = \cos 2\theta_q$ , and  $S_\beta = \sin \beta$  and  $C_\beta = \cos \beta$ .

combination of three physical, gauge independent operators [168, 253] constructed from the light degrees of freedom

$$\mathcal{L}_Y^{\text{eff}} = -\frac{h^{(0)}}{v^{(0)}} \left[ C_1^0 \mathcal{O}_1^0 + \sum_q (C_{2q}^0 \mathcal{O}_{2q}^0 + C_{3q}^0 \mathcal{O}_{3q}^0) \right], \quad (8.5)$$

where the coefficient functions  $C_i$ ,  $i = 1, 2q, 3q$ , parametrize the effects of the heavy particles on the low-energy phenomena. The superscript 0 labels bare quantities. The three operators are defined as

$$\begin{aligned} \mathcal{O}_1^0 &= (G_{\mu,\nu}^{0,\prime,a})^2, \\ \mathcal{O}_{2q}^0 &= m_q^{0,\prime} \bar{q}^{0,\prime} q^{0,\prime}, \\ \mathcal{O}_{3q}^0 &= \bar{q}^{0,\prime} (i \not{D}^{0,\prime} - m_q^{0,\prime}) q^{0,\prime}, \end{aligned} \quad (8.6)$$

where  $G_{\mu,\nu}^{0,\prime,a}$  and  $D_\mu^{0,\prime}$  are the gluon field strength tensor and the covariant derivative, respectively. The primes label the quantities in the effective theory. The relations between the parameters and fields in the full and effective theories have been derived in section 6.1. The explicit formulae can be read off from Eqs. (6.49). The operator  $\mathcal{O}_{3q}$  vanishes by the fermionic equation of motion and it will not contribute to physical observables. Thus, the last term in Eq. (8.5) might be omitted, once the coefficients  $C_1^0, C_{2q}^0$  are determined.

For convenience of the reader we reproduce the results for the renormalization constants of the operators  $\mathcal{O}_1^0$  and  $\mathcal{O}_{2q}^0$  that are of interest

$$\mathcal{O}_1 = Z_{11} \mathcal{O}_1^0 + Z_{12} \mathcal{O}_{2q}^0, \quad \mathcal{O}_{2q} = Z_{22} \mathcal{O}_{2q}^0, \quad \text{where} \\ Z_{11} = \left( 1 - \frac{\pi}{\alpha'_s} \frac{\beta(\alpha'_s)}{\epsilon} \right)^{-1}, \quad Z_{12} = -\frac{4\gamma_m(\alpha'_s)}{\epsilon} \left( 1 - \frac{\pi}{\alpha'_s} \frac{\beta(\alpha'_s)}{\epsilon} \right)^{-1}, \quad Z_{22} = 1, \quad (8.7)$$

$$C_1 = Z_{11}^{-1} C_1^0, \quad C_{2q} = C_{2q}^0 - \frac{Z_{12}}{Z_{11}} C_1^0. \quad (8.8)$$

In the above equations the beta function and quark mass anomalous dimension  $\gamma_m$  refer to QCD with  $n_l = 5$  active flavours evaluated in the  $\overline{\text{MS}}$  scheme. They are needed up to three-loop order and have been given explicitly in section 3.

The renormalized coefficient functions and operators are finite but not renormalization group (RG) invariant. In Ref. [254], a redefinition of the coefficient functions and operators was

introduced so that they are separately renormalization group invariant. The RG invariant operators are defined as follows

$$\begin{aligned}\mathcal{O}_g &= -\frac{2\pi}{\beta_0^{(5)}} \left( \frac{\pi\beta^{(5)}}{2\alpha_s^{(5)}} \mathcal{O}_1 - 2\gamma_m^{(5)} \sum_q \mathcal{O}_{2q} \right), \\ \mathcal{O}_q &= \mathcal{O}_{2q},\end{aligned}\tag{8.9}$$

where the superscript (5) marks that there are five active quarks to be considered in the formulas for the beta function and the mass anomalous dimension  $\gamma_m$ . Accordingly, the associated coefficient functions are given by

$$\begin{aligned}C_g &= -\frac{\alpha_s^{(5)}\beta_0^{(5)}}{\pi^2\beta^{(5)}}C_1, \\ C_q &= \frac{4\alpha_s^{(5)}\gamma_m^{(5)}}{\pi\beta^{(5)}}C_1 + C_{2q}.\end{aligned}\tag{8.10}$$

This procedure allows us to choose independent renormalization scales for coefficient functions and operators. In practice, one chooses  $\mu \approx M_h$  for the renormalization scale of the operators and  $\mu \approx \tilde{M}$  (where  $\tilde{M}$  denotes an averaged mass for the heavy supersymmetric particles) for the coefficient functions. Thus, Eq. (8.9) is to be evaluated at a low scale  $\mu \approx M_h$ , whereas Eq. (8.10) is to be utilized at a high scale  $\mu \approx \tilde{M}$ .

For the computation of the Higgs production and decay rates, it is however more convenient to re-express the effective Lagrangian in terms of the operators  $\mathcal{O}_1$  and  $\mathcal{O}_{2q}$ . However now, one keeps the separation of the scales for operators and coefficient functions as given in Eqs. (8.9) and (8.10). The new coefficient functions read [254]

$$\begin{aligned}C_1(\tilde{M}, M_h) &= \frac{\alpha'_s(\tilde{M})\beta^{(5)}(\alpha'_s(M_h))}{\alpha'_s(M_h)\beta^{(5)}(\alpha'_s(\tilde{M}))}C_1(\tilde{M}) = -\frac{\pi^2\beta^{(5)}(\alpha'_s(M_h))}{[\alpha'_s(M_h)]^2\beta_0^{(5)}}C_g(\tilde{M}), \\ C_2(\tilde{M}, M_h) &= \frac{4\alpha'_s(\tilde{M})}{\pi\beta^{(5)}(\alpha'_s(\tilde{M}))}[\gamma_m^{(5)}(\alpha'_s(\tilde{M})) - \gamma_m^{(5)}(\alpha'_s(M_h))]C_1(\tilde{M}) + C_{2q}(\tilde{M}),\end{aligned}\tag{8.11}$$

The explicit computation of the coefficient functions will be discussed in detail in the next section.

## 8.2 Computation of the coefficient functions $C_1$ and $C_{2q}$

To calculate the coefficient functions one has to consider appropriate Green functions in the full and the effective theory and relate them via the decoupling relations. For example, the amputated Green function involving the  $q\bar{q}$  pair and the zero-momentum insertion of the operator  $\mathcal{O}_h$  which mediates the couplings to the light Higgs boson  $h$  contains both coefficient functions  $C_{2q}$  and  $C_{3q}$ .

$$\begin{aligned}\Gamma_{\bar{q}q\mathcal{O}_h}^0(p, -p) &= i^2 \int dx dy e^{ip(x-y)} \langle T q^0(x) \bar{q}^0(y) \mathcal{O}_h(0) \rangle^{1\text{PI}} \\ &= -\zeta_2^{(0)} \int dx dy e^{ip(x-y)} \langle T q'^0(x) \bar{q}'^0(y) (C_{2q}\mathcal{O}_{2q} + C_{3q}\mathcal{O}_{3q}) \rangle^{1\text{PI}},\end{aligned}\tag{8.12}$$

where  $p$  is the outgoing momentum of the quark and we label the quantities in the effective theory with a prime.

Upon decomposition of the Green function  $\Gamma_{\bar{q}q\mathcal{O}_h}^0$  into its scalar and vector components and taking the limit  $p \rightarrow 0$ , one obtains for the coefficient function  $C_{2q}$  the following expression

$$C_{2q}^0 = \frac{\Gamma_{\bar{q}q\mathcal{O}_h;s}^{0,h}(0,0)}{1 - \Sigma_s^{0,h}(0)} + \frac{\Gamma_{\bar{q}q\mathcal{O}_h;v}^{0,h}(0,0)}{1 + \Sigma_v^{0,h}(0)}. \quad (8.13)$$

The quantities  $\Sigma_v^{0,h}(0)$  and  $\Sigma_s^{0,h}(0)$  have been defined in Eq. (6.50). The superscript  $h$  in the above equation marks that only the hard parts of the Green functions survive when one sets the external momenta to zero  $p^2 = p_h^2 = 0$ .

From the technical point of view, to separate the vector and scalar contributions to the vertex Green function  $\Gamma_{\bar{q}q\mathcal{O}_h}$  one has to perform a naive Taylor expansion up to linear order in the external momenta carried by quarks. After the projection on vector and scalar parts, the external momenta can be set to zero. Nevertheless, the light Higgs mass approximation  $M_h^2 = p_h^2 \approx 0$  can be applied from the very beginning, which implies that the quark momenta can be chosen to be equal. As a consequence, vertex diagrams are reduced to two-point functions with vanishing external momenta, that can be further mapped to vacuum integrals.

Similarly, one can compute the coefficient function  $C_1$  via the Green function formed by the coupling of the operators  $\mathcal{O}_h$  to two gluons

$$\begin{aligned} \delta^{ab}\Gamma_{GG\mathcal{O}_h}^{0,\mu\nu}(p_1, p_2) &= i^2 \int dx dy e^{i(p_1 \cdot x + p_2 \cdot y)} \langle T G^{0,a,\mu}(x) G^{0,b,\nu}(y) \mathcal{O}_h(0) \rangle^{\text{1PI}}, \\ &= \delta^{ab} (-g^{\mu\nu} p_1 \cdot p_2 + p_1^\nu p_2^\mu) \Gamma_{GG\mathcal{O}_h}^0(p_1, p_2), \end{aligned} \quad (8.14)$$

where  $p_1$  and  $p_2$  denote the outgoing momenta of the gluons with the colour indices  $a$  and  $b$ . One can show that [109, 254] the coefficient  $C_1$  is given by the following relation

$$\begin{aligned} C_1^0 &= -\frac{1}{4} \frac{1}{\zeta_3^0} \Gamma_{GG\mathcal{O}_h}^0(0, 0) \\ &= -\frac{1}{4} \frac{1}{\Pi^{0,h}(0)} \left( \frac{g_{\mu\nu} p_1 \cdot p_2 - p_{1,\nu} p_{2,\mu} - p_{1,\mu} p_{2,\nu}}{(d-2)(p_1 \cdot p_2)^2} \Gamma_{GG\mathcal{O}_h}^{0,\mu\nu}(p_1, p_2) \right) \Big|_{p_1^2=p_2^2=0}, \end{aligned} \quad (8.15)$$

where  $d$  denotes as usual the number of space-time dimensions in dimensional regularization scheme and  $\Pi^{0,h}(0)$  has been defined in Eq. (6.50). Let us mention at this point that the projector given in Eq. (8.15) projects out the coefficient of the term proportional to  $g^{\mu\nu}$  in Eq. (8.14). To explicitly verify the transversality of the Green function  $\Gamma_{GG\mathcal{O}_h}^{0,\mu\nu}(p_1, p_2)$ , one needs to compute also the coefficient of the Lorentz structure proportional to  $p_1^\nu p_2^\mu$  using a second projector (for the explicit formula see for example Ref. [114]).

In equation (8.15), one has to keep  $p_1 \neq 0$  and  $p_2 \neq 0$  until the projection is applied. When only heavy particles are running in the loops, a naive Taylor expansion to the linear order in the two external momenta is required. After the expansion, the factor  $(p_1 \cdot p_2)^2$  in the denominator cancels and the two external momenta can be set to zero. In this way the vertex topologies implied in Eq. (8.15) are reduced to vacuum integrals. Nevertheless, when light particles are present in the loops, *e.g.* bottom quarks, a naive Taylor expansion is not enough and one has to perform

an asymptotic expansion. In this case the resulting Feynman integrals can be decomposed into massive vacuum integrals and vertex integrals with external momenta satisfying  $p_1^2 = p_2^2 = 0$  and  $2p_1 \cdot p_2 = M_h^2$ , and light quark masses present in the loops. Up to now, the light quark mass effects have been evaluated at NLO in Refs. [255, 256], which requires the computation of two-loop massive vacuum integrals and 1-loop vertex integrals.

As explained above the computation of the coefficient functions  $C_1$  and  $C_{2q}$  involves vacuum integrals with several mass scales. Up to two-loop order such integrals are known exactly [257]. However, the three-loop multi-scale integrals are not known and the computation of the coefficient  $C_1$  at NNLO can be performed only for specific mass hierarchies between the SUSY particles, that requires application of the asymptotic expansion method (for details see Refs. [115, 142]).

In SM, the coefficient functions  $C_1$  and  $C_{2q}$  are known up to the third order in perturbation theory. The first order QCD corrections to  $C_1$  have been computed in Refs. [258–260], while the same order contribution to  $C_{2q}$  vanishes in the SM. The second order QCD corrections to the coefficients  $C_1$  and  $C_2$  can be found in Ref. [254]. The leading Yukawa corrections to the coefficient functions have been evaluated in Ref. [158]. For the coefficient function  $C_1$  the fourth order QCD corrections have been computed recently [169]. Using the low-energy theorem, the authors of Ref [261] computed even the fifth order QCD corrections to the coefficient  $C_1$  up to contributions originating in the  $n_l$ -dependent part of the five-loop QCD beta function, that are currently not known.

In the MSSM, the coefficient functions  $C_1$  and  $C_{2q}$  are known at the NNLO. The NLO corrections to  $C_1$  have been computed within SUSY-QCD for the first time in Refs. [177, 262] and confirmed analytically [263] and numerically [264] (see also Ref. [265]). In Refs. [266, 267] the squark loop contributions to Higgs boson production in the MSSM have been computed without assuming any mass hierarchy. In SUSY models with large values of  $\tan \beta$ , the radiative corrections due to the bottom sector can become large and they have been computed analytically at NLO in Refs. [255, 256] and confirmed numerically in Ref. [264]. For the coefficient function  $C_{2q}$  the NLO SUSY-QCD and top Yukawa corrections are known analytically since quite some time [180]. The dominant ( $\tan \beta$  enhanced) NNLO SUSY QCD and top Yukawa corrections to  $C_{2b}$  have been computed in Ref. [172]. The SUSY QCD contributions have been confirmed analytically in [268].

For completeness, we display here the one-loop order coefficients  $C_1$  and  $C_{2b}$  providing also  $\mathcal{O}(\epsilon)$  terms that are necessary for the higher order calculations.

$$\begin{aligned}
C_1 = & -\frac{\alpha_s}{3\pi} \left\{ + \frac{\sin \alpha}{\cos \beta} \left[ \frac{M_t^2 \mu_{\text{SUSY}} X_t}{4m_{\tilde{t}_1}^2 m_{\tilde{t}_2}^2 \tan \beta} - \epsilon \frac{M_t \mu_{\text{SUSY}} \sin 2\theta_t}{8 \tan \beta} \left( \frac{L_{\mu \tilde{t}_1}}{m_{\tilde{t}_1}^2} - \frac{L_{\mu \tilde{t}_2}}{m_{\tilde{t}_2}^2} \right) \right] \right. \\
& - \frac{\cos \alpha}{\sin \beta} \left[ \frac{4m_{\tilde{t}_1}^2 m_{\tilde{t}_2}^2 + m_{\tilde{t}_1}^2 M_t^2 + m_{\tilde{t}_2}^2 M_t^2 - A_t M_t^2 X_t}{4m_{\tilde{t}_1}^2 m_{\tilde{t}_2}^2} \right. \\
& \left. \left. + \epsilon \frac{A_t M_t \sin 2\theta_t}{8} \left( \frac{L_{\mu \tilde{t}_1}}{m_{\tilde{t}_1}^2} - \frac{L_{\mu \tilde{t}_2}}{m_{\tilde{t}_2}^2} \right) + \epsilon \frac{M_t^2}{4} \left( \frac{4L_{\mu t}}{M_t^2} + \frac{L_{\mu \tilde{t}_1}}{m_{\tilde{t}_1}^2} + \frac{L_{\mu \tilde{t}_2}}{m_{\tilde{t}_2}^2} \right) \right] \right\}, \quad (8.16)
\end{aligned}$$

$$\begin{aligned}
C_{2b} = & -\frac{\sin \alpha}{\cos \beta} \frac{1 + \frac{\alpha_s}{2\pi} C_F A_b m_{\tilde{g}} \left[ F_1(m_{\tilde{b}_1}^2, m_{\tilde{b}_2}^2, m_{\tilde{g}}^2) + \epsilon F_2(m_{\tilde{b}_1}^2, m_{\tilde{b}_2}^2, m_{\tilde{g}}^2) \right]}{1 + \frac{\alpha_s}{2\pi} C_F X_b m_{\tilde{g}} \left[ F_1(m_{\tilde{b}_1}^2, m_{\tilde{b}_2}^2, m_{\tilde{g}}^2) + \epsilon F_2(m_{\tilde{b}_1}^2, m_{\tilde{b}_2}^2, m_{\tilde{g}}^2) \right]} \\
& + \frac{\cos \alpha}{\sin \beta} \frac{\frac{\alpha_s}{2\pi} C_F (-\mu_{\text{SUSY}} \tan \beta) m_{\tilde{g}} \left[ F_1(m_{\tilde{b}_1}^2, m_{\tilde{b}_2}^2, m_{\tilde{g}}^2) + \epsilon F_2(m_{\tilde{b}_1}^2, m_{\tilde{b}_2}^2, m_{\tilde{g}}^2) \right]}{1 + \frac{\alpha_s}{2\pi} C_F X_b m_{\tilde{g}} \left[ F_1(m_{\tilde{b}_1}^2, m_{\tilde{b}_2}^2, m_{\tilde{g}}^2) + \epsilon F_2(m_{\tilde{b}_1}^2, m_{\tilde{b}_2}^2, m_{\tilde{g}}^2) \right]}, \quad (8.17)
\end{aligned}$$

where the functions  $F_1$  and  $F_2$  are defined through

$$\begin{aligned}
F_1(x, y, z) &= -\frac{xy \ln \frac{y}{x} + yz \ln \frac{z}{y} + zx \ln xz}{(x-y)(y-z)(z-x)}, \\
F_2(x, y, z) &= \frac{1}{(x-y)(y-z)(z-x)} \left[ xy \ln \frac{y}{x} \left( 1 + \frac{1}{2} \ln \frac{\mu^2}{\sqrt{xy}} \right) \right. \\
&\quad \left. + yz \ln \frac{z}{y} \left( 1 + \frac{1}{2} \ln \frac{\mu^2}{\sqrt{yz}} \right) + zx \ln xz \left( 1 + \frac{1}{2} \ln \frac{\mu^2}{\sqrt{xz}} \right) \right]. \quad (8.18)
\end{aligned}$$

The corresponding expression for up type quarks can be easily obtained by replacing  $\sin \alpha$  with  $\cos \alpha$  and  $\sin \beta$  with  $\cos \beta$  and vice versa.

The approach outlined above has the advantage that it simplifies significantly the calculation, once the limit  $M_h^2 = p_h^2 \approx 0$  is applied. The validity of this approximation has been proved within the SM at the NNLO [269, 270]<sup>26</sup>. Since the SUSY particle masses are expected to be considerably heavier than the top quark mass, we expect that this approximation holds in the MSSM even with higher accuracy.

### 8.2.1 Low Energy Theorem

A second possibility to compute the coefficient functions is to relate them via the Low Energy Theorem (LET) to vacuum polarization and quark self energy corrections. This approach resides heavily on the fact that the momenta carried by the Higgs boson can be set to zero. In this case, it was shown (within the SM) that the amplitude of a process containing  $(N+1)$  external particles from which, one is a Higgs boson with vanishing momenta, can be computed from the amplitude with  $N$  external particles, obtained in the absence of the Higgs external leg [271]:

$$\lim_{p_h \rightarrow 0} \Gamma^{h, A_1, A_2, \dots, A_N}(p_h, p_{A_1}, p_{A_2}, \dots, p_{A_N}) = \frac{\partial}{\partial v} \Gamma^{A_1, A_2, \dots, A_N}(p_{A_1}, p_{A_2}, \dots, p_{A_N}), \quad (8.19)$$

where  $v$  denotes the vacuum expectation value (VEV) of the theory. Beyond tree level, all kinematic parameters must be considered as bare quantities. For certain special theories and renormalization schemes the above equation holds even for renormalized parameters (for details see Ref. [272]). Within QCD all order formulae relating the coefficient functions of dimension four operators with the decoupling coefficients for the strong coupling and the quark masses have

<sup>26</sup>For the SM, it is known as the infinite top quark mass approximation.

been derived [168]. Within the MSSM, Eq. (8.19) has to be generalized to the case where two Higgs fields acquire VEVs. Nevertheless, it has been proved [173, 263, 268] that within SUSY-QCD the coefficient functions  $C_1$  and  $C_{2q}$  can be derived up to NNLO from the decoupling coefficients  $\zeta_s$  and  $\zeta_{m_q}$  through the following relations:

$$\begin{aligned} C_1^0 &= (-\sin \alpha \hat{D}_{\phi_1}^0 + \cos \alpha \hat{D}_{\phi_2}^0) \ln \zeta_s^0 \equiv \hat{D}_h^0 \ln \zeta_s^0, \\ C_{2q}^0 &= (-\sin \alpha \hat{D}_{\phi_1}^0 + \cos \alpha \hat{D}_{\phi_2}^0) \ln \zeta_{m_q}^0 \equiv \hat{D}_h^0 \ln \zeta_{m_q}^0. \end{aligned} \quad (8.20)$$

As usual, the superscript 0 labels bare quantities. The operators  $\hat{D}_{\phi_i}^0$ , with  $i = 1, 2$ , contain the derivatives w.r.t. the two VEVs of the MSSM. They have been derived using the field dependent definitions of quark and squark masses and mixing angles in Ref [263]. However, for the computation of the coefficient function  $C_1$  at the NNLO, also the dependence of the  $\varepsilon$ -scalar mass on the VEVs through the loop induced Higgs- $\varepsilon$ -scalar coupling has to be taken into account [173]. As can be understood from the Eqs. (21) and (22) in Ref. [263] the dominant contributions to the differential operators originate from the pure SUSY-QCD terms. For exemplification and to fix the normalization, we reproduce here the terms corresponding to the third generation quarks keeping only the linear terms in bottom quark masses<sup>27</sup>

$$\begin{aligned} \hat{D}_{\phi_1} &= \frac{1}{\cos \beta} (m_b A_b \mathcal{F}_b + m_b \mathcal{G}_b) - \frac{1}{\sin \beta} m_t \mu_{\text{SUSY}} \sin 2\theta_t \mathcal{F}_t, \\ \hat{D}_{\phi_2} &= \frac{1}{\cos \beta} (-m_b \mu_{\text{SUSY}} \mathcal{F}_b) + \frac{1}{\sin \beta} (m_t A_t \sin 2\theta_t \mathcal{F}_t + 2m_t^2 \mathcal{G}_t), \quad \text{with} \\ \mathcal{F}_b &= \frac{2}{m_{b_1}^2 - m_{b_2}^2} (1 - \sin^2 2\theta_b) \frac{\partial}{\partial \sin 2\theta_b}, \quad \mathcal{G}_b = \frac{\partial}{\partial m_b}, \\ \mathcal{F}_t &= \frac{\partial}{\partial m_{t_1}^2} - \frac{\partial}{\partial m_{t_2}^2} + \frac{2}{m_{t_1}^2 - m_{t_2}^2} \frac{(1 - \sin^2 2\theta_t)}{\sin 2\theta_t} \frac{\partial}{\partial \sin 2\theta_t}, \\ \mathcal{G}_t &= \frac{\partial}{\partial m_{t_1}^2} + \frac{\partial}{\partial m_{t_2}^2} + \frac{\partial}{\partial m_t^2}. \end{aligned} \quad (8.21)$$

On the r.h.s. of the above equations, all parameters are the bare ones. We omitted the superscript “0” to avoid clumsy notation. For large values of  $\tan \beta$  the dominant contributions to the coefficient functions, *i.e.* the terms proportional to  $\mu_{\text{SUSY}} \tan \beta$ , are generated through the term containing the derivative  $\mathcal{F}_b$  in  $\hat{D}_{\phi_2}$ . Taking into account the parametric dependence of the quark self energy  $\Sigma^{0,h}$  on masses and mixing angles, one can easily derive these contributions from the terms proportional to  $\sin 2\theta_b$  in  $\Sigma_s^{0,h}$ .

### 8.3 Hadronic Higgs decays

In this section we study the phenomenological applications of the computations discussed above. We concentrate on the calculation within the MSSM of the total decay rate into hadrons  $\Gamma(h \rightarrow \text{hadrons})$ , that is composed of the partial decay widths into quarks  $\Gamma(h \rightarrow q\bar{q})$  and gluons  $\Gamma(h \rightarrow gg)$ . Although, the channel  $\Gamma(h \rightarrow b\bar{b})$  gives the dominant contributions to the total Higgs decay rate, it was not used among the Higgs discovery channels at the LHC, due to its

<sup>27</sup>Please note the sign difference in the definition of parameter  $\mu_{\text{SUSY}}$  between Ref. [263] and Refs [173, 268].

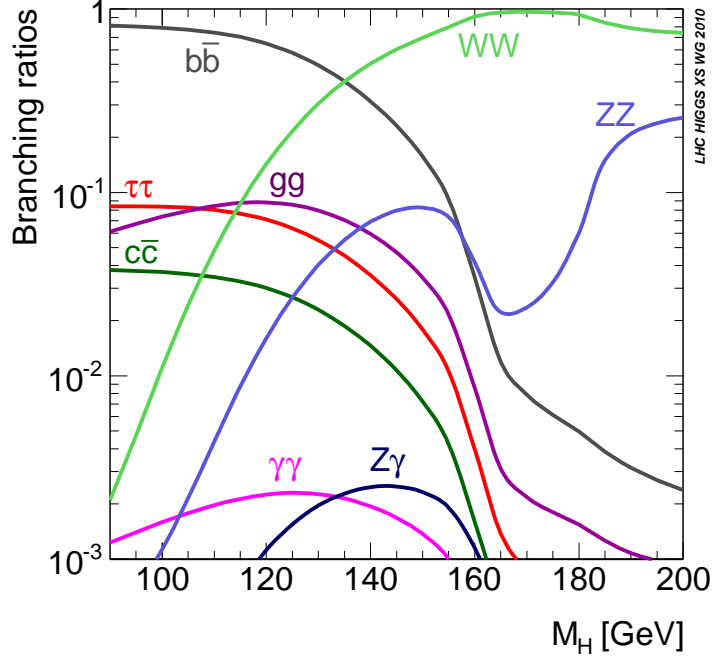


Figure 8.1: Higgs boson branching ratios in the SM at the LO from Ref. [273].

huge background. Nevertheless, it has a big impact on all branching ratios and is an important channel for the identification of the Higgs properties. Precisely, the uncertainties on the partial decay width  $\Gamma(h \rightarrow b\bar{b})$  translate into significant systematic errors for all the other non-leading branching ratios. For illustration we show in Figs. 8.1 from Ref. [273] the branching ratios of the Higgs boson in the SM at the LO. For precise analysis they have to be complemented by genuine SM radiative corrections together with corrections due to the supersymmetric particles, that can be embedded in the decoupling coefficients as discussed in the previous section.

Starting from the effective Lagrangian (8.5) one can derive the following formula for the total decay width into hadrons

$$\begin{aligned} \Gamma(h \rightarrow \text{hadrons}) = & (1 + \bar{\delta}_u)^2 \left\{ \sum_q \Gamma_{q\bar{q}}^{(0)} \left[ (1 + \Delta_{22})\mathcal{C}_2^2 + \Delta_{12}\mathcal{C}_1\mathcal{C}_2 \right] \right. \\ & \left. + \Gamma_{gg}^{(0)}(1 + \Delta_{11})\mathcal{C}_1^2 \right\}, \end{aligned} \quad (8.22)$$

where the coefficient functions  $\mathcal{C}_1$  and  $\mathcal{C}_2$  have been defined in Eq. (8.11).

At the lowest order in perturbation theory, the first line corresponds to  $\Gamma(h \rightarrow q\bar{q})$ , whereas the second one stands for  $\Gamma(h \rightarrow gg)$ . At higher orders, however, the splitting of Eq. (8.22) into the decay widths to fermions and gluons is not straightforward anymore, due to the occurrence of diagrams contributing to both channels.

The LO expressions for the branching ratios are given by

$$\Gamma_{q\bar{q}}^{(0)} = \frac{N_c G_F M_h m_q^2}{4\pi\sqrt{2}} \left(1 - \frac{4m_q^2}{M_h^2}\right)^{3/2} \quad \text{and} \quad \Gamma_{gg}^{(0)} = \frac{N_c C_F G_F M_h^3}{\pi\sqrt{2}}, \quad (8.23)$$

where  $G_F$  denotes the Fermi constant. As is well known [188, 260, 274], the large logarithms of the type  $\ln(M_h^2/m_q^2)$  can be resummed by taking  $m_q$  in Eq. (8.23) to be the  $\overline{\text{MS}}$  mass  $m_q^{\overline{\text{MS}}}(\mu)$  evaluated at the scale  $\mu = M_h$ .

The coefficients  $\Delta_{11}$ ,  $\Delta_{12}$ ,  $\Delta_{22}$  describe the low-energy physics. Therefore, they have to be computed in the effective theory and are independent of the heavy masses. Using the method of operators described in the previous section, they can be related via the optical theorem to the absorptive parts of the scalar correlators  $\Pi_{jk}$

$$\Delta_{jk} = \frac{1}{M_h} \text{Im}(\Pi_{jk}) = \frac{1}{M_h} \text{Im} \left( i \int dx e^{ipx} \langle 0 | T[\mathcal{O}_j(x) \mathcal{O}_k(0)] | 0 \rangle \Big|_{p^2=M_h^2} \right), \quad j, k = 1, 2, \quad (8.24)$$

where  $p$  is the momentum of the external Higgs boson. They have been computed within SM up to three-loop order<sup>28</sup>. For the analysis discussed in this section, their one- and two-loop QCD corrections are required. The two-loop QCD contributions to the coefficients  $\Delta_{22}$  and  $\Delta_{11}$  are given by [275, 276].

$$\begin{aligned} \Delta_{22} = & \frac{\alpha'_s(\mu)}{\pi} \left( \frac{17}{3} + 2 \ln \frac{\mu^2}{M_h^2} \right) \\ & + \left( \frac{\alpha'_s(\mu)}{\pi} \right)^2 \left[ \frac{10801}{144} - \frac{19}{2} \zeta(2) - \frac{39}{2} \zeta(3) + \frac{106}{3} \ln \frac{\mu^2}{M_h^2} + \frac{19}{4} \ln^2 \frac{\mu^2}{M_h^2} \right. \\ & \left. - n_l \left( \frac{65}{24} - \frac{1}{3} \zeta(2) - \frac{2}{3} \zeta(3) + \frac{11}{9} \ln \frac{\mu^2}{M_h^2} + \frac{1}{6} \ln^2 \frac{\mu^2}{M_h^2} \right) \right], \end{aligned} \quad (8.25)$$

$$\begin{aligned} \Delta_{11} = & \frac{\alpha'_s(\mu)}{\pi} \left[ \frac{73}{4} + \frac{11}{2} \ln \frac{\mu^2}{M_h^2} - n_l \left( \frac{7}{6} + \frac{1}{3} \ln \frac{\mu^2}{M_h^2} \right) \right] \\ & + \left( \frac{\alpha'_s(\mu)}{\pi} \right)^2 \left[ \frac{37631}{96} - \frac{363}{8} \zeta(2) - \frac{495}{8} \zeta(3) + \frac{2817}{16} \ln \frac{\mu^2}{M_h^2} + \frac{363}{16} \ln^2 \frac{\mu^2}{M_h^2} \right. \\ & \left. - n_l \left( \frac{7189}{144} - \frac{11}{2} \zeta(2) - \frac{5}{4} \zeta(3) + \frac{263}{12} \ln \frac{\mu^2}{M_h^2} + \frac{11}{4} \ln^2 \frac{\mu^2}{M_h^2} \right) \right. \\ & \left. + n_l^2 \left( \frac{127}{108} - \frac{1}{6} \zeta(2) + \frac{7}{12} \ln \frac{\mu^2}{M_h^2} + \frac{1}{12} \ln^2 \frac{\mu^2}{M_h^2} \right) \right], \end{aligned} \quad (8.26)$$

with  $\zeta(x)$  being the Riemann's zeta function.

The additional QCD correction  $\Delta_{12}$  is generated through double-triangle topologies. It was first computed in Ref. [254] and it reads

$$\Delta_{12} = \frac{\alpha'_s(\mu)}{\pi} C_F \left( -19 + 6\zeta(2) - \ln^2 \frac{m_q^2}{M_h^2} - 6 \ln \frac{\mu^2}{M_h^2} \right). \quad (8.27)$$

---

<sup>28</sup>See Ref. [120] for a comprehensive review on this topic.



The universal corrections  $\bar{\delta}_u$  of  $\mathcal{O}(\alpha_s^n x_t)$ , where  $x_t = (\alpha_t/4\pi)^2 = G_F M_t^2/(8\pi^2\sqrt{2})$ , with  $\alpha_t$  the top-Yukawa coupling, contain the contributions from the renormalization of the Higgs wave function and the vacuum expectation value [277]. It is given by

$$\bar{\delta}_u = x_t \left[ \frac{7}{2} + \frac{\alpha'_s(\mu)}{\pi} \left( \frac{19}{3} - 2\zeta(2) + 7 \ln \frac{\mu^2}{M_t^2} \right) + \mathcal{O}(\alpha_s^2) \right]. \quad (8.28)$$

Now, we are in a position to interpret the phenomenological significance of Eq. (8.22). In the following section we concentrate on the numerical effects of the radiative corrections to the hadronic Higgs decay.

### 8.3.1 Numerical analysis

The SM input parameters are the strong coupling constant at the Z-boson mass scale  $\alpha_s(M_Z) = 0.1184$  [164], the top quark pole mass  $M_t = 173.1$  GeV [160] and the running bottom quark mass in the  $\overline{\text{MS}}$  scheme  $m_b(m_b) = 4.163$  GeV [278]. For the supersymmetric parameters we adopted the corresponding values of the “modified  $m_h^{\text{max}}$ ” scenario as described in section 7.2.2 (for details see Ref. [115]).

In Fig. 8.2 we focus on the decay channel  $h \rightarrow b\bar{b}$  and display the decay width as a function of the Higgs boson mass  $M_h$ . We chose in this case  $\tan\beta = 50$ . The two-loop genuine QCD and electroweak corrections (i.e. computed in the effective theory) to the process  $h \rightarrow b\bar{b}$ , as well as the two-loop SUSY-QCD corrections to the Higgs boson mass are depicted by the dotted line. More precisely, they are derived from Eq. (8.22), where the coefficient functions  $\mathcal{C}_1$  and  $\mathcal{C}_2$  are set to their tree-level values. The additional SUSY-QCD vertex corrections parametrized through the coefficient functions  $\mathcal{C}_1$  and  $\mathcal{C}_2$  are represented at the one- and two-loop order by the dashed and solid lines, respectively. We also take into account the one-loop SUSY-EW corrections to the coefficient function  $\mathcal{C}_2$  and fix their renormalization scale at  $\mu_{\text{SEW}} = (m_{\tilde{t}_1} + m_{\tilde{t}_2} + \mu_{\text{SUSY}})/15$ , for which the two-loop SUSY-EW corrections become negligible [172]. The genuine two-loop corrections are negligible. Nevertheless, they are essential tools for the proof of the convergence of the perturbative expansion.

The large one-loop SUSY-QCD radiative corrections to  $\Gamma(h \rightarrow b\bar{b})$  have only a relatively small impact on the branching ratio  $BR(h \rightarrow b\bar{b})$ , but they can have a large impact on  $BR(h \rightarrow \tau^+\tau^-)$ . For sufficiently large  $\tan\beta$  and  $\mu_{\text{SUSY}}$ , the measurement of  $BR(h \rightarrow \tau^+\tau^-)$  can provide information about the distinction between the SM and MSSM predictions.

The gluonic Higgs decay rate can be directly measured only at  $e^+e^-$  colliders. At hadron colliders, they can be measured only indirectly with rather bad accuracy of the order of 20%. As it has been shown, the genuine SUSY-QCD corrections to the gluonic Higgs decay are rather small [281]. For the experimental analysis relevant at the LHC they can be neglected with respect to the standard quark contributions to the hadronic decay rate. The QCD corrections are known in the SM up to the NNNLO [169, 261] in the heavy-top-mass limit.<sup>29</sup> Even the mixed QCD-electroweak corrections at the three-loop level are known [158] in the same approximations. The genuine NLO SUSY-QCD corrections have been evaluated in Refs. [177, 263] and amount to about  $-5\%$  from the QCD corrections at NLO.

<sup>29</sup>Here, the mass of the Higgs boson is assumed to be much smaller than the mass of the top quark.

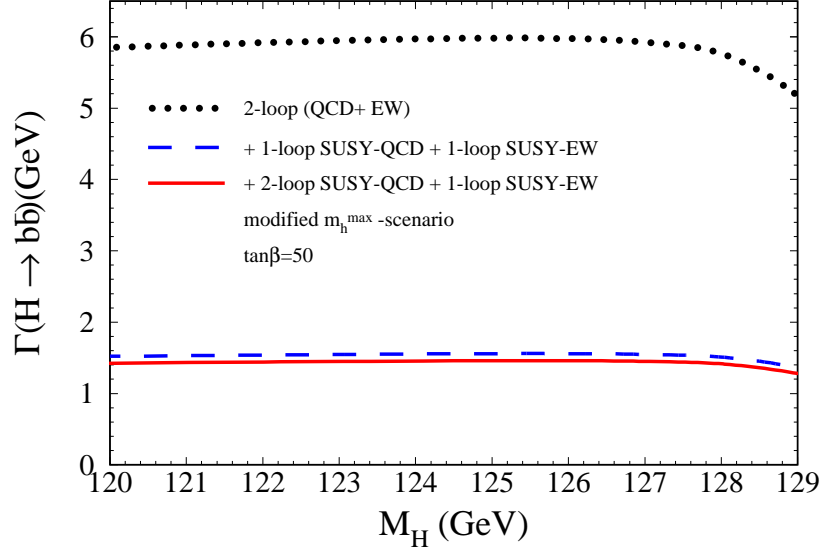


Figure 8.2:  $\Gamma(h \rightarrow b\bar{b})$  for the “modified  $m_h^{max}$ ” scenario as a function of  $M_h$ . The dotted line displays the two-loop QCD and electroweak corrections together with two-loop corrections to the Higgs boson propagator. The dashed and solid lines depict in addition the one- and two-loop SUSY-QCD vertex corrections, respectively.

A much more interesting Higgs decay channel from the perspective of the ongoing experiments conducted at the LHC is the rare  $h \rightarrow \gamma\gamma$  channel. In this case the coupling of the Higgs to photons is mediated by loops containing electrically charged particles. If the masses of the particles inside loops are generated through the Higgs mechanism, as in the case of the SM, the couplings to the Higgs boson grow with the masses, balancing the decrease due to rising loop masses. If the masses of the particles are generated by different mechanisms, as is the case in SUSY, the effect of the heavy particles on the  $h\gamma\gamma$  coupling is in general small.

In SM with the Higgs boson mass of about 125 GeV only the top quark and the W boson effectively contribute and they interfere destructively. The radiative corrections are well under control. The QCD contributions are known up to NNLO [282] and the electroweak corrections to NLO [283]. The SUSY-QCD corrections to  $\Gamma(h \rightarrow \gamma\gamma)$  are known with the same accuracy as in the case of  $\Gamma(h \rightarrow gg)$ . The NLO corrections have been computed in Refs. [281, 284] and the NNLO contributions can be found in Ref. [285]. Also for this channel, the SUSY corrections are small as compared to the SM ones.

### 8.3.2 Mass corrections to hadronic Higgs decays

For an intermediate Higgs mass of about 125 GeV it is legitimate to investigate the quality of the approximation discussed in the previous section. For accurate results, one has to take into consideration in Eq. (8.5) also operators of dimension six and higher, that are suppressed

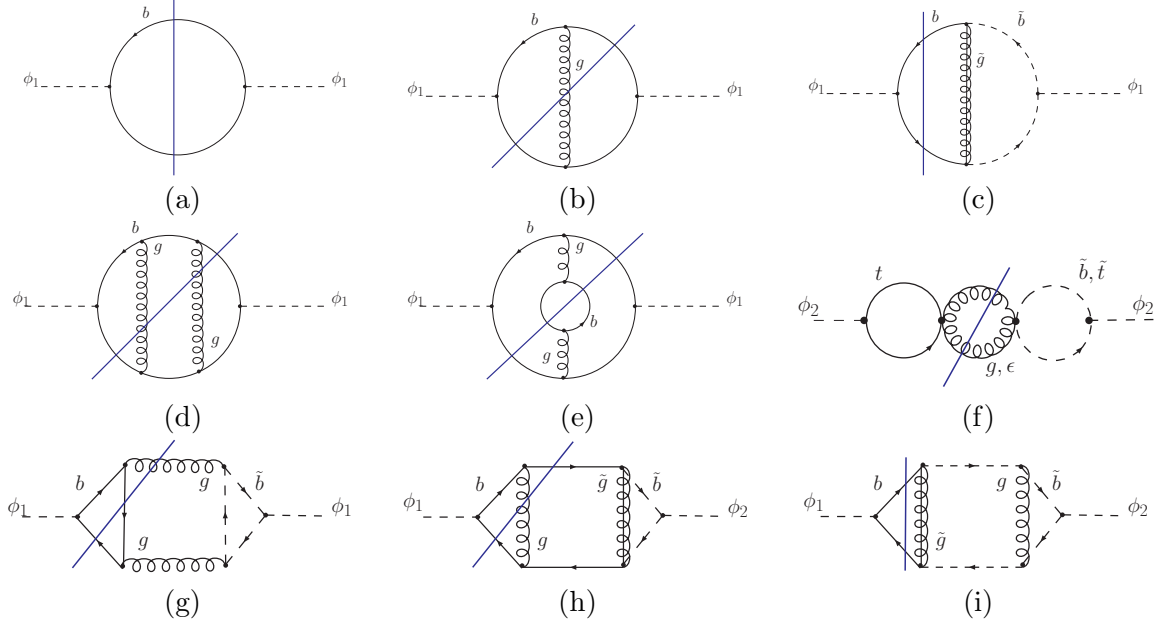


Figure 8.3: One-, two- and three-loop Feynman diagrams contributing to the Higgs boson propagator in SUSY-QCD. Dashed lines denote Higgs bosons, whereas oriented dashed lines represent the squarks. For the other particles we use the same convention as before.

at least by a factor  $M_h^2/M_t^2$ . However, the application of higher dimensional operators in the context of SUSY is quite tedious. A more familiar method for this purpose is to use the optical theorem. Hereby, one has to consider corrections to the Higgs boson self-energy  $\Pi_h(q^2)$ . The imaginary part of this quantity provides us with the total decay rate of the Higgs boson

$$\Gamma_h = \frac{1}{M_h} \text{Im} \Pi_h(M_h^2) \quad (8.29)$$

According to the Cutkosky cut rules, non-vanishing contributions to the imaginary part of the Higgs boson self energy will provide only those diagrams, that can be cut in such a way that all resulting final state particles can be set simultaneously on their mass-shell. Sample diagrams contributing to the hadronic decay rate can be seen in Fig. 8.3.

The imaginary parts originate from the  $i\epsilon$ -prescription for on-shell propagators. In the results obtained using DRED they are embedded in complex logarithms occurring in the  $\epsilon$ -expansion of the expression

$$\left( \frac{-\mu^2}{q^2 + i\epsilon} \right)^\epsilon = 1 - \epsilon \log \left( \frac{-q^2 - i\epsilon}{\mu^2} \right) + \frac{1}{2} \epsilon^2 \log^2 \left( \frac{-q^2 - i\epsilon}{\mu^2} \right) + \mathcal{O}(\epsilon^3). \quad (8.30)$$

After setting the external momenta on the Higgs mass shell  $q^2 = M_h^2$ , one obtains further

$$\log \left( \frac{-q^2 - i\epsilon}{\mu^2} \right) = \log \left( \frac{M_h^2}{\mu^2} \right) - i\pi. \quad (8.31)$$

The analytic calculation of the three-loop diagrams contributing to  $\Gamma_h$  in SUSY-QCD is not yet possible. Nevertheless, for fixed mass hierarchies between the occurring particles, the method

of asymptotic expansion can be successfully applied. For illustration, we consider a degenerate SUSY mass spectrum satisfying the following inequality with respect to the SM particle masses

$$m_q \ll M_h \ll m_t \ll M_S \equiv m_{\tilde{g}} = m_{\tilde{q}}. \quad (8.32)$$

Similar with the computation of three-loop SUSY-QCD corrections to the light Higgs bosons mass, also in this calculation one has to make an additional Taylor expansion of bottom squark propagator in bottom squark mass differences  $\Delta_b$  defined like

$$\Delta_b = \frac{m_{\tilde{b}_1}^2 - m_{\tilde{b}_2}^2}{m_{\tilde{b}_1}^2}. \quad (8.33)$$

This procedure allows to correctly take into account the contributions generated by the bottom squark mixing angle renormalization.

In the following we consider the same renormalization scheme as in section 7.2.1. The results for  $\Gamma_h$  including the dominant mass corrections at  $\mathcal{O}(\alpha_s^2)$  read [286]

$$\begin{aligned} \Gamma_h = & \Gamma_{qq}^{(0)} \left( \frac{\sin \alpha}{\cos \beta} \right)^2 \left\{ 1 + \frac{4}{3} \frac{\alpha_s}{\pi} \left[ \frac{19}{4} + \frac{3}{2} L_{\mu h} - \frac{1}{2} L_{\mu S} + \left( -\frac{15}{2} - 9 L_{\mu h} + 3 L_{\mu S} \right) \frac{m_b^2}{M_h^2} + \frac{5}{12} \frac{m_b^2}{M_S^2} \right. \right. \\ & + \frac{1}{15} \frac{m_b^2 M_h^2}{M_S^4} - \frac{A_b - \mu_{\text{SUSY}} \cot \alpha}{M_S} \left( \frac{1}{2} + \frac{1}{12} \frac{m_b^2}{M_S^2} + \frac{1}{24} \frac{M_h^2}{M_S^2} \right) \Big] + \left( \frac{\alpha_s}{\pi} \right)^2 \left[ \frac{14093}{216} + \frac{541}{18} L_{\mu h} \right. \\ & + \frac{47}{12} L_{\mu h}^2 - \frac{559}{36} L_{\mu S} - \frac{10}{3} L_{\mu h} L_{\mu S} + \frac{35}{36} L_{\mu S}^2 - \frac{11}{9} L_{\mu t} - \frac{1}{3} L_{\mu h} L_{\mu t} + \frac{1}{6} L_{\mu t}^2 - \frac{97}{6} \zeta(3) \\ & + \left( \frac{107}{675} + \frac{2}{45} L_{\mu h} - \frac{2}{45} L_{\mu t} \right) \frac{M_h^2}{m_t^2} + \left( -\frac{529}{88200} - \frac{1}{420} L_{\mu h} + \frac{1}{420} L_{\mu t} \right) \frac{M_h^4}{m_t^4} \\ & + \left( \frac{7}{108} + \frac{1}{9} L_{\mu S} - \frac{1}{9} L_{\mu t} \right) \frac{m_t^2}{M_S^2} + \left( \frac{5821}{16200} + \frac{17}{135} L_{\mu h} - \frac{17}{135} L_{\mu S} \right) \frac{M_h^2}{M_S^2} \\ & + \frac{(A_b - \mu_{\text{SUSY}} \cot \alpha)^2}{M_S^2} \left( \frac{1}{9} + \frac{1}{54} \frac{M_h^2}{M_S^2} \right) + \frac{A_b - \mu_{\text{SUSY}} \cot \alpha}{M_S} \left[ -\frac{119}{18} - \frac{4}{3} L_{\mu h} - \frac{1}{18} L_{\mu S} \right. \\ & + \left. \left( -\frac{7}{54} - \frac{1}{18} L_{\mu S} + \frac{1}{18} L_{\mu t} \right) \frac{m_t^2}{M_S^2} + \left( -\frac{62}{81} - \frac{1}{9} L_{\mu h} - \frac{1}{216} L_{\mu S} \right) \frac{M_h^2}{M_S^2} \right] \\ & + \frac{\tan \beta}{\sin \alpha} \left[ -\frac{28}{9} - \frac{2}{3} L_{\mu h} + \frac{2}{3} L_{\mu t} + \frac{5}{54} \frac{X_t m_t^2}{M_S^2} + \left( -\frac{2011}{24300} - \frac{41}{1620} L_{\mu h} + \frac{41}{1620} L_{\mu t} \right) \frac{M_h^2}{m_t^2} \right. \\ & + \left( -\frac{28307}{4762800} - \frac{47}{22680} L_{\mu h} + \frac{47}{22680} L_{\mu t} \right) \frac{M_h^4}{m_t^4} + \left( -\frac{85}{54} - \frac{1}{3} L_{\mu h} + \frac{1}{3} L_{\mu S} \right) \frac{m_t^2}{M_S^2} - \frac{1}{27} \frac{M_h^2}{M_S^2} \\ & \left. \left. - \frac{7}{3240} \frac{M_h^4}{m_t^2 M_S^2} \right] \right\} + \Gamma_{gg}^{(0)} \left( \frac{\cos \alpha}{\sin \beta} \right)^2 \left( \frac{\alpha_s}{\pi} \right)^2 \left[ \frac{1}{144} + \frac{1}{144} \frac{m_t^2}{M_S^2} + \frac{7}{8640} \frac{M_h^2}{m_t^2} + \frac{7}{17280} \frac{M_h^2}{M_S^2} \right. \\ & \left. + \frac{169}{2073600} \frac{M_h^4}{m_t^4} + \frac{1}{24192} \frac{M_h^4}{m_t^2 M_S^2} \right] + \mathcal{O} \left( \frac{M_h^4}{M_S^4}, \frac{M_t^4}{M_S^4}, \frac{M_h^6}{m_t^6} \right). \quad (8.34) \end{aligned}$$

For a light Higgs mass  $M_h = 125$  GeV and SUSY masses of about 1 TeV,  $\tan \beta = 40$  and SM parameters chosen as in the previous sections the mass corrections at NLO and NNLO amount to below one percent from the dominant contribution (*i.e.* computed in the EFT) at the corresponding order in perturbation theory. They are beyond the reach of the LHC accuracy, but they might be of phenomenological interest at a future linear collider.

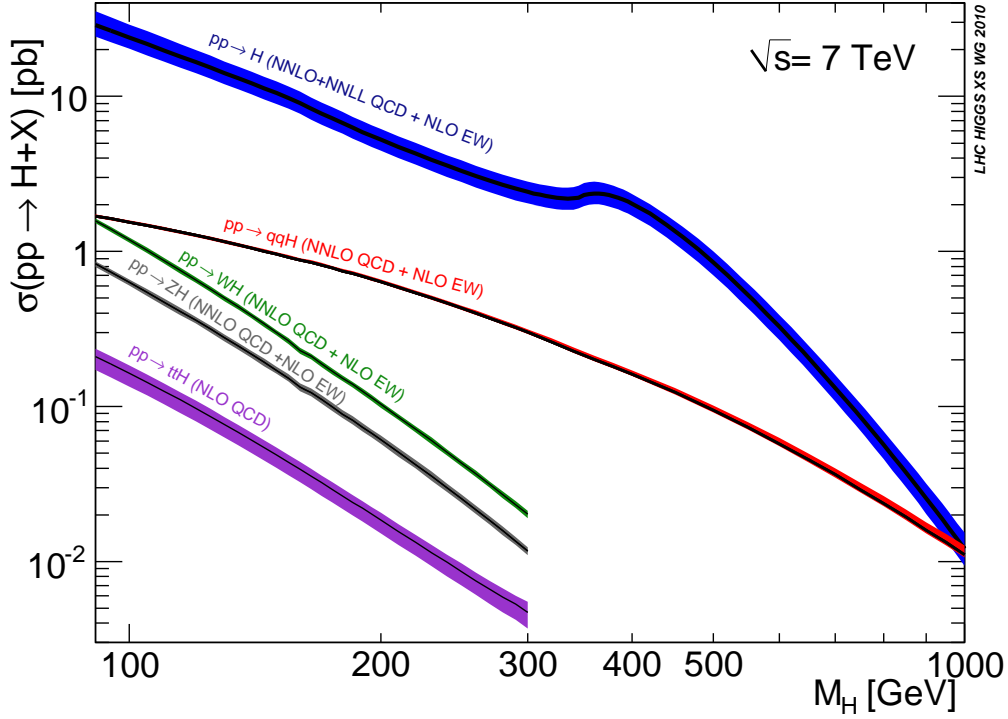


Figure 8.4: Higgs production cross sections at the LHC for  $\sqrt{s} = 8$  TeV together with the uncertainties from the missing higher order corrections and the parton density functions from Ref. [273].

## 8.4 Hadronic Higgs production

During the last years, a lot of effort has been devoted to precise predictions for Higgs production at hadron colliders (for reviews, see Refs. [34, 287, 288]). They constituted basic ingredients for the discovery of the new scalar particle at the LHC. The main production channel for the SM Higgs boson at the LHC is the loop-induced gluon-fusion channel. For illustration, we reproduce in Fig 8.4 from Ref. [273] the theoretical predictions for the main Higgs production channels together with the uncertainties due to missing higher order corrections and to the uncertainties on the parton density functions (PDFs).

An important application of the Higgs discovery is to constrain the parameters of theories predicting physics beyond the SM. This is also the case for SUSY theories. Given the high sensitivity of the Higgs observables (its mass, production cross sections and decay rates) on the parameters of the top sector in the MSSM, one can derive lower bounds for top squark masses and set constraints for their mixing angle. For this task one needs, among other ingredients, precise predictions for the Higgs production cross section, including even NNLO SUSY-QCD corrections. As discussed in section 8.2, exact analytic calculations at this order in perturbation theory are not yet feasible. Instead one has to use the EFT approach together with the method of asymptotic expansions. In the SM, it was shown [269, 270, 289–292] that the exact result for

the hadronic cross section for intermediate Higgs masses ( $M_h < 2m_t$ ) is approximated to better than 1% level by the result derived with EFT approach, if the full top mass dependence at LO is factored out.

Following the same reasoning for the case of the MSSM, one can write the hadronic cross section  $\sigma \equiv \sigma(pp \rightarrow h + X)$  as a function of the hadronic center-of-mass energy  $\sqrt{s}$ . It reads [177]

$$\sigma(z) = \rho_0 \sigma_0 \left( -3\pi \frac{C_g(\mu_h)}{c_1^{(0)}} \right)^2 \left[ \Sigma^{(0)}(z) + \frac{\alpha_s(\mu_s)}{\pi} \Sigma^{(1)}(z) + \left( \frac{\alpha_s(\mu_s)}{\pi} \right)^2 \Sigma^{(2)}(z) + \dots \right], \quad (8.35)$$

The exact LO contribution, denoted here  $\sigma_0$ , is factored out, as discussed above. The higher order corrections are computed within the EFT approach and the separation of short and long distance contributions is explicit in Eq. (8.35). For a better convergence of the perturbative expansion and to avoid the occurrence of large logarithms, one makes use of scale separation as discussed in section 8.1. Thus, the coefficient functions  $C_g$  and  $c_1^{(0)}$  that contain the radiative corrections due to heavy particles are evaluated at a heavy scale of the order of the SUSY particle masses  $\mu_h = \mathcal{O}(\tilde{M})$ . The partonic cross sections  $\Sigma^{(n)}(z)$  are computed at a low-scale of the order of the Higgs mass  $\mu_s = \mathcal{O}(M_h)$ . The individual building blocks in Eq. (8.35) are discussed below.

The normalization coefficient  $\rho_0$  is given by

$$\rho_0 = \frac{G_F [\alpha_s(\mu_s)]^2}{288\pi\sqrt{2}}, \quad (8.36)$$

where the presence of the strong coupling evaluated at the low energy scale  $\mu_s$  is due to the use of renormalization group invariant operators and coefficient functions as given in Eqs. (8.9) and (8.11).

$\sigma_0$  contains the exact dependence on all masses and momenta at the LO. Its analytic expression is known for quite long time. For convenience of the reader, we reproduce it here, in the normalization of Ref. [115]

$$\begin{aligned} \sigma_0 = & \left| \frac{3 \cos \alpha}{2 \sin \beta} \left\{ A(\tau_t) + \sum_{i=1,2} (-1)^i \left[ \frac{\sin(2\theta_t)}{2} \left( \tan \alpha + \frac{1}{\tan \beta} \right) \frac{m_t \mu_{\text{SUSY}}}{2m_{t_i}^2} \right. \right. \right. \\ & \left. \left. + \frac{m_t^2}{8m_{t_i}^2} \left( \sin^2(2\theta_t) \frac{m_{t_1}^2 - m_{t_2}^2}{m_t^2} - 4(-1)^i \right) \right] \tilde{A}(\tau_{t_i}) \right\} + \mathcal{O} \left( \frac{M_Z^2}{m_{t_i}^2} \right) \right|^2, \end{aligned} \quad (8.37)$$

with

$$\begin{aligned} \tau_i &= \frac{4m_i^2}{M_h^2}, \quad A(\tau) = \tau[1 + (1 - \tau)f(\tau)], \quad \tilde{A}(\tau) = \tau(1 - \tau f(\tau)), \\ f(\tau) &= \begin{cases} \arcsin^2(1/\sqrt{\tau}), & \tau \geq 1, \\ -\frac{1}{4} \left( \ln \frac{1+\sqrt{1-\tau}}{1-\sqrt{1-\tau}} - i\pi \right)^2, & \tau < 1. \end{cases} \end{aligned} \quad (8.38)$$

The coefficient  $c_1^0$  is defined through the one-loop relation

$$c_1^0 = -\frac{3\pi}{\alpha_s} C_1^{(1-\text{loop})}. \quad (8.39)$$

Its SUSY-QCD part can be read of directly from Eq. (8.16). The coefficient  $c_1^0$  is factored out because it is already contained in the LO contribution  $\sigma_0$  as can be easily understood from Eq. (8.37). Indeed, in the limit of light Higgs masses  $M_h \ll m_t, m_{\tilde{t}}, m_{\tilde{g}}$  and neglecting mass suppressed contributions of the order of  $\mathcal{O}(M_h^2/m_t^2)$ ,  $\mathcal{O}(M_h^2/m_{\tilde{t}}^2)$ , and  $\mathcal{O}(M_Z^2/m_{\tilde{t}}^2)$  the LO contribution  $\sigma_0$  takes the form <sup>30</sup>

$$\sigma_0 \rightarrow \left| c_1^{(0)} \right|^2. \quad (8.40)$$

The coefficient  $C_g$  was defined in Eq. (8.10) and has to be evaluated at the heavy scale. Let us point out that the factor  $-3\pi C_g(\mu_h)/c_1^0$  expanded in the strong coupling  $\alpha_s(\mu_h)$  takes the form

$$-3\pi \frac{C_g(\mu_h)}{c_1^0} = 1 + \frac{\alpha_s(\mu_h)}{\pi} c_g^{(1)} + \left( \frac{\alpha_s(\mu_h)}{\pi} \right)^2 c_g^{(2)} + \dots, \quad (8.41)$$

where the coefficients  $c_g^{(i)}$ , with  $i = 1, 2$ , are known, once the coefficient  $C_1$  is computed up to the NNLO.

Finally,  $\Sigma^{(n)}(z)$  is defined through the convolution

$$\Sigma^{(n)}(z) = \sum_{i,j \in \{q\bar{q}g\}} \int_z^1 dx_1 \int_{z/x_1}^1 dx_2 f_{i/p}(x_1) f_{j/p}(x_2) \hat{\Sigma}_{ij}^{(n)} \left( \frac{z}{x_1 x_2} \right), \quad z \equiv \frac{M_h^2}{s}, \quad (8.42)$$

of  $f_{j/p}(x)$  the density of parton  $i$  inside the proton and  $\hat{\Sigma}_{ij}^{(n)}(x)$  the partonic cross section expanded up to the  $n$ -th order in  $\alpha_s(\mu_s)$  and computed in the effective-theory approach. At the LO, it reads

$$\hat{\Sigma}_{ij}^{(0)}(x) = \delta_{ig} \delta_{jg} \delta(1-x). \quad (8.43)$$

The NLO and NNLO contributions contain the real and virtual corrections associated with the operator  $\mathcal{O}_1$  and its mixture with the operator  $\mathcal{O}_2$ . Since they are computed within the effective theory, they can be taken over from the SM computations reported in Refs. [258, 259, 269, 292].

Let us mention, that there is also a third scale present in Eq. (8.35), namely the factorization scale  $\mu_F$  embedded in the PDFs. Usually it is chosen to be equal to the low-scale  $\mu_s$ , *i.e.*  $\mu_F = \mu_s$ . The choice of scales plays an important role in precision calculations of the hadronic Higgs production cross section, especially when particles much heavier than the SM ones are present. We discuss in the next section the phenomenological impact of the NNLO corrections.

#### 8.4.1 Numerical analysis

For the numerical analysis we choose a supersymmetric mass spectrum in the so-called “modified  $m_h^{\max}$  scenario” as defined in Ref [115]. It is a modification of the original “ $m_h^{\max}$ ” scenario [279] such that one of the top squarks becomes light and the other one remains heavy, at the TeV scale. At the same time Higgs masses as large as 127 GeV can be achieved.

For illustration, we reproduce in Fig. 8.5 the results of Ref. [115] that constitute the most precise prediction for the hadronic cross section in the gluon fusion channel in the framework of the

---

<sup>30</sup>We adopt here the normalization of Ref. [115].

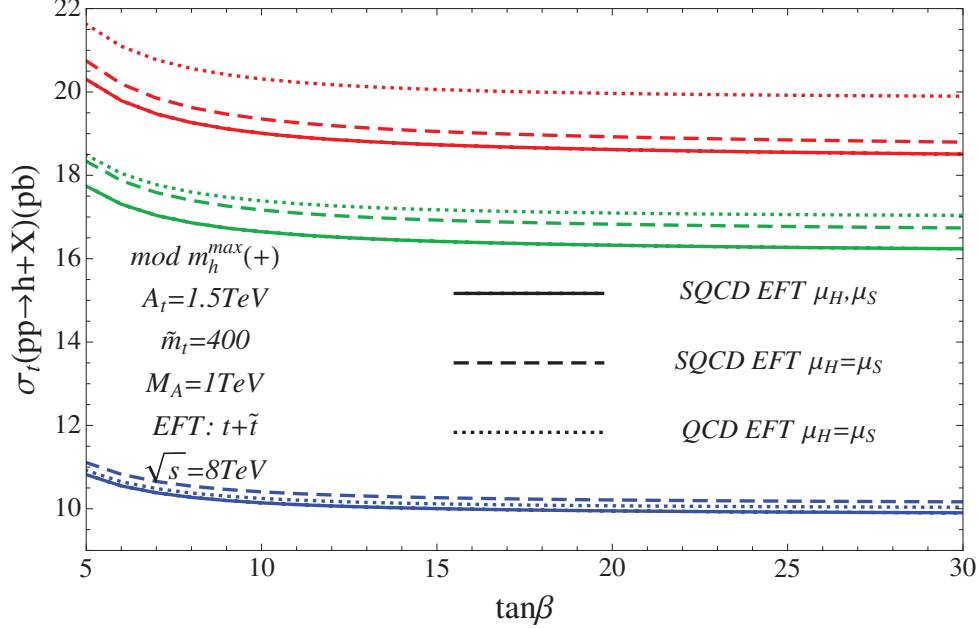


Figure 8.5: The cross section  $\sigma_t^{\text{SUSY-QCD}}(\mu_s, \mu_h)$  as a function of  $\tan \beta$  using the parameters in to LO (bottom), NLO (middle) and NNLO (top) from Ref. [115]. The dotted line corresponds to the SM and the dashed and solid lines to the MSSM.

MSSM. Here,  $\sigma_t^{\text{SUSY-QCD}}(\mu_s, \mu_h)$  denotes the dominant contribution originating from the top-sector. From bottom to top, the LO, NLO and NNLO results are depicted for  $5 \leq \tan \beta \leq 30$  and choosing  $m_{\tilde{t}_1} = 400$  GeV. The dotted lines represent the SM results. The solid and the dashed lines show the MSSM predictions for two different scale choices:  $\mu_h = M_t$  and  $\mu_s = M_h/2$  and  $\mu_h = \mu_s = M_h/2$ , respectively. The MSSM results are reduced by a few percent as compared to the SM prediction. This effect increases when going from LO to NLO and finally to NNLO where a difference of about 5% is observed. This behaviour is specific for supersymmetric mass spectra containing at least one light squark of the third generation. For the case when all SUSY particles are heavy, at the TeV scale, (the so called decoupling limit) the genuine SUSY-QCD corrections to the production cross section become negligible. The fact that the difference between the SM and MSSM predictions increases when higher order radiative corrections are taken into account can be explained by the occurrence of many new SUSY contributions.

As can be seen from the figure, the effect of scale choice is not negligible: the results for  $\mu_h = \mu_s$  are in general a few percent above the ones with  $\mu_h \neq \mu_s$ . At NLO, the scale dependence increases as compared to the LO case as a consequence of the special organisation of the perturbative series. Nevertheless, the scale dependence decreases when going from NLO to NNLO as expected.

## 9 Conclusions

In this review we report on precision calculations in supersymmetric theories. They are important ingredients not only for the development of quantum field theories in general, but they are also required by the current experimental analyses searching for indirect manifestations of



SUSY in collider experiments at the TeV scale. The latter topic is of utmost importance for particle physics: the non-observation of any supersymmetric particle at the TeV scale renders low-energy supersymmetric theories debatable. Obviously, to prove or disprove a theory for which enormous efforts both at theoretical and experimental level have been devoted over the last four decades, is a very complex task. In this review, we concentrate on the indirect searches for SUSY that can be carried through precision tests of the gauge coupling unification hypothesis, the prediction of a light Higgs boson mass and the interaction properties of the Higgs boson with the SM particles.

It turns out, that the hypothesis of gauge coupling unification even in the framework of minimal SUSY SU(5) model cannot be falsified with the help of currently available experimental data. Let us mention that the contributions at the three-loop order in perturbation theory are essential in this analysis. The conclusion drawn from precision calculations reconfirm earlier results derived from model building arguments.

Furthermore, the theoretical prediction of the light Higgs boson mass within SUSY with an accuracy comparable with the one reached by the ongoing experimental analyses conducted at the LHC is an important tool for constraining the supersymmetric parameter space. For this purpose one needs to calculate even three-loop Feynman integrals involving many different mass scales. At present, an exact analytic computation is not feasible. Nevertheless, the method of asymptotic expansion can be applied successfully also in SUSY theories and provides us with precise results. Specifically, the lightest Higgs bosons mass within the MSSM can be predicted at present with an accuracy of about 1 GeV for the parameter space of phenomenological interest.

Moreover, after the recent discovery of the Higgs boson at the LHC, the natural question is whether it has the characteristics of the particle predicted by the SM or new theories are required to describe it. To answer this question from the perspective of supersymmetric theories, one needs predictions of the hadronic Higgs production cross section and its decay rates into SM particles with the same precision as in the SM. To achieve such an accuracy, again multi-loop calculations up to the three-loop order are required.

Detailed analyses of the data taken or to be taken at the LHC running at energies up to 14 TeV are expected to provide us with new insights into the particle physics and hopefully with the answer to the question whether low-energy supersymmetry is the right theory to describe the phenomena at the TeV scale.

## Acknowledgements

I am grateful to M. Steinhauser and J.H. Kühn for carefully reading the manuscript and for many valuable comments and discussions. Furthermore, I would like to thank J.H. Kühn and M. Steinhauser for encouraging me to complete this work. This work was supported by the DFG through SFB/TR 9 “Computational Particle Physics”.

## A Group Theory

We consider a gauge group  $\mathcal{G}$  with generators  $R^a$  satisfying the Lie algebra<sup>31</sup>

$$[R^a, R^b] = if^{abc}R^c. \quad (\text{A.44})$$

We work throughout with a fermion representation consisting of  $N_f$  sets of Dirac fermions or  $2N_f$  sets of two-component fermions, in irreducible representations with identical Casimir invariants, using  $R^a$  to denote the generators in one such representation. Thus  $R^a R^a$  is proportional to the unit matrix:

$$R^a R^a = C_R \cdot I \quad (\text{A.45})$$

For the adjoint representation we have

$$C_A \delta_{ab} = f_{acd} f_{bcd}. \quad (\text{A.46})$$

$I_2(R)$  is defined by

$$\text{Tr}[R^a R^b] = I_2(R) \delta^{ab}. \quad (\text{A.47})$$

Thus we have

$$C_R d_R = I_2(R) N_A \quad (\text{A.48})$$

where  $N_A$  is the number of generators and  $d_R$  is the dimensionality of the representation  $R$ . Evidently  $I_2(A) = C_A$ . The fully symmetric tensors  $d_R^{abcd}$  and  $d_A^{abcd}$  are defined by

$$\begin{aligned} d_R^{abcd} &= \frac{1}{6} \text{Tr}[R^{(a} R^b R^c R^{d)}], \\ d_A^{abcd} &= \frac{1}{6} \text{Tr}[F^{(a} F^b F^c F^{d)}], \end{aligned} \quad (\text{A.49})$$

where

$$(F^a)^{bc} = if^{bac} \quad (\text{A.50})$$

and

$$\begin{aligned} R^{(a} R^b R^c R^{d)} &= R^a R^b R^c R^d + R^a R^b R^d R^c + R^a R^c R^b R^d \\ &+ R^a R^c R^d R^b + R^a R^d R^b R^c + R^a R^d R^c R^b, \end{aligned} \quad (\text{A.51})$$

(similarly for  $F^{(a} F^b F^c F^{d)}$ ).

The additional tensor invariants occurring in the results are defined as

$$\begin{aligned} D_3(RR) &= d_A^{abc} d_A^{abc} / N_A \\ D_4(AA) &= d_A^{abcd} d_A^{abcd} / N_A \\ D_4(RA) &= d_R^{abcd} d_A^{abcd} / N_A \\ D_4(AAA) &= d_A^{abcd} d_A^{cdef} d_A^{abef} / N_A \\ D_4(RAA) &= d_R^{abcd} d_A^{cdef} d_A^{abef} / N_A. \end{aligned} \quad (\text{A.52})$$

In table A.2-A.4 we present results for the various tensor invariants for the groups  $SU(N)$ ,  $SO(N)$  and  $Sp(N)$ , when the fermion representation  $R$  is the fundamental representation.

The canonical choice of  $b$  is  $b = 1$  for all groups, but sometimes different choices are more convenient [125].

---

<sup>31</sup>Useful sources for some of the material in this section have included Refs. [104, 122, 125].

| Group      | $SU(N)$                                  |
|------------|--|
| $C_A$      | $bN$                                     |
| $C_R$      | $b\frac{N^2-1}{2N}$                      |
| $I_2(A)$   | $bN$                                     |
| $I_2(R)$   | $\frac{b}{2}$                            |
| $N_A$      | $N^2 - 1$                                |
| $D_4(AA)$  | $\frac{b^4}{24}(N^2 + 36)N^2$            |
| $D_4(RA)$  | $\frac{b^4}{48}N(N^2 + 6)$               |
| $D_4(RR)$  | $\frac{b^4}{96N^2}(18 - 6N^2 + N^4)$     |
| $D_4(AAA)$ | $\frac{b^6}{216}N^2(324 + 135N^2 + N^4)$ |
| $D_4(RAA)$ | $\frac{b^6}{432}N^3(51 + N^2)$           |

Table A.2:  $SU(N)$  Group invariants (here  $R$  is the fundamental representation).

| Group      | $SO(N)$   |
|------------|---|
| $C_A$      | $b(N - 2)$  |
| $C_R$      | $\frac{b}{2}(N - 1)$  |
| $I_2(A)$   | $b(N - 2)$  |
| $I_2(R)$   | $b$   |
| $N_A$      | $\frac{1}{2}N(N - 1)$   |
| $D_4(AA)$  | $\frac{b^4}{24}(N - 2)(-296 + 138N - 15N^2 + N^3)$                          |
| $D_4(RA)$  | $\frac{b^4}{24}(N - 2)(22 - 7N + N^2)$                                      |
| $D_4(RR)$  | $\frac{b^4}{24}(4 - N + N^2)$   |
| $D_4(AAA)$ | $\frac{b^6}{432}(N - 2)(-29440 + 23272N - 7018N^2 + 971N^3 - 47N^4 + 2N^5)$ |
| $D_4(RAA)$ | $\frac{b^6}{432}(N - 2)(2048 - 1582N + 387N^2 - 31N^3 + 2N^4)$              |

Table A.3:  $SO(N)$  Group invariants (here  $R$  is the fundamental representation).

## B Modification of the $\overline{\text{DR}}$ scheme: $\overline{\text{MDR}}$

In the following we provide analytic expressions for the finite shifts introduced in the top squark mass counter-terms as compared to the  $\overline{\text{DR}}$  scheme. According to the discussion in section 7, one can distinguish four cases for the mass hierarchies.

Case (i):  $m_{\tilde{q}} \gg m_{\tilde{t}_i}$ , ( $i = 1, 2$ )

$$\left(\frac{m_{\tilde{t}_i}^{\overline{\text{MDR}}}}{m_{\tilde{t}_i}}\right)^2 = 1 - (\alpha_s)^2 C_R N_q I_2(R) \left(-\frac{1}{2} + L_{\mu\tilde{q}} + \zeta(2)\right) \frac{m_{\tilde{q}}^2}{m_{\tilde{t}_i}^2}. \quad (\text{B.53})$$

The label  $N_q = 5$  has been introduced for convenience and for the logarithms the abbreviation  $L_{\mu\tilde{q}} = \ln(\mu^2/m_{\tilde{q}}^2)$  has been introduced.

| Group      | $Sp(N)$  |
|------------|--|
| $C_A$      | $b(N+2)$   |
| $C_R$      | $\frac{b}{4}(N+1)$   |
| $I_2(A)$   | $b(N+2)$   |
| $I_2(R)$   | $\frac{b}{2}$  |
| $N_A$      | $\frac{1}{2}N(N+1)$  |
| $D_4(AA)$  | $\frac{b^4}{384}(N+2)(296+138N+15N^2+N^3)$                       |
| $D_4(RA)$  | $\frac{b^4}{384}(N+2)(22+7N+N^2)$                                |
| $D_4(RR)$  | $\frac{b^4}{384}(4+N+N^2)$                                       |
| $D_4(AAA)$ | $\frac{b^6}{27648}(N+2)(29440+23272N+7018N^2+971N^3+47N^4+2N^5)$ |
| $D_4(RAA)$ | $\frac{b^6}{27648}(N+2)(2048+1582N+387N^2+31N^3+2N^4)$           |

Table A.4:  $Sp(N)$  Group invariants (here  $R$  is the fundamental representation).

Case (ii):  $m_{\tilde{t}_2} \gg m_{\tilde{t}_1}$

$$\left(\frac{m_{\tilde{t}_1}^{\overline{\text{MDR}}}}{m_{\tilde{t}_1}}\right)^2 = 1 - (\alpha_s)^2 C_R I_2(R) \left(-\frac{1}{4} + \frac{1}{2}L_{\mu\tilde{t}_2} + \frac{1}{2}\zeta(2)\right) \frac{m_{\tilde{t}_2}^2}{m_{\tilde{t}_1}^2}. \quad (\text{B.54})$$

In this equation we have  $L_{\mu\tilde{t}_2} = \ln(\mu^2/m_{\tilde{t}_2}^2)$ .

Case (iii):  $m_{\tilde{g}} \gg m_{\tilde{t}_i}$ , ( $i = 1, 2$ ) and  $m_{\tilde{q}} \gg m_{\tilde{g}}$

$$\begin{aligned} \left(\frac{m_{\tilde{t}_i}^{\overline{\text{MDR}}}}{m_{\tilde{t}_i}}\right)^2 &= 1 + \alpha_s C_R [1 + L_{\mu\tilde{g}}] \frac{m_{\tilde{g}}^2}{m_{\tilde{t}_i}^2} + (\alpha_s)^2 \left\{ C_R^2 \left[-\frac{11}{4} - \frac{3}{2}L_{\mu\tilde{g}} + \zeta(2)\right] \frac{m_{\tilde{g}}^2}{m_{\tilde{t}_i}^2} \right. \\ &+ C_A C_R \left[\frac{21}{8} + \frac{7}{2}L_{\mu\tilde{g}} + \frac{9}{8}L_{\mu\tilde{g}}^2 - \frac{1}{4}\zeta(2)\right] \frac{m_{\tilde{g}}^2}{m_{\tilde{t}_i}^2} \\ &+ C_R N_t I_2(R) \left[-\left(2 + 2L_{\mu\tilde{g}} + \frac{3}{4}L_{\mu\tilde{g}}^2\right) \frac{m_{\tilde{g}}^2}{m_{\tilde{t}_i}^2} + (1 - 2\zeta(2)) \frac{m_{\tilde{g}}(m_{\tilde{g}} - m_{\tilde{t}_2})}{m_{\tilde{t}_i}^2} \right. \\ &+ \left.\left.\left(\frac{1}{4} - \frac{1}{2}L_{\mu\tilde{t}_2} - \frac{1}{2}\zeta(2)\right) \frac{m_{\tilde{t}_2}^2}{m_{\tilde{t}_i}^2}\right] \right. \\ &+ C_R N_q I_2(R) \left[\left(-\frac{5}{8} - \frac{3}{4}L_{\mu\tilde{g}} - \frac{5}{4}L_{\mu\tilde{q}} - \frac{3}{2}L_{\mu\tilde{g}}L_{\mu\tilde{q}} + \frac{3}{4}L_{\mu\tilde{q}}^2 + \frac{3}{2}\zeta(2)\right) \frac{m_{\tilde{g}}^2}{m_{\tilde{t}_i}^2} \right. \\ &+ \left(-\frac{43}{36} - \frac{5}{6}L_{\tilde{q}\tilde{g}}\right) \frac{m_{\tilde{q}}^4}{m_{\tilde{q}}^2 m_{\tilde{t}_i}^2} + \left(-\frac{67}{288} - \frac{7}{24}L_{\tilde{q}\tilde{g}}\right) \frac{m_{\tilde{q}}^6}{m_{\tilde{q}}^4 m_{\tilde{t}_i}^2} \\ &+ \left.\left.\left(+\frac{1}{2} - L_{\mu\tilde{q}} - \zeta(2)\right) \frac{m_{\tilde{q}}^2}{m_{\tilde{t}_i}^2}\right] \right\}. \quad (\text{B.55}) \end{aligned}$$

Here  $N_t = 1$ ,  $L_{\mu\tilde{g}} = \ln(\mu^2/m_{\tilde{g}}^2)$  and  $L_{\tilde{q}\tilde{g}} = \ln(m_{\tilde{q}}^2/m_{\tilde{g}}^2)$ .

Case (iv):  $m_{\tilde{g}} \gg m_{\tilde{t}_1}$ , and  $m_{\tilde{q}} \approx m_{\tilde{g}}$

$$\begin{aligned}
\left(\frac{m_{\tilde{t}_i}^{\overline{\text{MDR}}}}{m_{\tilde{t}_i}}\right)^2 &= 1 + \alpha_s C_R [1 + L_{\mu\tilde{g}}] \frac{m_{\tilde{g}}^2}{m_{\tilde{t}_i}^2} + (\alpha_s)^2 \left\{ C_R^2 \left[ -\frac{11}{4} - \frac{3}{2} L_{\mu\tilde{g}} + \zeta(2) \right] \frac{m_{\tilde{g}}^2}{m_{\tilde{t}_i}^2} \right. \\
&+ C_A C_R \left[ \frac{21}{8} + \frac{7}{2} L_{\mu\tilde{g}} + \frac{9}{8} L_{\mu\tilde{g}}^2 - \frac{1}{4} \zeta(2) \right] \frac{m_{\tilde{g}}^2}{m_{\tilde{t}_i}^2} \\
&+ C_R N_t I_2(R) \left[ - \left( 2 + 2L_{\mu\tilde{g}} + \frac{3}{4} L_{\mu\tilde{g}}^2 \right) \frac{m_{\tilde{g}}^2}{m_{\tilde{t}_i}^2} + (1 - 2\zeta(2)) \frac{m_{\tilde{g}}(m_{\tilde{g}} - m_{\tilde{t}_2})}{m_{\tilde{t}_i}^2} \right. \\
&+ \left. \left( \frac{1}{4} - \frac{1}{2} L_{\mu\tilde{t}_2} - \frac{1}{2} \zeta(2) \right) \frac{m_{\tilde{t}_2}^2}{m_{\tilde{t}_i}^2} \right] \\
&+ C_R N_q I_2(R) \left[ \left( -\frac{3}{4} L_{\mu\tilde{g}} - \frac{5}{4} L_{\mu\tilde{q}} - \frac{3}{2} L_{\mu\tilde{g}} L_{\mu\tilde{q}} + \frac{3}{4} L_{\mu\tilde{q}}^2 + \frac{3}{2} \zeta(2) \right) \frac{m_{\tilde{g}}^2}{m_{\tilde{t}_i}^2} \right. \\
&- \left. 4\zeta(2) \frac{m_{\tilde{g}}(m_{\tilde{g}} - m_{\tilde{t}_2})}{m_{\tilde{t}_i}^2} - \left( \frac{7}{4} + L_{\mu\tilde{q}} + \zeta(2) \right) \frac{m_{\tilde{q}}^2}{m_{\tilde{t}_i}^2} \right] \Big\}. \tag{B.56}
\end{aligned}$$

All the masses on the r.h.s. of the Eqs. (B.53), (B.54), (B.55) and (B.56) are  $\overline{\text{DR}}$  masses. Let us also mention that the above formulae are valid for the case  $M_\varepsilon = 0$ . The finite shifts given for the cases (iii) and (iv) can also be used for other mass hierarchies like for example  $m_{\tilde{q}} \gg m_{\tilde{t}_2} \approx m_{\tilde{g}} \gg m_{\tilde{t}_1}$  or  $m_{\tilde{q}} \approx m_{\tilde{t}_2} \approx m_{\tilde{g}} \gg m_{\tilde{t}_1}$ .

## References

- [1] S. L. Glashow, Nucl. Phys. **22** (1961) 579.
- [2] S. Weinberg, Phys. Rev. Lett. **19** (1967) 1264.
- [3] A. Salam, *In the Proceedings of 8th Nobel Symposium, Lerum, Sweden, 19-25 May 1968*, pp 367-377.
- [4] M. Gell-Mann, Acta Phys. Austriaca Suppl. **9** (1972) 733;  
H. Fritzsch, M. Gell-Mann and H. Leutwyler, Phys. Lett. B **47** (1973) 365.
- [5] D. J. Gross and F. Wilczek, Phys. Rev. Lett. **30** (1973) 1343; D. J. Gross and F. Wilczek, Phys. Rev. D **8** (1973) 3633;  
H. D. Politzer, Phys. Rev. Lett. **30** (1973) 1346.
- [6] S. R. Coleman and J. Mandula, Phys. Rev. **159** (1967) 1251.
- [7] R. Haag, J. T. Lopuszanski and M. Sohnius, Nucl. Phys. B **88** (1975) 257.
- [8] Y. A. Golfand and E. P. Likhtman, JETP Lett. **13** (1971) 323 [Pisma Zh. Eksp. Teor. Fiz. **13** (1971) 452].

- [9] D. V. Volkov and V. P. Akulov, JETP Lett. **16** (1972) 438 [Pisma Zh. Eksp. Teor. Fiz. **16** (1972) 621].
- [10] J. Wess and B. Zumino, Nucl. Phys. B **70** (1974) 39.
- [11] A. Salam and J. A. Strathdee, Nucl. Phys. B **76** (1974) 477.
- [12] B. Zumino, Nucl. Phys. B **89** (1975) 535.
- [13] P. C. West, Nucl. Phys. B **106** (1976) 219.
- [14] M. T. Grisaru, W. Siegel and M. Rocek, Nucl. Phys. B **159** (1979) 429.
- [15] L. Girardello and M. T. Grisaru, Nucl. Phys. B **194** (1982) 65.
- [16] A. V. Gladyshev and D. I. Kazakov, arXiv:1212.2548 [hep-ph].
- [17] <http://lepewwg.web.cern.ch/LEPEWWG/>
- [18] J. R. Ellis, S. Kelley and D. V. Nanopoulos, Phys. Lett. B **260** (1991) 131.
- [19] U. Amaldi, W. de Boer and H. Furstenau, Phys. Lett. B **260** (1991) 447.
- [20] P. Langacker and M. x. Luo, Phys. Rev. D **44** (1991) 817.
- [21] Y. Sofue and V. Rubin, Ann. Rev. Astron. Astrophys. **39** (2001) 137 [astro-ph/0010594].
- [22] N. Kaiser and G. Squires, Astrophys. J. **404** (1993) 441.
- [23] C. S. Kochanek, Astrophys. J. **453** (1995) 545 [astro-ph/9411082].
- [24] S. Eidelman *et al.* [Particle Data Group Collaboration], Phys. Lett. B **592** (2004) 1.
- [25] <https://twiki.cern.ch/twiki/bin/view/AtlasPublic/SupersymmetryPublicResults>
- [26] J. Angle *et al.* [XENON10 Collaboration], Phys. Rev. Lett. **107** (2011) 051301 [arXiv:1104.3088 [astro-ph.CO]].
- [27] <http://map.gsfc.nasa.gov/>
- [28] G. W. Bennett *et al.* [Muon G-2 Collaboration], Phys. Rev. D **73** (2006) 072003 [hep-ex/0602035].
- [29] <https://twiki.cern.ch/twiki/bin/view/AtlasPublic/HiggsPublicResults>
- [30] <https://twiki.cern.ch/twiki/bin/view/CMSPublic/PhysicsResults>
- [31] S. Heinemeyer, W. Hollik and G. Weiglein, Phys. Rept. **425** (2006) 265 [hep-ph/0412214].
- [32] D. Stockinger, J. Phys. G **34** (2007) R45 [hep-ph/0609168].
- [33] F. del Aguila, J. A. Aguilar-Saavedra, B. C. Allanach, J. Alwall, Y. .Andreev, D. Aristizabal Sierra, A. Bartl and M. Beccaria *et al.*, Eur. Phys. J. C **57** (2008) 183 [arXiv:0801.1800 [hep-ph]].

- [34] S. Dittmaier *et al.* [LHC Higgs Cross Section Working Group Collaboration], arXiv:1101.0593 [hep-ph].
- [35] M. A. Shifman and A. I. Vainshtein, Nucl. Phys. B **277** (1986) 456 [Sov. Phys. JETP **64** (1986) 428] [Zh. Eksp. Teor. Fiz. **91** (1986) 723].
- [36] N. Arkani-Hamed and H. Murayama, JHEP **0006** (2000) 030 [arXiv:hep-th/9707133].
- [37] K. G. Wilson and J. B. Kogut, Phys. Rept. **12** (1974) 75.
- [38] M. Gell-Mann and F. E. Low, Phys. Rev. **95**, 1300 (1954).
- [39] C. G. . Callan, Phys. Rev. D **2** (1970) 1541.
- [40] K. Symanzik, Commun. Math. Phys. **18** (1970) 227.
- [41] M. T. Grisaru, B. Milewski and D. Zanon, Phys. Lett. B **155** (1985) 357.
- [42] J. Hisano and M. A. Shifman, Phys. Rev. D **56** (1997) 5475 [arXiv:hep-ph/9705417].
- [43] N. Arkani-Hamed, G. F. Giudice, M. A. Luty and R. Rattazzi, Phys. Rev. D **58**, 115005 (1998) [arXiv:hep-ph/9803290].
- [44] Y. Yamada, Phys. Rev. D **50** (1994) 3537 [arXiv:hep-ph/9401241].
- [45] L. V. Avdeev, D. I. Kazakov and I. N. Kondrashuk, Nucl. Phys. B **510** (1998) 289 [arXiv:hep-ph/9709397].
- [46] D. I. Kazakov and V. N. Velizhanin, Phys. Lett. B **485** (2000) 393 [hep-ph/0005185].
- [47] V. A. Novikov, M. A. Shifman, A. I. Vainshtein and V. I. Zakharov, Phys. Lett. B **166** (1986) 329 [Sov. J. Nucl. Phys. **43** (1986) 294] [Yad. Fiz. **43** (1986) 459].
- [48] W. Siegel, Phys. Lett. B **84** (1979) 193.
- [49] W. Siegel, Phys. Lett. B **94** (1980) 37.
- [50] L.V. Avdeev, G.A. Chochia and A.A. Vladimirov, Phys. Lett. B **105** (1981) 272.
- [51] L. V. Avdeev and A. A. Vladimirov, Nucl. Phys. B **219** (1983) 262.
- [52] I. Jack and D. R. T. Jones, Phys. Lett. B **415** (1997) 383 [hep-ph/9709364].
- [53] I. Jack, D. R. T. Jones, A. Pickering, Phys. Lett. **B432** (1998) 114-119. [hep-ph/9803405].
- [54] I. Jack, D. R. T. Jones and C. G. North, Nucl. Phys. B **473** (1996) 308 [arXiv:hep-ph/9603386].
- [55] I. Jack, D. R. T. Jones and C. G. North, Phys. Lett. B **386** (1996) 138 [arXiv:hep-ph/9606323].
- [56] I. Jack, D. R. T. Jones and C. G. North, Nucl. Phys. B **486** (1997) 479 [arXiv:hep-ph/9609325].

- [57] I. Jack, D. R. T. Jones and K. L. Roberts, Z. Phys. C **63** (1994) 151 [arXiv:hep-ph/9401349].
- [58] L. V. Avdeev and O. V. Tarasov, Phys. Lett. B **112**, 356 (1982).
- [59] C.G. Bollini and J.J. Giambiagi, Nuovo Cim. B **12** (1972) 20.
- [60] G. 't Hooft and M. J. G. Veltman, Nucl. Phys. B **44** (1972) 189.
- [61] O. Piguet, K. Sibold and M. Schweda, Nucl. Phys. B **174** (1980) 183.
- [62] J. C. Ward, Phys. Rev. **78** (1950) 182;  
Y. Takahashi, Nuovo Cim. **6** (1957) 371.
- [63] A. A. Slavnov, Theor. Math. Phys. **10** (1972) 99 [Teor. Mat. Fiz. **10** (1972) 153].
- [64] D. Stöckinger, JHEP **0503** (2005) 076 [arXiv:hep-ph/0503129].
- [65] J. Collins, *Renormalization*, Cambridge University Press, Cambridge 1984.
- [66] J. G. Korner and M. M. Tung, Z. Phys. C **64** (1994) 255.
- [67] M. Misiak, Phys. Lett. B **321** (1994) 113 [arXiv:hep-ph/9309236].
- [68] Z. Kunszt, A. Signer and Z. Trocsanyi, Nucl. Phys. B **411** (1994) 397 [arXiv:hep-ph/9305239].
- [69] J. Smith and W. L. van Neerven, Eur. Phys. J. C **40** (2005) 199 [arXiv:hep-ph/0411357].
- [70] G. Altarelli, G. Curci, G. Martinelli and S. Petrarca, Nucl. Phys. B **187** (1981) 461.
- [71] D. M. Capper, D. R. T. Jones and P. van Nieuwenhuizen, Nucl. Phys. B **167** (1980) 479.
- [72] H. Nicolai and P. K. Townsend, Phys. Lett. B **93** (1980) 111.
- [73] D. R. T. Jones and J. P. Leveille, Nucl. Phys. B **206** (1982) 473; [Erratum-ibid. B **222** (1983) 517].
- [74] S. L. Adler and W. A. Bardeen, Phys. Rev. **182** (1969) 1517.
- [75] T. L. Trueman, Z. Phys. C **69** (1996) 525 [arXiv:hep-ph/9504315].
- [76] S. A. Larin, Phys. Lett. B **303** (1993) 113 [arXiv:hep-ph/9302240].
- [77] K. G. Chetyrkin, B. A. Kniehl, M. Steinhauser and W. A. Bardeen, Nucl. Phys. B **535** (1998) 3 [arXiv:hep-ph/9807241].
- [78] S. L. Adler, Phys. Rev. **177** (1969) 2426;  
J. S. Bell and R. Jackiw, Nuovo Cim. A **60** (1969) 47;  
W. A. Bardeen, Phys. Rev. **184** (1969) 1848.
- [79] W. A. Bardeen, R. Gastmans and B. Lautrup, Nucl. Phys. B **46** (1972) 319.
- [80] M. S. Chanowitz, M. Furman and I. Hinchliffe, Nucl. Phys. B **159** (1979) 225.



- [81] F. Jegerlehner, Eur. Phys. J. C **18** (2001) 673 [arXiv:hep-th/0005255].
- [82] J. Fleischer, O. V. Tarasov and F. Jegerlehner, Phys. Lett. B **319** (1993) 249;  
J. Fleischer, O. V. Tarasov, F. Jegerlehner and P. Raczka, Phys. Lett. B **293** (1992) 437.
- [83] A. Freitas, W. Hollik, W. Walter and G. Weiglein, Phys. Lett. B **495** (2000) 338 [Erratum-  
ibid. B **570** (2003) 260] [arXiv:hep-ph/0007091];  
A. Freitas, W. Hollik, W. Walter and G. Weiglein, Nucl. Phys. B **632** (2002) 189 [Erratum-  
ibid. B **666** (2003) 305] [arXiv:hep-ph/0202131].
- [84] L. Avdeev, J. Fleischer, S. Mikhailov and O. Tarasov, Phys. Lett. B **336** (1994) 560  
[Erratum-ibid. B **349** (1995) 597] [arXiv:hep-ph/9406363].
- [85] K. G. Chetyrkin, J. H. Kuhn and M. Steinhauser, Phys. Lett. B **351** (1995) 331  
[hep-ph/9502291].
- [86] S. Heinemeyer, D. Stockinger and G. Weiglein, Nucl. Phys. B **699** (2004) 103  
[arXiv:hep-ph/0405255].
- [87] A. G. M. Pickering, J. A. Gracey and D. R. T. Jones, Phys. Lett. B **510** (2001) 347 [Phys.  
Lett. B **512** (2001 ERRATUM, B535, 377.2002) 230] [arXiv:hep-ph/0104247].
- [88] R. V. Harlander, L. Mihaila and M. Steinhauser, Eur. Phys. J. C **63** (2009) 383  
[arXiv:0905.4807 [hep-ph]].
- [89] G. 't Hooft, Nucl. Phys. B **61** (1973) 455.
- [90] W. A. Bardeen, A. J. Buras, D. W. Duke and T. Muta, Phys. Rev. D **18** (1978) 3998.
- [91] J. C. Collins, Nucl. Phys. B **80** (1974) 341; Nucl. Phys. B **92** (1975) 477.
- [92] K. G. Chetyrkin and V. A. Smirnov, Phys. Lett. B **144** (1984) 419.
- [93] A. A. Vladimirov, Theor. Math. Phys. **43** (1980) 417 [Teor. Mat. Fiz. **43** (1980) 210].
- [94] K. G. Chetyrkin, A. L. Kataev and F. V. Tkachov, Nucl. Phys. B **174** (1980) 345.
- [95] O. V. Tarasov, A. A. Vladimirov and A. Y. Zharkov, Phys. Lett. B **93** (1980) 429.
- [96] S. A. Larin and J. A. M. Vermaseren, Phys. Lett. B **303** (1993) 334 [arXiv:hep-ph/9302208].
- [97] R. Harlander, P. Kant, L. Mihaila and M. Steinhauser, JHEP **0609** (2006) 053  
[arXiv:hep-ph/0607240].
- [98] K. G. Chetyrkin and M. F. Zoller, JHEP **1206** (2012) 033 [arXiv:1205.2892 [hep-ph]].
- [99] L. N. Mihaila, J. Salomon and M. Steinhauser, Phys. Rev. Lett. **108** (2012) 151602  
[arXiv:1201.5868 [hep-ph]].
- [100] S. A. Larin, F. V. Tkachov and J. A. M. Vermaseren, preprint NIKHEF-H-91-18 (1991).
- [101] J. A. M. Vermaseren, arXiv:math-ph/0010025.

- [102] K. G. Chetyrkin, M. Misiak and M. Munz, Nucl. Phys. B **518** (1998) 473 [arXiv:hep-ph/9711266].
- [103] K. G. Chetyrkin, Phys. Lett. B **404** (1997) 161 [hep-ph/9703278].
- [104] T. van Ritbergen, J. A. M. Vermaseren and S. A. Larin, Phys. Lett. B **400** (1997) 379 [hep-ph/9701390].
- [105] J. A. M. Vermaseren, S. A. Larin and T. van Ritbergen, Phys. Lett. B **405** (1997) 327 [hep-ph/9703284].
- [106] M. Czakon, Nucl. Phys. B **710** (2005) 485 [hep-ph/0411261].
- [107] T. Curtright, Phys. Rev. D **21** (1980) 1543.
- [108] D. R. T. Jones, Phys. Rev. D **22** (1980) 3140.
- [109] M. Steinhauser, Comput. Phys. Commun. **134** (2001) 335 [arXiv:hep-ph/0009029].
- [110] K. G. Chetyrkin, Phys. Lett. B **391** (1997) 402 [arXiv:hep-ph/9608480].
- [111] K. G. Chetyrkin, Phys. Lett. B **390** (1997) 309 [arXiv:hep-ph/9608318].
- [112] P. M. Ferreira, I. Jack and D. R. T. Jones, Phys. Lett. B **387**, 80 (1996) [arXiv:hep-ph/9605440].
- [113] Z. Bern, A. De Freitas, L. J. Dixon and H. L. Wong, Phys. Rev. D **66** (2002) 085002 [arXiv:hep-ph/0202271].
- [114] A. Pak, M. Steinhauser and N. Zerf, Eur. Phys. J. C **71** (2011) 1602 [arXiv:1012.0639 [hep-ph]].
- [115] A. Pak, M. Steinhauser and N. Zerf, JHEP **1209** (2012) 118 [arXiv:1208.1588 [hep-ph]].
- [116] P. Kant, PhD thesis, University of Karlsruhe (2008).
- [117] D.R.T. Jones (unpublished) 1979;  
see also W. Siegel, P.K. Townsend and P. van Nieuwenhuizen, Proc. 1980 Cambridge meeting on supergravity, ITP-SB-80-65.
- [118] R. van Damme and G. 't Hooft, Phys. Lett. B **150** (1985) 133.
- [119] I. Jack, D. R. T. Jones and K. L. Roberts, Z. Phys. C **62** (1994) 161 [arXiv:hep-ph/9310301].
- [120] M. Steinhauser, Phys. Rept. **364** (2002) 247 [hep-ph/0201075].
- [121] I. Jack, D. R. T. Jones, P. Kant and L. Mihaila, JHEP **0709** (2007) 058 [arXiv:0707.3055 [hep-th]].
- [122] P. Cvitanovic, Phys. Rev. D **14** (1976) 1536.
- [123] P. Dittner, Commun. Math. Phys. **27** (1972) 44.

- [124] A.J. MacFarlane, A. Sudbery and P.H. Weisz, Commun. Math. Phys. **11** (1968) 77.
- [125] T. van Ritbergen, A.N. Schellekens and J.A.M. Vermaseren, Int. J. Mod. Phys. A **14** (1999) 41 [arXiv:hep-ph/9802376].
- [126] T. P. Cheng, E. Eichten and L. F. Li, Phys. Rev. D **9** (1974) 2259.
- [127] P. Nogueira, J. Comput. Phys. **105** (1993) 279.
- [128] T. Seidensticker, [hep-ph/9905298].
- [129] R. Harlander, T. Seidensticker and M. Steinhauser, Phys. Lett. B **426** (1998) 125 [hep-ph/9712228].
- [130] R. V. Harlander, D. R. T. Jones, P. Kant, L. Mihaila and M. Steinhauser, JHEP **0612** (2006) 024 [arXiv:hep-ph/0610206].
- [131] P. A. Baikov, K. G. Chetyrkin and J. H. Kuhn, Phys. Rev. Lett. **101** (2008) 012002 [arXiv:0801.1821 [hep-ph]].
- [132] P. A. Baikov, K. G. Chetyrkin and J. H. Kuhn, Nucl. Phys. Proc. Suppl. **205-206** (2010) 237 [arXiv:1007.0478 [hep-ph]].
- [133] I. Jack, D. R. T. Jones, A. Pickering, Phys. Lett. **B435** (1998) 61-66. [hep-ph/9805482].
- [134] D.R.T. Jones, Phys. Lett. B **123** (1983) 45.
- [135] V.A. Novikov, M.A. Shifman, A.I. Vainshtein and V.I. Zakharov, Nucl. Phys. B **229** (1983) 407.
- [136] V. A. Smirnov, “Applied asymptotic expansions in momenta and masses,” Springer Tracts Mod. Phys. **177** (2002) 1.
- [137] P. Marquard, L. Mihaila, J. H. Piclum and M. Steinhauser, Nucl. Phys. B **773** (2007) 1 [arXiv:hep-ph/0702185].
- [138] S. P. Martin, Phys. Rev. D **65** (2002) 116003 [arXiv:hep-ph/0111209].
- [139] <http://www.fnal.gov/pub/science/experiments/energy/tevatron/>
- [140] S. Heinemeyer, Int. J. Mod. Phys. A **21** (2006) 2659 [arXiv:hep-ph/0407244].
- [141] G. Degrossi and P. Slavich, Nucl. Phys. B **825** (2010) 119 [arXiv:0907.4682 [hep-ph]].
- [142] P. Kant, R. V. Harlander, L. Mihaila and M. Steinhauser, JHEP **1008** (2010) 104 [arXiv:1005.5709 [hep-ph]].
- [143] V. A. Novikov, M. A. Shifman, A. I. Vainshtein and V. I. Zakharov, Nucl. Phys. B **229** (1983) 381.
- [144] I. Jack, D. R. T. Jones and A. F. Kord, Phys. Lett. B **579** (2004) 180 [arXiv:hep-ph/0308231].  
I. Jack, D. R. T. Jones and A. F. Kord, Annals Phys. **316** (2005) 213 [arXiv:hep-ph/0408128].

- [145] L. N. Mihaila, J. Salomon and M. Steinhauser, Phys. Rev. D **86** (2012) 096008 [arXiv:1208.3357 [hep-ph]].
- [146] T. Hermann, L. Mihaila and M. Steinhauser, Phys. Lett. B **703** (2011) 51 [arXiv:1106.1060 [hep-ph]].
- [147] W. Hollik, E. Kraus, M. Roth, C. Rupp, K. Sibold and D. Stockinger, Nucl. Phys. B **639** (2002) 3 [hep-ph/0204350].  
W. Hollik, E. Kraus and D. Stockinger, Eur. Phys. J. C **23** (2002) 735 [hep-ph/0007134].
- [148] I. Jack, D. R. T. Jones, S. P. Martin, M. T. Vaughn and Y. Yamada, Phys. Rev. D **50** (1994) 5481 [arXiv:hep-ph/9407291].
- [149] H. D. Politzer, Phys. Rev. Lett. **30** (1973) 1346.
- [150] D. R. T. Jones, Nucl. Phys. B **75**, 531 (1974).
- [151] O. V. Tarasov and A. A. Vladimirov, Sov. J. Nucl. Phys. **25** (1977) 585 [Yad. Fiz. **25** (1977) 1104].
- [152] W. E. Caswell, Phys. Rev. Lett. **33** (1974) 244.
- [153] E. Egorian and O. V. Tarasov, Teor. Mat. Fiz. **41** (1979) 26 [Theor. Math. Phys. **41** (1979) 863].
- [154] D. R. T. Jones, Phys. Rev. D **25** (1982) 581.
- [155] M. S. Fischler and C. T. Hill, Nucl. Phys. B **193** (1981) 53.
- [156] M. E. Machacek and M. T. Vaughn, Nucl. Phys. B **222** (1983) 83; Nucl. Phys. B **236** (1984) 221; Nucl. Phys. B **249** (1985) 70.
- [157] I. Jack and H. Osborn, Nucl. Phys. B **249** (1985) 472.
- [158] M. Steinhauser, Phys. Rev. D **59** (1999) 054005 [hep-ph/9809507].
- [159] A. V. Bednyakov, A. F. Pikelner and V. N. Velizhanin, JHEP **1301** (2013) 017 [arXiv:1210.6873 [hep-ph]].
- [160] K. Nakamura *et al.* [Particle Data Group Collaboration], J. Phys. G **37** (2010) 075021.
- [161] L. F. Abbott, Nucl. Phys. B **185** (1981) 189.
- [162] A. Denner, G. Weiglein and S. Dittmaier, Nucl. Phys. B **440** (1995) 95 [hep-ph/9410338].
- [163] M. E. Peskin and D. V. Schroeder, *An Introduction to quantum field theory*, Reading, USA: Addison-Wesley (1995) 842 p.
- [164] S. Bethke, Eur. Phys. J. C **64** (2009) 689 [arXiv:0908.1135 [hep-ph]].
- [165] R. Harlander, L. Mihaila and M. Steinhauser, Phys. Rev. D **72** (2005) 095009 [hep-ph/0509048].

- [166] A. Bauer, L. Mihaila and J. Salomon, JHEP **0902** (2009) 037 [arXiv:0810.5101 [hep-ph]].
- [167] T. Appelquist and J. Carazzone, Phys. Rev. D **11** (1975) 2856.
- [168] K. G. Chetyrkin, B. A. Kniehl and M. Steinhauser, Nucl. Phys. B **510** (1998) 61 [hep-ph/9708255].
- [169] Y. Schroder and M. Steinhauser, JHEP **0601** (2006) 051 [hep-ph/0512058];  
K. G. Chetyrkin, J. H. Kuhn and C. Sturm, Nucl. Phys. B **744** (2006) 121 [hep-ph/0512060].
- [170] A. V. Bednyakov, Int. J. Mod. Phys. A **22** (2007) 5245.
- [171] A. V. Bednyakov, Int. J. Mod. Phys. A **25** (2010) 2437.
- [172] D. Noth and M. Spira, Phys. Rev. Lett. **101** (2008) 181801 [arXiv:0808.0087 [hep-ph]];  
D. Noth and M. Spira, JHEP **1106** (2011) 084 [arXiv:1001.1935 [hep-ph]].
- [173] A. Kurz, M. Steinhauser and N. Zerf, JHEP **1207** (2012) 138 [arXiv:1206.6675 [hep-ph]].
- [174] I. Jack and D. R. T. Jones, Phys. Lett. B **333** (1994) 372 [arXiv:hep-ph/9405233].
- [175] A. Bednyakov, A. Onishchenko, V. Velizhanin and O. Veretin, Eur. Phys. J. C **29** (2003) 87 [hep-ph/0210258].
- [176] D. M. Pierce, J. A. Bagger, K. T. Matchev and R. j. Zhang, Nucl. Phys. B **491**, 3 (1997) [arXiv:hep-ph/9606211].
- [177] R. V. Harlander and M. Steinhauser, JHEP **0409** (2004) 066 [hep-ph/0409010].
- [178] S. P. Martin and D. G. Robertson, Comput. Phys. Commun. **174** (2006) 133 [hep-ph/0501132].
- [179] M. A. Shifman, A. I. Vainshtein and V. I. Zakharov, Phys. Lett. B **78** (1978) 443.
- [180] M. Carena, D. Garcia, U. Nierste and C. E. M. Wagner, Nucl. Phys. B **577** (2000) 88 [hep-ph/9912516].
- [181] R. V. Harlander, L. Mihaila and M. Steinhauser, Phys. Rev. D **76** (2007) 055002 [arXiv:0706.2953 [hep-ph]].
- [182] L. Mihaila, Phys. Lett. B **681** (2009) 52 [arXiv:0908.3403 [hep-ph]].
- [183] D. Stockinger and P. Varso, Comput. Phys. Commun. **183** (2012) 422 [arXiv:1109.6484 [hep-ph]].
- [184] S. Bethke, Prog. Part. Nucl. Phys. **58** (2007) 351 [hep-ex/0606035].
- [185] J. A. Aguilar-Saavedra, A. Ali, B. C. Allanach, R. L. Arnowitt, H. A. Baer, J. A. Bagger, C. Balazs and V. D. Barger *et al.*, Eur. Phys. J. C **46** (2006) 43 [hep-ph/0511344].
- [186] N. Ghodbane and H. U. Martyn, in *Proc. of the APS/DPF/DPB Summer Study on the Future of Particle Physics (Snowmass 2001)* ed. N. Graf, [arXiv:hep-ph/0201233].

- [187] S. Dimopoulos and H. Georgi, Nucl. Phys. B **193** (1981) 150.
- [188] N. Sakai, Z. Phys. C **11** (1981) 153.
- [189] T. Goto and T. Nihei, Phys. Rev. D **59** (1999) 115009 [arXiv:hep-ph/9808255].
- [190] H. Murayama and A. Pierce, Phys. Rev. D **65**, 055009 (2002) [arXiv:hep-ph/0108104].
- [191] B. Bajc, P. Fileviez Perez and G. Senjanovic, Phys. Rev. D **66** (2002) 075005 [arXiv:hep-ph/0204311].
- [192] D. Emmanuel-Costa and S. Wiesenfeldt, Nucl. Phys. B **661** (2003) 62 [arXiv:hep-ph/0302272].
- [193] S. Wiesenfeldt, PhD thesis, University of Hamburg (2004).
- [194] B. Bajc, P. Fileviez Perez and G. Senjanovic, arXiv:hep-ph/0210374.
- [195] Y. Yamada, Z. Phys. C **60** (1993) 83.
- [196] L. J. Hall, Nucl. Phys. B **178** (1981) 75.
- [197] S. Weinberg, Phys. Lett. B **91** (1980) 51.
- [198] M. B. Einhorn and D. R. T. Jones, Nucl. Phys. B **196** (1982) 475.
- [199] K. Hagiwara and Y. Yamada, Phys. Rev. Lett. **70** (1993) 709.
- [200] A. Dedes, A. B. Lahanas, J. Rizos and K. Tamvakis, Phys. Rev. D **55** (1997) 2955 [arXiv:hep-ph/9610271].
- [201] J. Hisano, H. Murayama and T. Yanagida, Nucl. Phys. B **402** (1993) 46 [arXiv:hep-ph/9207279].
- [202] C. Amsler *et al.* [Particle Data Group], Phys. Lett. B **667** (2008) 1.
- [203] T. Teubner, K. Hagiwara, R. Liao, A. D. Martin and D. Nomura, Chin. Phys. C **34** (2010) 728 [arXiv:1001.5401 [hep-ph]].
- [204] M. Steinhauser, Phys. Lett. B **429** (1998) 158 [arXiv:hep-ph/9803313].
- [205] J. H. Kuhn and M. Steinhauser, Phys. Lett. B **437** (1998) 425 [arXiv:hep-ph/9802241].
- [206] S. Fanchiotti, B. A. Kniehl and A. Sirlin, Phys. Rev. D **48** (1993) 307 [arXiv:hep-ph/9212285].
- [207] K. G. Chetyrkin, J. H. Kühn and M. Steinhauser, Comput. Phys. Commun. **133** (2000) 43 [arXiv:hep-ph/0004189].
- [208] A. Dedes, A. B. Lahanas and K. Tamvakis, Phys. Rev. D **59** (1999) 015019 [arXiv:hep-ph/9801425].
- [209] A. H. Chamseddine, R. L. Arnowitt and P. Nath, Phys. Rev. Lett. **49** (1982) 970.

- [210] B. C. Allanach, Comput. Phys. Commun. **143** (2002) 305 [arXiv:hep-ph/0104145].
- [211] W. Martens, L. Mihaila, J. Salomon and M. Steinhauser, Phys. Rev. D **82** (2010) 095013 [arXiv:1008.3070 [hep-ph]].
- [212] K. Kobayashi *et al.* [Super-Kamiokande Collaboration], Phys. Rev. D **72** (2005) 052007 [arXiv:hep-ex/0502026].
- [213] Y. Nambu, Phys. Rev. Lett. **4** (1960) 380.
- [214] F. Englert and R. Brout, Phys. Rev. Lett. **13** (1964) 321.
- [215] P. W. Higgs, Phys. Lett. **12** (1964) 132.
- [216] P. W. Higgs, Phys. Rev. Lett. **13** (1964) 508.
- [217] G. 't Hooft, Nucl. Phys. B **35** (1971) 167.
- [218] R. Barate *et al.* [LEP Working Group for Higgs boson searches and ALEPH and DELPHI and L3 and OPAL Collaborations], Phys. Lett. B **565** (2003) 61 [hep-ex/0306033].
- [219] M. Baak, M. Goebel, J. Haller, A. Hoecker, D. Kennedy, R. Kogler, K. Moenig and M. Schott *et al.*, Eur. Phys. J. C **72** (2012) 2205 [arXiv:1209.2716 [hep-ph]].
- [220] [TEVNPH (Tevatron New Phenomena and Higgs Working Group) and CDF and D0 Coll], [arXiv:1203.3774 [hep-ex]].
- [221] J. Ellis, J. R. Espinosa, G. F. Giudice, A. Hoecker and A. Riotto, Phys. Lett. B **679** (2009) 369 [arXiv:0906.0954 [hep-ph]].
- [222] J. Elias-Miro, J. R. Espinosa, G. F. Giudice, G. Isidori, A. Riotto and A. Strumia, Phys. Lett. B **709** (2012) 222 [arXiv:1112.3022 [hep-ph]].
- [223] F. Bezrukov, M. Y. Kalmykov, B. A. Kniehl and M. Shaposhnikov, JHEP **1210** (2012) 140 [arXiv:1205.2893 [hep-ph]].
- [224] G. Degrandi, S. Di Vita, J. Elias-Miro, J. R. Espinosa, G. F. Giudice, G. Isidori and A. Strumia, JHEP **1208** (2012) 098 [arXiv:1205.6497 [hep-ph]].
- [225] J. R. Ellis, G. Ridolfi and F. Zwirner, Phys. Lett. B **257** (1991) 83; Phys. Lett. B **262** (1991) 477.
- [226] Y. Okada, M. Yamaguchi and T. Yanagida, Prog. Theor. Phys. **85** (1991) 1.
- [227] H. E. Haber and R. Hempfling, Phys. Rev. Lett. **66** (1991) 1815.
- [228] B. C. Allanach *et al.*, in *Proc. of the APS/DPF/DPB Summer Study on the Future of Particle Physics (Snowmass 2001)* ed. N. Graf, Eur. Phys. J. C **25** (2002) 113 [arXiv:hep-ph/0202233].
- [229] P. H. Chankowski, S. Pokorski and J. Rosiek, Phys. Lett. B **274** (1992) 191.
- [230] A. Brignole, Phys. Lett. B **281**, 284 (1992).

- [231] A. Dabelstein, Z. Phys. C **67**, 495 (1995) [arXiv:hep-ph/9409375].
- [232] B. C. Allanach, A. Djouadi, J. L. Kneur, W. Porod and P. Slavich, JHEP **0409** (2004) 044 [arXiv:hep-ph/0406166].
- [233] M. Frank, T. Hahn, S. Heinemeyer, W. Hollik, H. Rzehak and G. Weiglein, JHEP **0702** (2007) 047 [arXiv:hep-ph/0611326].
- [234] S. Heinemeyer, W. Hollik, H. Rzehak and G. Weiglein, Phys. Lett. B **652** (2007) 300 [arXiv:0705.0746 [hep-ph]].
- [235] M. S. Carena, J. R. Ellis, A. Pilaftsis and C. E. M. Wagner, Nucl. Phys. B **586** (2000) 92 [hep-ph/0003180].
- [236] S. P. Martin, Phys. Rev. D **67** (2003) 095012 [arXiv:hep-ph/0211366].
- [237] S. P. Martin, Phys. Rev. D **75** (2007) 055005 [arXiv:hep-ph/0701051].
- [238] R. V. Harlander, P. Kant, L. Mihaila and M. Steinhauser, Phys. Rev. Lett. **100** (2008) 191602 [Phys. Rev. Lett. **101** (2008) 039901] [arXiv:0803.0672 [hep-ph]].
- [239] S. Heinemeyer, W. Hollik and G. Weiglein, Comput. Phys. Commun. **124** (2000) 76 [arXiv:hep-ph/9812320].
- [240] G. Degrandi, S. Heinemeyer, W. Hollik, P. Slavich and G. Weiglein, Eur. Phys. J. C **28** (2003) 133 [arXiv:hep-ph/0212020].
- [241] T. Hahn, S. Heinemeyer, W. Hollik, H. Rzehak and G. Weiglein, Comput. Phys. Commun. **180** (2009) 1426.
- [242] J. S. Lee, A. Pilaftsis, M. S. Carena, S. Y. Choi, M. Drees, J. R. Ellis and C. E. M. Wagner, Comput. Phys. Commun. **156** (2004) 283 [arXiv:hep-ph/0307377].
- [243] J. S. Lee, M. Carena, J. Ellis, A. Pilaftsis and C. E. M. Wagner, Comput. Phys. Commun. **180** (2009) 312 [arXiv:0712.2360 [hep-ph]].
- [244] <http://www-ttp.particle.uni-karlsruhe.de/Progdata/ttp10/ttp10-23/>
- [245] <http://www.feynhiggs.de/>
- [246] Y. Schroder and M. Steinhauser, Phys. Lett. B **622** (2005) 124 [hep-ph/0504055].
- [247] K. G. Chetyrkin, M. Faisst, J. H. Kuhn, P. Maierhofer and C. Sturm, Phys. Rev. Lett. **97** (2006) 102003 [hep-ph/0605201].
- [248] R. Boughezal and M. Czakon, Nucl. Phys. B **755** (2006) 221 [hep-ph/0606232].
- [249] G. Degrandi, P. Slavich and F. Zwirner, Nucl. Phys. B **611** (2001) 403 [hep-ph/0105096].
- [250] K. G. Wilson, Phys. Rev. **179** (1969) 1499.
- [251] H. Kluberg-Stern and J. B. Zuber, Phys. Rev. D **12** (1975) 3159.



- [252] N. K. Nielsen, Nucl. Phys. B **97** (1975) 527.
- [253] V. P. Spiridonov, Report No. INR P-0378, Moscow, 1984.
- [254] K. G. Chetyrkin, B. A. Kniehl and M. Steinhauser, Nucl. Phys. B **490** (1997) 19 [hep-ph/9701277].
- [255] G. Degrassi and P. Slavich, JHEP **1011** (2010) 044 [arXiv:1007.3465 [hep-ph]].
- [256] R. V. Harlander, F. Hofmann and H. Mantler, JHEP **1102** (2011) 055 [arXiv:1012.3361 [hep-ph]].
- [257] A. I. Davydychev and J. B. Tausk, Nucl. Phys. B **397** (1993) 123.
- [258] S. Dawson, Nucl. Phys. B **359** (1991) 283.
- [259] A. Djouadi, M. Spira and P. M. Zerwas, Phys. Lett. B **264** (1991) 440.
- [260] T. Inami, T. Kubota and Y. Okada, Z. Phys. C **18** (1983) 69.
- [261] P. A. Baikov and K. G. Chetyrkin, Phys. Rev. Lett. **97** (2006) 061803 [hep-ph/0604194].
- [262] R. V. Harlander and M. Steinhauser, Phys. Lett. B **574** (2003) 258 [hep-ph/0307346].
- [263] G. Degrassi and P. Slavich, Nucl. Phys. B **805** (2008) 267 [arXiv:0806.1495 [hep-ph]].
- [264] C. Anastasiou, S. Beerli and A. Daleo, Phys. Rev. Lett. **100** (2008) 241806 [arXiv:0803.3065 [hep-ph]].
- [265] M. Muhlleitner, H. Rzehak and M. Spira, JHEP **0904** (2009) 023 [arXiv:0812.3815 [hep-ph]].
- [266] M. Muhlleitner and M. Spira, Nucl. Phys. B **790** (2008) 1 [hep-ph/0612254].
- [267] R. Bonciani, G. Degrassi and A. Vicini, JHEP **0711** (2007) 095 [arXiv:0709.4227 [hep-ph]].
- [268] L. Mihaila and C. Reisser, JHEP **1008** (2010) 021 [arXiv:1007.0693 [hep-ph]].
- [269] R. V. Harlander and K. J. Ozeren, JHEP **0911** (2009) 088 [arXiv:0909.3420 [hep-ph]].
- [270] A. Pak, M. Rogal and M. Steinhauser, JHEP **1002** (2010) 025 [arXiv:0911.4662 [hep-ph]].
- [271] J. R. Ellis, M. K. Gaillard and D. V. Nanopoulos, Nucl. Phys. B **106** (1976) 292;  
M. A. Shifman, A. I. Vainshtein and V. I. Zakharov, Phys. Lett. B **78** (1978) 443;  
M. A. Shifman, A. I. Vainshtein, M. B. Voloshin and V. I. Zakharov, Sov. J. Nucl. Phys. **30** (1979) 711 [Yad. Fiz. **30** (1979) 1368];  
A. I. Vainshtein, V. I. Zakharov and M. A. Shifman, Sov. Phys. Usp. **23** (1980) 429 [Usp. Fiz. Nauk **131** (1980) 537];  
B. A. Kniehl and M. Spira, Z. Phys. C **69** (1995) 77 [hep-ph/9505225];  
M. Spira, A. Djouadi, D. Graudenz and P. M. Zerwas, Nucl. Phys. B **453** (1995) 17 [hep-ph/9504378].
- [272] W. Kilian, Z. Phys. C **69** (1995) 89 [hep-ph/9505309].

- [273] <https://twiki.cern.ch/twiki/bin/view/LHCPhysics/CrossSections>
- [274] E. Braaten and J. P. Leveille, Phys. Rev. D **22** (1980) 715.
- [275] S. G. Gorishnii, A. L. Kataev, S. A. Larin and L. R. Surguladze, Mod. Phys. Lett. A **5** (1990) 2703.
- [276] K. G. Chetyrkin, B. A. Kniehl and M. Steinhauser, Phys. Rev. Lett. **79** (1997) 2184 [hep-ph/9706430].
- [277] A. Kwiatkowski and M. Steinhauser, Phys. Lett. B **338** (1994) 66 [Erratum-ibid. B **342** (1995) 455] [hep-ph/9405308].
- [278] K. G. Chetyrkin, J. H. Kuhn, A. Maier, P. Maierhofer, P. Marquard, M. Steinhauser and C. Sturm, Phys. Rev. D **80** (2009) 074010 [arXiv:0907.2110 [hep-ph]].
- [279] M. S. Carena, S. Heinemeyer, C. E. M. Wagner and G. Weiglein, Eur. Phys. J. C **26** (2003) 601 [hep-ph/0202167].
- [280] J. Guasch, P. Hafliger and M. Spira, Phys. Rev. D **68** (2003) 115001 [hep-ph/0305101].
- [281] M. Spira, A. Djouadi, D. Graudenz and P. M. Zerwas, Nucl. Phys. B **453** (1995) 17 [hep-ph/9504378].
- [282] M. Steinhauser, In \*Tegernsee 1996, The Higgs puzzle\* 177-185 [hep-ph/9612395].
- [283] U. Aglietti, R. Bonciani, G. Degrossi and A. Vicini, Phys. Lett. B **595** (2004) 432 [hep-ph/0404071];  
F. Fugel, B. A. Kniehl and M. Steinhauser, Nucl. Phys. B **702** (2004) 333 [hep-ph/0405232];  
G. Degrossi and F. Maltoni, Nucl. Phys. B **724** (2005) 183 [hep-ph/0504137].
- [284] R. Harlander and P. Kant, JHEP **0512** (2005) 015 [hep-ph/0509189].
- [285] A. Kurz, Diploma thesis, Karlsruhe Institute of Technology (2010).
- [286] J. Kleine, Diploma thesis, Karlsruhe Institute of Technology (2010).
- [287] A. Djouadi, Phys. Rept. **457** (2008) 1 [hep-ph/0503172];  
A. Djouadi, Phys. Rept. **459** (2008) 1 [hep-ph/0503173].
- [288] R. Harlander, J. Phys. G **35** (2008) 033001.
- [289] R. V. Harlander and K. J. Ozeren, Phys. Lett. B **679** (2009) 467 [arXiv:0907.2997 [hep-ph]].
- [290] R. V. Harlander, H. Mantler, S. Marzani and K. J. Ozeren, Eur. Phys. J. C **66** (2010) 359 [arXiv:0912.2104 [hep-ph]].
- [291] A. Pak, M. Rogal and M. Steinhauser, Phys. Lett. B **679** (2009) 473 [arXiv:0907.2998 [hep-ph]].
- [292] A. Pak, M. Rogal and M. Steinhauser, JHEP **1109** (2011) 088 [arXiv:1107.3391 [hep-ph]].